UNIVERSITÀ
DEGLI STUDI
DI PADOVA

Sede Amministrativa: Università degli Studi di Padova

Dipartimento di Ingegneria dell'Informazione

Corso di Dottorato di Ricerca in: Ingegneria dell'Informazione
Curriculum: Information and Communication Technology
Ciclo: 34°

PREDICTIVE CONSTRAINED CONTROL OVER WIRELESS FROM STABILITY TO SAFETY

Coordinatore: Prof. Andrea Neviani

Supervisore: Prof. Luca Schenato

Dottorando: Matthias Pezzutto

University of Padova

Department of Information Engineering

Predictive Constrained Control over Wireless

From Stability to Safety

Supervisor
Prof. Luca Schenato
University of Padova

Candidate
Matthias Pezzutto

Abstract

The convergence of wireless networks and control theory has been the key factor for many successful applications like smart homes, smart cities, smart factories, and smart agriculture. Today, new wireless control applications with small sampling periods, e.g. in cooperative robotics, are feasible thanks to the latest high-speed 5G and Wi-Fi networks. However, they are still relegated to research laboratories. The reason is that, differently from systems with ideal communications, stability does not imply reliability. Temporary large deviations from the expected trajectory are likely to occur even if stability is theoretically guaranteed, especially with high-speed wireless networks. Motivated by practical examples, we propose to move from the concept of stability to the concept of safety, defined as the satisfaction of suitable constraints.

Solutions available in the literature guarantee safety of the control system over wireless only if communication blackouts are excluded. Since this is not possible with high-speed wireless networks, we study new predictive control strategies able to enforce the constraints even in presence of blackouts. The key idea is to consider two control loops: the inner control loop makes use of a simple controller, to be implemented at the plant side, able to stabilize the system, possibly used only during blackouts, while the outer control loop comprises a sophisticated predictive constrained controller, specifically designed to enforce constraints and to track reference signals despite packet loss.

In this thesis, we propose three novel solutions: the first based on Reference Governor, the second based on MPC for Tracking, and the third based on Reference Governor tailored for multi-agent systems. For any proposed strategy, we theoretically verify the recursive feasibility of the underlying optimization problem, the constraint satisfaction with probability 1 without any assumption on the communication network, and the convergence to the desired set-point under very mild hypotheses. All the algorithms achieve good results with real Wi-Fi networks. The solutions are both robust when the channel is bad and high-performing when the channel is good. Preliminary experimental tests show the validity of the proposed approach.

The thesis concludes with a sensor transmission power allocation algorithm for remote estimation that explicitly takes advantage of the latest wireless technologies. It is suitable both for multi-agent systems controlled by a central unit and for general monitoring applications relying on the Internet of Things.

Acknowledgments

I would like to thank my advisor, professor Luca Schenato, for being the best model for a PhD student. His vision and his foresight overshadow his outstanding knowledge of the field. I am very grateful for his encouragement at the right moment and his lessons on the way of approaching research.

I would like to express my gratitude to all the professors and researchers with whom I have worked in the last three years, professor Dey, professor Farina, professor Carli, professor Tramarin, and professor Garone, for his crazy ideas. Special thanks go to dr. Branz and dr. Antonello, probably the most skilled engineer in the world, that make the great part of the experimental setup used in this thesis.

I want to thank also all my colleagues from the University of Padova and from the Université Libre de Bruxelles, for all the time spent together and all the interesting scientific discussions.

Finally, I am indebted to my parents, for their unconditional and immeasurable help, and to Lisa, for being my support and for feeding me while writing this thesis.

Contents

1 Introduction

The wireless revolution of the last decades has impacted everyday life far beyond the mere way of communicating. The easy connection of wireless networks has enabled the connected world where we live in, where both people and devices are constantly linked in a networked fashion. This trend is expected to increase and wireless communications will find even more space in the next few years.

Control engineers have looked with interest at the advent of new communication technologies as witnessed by the large attention paid to Networked Control Systems (NCSs). Differently from the standard control architecture, where the sensors and the actuators are connected to the control unit by means of point-to-point dedicated cables, a NCS consists of a control system where at least a link between the plant and the controller is implemented through a communication network, either wired or wireless.

The interest in NCSs specifically relying on wireless networks is supported by several practical reasons. In fact, wiring can be drastically reduced, reconfigurability and interoperability are enhanced, troubleshooting is simplified. Most importantly, fewer computational capabilities can be allocated to the plant, and more complex control algorithms can be implemented. For these reasons, wireless communications are very appealing for many relevant control applications like industrial plants covering wide areas, and systems with many sensors and actuators. Also, in modern factories, the new Industry 4.0 paradigm [1] and the Industrial Internet-of-Things [2] call for a more pervasive use of wireless networks. Smart buildings [3], smart cities [4], and smart grids [5] can effectively rely on wireless networks. For other applications, like mobile and multi-agent robotics, wireless communications are not only convenient but required.

Unfortunately, wireless networks are not as reliable as point-to-point connections or wired networks and they cannot be assumed ideal in the control design. Packet loss and delays are the two main non-idealities that affect communications over wireless. In order to close the feedback loop over wireless, their effects on the system have to be carefully studied and adequately addressed, both in the communication network design and in the control design.

1.1 State of the Art

In the following, we show how the interplay of communication and control has been studied from the network science perspective and from the control theory perspective. We conclude the section with an overall picture of the current deployment of wireless networks in real control applications.

1.1.1 Communication for Control

Existing wireless networks can be essentially divided in two groups: networks for automation purposes and networks for general purposes.

The most widespread and settled solutions for automation are WirelessHart and ISA 100.11a, both based on the IEEE 802.15.4 standard [6]. These networks have been specifically designed to guarantee high reliability (few corrupted received packets) and small latencies (few out-to-date receptions), see [6]. They provide a raw data-rate of 250 kbit/s over a time-slotted channel. Unfortunately, the minimum time slot duration is equal to 10 ms, so, even in the simplest case with a single sensor and a single actuator, the sampling period cannot be decreased below 20 ms [7]. In the case of multiple sensors and actuators, like in the case of multi-agent systems, the sampling period fatally increases and the performances are limited.

Nowadays, the most popular wireless networks for general purposes are Wi-Fi, based on IEEE 802.11 standard, and 5G. These networks are throughput-oriented, so the total amount of delivered data is favored over the timeliness in delivering each data packet [8]. To this end, they provide high data-rates and more efficient medium access protocols [8]. Consequently, when they are used for control applications, smaller sampling periods can be achieved but the stochasticity in the feedback loop, represented by packet losses and delays, is largely increased. To achieve both high performances and high safety, we are forced to use general purposes wireless networks and to cope with the resulting unreliability.

A first approach to deal with control over general purpose wireless networks is to reduce the unreliability through a suitable design of the communication parameters. Several solutions are available in the literature, mainly tailored for Wi-Fi. At the Physical layer, both the transmission power and the data-rate can be adapted according to the channel condition on a packet basis. In fact, the transmission power can be increased when the channel noise is high to decrease the loss probability, while it can be decreased when the channel noise is low to save energy [9]. Similarly, high data-rates can be selected in good channel conditions to decrease the sampling period, while low data-rates employing more robust modulations can be selected in bad channel conditions to reduce packet losses [10]. Along this line, an adaptive transmission rate scheme based on LQG cost is studied in [11], while a model-free data-driven scheme is devised in [12]. Moreover, the presence of

multiple antennas can be exploited to increase the reliability of the communication, see the proof of concept [8]. Alternatively, it is possible to act at the Data Link layer as suggested in [13]. Refined solutions can be obtained following the approach of [14], which exploits the analytical model of the MAC layer of IEEE 802.15.4 standard to optimize the number of retransmissions, the minimum backoff exponent, and the maximum number of backoffs. A more radical solution is the ad-hoc wireless protocol tested in [15] called Real Time Wi-Fi (RT-WiFi). It exploits the Physical layer of the IEEE 802.11 standard to guarantee high transmission rates and a Data Link layer based on TDMA to enforce determinism in the communication. Experimental tests show that RT-WiFi outperforms Wi-Fi in terms of latencies and thus it is more suitable for control applications. The authors argue that (aggregate) transmission rates up to 6 kHz are possible with RT-WiFi. The idea of combining the data-rates of the Physical layer of IEEE 802.11 standard and the determinism of TDMA protocol at the Data Link layer is used also in WIA-FA networks, based on the recently approved IEC 62948 standard [16].

A second approach is to cope with the network unreliability in the control design. Clearly, a suitable model of the wireless network is important in order to design an effective control algorithm. In most of the existing works on NCSs, packet losses are modeled as independent and identically distributed random variables with Bernoulli distribution. This model is attractive because of its simplicity but it is not able to capture the experimental behavior of general purpose wireless networks. A more accurate model is the well-known Gilbert-Elliott model, whose main idea is proposed in [17][18]. The channel is modeled through a Markov chain with two states, usually referred to as "Good" and "Bad". Accordingly, the probability of transition from a state to another depends only on the current state. In the more general formulation, losses can occur in every channel state as independent events, and the loss probability depends only on the channel state. This includes the special case where the packet is always lost in Bad state and always delivered in Good state, which in turn includes the case of independent losses when the transition probabilities are taken symmetric. The idea can be easily generalized to consider more states, possibly characterized by SNR [19], or higher-dimensional Markov chains, where the packet loss probability depends on the number of consecutive packet losses so far [20]. Along the same line, Hidden Markov Models are used [21]. An overview of the existing models tailored for Wi-Fi can be found in the recent work [22].

The validity of these models depends on the network standard and on the environment. For this reason, experimental tests are necessary to understand their applicability to the specific case. For Wi-Fi, detailed experimental campaigns are carried out e.g. in [8] and [23]. For illustrative purposes, we report some experimental data obtained in our laboratory.

The experimental setup, originally devised in [23], comprises a host PC and a target board connected through a Wi-Fi network in an office-like environment. Network

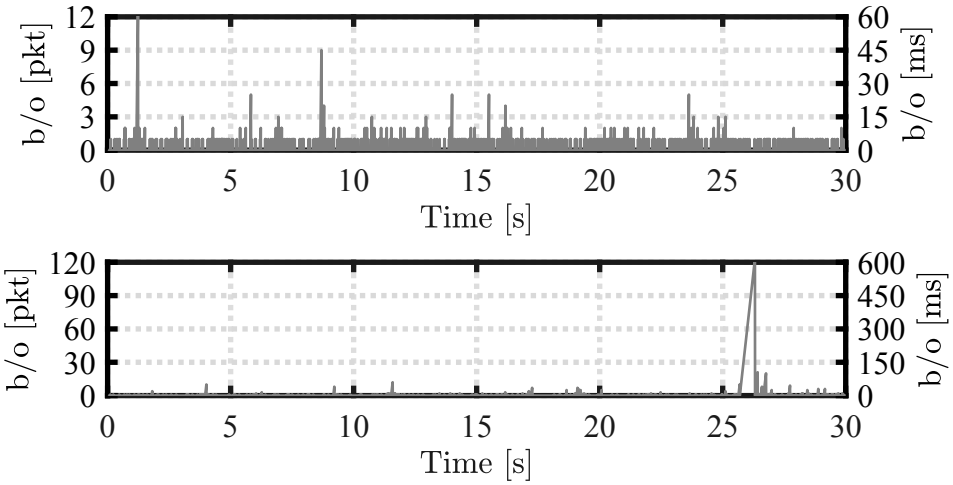

Figure 1.1: Blackouts (b/o) with good channel conditions. In the bottom panel, we can see that long blackouts are possible even with good channel conditions.

parameters are set according to [24]. The experiment consists of the transmission of time-stamped packets from the host PC to the target board and the other way around. At each side, a fixed time-span T elapses between two following transmissions, mimicking sampling instants and thus the communication between a plant and a remote control unit. Using the time-stamps, we retrieve the arrival processes and compute the communication blackouts that occurred during the experiment. Formally, at time instant t, the blackout b/o is the period elapsed since the last received packet. For a complete description of the experimental setup see Appendix A.3. The interested reader is referred to [23] for an exhaustive experimental campaign for different T and a detailed description of the results in terms of delays and packet losses. In the following, we give a taste of the typical behavior of the Wi-Fi network for the case of $T = 5$ ms focusing on communication blackouts.

In top panel of Figure 1.1 we can see the behavior of the network in good channel conditions. We can see that only 15 times over 30 s (6000 packets) more than two consecutive packets have been lost. The longest blackout has a length of 12 packets, corresponding to 60 ms. This network evolution, in general, allows control applications.

Bottom panel of Figure 1.1 still reports the network evolution under good channel conditions. However, in this case, we see a very long communication blackout of 120 packets, corresponding to 600 ms. This is particularly annoying because the blackout was almost unexpected, since the network performances were satisfactory so far. If the open-loop system is unstable, we may expect the trajectory to diverge.

Since the above experimental data have been collected in ideal conditions, with only minor interference from other networks, we introduce a new Wi-Fi network in the laboratory. This is a very realistic setup, since it is reasonable to consider other Wi-Fi networks in the environment, both for general traffic and possibly for other control applications.

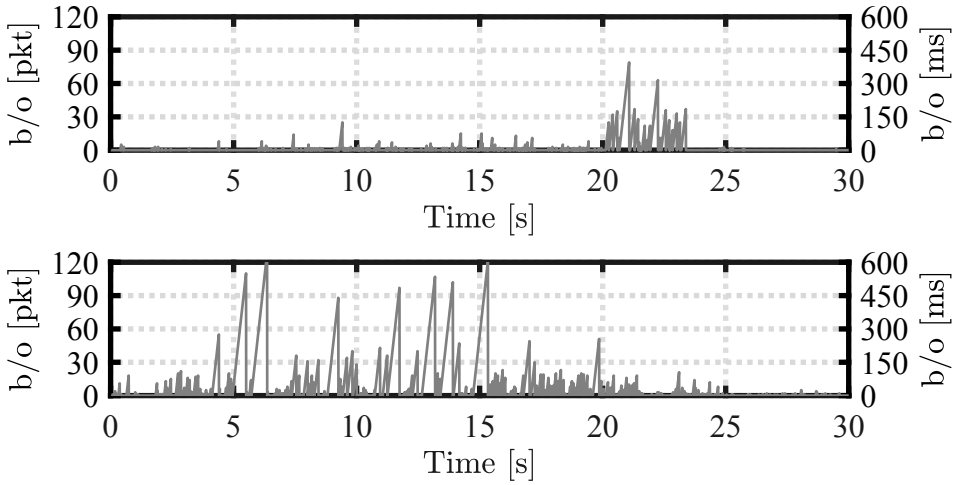

Figure 1.2: Blackouts (b/o) with bad channel conditions. We can see that bad channel conditions can last for both short (top panel) and long periods (bottom panel)

It follows that the channel experienced by the considered network depends on the traffic on the other network. As shown in top panel of Figure 1.2, the channel condition can be good for long periods (see from 0 to 20 s), but long blackouts can still occur in a short period of time (less than 4 s) due to a temporary disturbed channel. Moreover, in the same configuration, bad channel conditions can last for a long period, see bottom panel of Figure 1.2. In that case, the average packet loss probability in the period from 5 s to 20 s is 0.7 and 5 blackouts longer than 100 packets occur. Control applications in these conditions are really challenging and performances may be unsatisfactory.

These experimental results give important insight on the problem. First, we can see that communication blackouts are possible even in good channel conditions. In general, this behavior prevents the remote stabilization of an unstable plant. Second, we see that channel conditions are strongly time-varying. Control algorithms have to adapt to the channel conditions, to avoid both instability in bad channel conditions and conservativeness in good channel conditions.

1.1.2 Theory of Networked Control Systems

Different approaches have been proposed to theoretically study control system over wireless networks.

Following e.g. [25][26][27][28][29], the plant is modeled as a continuous-time system but, due to the presence of the wireless network, transmissions (of the measurements and of the control inputs) occur only at sampled time instants. Transmission instants may be governed by the medium access protocol or by event-trigger mechanisms [30], while the network may introduce delays on the reception (and so on the application) instant of the packet. According to this model, a packet is used as soon as it has been received. Typically, the controller is designed as if the network is not present and most of the

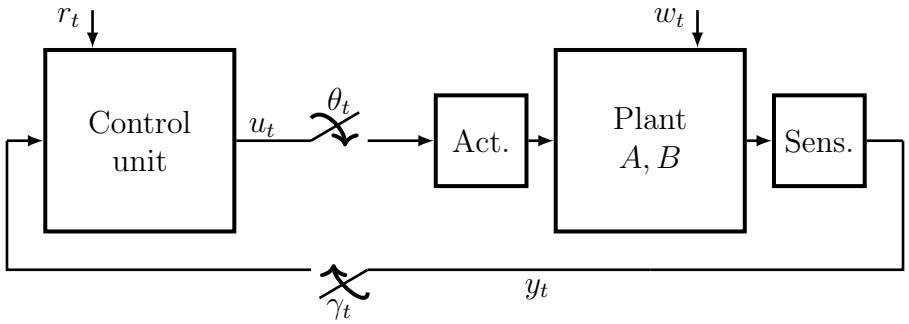

Figure 1.3: Standard setup considered in the literature. The switches indicate an intermittent communication. Note that sensor and actuator do not directly communicate.

effort is dedicated to deriving the Maximum Allowable Transmission Interval (MATI) that preserves stability. The resulting control design is called Emulation-based and is widely adopted in the literature [31][32][33][34].

An alternative approach, used e.g. in [35][36][37][38][39], proposes to model the plant as a discrete-time system with transmissions occurring at sampling instants. According to this model, a packet is used at the sampling instant following its reception. In this sense, any delay smaller than a sampling period has the same effect on the system. Since this is the model used in this thesis, we summarize some relevant results obtained using this approach and we use them to illustrate the main known drawbacks of control over wireless. We consider linear systems with Gaussian noise. Since the results are simpler, by way of example, we focus on the TCP-like case.

The first problem when controlling a remote plant is to estimate the state of the system. Interestingly, the **optimal filter** for linear systems in presence of packet loss can be easily obtained using the Kalman filter for time-varying systems: in fact, the resulting system is equivalent to the original system but with time-varying output matrix, equal to the original one when the packet is arrived and equal to the null matrix when the packet is lost [35]. The optimal estimate is obtained applying a closed-loop update (i.e. the Kalman filter update with the original non-null output matrix) if the packet is arrived or applying an open-loop update using only the model (corresponding to the Kalman filter update with the null output matrix) if the packet is lost. As a consequence, the error covariance does not converge due to the dependence on the arrival process and the optimal gain is time-varying.

The first drawback then is that, differently from the system with ideal channels, the estimation error covariance is not always bounded. It has been shown that, if packets are lost according to independent Bernoulli random variables, there exists a critical threshold λ_c on the arrival probability below which the expected error covariance diverges [35]. Similar results hold for more general channel models [39]. This limits the application of control over wireless networks to the cases where some minimal average channel

requirements are guaranteed.

With the aim of providing a full understanding of the channel requirements to apply control over wireless, large efforts have been made to characterize the critical threshold λ_c. The simple upper bound $\bar{\lambda} = 1 - 1/\prod_i |\lambda_i|^2$ where λ_i are the unstable eigenvalues of the system matrix A has been provided in [38] following [36]. The well-known lower bound $\underline{\lambda} = 1 - 1/|\lambda_{\max}|^2$ where $\lambda_{\max}$ is the largest eigenvalue of A is given in [35]. It has been shown that the exact value coincides with the lower bound when the output matrix C is invertible, when A has a unique unstable eigenvalue, and when A is diagonalizable with simple and distinct eigenvalues [40]. The equivalence between the critical value and the lower bound has been proved in [41] if the submatrix of C relative to the observable space of the system is invertible and in [42] if A is diagonalizable and the system is non-degenerate. The latter result has been generalized for more general channel models in [43].

The problem of remote estimation over wireless networks has been extended to consider multiple sensors [44] and delays [45], expressed in terms of number of sampling periods. Notably, in these cases, the algorithms are natural extensions of the original Kalman filtering with packet loss [35]. The work [46] studies how to optimally encode the information transmitted from the sensor to the remote estimator. Interestingly, the optimal scheme among all causal algorithms for any packet loss model is a standard Kalman filter at the sensor. Then, the optimal estimate at the remote estimator is set equal to the estimate of the local estimator if the packet is arrived, or it is obtained with an open-loop update using the system model if the packet is lost. If packets are lost according to independent Bernoulli random variables, also in this case, there exists a critical threshold on the arrival probability and it coincides with the lower bound of the critical threshold for the case where the raw measurement is transmitted. It follows that, for systems for which the exact critical threshold and the lower bound coincide, stability is not enhanced if the optimal state estimate is transmitted instead of the raw measurement.

The second problem when controlling a remote plant is to design the controller. It has been shown that the **optimal controller** is a linear function of the state estimate and is independent of the arrival processes. While the standard optimal regulator always stabilizes the original system, when packets are lost according to independent Bernoulli random variables, the stability can be lost if the arrival probabilities are below a certain threshold. In that case, the LQG cost is unbounded and the state covariance diverges [38]. Since the duality of the optimal control and estimation problems holds, many results achieved for remote estimation can be obtained also for remote control, in particular for what concerns the critical threshold. It follows that, in several cases, the critical arrival probability is equal to $1 - 1/|\lambda_{\max}|^2$ where $\lambda_{\max}$ is the largest eigenvalue of A. We can conclude that, as in the estimation problem, minimal average channel requirements have to be met in order to remotely control the plant.

The problem of remote control over wireless networks has been extended to consider multiple actuators [47]. The work [48] studies the problem of how to compute the control input at the actuator when the packet transmitted from the remote controller is not arrived. It has been shown that the stability conditions are not improved for any possible algorithm implemented at the actuator, even if it can exploit the system model. Clearly, the performances in terms of LQG cost change depending on the algorithm used. For instance, the work [49] considers the two simplest strategies, namely the zero-input strategy, where the control input is set to zero when a packet is lost, and the hold-input strategy, where the previous control input is kept. For scalar systems, it has been shown that the hold-input strategy outperforms the zero-input strategy for small packet loss probabilities and high input penalization.

A particular instance of the control problem over wireless networks is the design of the **constrained controller**. Differently from unconstrained problems, where the requirements are on the average state, constraints have to be enforced point-wise in time. In the literature, different designs based on Model Predictive Control (MPC) have been proposed. The main idea is to use the sequence of future inputs, that is computed by MPC as by-product to obtain the current control input, to cope with future communication flaws. The work [50] studies the case where the link between sensor and MPC is ideal for nonlinear systems without disturbances. The solution has been extended in [51] for the case with bounded disturbances. In the work [52], the optimization is not solved at each time instant but only if either a new measurement has been arrived, or the last measurement has been arrived i steps ago and all the last i control sequences have been lost. The work [53] proposes to introduce a fictitious delay before using a new control sequence in order to preserve the admissibility of any applied input. In general, it has been shown that state constraints are satisfied if the number of consecutive packet losses is smaller than the horizon of the MPC. So, the second drawback of control over wireless is that, differently from the system with ideal channels, constraints are not always satisfied but the number of consecutive packet losses has to be bounded and known in advance. We can conclude that, in order to satisfactorily control a remote plant over wireless, the network has to satisfy both average requirements on the channel, namely the minimal arrival rate, and instantaneous requirements, namely the bound on the number of consecutive packet losses.

In the UDP-like case, the control design is much more challenging. In particular, it has been shown that the separation principle does not hold even in the linear case [38]. In particular, the control input is a nonlinear function of the state estimate and the optimal estimate is a nonlinear function of the control input. The same holds also in the realistic case where the acknowledgment is randomly lost [54]. Since the exact optimal estimate and control have been shown to be intractable [55][56], several suboptimal solutions have been proposed. For instance, the state estimate can be computed using the expected

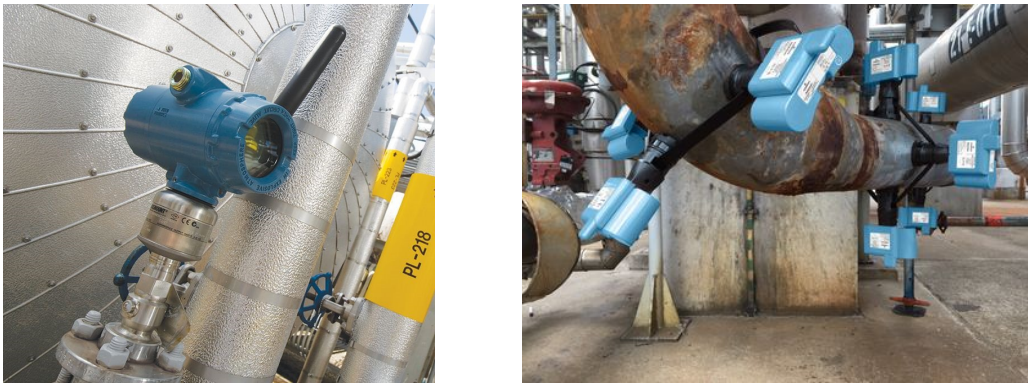

Figure 1.4: Practical deployment of wireless sensors. Courtesy of Emerson™. Left panel: pressure sensor. Right panel: corrosion sensor.

applied input in the Kalman filter [37], estimating the applied input based on the received measurement [57], or using optimal static gains [58]. When constraints are present, with UDP-like protocol, the solutions are usually more conservative [59].

1.1.3 From theory to practice

To date, wireless networks are deployed in many control applications. In the simplest case, the wireless network is used to connect a set of spatially distributed sensors to a central monitoring unit. This application, referred to as Wireless Sensor Network (WSN), is today widely established and several off-the-shelf solutions are now provided by important companies like Siemens, Emerson, and ABB, just to mention a few. Two examples of wireless sensors available on the market are reported in Figure 1.4. Extensive use of WSNs has been made for monitoring purposes in industrial environment since the seminal successful application at Cherry Point refinery in 2006 [60]. Another interesting application of WSNs is the monitoring of civil infrastructures, like bridges, skyscrapers, and other buildings. A curious early implementation has been deployed in the Golden Gate Bridge in San Francisco bay [61] (based on TinyOS). Other interesting applications of WSNs can be found in the medical area, see [62] for a detailed survey. In this field, an interesting pilot application has been implemented at Johns Hopkins Hospital Emergency Department [63]. Each patient is provided with a compact device including a small microprocessor, an IEEE 802.15.4 chip, and a sensor board connected to a pulse oximetry probe. The overall architecture, called MEDiSN, comprises relay nodes, a gateway, and a central server. Using an ad-hoc communication suite and app services, the WSN allows doctors to monitor patient data from remote in an efficient way. A similar architecture, called CodeBlue, has been experimentally tested in [64].

The aforementioned applications are limited to sensing and no control action is transmitted over wireless. In the last years, however, in several cases, wireless networks have been used for both the links of the control loop. Smart homes are one of the most prolific

application fields. In fact, a home can be seen as a dynamical system with several outputs, e.g. the temperature and the room light, and input, e.g. air conditioning, heating, and the light switches. In this context, typical applications are temperature control and light control. For instance, the work [65] implements a light controller in an office environment using light sensors, motion sensors, a central computational unit, and local LED drivers, connected through a wireless network (ZigBee). Results are really promising: the control system reduces the total power consumption by 55% during a six months period. The work [66] implements a temperature control in an office in Hong Kong using occupancy sensors, temperature sensors, a central computational unit, and a variable-air-volume conditioning system, connected by wireless. The control law regulates the supply airflow rate by acting on the opening rate of the variable-air-volume boxes. The solution outperforms significantly the conventional control in terms of total power consumption and improves the comfort of persons in the room.

Also agriculture is a breeding ground for control over wireless. For instance, a scheme employing local (ZigBee) and cellular (GPRS) wireless communications have been used in an automated irrigation system for sage, thyme, origanum, and basil, in Mexico [67]. Results are outstanding: the system achieves water savings of up to 90% compared with traditional irrigation practices. Along this line, international research projects [68][69] have been funded to put into practice smart agriculture solutions exploiting control and wireless technologies.

Wireless communications have been successfully used also in process control. A notable work is [70] where a wireless control system has been implemented for a starch cooker process at the Iggesund paper mill in Sweden. The considered application comprises three stages of the overall process. First, a starch-water mixture is cooked through steam injection, then it is diluted and opportunely mixed, and finally it is sent to a storage tank. The process is regulated by three independent controllers: the temperature during the cooking is controlled regulating the steam injection, the concentration after the dilution is controlled regulating the water flow, and the pressure is controlled regulating the flow to the storage. The three controllers, taken identical to the preexisting PID controllers, are implemented in a central computational unit connected with the sensors and the actuators through a wireless network. Interestingly, the paper mill operators could not distinguish if the paper was produced using the wireless control system or using the preexisting wired controllers.

As shown in the examples above taken from smart homes and smart agriculture, wireless networks have promoted a technological shift by enabling control strategies in applications where it was difficult or almost impossible to close a feedback loop. Large improvements can be achieved also in process control by connecting many sensors, actuators, and advanced remote computational units. Notably, from the theoretical point of view, standard control strategies apply in these cases since transmission rates are really

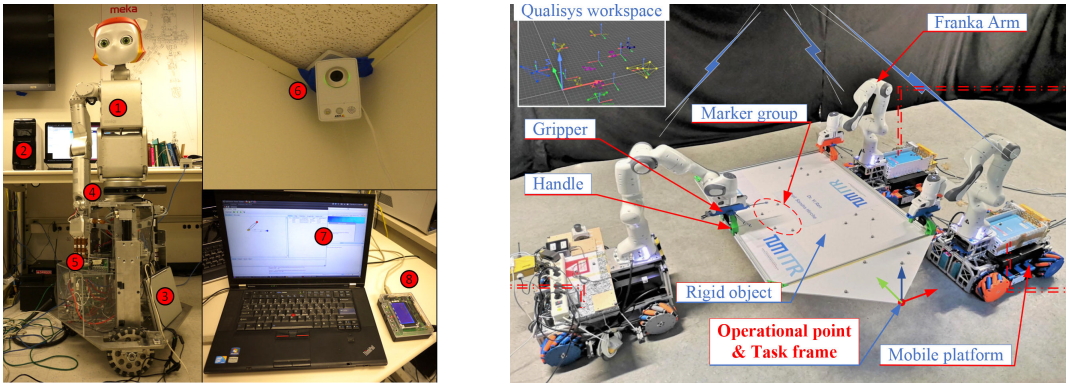

Figure 1.5: Case study of NCSs. Left panel: architecture of the cyberphysical avatar by [71]. Right panel: three mobile manipulators used in [75]. So far, high-frequency control applications over wireless are limited to research laboratories.

low (generally speaking, less than 1 transmission per second) and the communication can be made sufficiently reliable.

We argue that a similar technological shift that enables the large deployment of multi-agent robotic systems can be achieved thanks to wireless communications. So far, however, despite the large body of literature on control with packet losses, this application is only at its infancy. To date, just a few practical implementations have been done. A complete architecture of a cyber-physical avatar employing both Wi-Fi and WirelessHart is presented in [71]. The control of inverted pendulum systems has been implemented in the early work [72] using Bluetooth, in [73] on IEEE 802.15.4, and in the more recent work [24] using Wi-Fi. A case study involving multiple inverted pendulum systems with independent control loops has been experimentally tested in [74].

A notable application is the mobile gait rehabilitation system presented in [76]. The core of the system is a compact rotary series elastic actuator (RSEA) that provides assistive torque to the patient's knee joints. The mechanism simply consists of a DC motor and a link attached to the patient leg connected by a torsional spring. The sensors included in the system are the encoders on the motor and on the knee, several IMU motion sensors, and two smart shoes with air pressure sensors. A control algorithm is implemented on a computer connected to the system through a wireless networks. Several control strategies and wireless networks have been integrated in the system, see [77][78], proving the feasibility of the application. In this case, the possibility of using a computer to implement the control algorithm allows to keep the hardware simple and cost effective. More recently, the work [75] successfully implements a system of three mobile manipulators that grasp and manipulate a rigid object. The solution uses a distributed control algorithm and a wireless network providing fast communications. The experiments show the feasibility of robotic manipulation with ideal channel conditions.

These applications, however, are academic and, even if promising, to date they are not readily implementable on real system on uncontrolled environment.

1.2 Contribution

This thesis tries to address the constrained control problem over wireless both from a theoretical point of view and from a practical perspective. In this section, we retrace the reasoning done to understand the problem, to solve the limits of the existing solutions, and to test the proposed algorithms.

1.2.1 Theoretical advances in NCSs

As shown in section 1.1.2, a lot of attention has been paid to the characterization of the conditions for the stability of the system in mean-square sense. However, much less attention has been paid to understand which conditions ensure safety of the closed-loop system with wireless communications. For common stochastic systems, safety is usually implied by stability. Indeed, with the optimal regulator, the state and the error covariances are known in advance and converge. Based on their values, it is possible to obtain bounds, satisfied with very high probability, on the deviations of the system state and of the estimation error from their expected values. Since both the state and the error are Gaussian, the bounds are generally small. For instance, the error norm is smaller than 3 times the square root of the error covariance with 99,7% probability. If measurement noise is negligible, the bound is equal to the process noise standard deviation.

It is natural to wonder if the same holds for control over wireless. In particular, is the qualitative behavior of an unstable stochastic system with ideal communications the same as an unstable stochastic system with lossy communications? Even more, is the qualitative behavior of a stable stochastic system with ideal communications the same as a stable stochastic system with lossy communications? Surprisingly, the answer to these questions is no. In fact, differently from the standard case, we show in chapter 2 that the estimation error has heavy-tailed distribution. Informally, this means that the probability of deviations larger than an arbitrary threshold is higher than the probability in the Gaussian case. It follows that, if we compare a stable system with ideal communications and a stable system with wireless communications, in the latter we see larger deviations more often. These deviations can result in dangerous system responses, like oscillations or unexpected overshoots, and suggest that stability is not sufficient to guarantee safety.

Interestingly, we also show that there exist loss probabilities for which the error has unbounded covariance (so the estimator is not mean-square stable) but admits a steady-state distribution (and so it is bounded in probability). It follows that, even if we have a mean-square unstable system with wireless communications, the evolution of the error may not divergent. We can conclude that, *even if the works on stabilization through wireless networks have advanced the understanding of stochastic control and triggered the development of several useful methodological tools, stability does not seem the right objective to boost the adoption of control over wireless.*

To increase the impact of control over wireless, it is important to provide the reliability guarantees required by most control applications. Informally, what is required is to guarantee safety by avoiding both catastrophic and dangerous events. Typical examples are collisions with obstacles, violations of the prescribed physical limits, the damage of the load due to undesired oscillations, and stress on the systems due to uncoordinated actions (e.g. in the case of cooperative robotics). More properly, safety can be identified through suitable constraints. Then, we may say that the system is safe if constraints are satisfied with probability 1. We use this concept as guideline in the design of the control algorithms proposed in this thesis.

As outlined in the previous section, existing constrained control algorithms require that the number of consecutive packet losses is bounded and known in advance. Unfortunately, communication blackouts are present in real wireless networks, especially when the channel is pushed to the limit by the control application e.g. through a low sampling period. Even if the network condition is usually good, with only sporadic packet losses, the presence of temporary blackouts is a common experience when using a wireless connection. Blackouts may arise due to routine internal processes of the network stack, to the presence of a new node trying to access the network, to other communications on the same network, to the interference of other networks, or to temporary electromagnetic noise. In section 1.1.1 we show that long blackouts in Wi-Fi networks may arise even in good channel conditions and lasting poor conditions can be caused by the presence of other interfering networks. Novel constrained control strategies are needed to deal with communication blackouts. This is the core of the thesis.

For example, consider now a remote linear system with disturbances and a zero-order hold at the actuator to compensate for packet losses. Assume that the state is required to belong to a compact set. It is easy to show that, if the system is unstable, there always exists a blackout length such that constraints are violated. On the other hand, if the system is stable and the current state satisfies the constraints, we know from the literature that there exists an input that can be kept constant for any arbitrary long period without violating the constraints. These considerations imply an important conclusion: *in order to satisfy constraints with communication blackouts, the system needs to be stabilized at the plant side.* For this reason, in chapter 3 we assume that the system is stable, possibly thanks to an inner control loop. In chapter 4 this assumption is relaxed and we assume that a smart actuator has access to the system state to apply a stabilizing control law during long blackouts. In both cases, the plant is assumed to be provided with a small computational unit not sufficient to implement the sophisticated control algorithms required to enforce constraints. On the other side, the remote control unit is provided with high computational power to tackle the problem of reference tracking under constraints. This setup is graphically depicted in Figure 1.6. We can see that the resulting control system consists of two control loops. An inner control loop, implemented

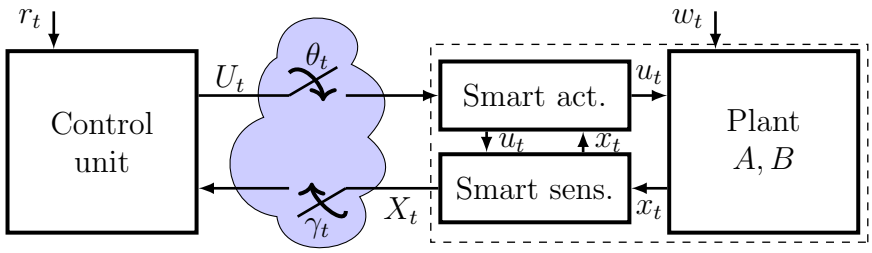

Figure 1.6: Setup considered in chapters 3 and 4. Sensor and actuator are co-located.

at the plant side, is used to be robust against blackouts. This controller is usually simple, it is designed to stabilize the system and to achieve good system responses, but it is not able to enforce constraints. The outer control loop, closed over a wireless network, is used to enforce constraints while tracking a reference signal.

Due to the presence of blackouts, the plant has to be able to autonomously evolve for arbitrarily long periods without violating the constraints. This does not only require the system to be stabilized at the plant side but also the inputs transmitted to the plant have to be specifically designed to be valid in the future. *The capability of enforcing constraints even in presence of future blackouts can be achieved using predictive control strategies.* In this thesis we employ the Reference Governor (RG) [79] and the Model Predictive Control (MPC) [80]. In both cases, the system evolution is predicted to guarantee that also future states are admissible. Moreover, predictive control strategies are known to improve the performances of the system by exploiting the model, thus taking advantage of the knowledge on the system.

To recap, in order to guarantee safety in the presence of blackouts, we have to design a simple local control strategy, able to stabilize the system, and a remote predictive constrained control algorithm, that takes into account the missing information from the plant (due to past states that have been lost) and the missing information at the plant (due to the future control inputs that may be lost).

In this thesis, we have proposed a solution based on RG (chapter 3), a solution based on MPC for Tracking (chapter 4), and a solution based on RG tailored for multi-agent systems (chapter 5). For any proposed strategy, we have theoretically verified the recursive feasibility of the underlying optimization problem, the constraint satisfaction with probability 1 without any assumption on the network, and the convergence to the desired set-point under very mild hypotheses.

Finally, the thesis concludes with a smart transmission power allocation algorithm (chapter 6). It is suitable both for multi-agent systems controlled by a central unit and for general monitoring applications relying on Internet-of-Things. It explicitly takes advantage of the latest wireless technologies using advanced reception techniques.

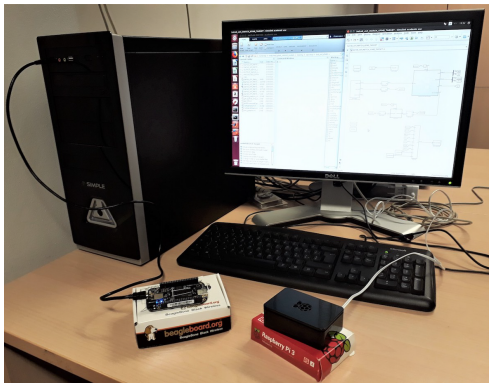
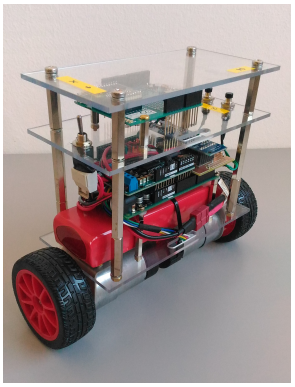

Figure 1.7: Experimental setup used in the thesis. Left panel: PC and board used to collect Wi-Fi communication data. Right panel: Segway.

1.2.2 From theory to practice

In order to test the validity of the proposed constrained algorithms for future robotics, we have conducted an accurate experimental campaign on the two-wheeled balancing robot of Figure 1.7. As we can see, it consists of a rigid chassis, with dimension 20 cm $\times$ 20 cm $\times$ 10 cm, and two wheels, with radius 3.4 cm. We often refer to it as Segway-like robot or simply Segway since, due to its structure, its dynamics are similar to a Segway electric vehicle.

The Segway is an interesting testbed because the open-loop system is nonlinear and unstable. Even if it can be linearized around the vertical position and stabilized with standard techniques, deviations from the equilibrium quickly deteriorate the accuracy of the linearization and the performances of the controller. If large tilt angles are not avoided, the Segway will be out of control and it will dramatically fall. It is natural to require the tilt angle to be limited in a suitable interval to preserve the integrity of the system while moving to any desired point of the plant. Indeed, in this case, the relation between constraint satisfaction and safety is clear. Additionally, the presence of limits on the actuators makes the control problem even more challenging. More details on the Segway are given in Appendix A.2

We proceed step-by-step. First, we start with WiFi-in-the-loop experiments where a real Wi-Fi network is used while the Segway is emulated. In particular, communication data have been collected in an experimental campaign carried in our laboratory. The experiments consist of the transmission of time-stamped packets from a host PC to a target board, and the other way around, with a given periodicity. A detailed description of the experimental setup is given in Appendix A.3 and some representative channel evolutions are shown in section 1.1.1. The collected data have been included in a Simulink model where the plant model and the control unit have been implemented. In this way, we accurately simulate the nonlinear plant dynamics, the sensing devices (encoders and MPU), the actuator saturation, and the network, based on the experimental data. In

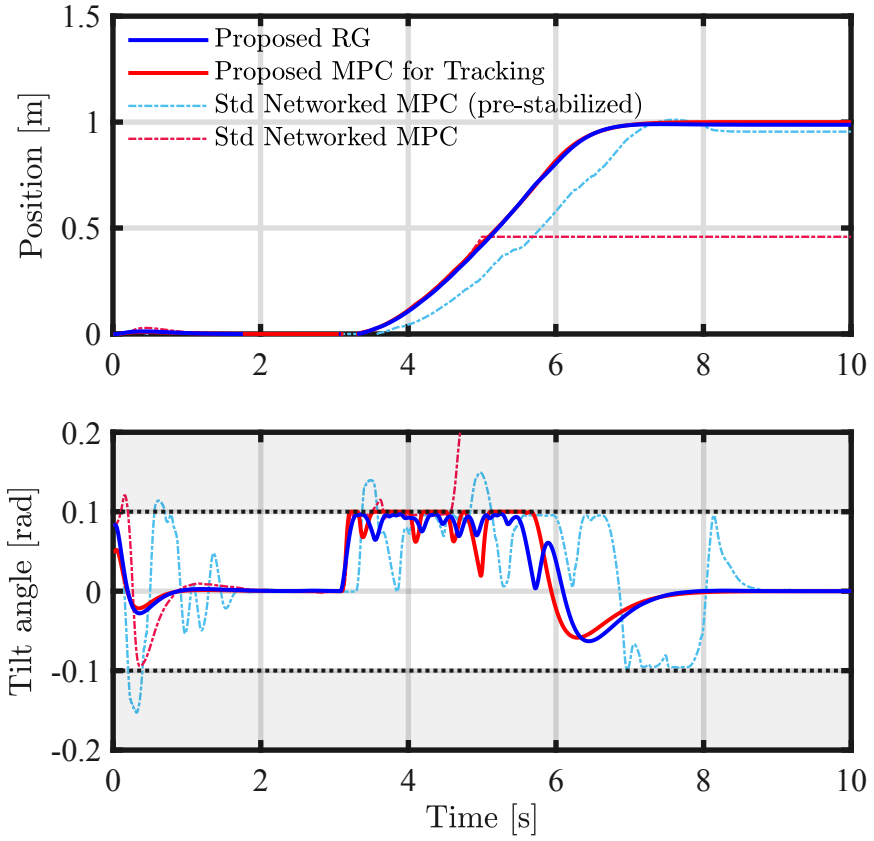

Figure 1.8: System response with WiFi-in-the-loop setup. Comparison between proposed strategies and standard Networked MPC [59]. Constraints are indicated in dark gray.

this framework, we have tested the RG with packet losses devised in chapter 3 and the MPC for Tracking over wireless devised in chapter 4.

Typical results under bad channel conditions are reported in Figure 1.8. We can see that the Networked MPC [59] is not able to enforce the constraints due to long blackouts. If the Segway is pre-stabilized by a local controller, the violations are modest, but still up to 0.05 rad on a limit of 0.1 rad, and the reference is reached, but 1 s later than the proposed strategies. If the Segway is not equipped with a local controller, the consequences are catastrophic: the Segway falls down (the tilt angle is equal to $\pi/2$) and cannot proceed anymore. Conversely, both the proposed RG and the proposed MPC for Tracking succeed in reaching the desired set-point. The performances are almost identical, but we can see more but smaller oscillations with the proposed RG with respect to the proposed MPC for Tracking. Most importantly, the constraints are always satisfied. Notably, we have repeatedly tested the proposed strategies with different channel conditions, network parameters, control design parameters, and sampling periods, and we have seen that safety is achieved in any case.

Due to the promising results, the WiFi-in-the-loop validation is followed by a full experimental test. Since RG over wireless and MPC for Tracking over wireless give

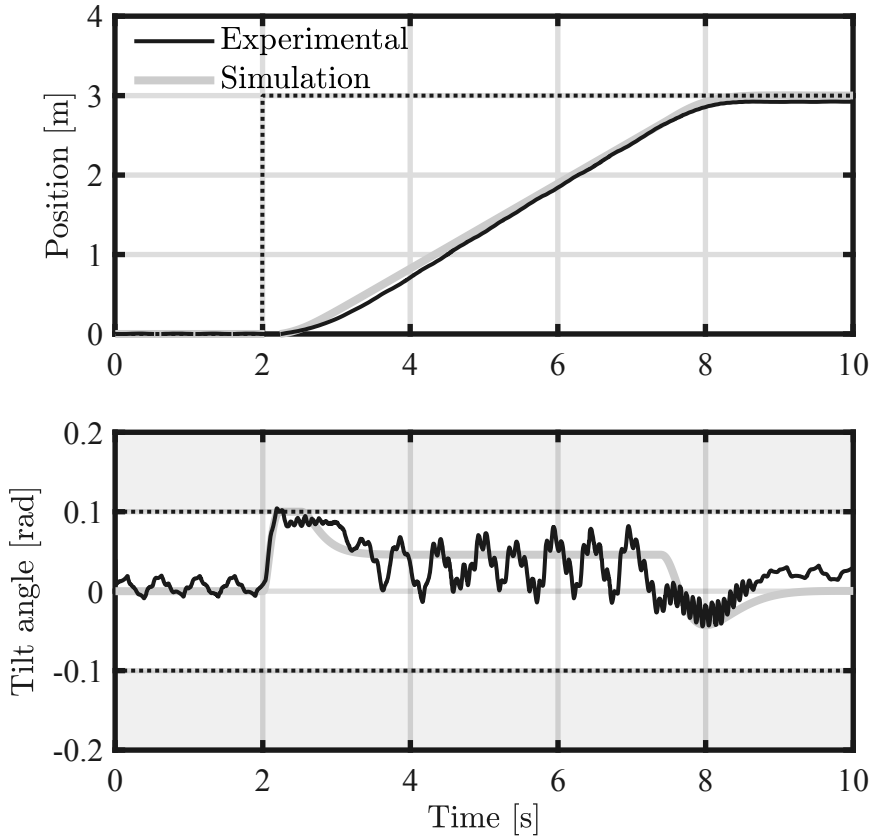

Figure 1.9: System response with proposed RG. Simulation with ideal communication and full experiment on Segway.

comparable performances in the WiFi-in-the-loop tests, we choose to put in practice the proposed RG because of the simplicity of the implementation. Indeed, the size of the optimization variable is much smaller: it is m for RG, while it is $(N+1)m+n$ for the MPC for Tracking, where m is the dimension of the input, n is the dimension of the state, and N the horizon of MPC. For the case at hand, $m=1$, $n=4$, and $N=50$. Moreover, in good channel conditions, the number of constraints is smaller with RG, since the constraints with RG coincide with the terminal constraints of MPC for Tracking. Since the optimization variable is scalar, RG does not neither need optimization algorithms (e.g. gradient descent) since the optimal point can be found with a linear search in an array with length equal to the number of constraints. Also the smart actuator is extremely simple.

In the full experimental setup, the proposed RG is implemented on a host PC, while the Segway is equipped with an Arduino microcrontroller, where the stabilizing inner loop is implemented, and a Raspberry board, used to manage the communication between the plant and the control unit. All the details are given in Appendix A.4.

In this experiment, we have to deal with both the network non-idealities and the physical system non-idealities. While the effects of the former have been already tested

in the WiFi-in-the-loop experiments, the latter were not considered yet. In fact, even if the dynamics were accurately simulated in the WiFi-in-the-loop tests, the parameters used in the control design were matched with the parameters of the simulated model. Unfortunately, in practice, the Segway prototype cannot be adequately identified due to its complicated physical structure. Moreover, the mechanical design of the robot is affected by some inaccuracies, like non-ideal mass distribution, that give oscillations. All these features make the control of the robot challenging, especially if limits on the tilt angles are required.

The obtained results are depicted in Figure 1.9. We can see that the system evolution is affected by oscillations, but constraints are satisfied, and the system quickly converges to the set point. We believe that the performances are satisfactory, provided the scarce knowledge on the plant parameters and its intrinsic mechanical limitations.

From the outcomes of the experiments, we think that the proposed solution under average channel conditions is able to achieve the same performances of classic solutions that require wired dedicated cables. From the outcomes of the WiFi-in-the-loop experiments, we believe that the proposed algorithm guarantees safety also with bad channel conditions. These results, still preliminary, indicate that to use a local simple controller to stabilize the system and a wireless controller to enforce constraints is a promising direction for advanced control applications.

1.2.3 Outline

The thesis is structured as follows. In chapter 2 we consider the problem of remote estimation with intermittent observations, showing that the distribution of the estimation error is heavy-tailed. We then address the problem of constrained control over wireless networks. In chapter 3, we propose a solution based on RG, while in chapter 4 we devise a solution based on MPC for Tracking. The problem is generalized to case with multiple actuators and sensors in chapter 5, where an algorithm based on RG is proposed. Finally, chapter 6 addresses the problem of transmission power allocation for remote estimation.

2

Heavy-Tails Everywhere

According to [81], for the scalar case, the distribution of a random variable X is heavy-tailed if and only if $\lim_{x\to+\infty} e^{\alpha x}\mathbf{P}(X > x) = +\infty$ for any $\alpha > 0$. Informally, this means that heavy-tailed distributions are those that converge to 0 more slowly than an exponential function. This also means that the probability of the tail, namely of values larger than an arbitrary large threshold, of a heavy-tailed distribution is higher than the probability of the tail of an exponential random variable, and therefore of a Gaussian random variable as well. A pictorial comparison is reported in Figure 2.1.

In the past, it has been shown that heavy-tailed distributions appear in many different domains, like in economics (e.g. the financial asset returns [82]), in computer science (e.g. the sizes of files stored on servers available on the World Wide Web [83]), as well as in many aspects of human behavior (e.g. the email activity pattern [84]). As nicely explained in [85], heavy-tails in human behavior appear because the decision on when executing a task is based on some perceived priority, so that many tasks are immediately executed while others are long delayed. In the recent work [86], it has been outlined that heavy-tails appear in feedback systems with stochastic multiplicative noise.

Heavy-tails are ubiquitous also in control over wireless networks, both on the control side and on the network side. We first show the presence of heavy-tails in wireless networks experimentally. We make use of the experimental setup described in Appendix A.3 featuring a host PC and a target board connected through a Wi-Fi network. The experiment consists of the transmission of a time-stamped packet every $T = 5$ ms. From the time-stamps of the received packets we retrieve the lengths of the communication blackouts, i.e. the periods between two following packets received with at most a delay T. The experimental probability density function of the blackouts is reported in left panel of Figure 2.2. For sake of comparison, we also report the case where packet losses are independent and identically distributed (i.i.d.) random variables with Bernoulli distribution and mean equal to the average packet loss probability occurred during the whole experiment. We can see that blackouts longer than 10 packets have a higher probability in the experimental data. To better understand if the distribution of blackouts is heavy-tailed,

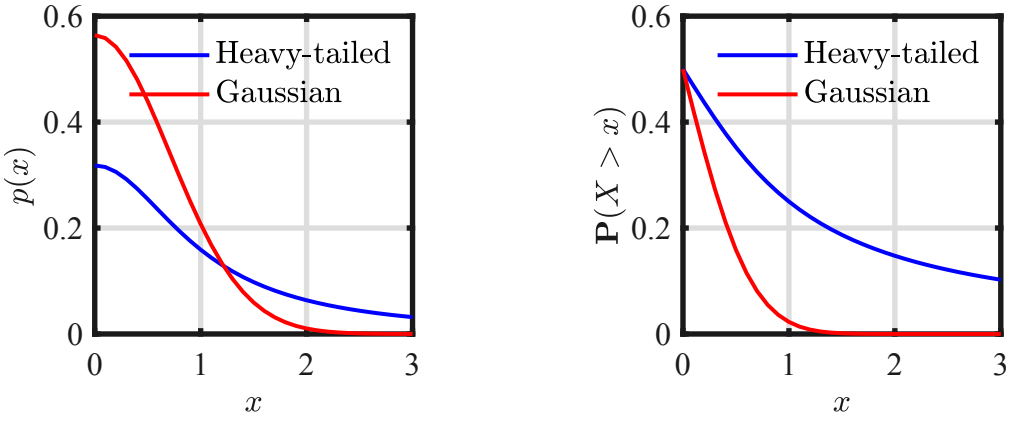

Figure 2.1: Comparison between a Gaussian distribution and a heavy-tailed distribution. Left panel: probability density function. Right panel: tail distribution.

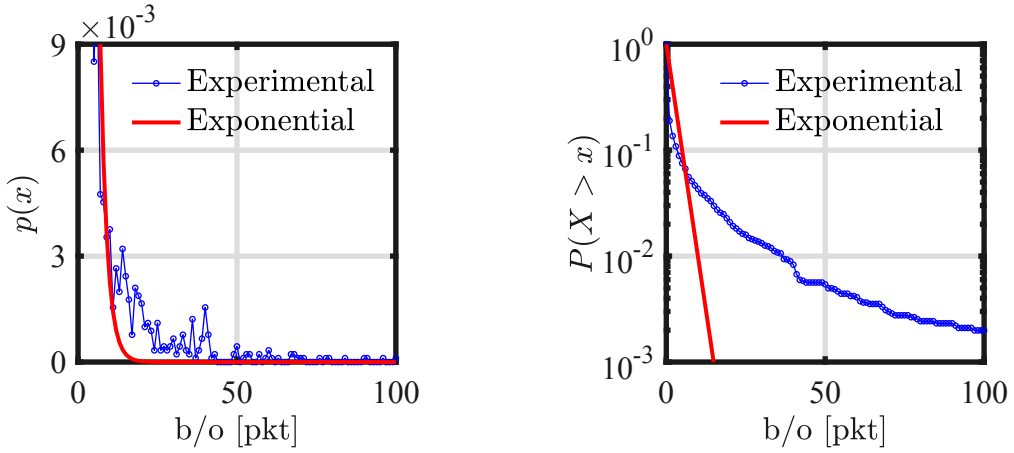

Figure 2.2: Blackouts (b/o) for an i.i.d. channel and an experimental Wi-Fi channel. Left panel: probability density function. Right panel: tail distribution. While blackout distribution is exponential with i.i.d. channel, it is heavy-tailed with Wi-Fi.

as suggested in [87], we plot the tail distribution, also referred to as complementary cumulative distribution function, with log scale. Indeed, if the distribution is exponential, the tail distribution is $\mathbf{P}(X > x) = e^{-\alpha x}$ and $\log(\mathbf{P}(X > x)) = -\alpha x$, so, in log scale, the tail distribution is a line passing through the origin. The plot is reported in right panel of Figure 2.2. We can see that, with i.i.d. packet losses, the blackouts are exponentially distributed, while the distribution of experimental blackouts results to be heavy-tailed. This has an important consequence: the well-known i.i.d. channel model, even with a conservative estimate of the loss probability, is optimistic for fast communications over fast wireless networks (Wi-Fi). We have also experimentally shown that the delay of received packets, defined as the difference between the time-stamp of the packet and the current local time-stamp, are heavy-tailed (see [24]).

In the following, we theoretically show that heavy-tailed distributions appear in the

problem of remote estimation over lossy networks. In particular, differently from works [88][89][90][42] that focus on the distribution of the error covariance of the optimal estimator, we directly focus on the distribution of the error, whose effects are immediately visible in practical implementation, and we consider a general linear estimator. We show that, if the sequence of estimation errors converges to a stationary distribution, it is heavy-tailed. Then, we obtain a sufficient condition for which the stationary distribution exists. The condition is weaker than the stability condition of the optimal estimator studied in [35][40][41][42][43]. This does not mean that the stability condition of the optimal estimator is actually conservative, but that the error does not show a threshold behavior. For this reason, increasing the packet loss probability, the estimation performances smoothly deteriorate, rather than diverging once the stability threshold is violated. Finally, we provide further insight on the problem focusing on the scalar case, for which we obtain an accurate characterization of the tail distribution.

2.1 Problem formulation

We consider a discrete-time linear system

$$x_{t+1} = Ax_t + w_t \tag{2.1}$$

$$y_t = Cx_t + v_t \tag{2.2}$$

where $x_t \in \mathbb{R}^n$ is the system state, $w_t \in \mathbb{R}^n$ is the process noise, $y_t \in \mathbb{R}^p$ is the system output, and $v_t \in \mathbb{R}^p$ is the measurement noise. We assume that process and measurement noises are independent and identically distributed random vectors with Gaussian distribution, namely $w_t \sim \mathcal{N}(0, Q)$ for $t \geq 0$, $v_t \sim \mathcal{N}(0, R)$ for $t \geq 0$, w_t is independent of w_k for $t \neq k$, v_t is independent of v_k for $t \neq k$, and w_t is independent of v_k for any $t, k \geq 0$. We also assume that the initial state x_0 is a Gaussian random variable independent of the process and measurement noise, namely $x_0 \sim \mathcal{N}(\bar{x}_0, \bar{P}_0)$ and x_0 is independent of w_t and v_t for any $t \geq 0$.

The measurements are transmitted to a remote estimator over a wireless network affected by packet loss. More formally, we introduce the arrival process $\gamma_t \in \{0, 1\}$ defined as

$$\gamma_t = \begin{cases} 1 & \text{if } y_t \text{ is available to the estimator} \\ 0 & \text{otherwise} \end{cases} \tag{2.3}$$

We assume that γ_t are independent and identically distributed random variables with Bernulli distribution and mean γ, namely $\gamma_t \sim \mathcal{B}(\gamma)$ for $t \geq 0$ and γ_t is independent of γ_k for $t \neq k$. The process mean γ is referred to as arrival rate, while $1 - \gamma$ is the packet loss probability.

Let $\hat{x}(t|t) \in \mathbb{R}^n$ denote the estimate of the state x_t. We consider a general linear

estimator expressed as

$$\hat{x}_{t+1|t+1} = A\hat{x}_{t|t} - \gamma_t K_t \left(y_t - C\hat{x}_{t|t}\right) \tag{2.4}$$

starting from a given $\hat{x}_{0|0}$, where K_t is the estimator gain, possibly time-varying. Note that this general formulation includes the well-known Kalman filter with packet losses. Let $e_t \in \mathbb{R}^n$ denote the estimation error, defined as

$$e_t = x_t - \hat{x}_{t|t}. \tag{2.5}$$

We can easily show that the error dynamics are

$$e_{t+1} = (A - \gamma_t K_t C)e_t + (w_t - \gamma_t K_t v_t) \tag{2.6}$$

Since $A - \gamma_t K_t C$ is a random matrix, the characterization of the process e_t is not trivial. In the following, we address this problem.

2.2 Larger errors, more often

Besides the intuitive definition given in the introductory paragraph, for the results of this chapter, it is convenient to use the following equivalent definition.

Definition 2.1. Let $X \in \mathbb{R}^n$ be a random vector. The distribution of X is said heavy-tailed if there exists a finite $r \in \mathbb{R}$ such that $\mathbb{E}[\|X\|^r] = +\infty$.

We are now ready to state the main theorem of this section.

Proposition 2.1. *Assume that the matrix A is strictly unstable and assume that the pair $(A, Q^{\frac{1}{2}})$ is reachable. Assume that the arrival rate is $\gamma < 1$. If the sequence e_t converges to a stationary distribution, it must be heavy-tailed.*

Proof. Using the law of total expectation, we get

$$\begin{aligned}
\mathbb{E}[\|e_{t+1}\|^r] &= \mathbb{E}[\|e_{t+1}\|^r|\gamma_t = 1]\mathbf{P}(\gamma_t = 1) + \mathbb{E}[\|e_{t+1}\|^r|\gamma_t = 0]\mathbf{P}(\gamma_t = 0) \\
&\geq \mathbb{E}[\|e_{t+1}\|^r|\gamma_t = 0]\mathbf{P}(\gamma_t = 0) \\
&= (1-\gamma)\mathbb{E}[\|Ae_t + w_t\|^r|\gamma_t = 0] \\
&\geq (1-\gamma)\mathbb{E}[\|Ae_t\|^r]
\end{aligned}$$

where the last inequality holds since e_t and w_t are independent (see [91], page 275). Iterating, we get

$$\mathbb{E}[\|e_{t+1}\|^r] \geq (1-\gamma)^t \mathbb{E}[\|A^t e_1\|^r]$$

Manipulating the norm we obtain

$$\begin{aligned}\mathbb{E}[\|e_{t+1}\|^r] &\geq (1-\gamma)^t \mathbb{E}\left[\left(e_1'(A^t)'A^t e_1\right)^{\frac{r}{2}}\right] \\ &= (1-\gamma)^t \mathbb{E}\left[\left(\text{trace}\left[e_1'(A^t)'A^t e_1\right]\right)^{\frac{r}{2}}\right] \\ &= (1-\gamma)^t \mathbb{E}\left[\left(\text{trace}\left[A^t e_1 e_1'(A^t)'\right]\right)^{\frac{r}{2}}\right] \\ &\geq (1-\gamma)^t \left(\text{trace}\left[A^t \mathbb{E}\left[e_1 e_1'\right](A^t)'\right]\right)^{\frac{r}{2}}\end{aligned}$$

where the last step follows from the Jensen's inequality, that holds for $r \geq 2$. By definition, we immediately get

$$\mathbb{E}\left[e_1 e_1'\right] \geq \mathbb{E}[w_0 w_0'] = Q$$

using the independence of w_0, v_0, x_0, γ_0 and the fact that w_0, v_0 have null expectation. Consequently

$$\mathbb{E}[\|e_{t+1}\|^r] \geq (1-\gamma)^t \left(\text{trace}\left[A^t Q (A^t)'\right]\right)^{\frac{r}{2}}$$

Since the pair $(A, Q^{\frac{1}{2}})$ is reachable, there exist a $\bar{t} \in \mathbb{Z}$ and $c > 0$ such that

$$\text{trace}\left[A^t Q (A^t)'\right] \geq c|\lambda_{\max}|^{2t}$$

for any $t \geq \bar{t}$. It follows that

$$\mathbb{E}[\|e_{t+1}\|^r] \geq (1-\gamma)^t (c|\lambda_{\max}|^{2t})^{\frac{r}{2}} = c^{\frac{r}{2}} \left((1-\gamma)|\lambda_{\max}|^r\right)^t$$

Choose now $\bar{r} = -\frac{\log(1-\gamma)}{\log|\lambda_{\max}|}$. Note that $\bar{r} > 0$ and it is finite since $\gamma < 1$. Under the assumption that $|\lambda_{\max}| > 1$ and that $\gamma < 1$, it holds that $\lim_{t\to+\infty} \left((1-\gamma)|\lambda_{\max}|^r\right)^t = +\infty$ for any $r > \max\{2, \bar{r}\}$. If the sequence e_t converges to a stationary distribution, we can conclude that it is heavy-tailed. □

This result has important practical consequences. When controlling an unstable system over unreliable links, large deviations of the estimation error are not as rare as in the case of reliable links. While, in the ideal case, violations of safety margins can be neglected thanks to the exponential decay of the Gaussian distribution of the error, safety guarantees are ruined due to the presence of heavy-tails. We clarify this claim through a toy example. Consider the scalar system with $A = 1.2$, $C = 1$, $K = A$, $Q = 1$, $R = 0$, and arrival rate equal to 0.4. In Figure 2.3, we report the error evolution for the toy system (blue line). For sake of comparison, we report a sequence of independent Gaussian random variables with variance equal to the sample variance of the error evolution obtained from the toy system (red line). This can be seen as the error evolution if it were Gaussian, as in the case with ideal channel. We can see that, in the Gaussian case, almost

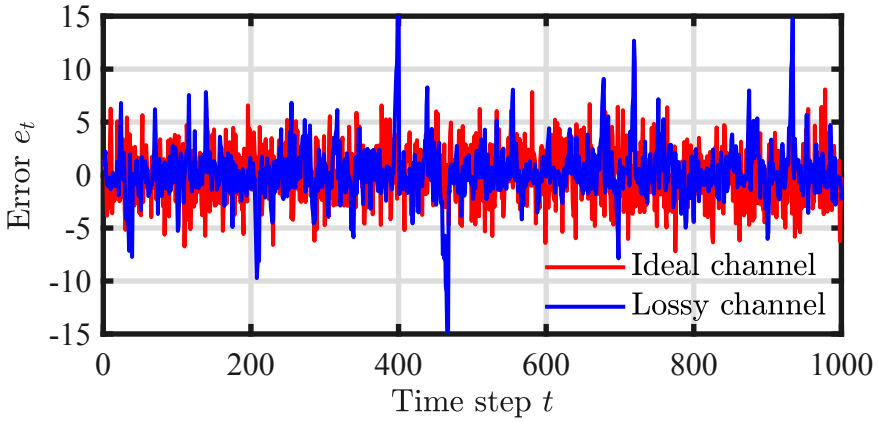

Figure 2.3: Error evolution for a toy system. Large deviations are present with lossy channels, while they are not in a comparable scenario with ideal channel.

every samples are in the set $[-5, 5]$, with only rare and small excesses. The largest value obtained over 1000 steps is equal to 7.5. The real error evolution is often smaller than the sample from the Gaussian random variable. However, the error is more often outside the set $[-5, 5]$, and also large deviations are present. The largest value obtained is around 15, and it occurs several times. The closed-loop system, even if it is stable, exhibits an unsatisfactory behavior and the large deviations may lead to critical conditions that have to be avoided in many applications.

The previous proposition theoretically motivates the widespread mistrust of control over wireless for safety-critical and industrial applications. Unfortunately, this cannot be avoided with simple (linear) control strategies and motivates the change of perspective that is proposed in this thesis.

Note that the previous proposition applies for the general class of time-varying linear estimator and therefore for the well-known Kalman filter with packet loss [35]. It follows that no linear estimation strategy can avoid the presence of heavy-tails in the error distribution. The results are also valid for more general noise and arrival process models. In fact, the proof simply requires w_t and e_t to be independent, and the covariance Q of the process noise w_t to be finite.

A critical assumption of the previous proposition is that the error sequence converges to a stationary distribution. Indeed, when the optimal time-varying estimator is considered, it is not trivial to show that a stationary distribution of the error exists. In the following section, we focus on the case of constant estimators, for which we are able to identify a sufficient condition for the existence of the stationary distribution. Based on this result, we are able to explain another important difference between stochastic systems with ideal links and with lossy links, namely the absence of a clear threshold behavior.

2.3 No threshold behavior of the error

In this section we assume that $K_t = K$ for any $t \geq 0$. It follows that the error dynamics is

$$e_{t+1} = (A - \gamma_t KC)e_t + (w_t - \gamma_t K v_t) \tag{2.7}$$

The main results of this section rely on the Renewal theory and on its application to the theory of random difference equations. We formalize the preliminary results needed for our study in the following two theorems.

Theorem 2.1 (Theorem 6 [92]). *Consider the following stochastic dynamic system*

$$E_{t+1} = F_t E_t + Z_t$$

where $E_t \in \mathbb{R}^n$, $Z_t \in \mathbb{R}^n$ are random vector and $F_t \in \mathbb{R}^{n\times n}$ is a random matrix. Assume that the pairs (F_t, Z_t), $t \geq 0$, are independent and identically distributed. Define the following quantities

$$S_t = \sum_{k=0}^{t-1} F_0 \cdots F_{k-1} Z_k, \qquad S = \sum_{k=0}^{\infty} F_0 \cdots F_{k-1} Z_k, \qquad \lambda = \lim_{k\to\infty} \frac{1}{k} \log\left(\|F_0 \cdots F_k\|\right).$$

Then, the following properties hold true:

1. *The random vector E_t has the same distribution as $S_t + F_{t-1}F_{t-2}\cdots F_0 E_0$.*
2. *If $\mathbb{E}\left(\log^+ \|F_0\|\right) < +\infty$, then λ exists with probability 1.*
3. *If $\lambda < 0$ with probability 1 and there exists $r > 0$ such that $\mathbb{E}\left(\|Z_0\|^r\right) < +\infty$, then S converges with probability 1.*
4. *If $\lambda < 0$ with probability 1, then $F_{t-1}F_{t-2}\cdots F_0 E_0$ converges to 0 with probability 1.*
5. *If $\lambda < 0$ with probability 1 and there exists $r > 0$ such that $\mathbb{E}\left(\|Z_0\|^r\right) < +\infty$, then the distribution of E_t converges to the distribution of S.*

Theorem 2.2 (Theorem 2 [93] and Lemma E.0.1 [94]). *If $\mathbb{E}\left(\log^+ \|F_0\|\right) < +\infty$, it holds that*

$$\lambda = \lim_{k\to+\infty} \frac{1}{k} \log\left(\|F_0 \cdots F_k\|\right) = \lim_{k\to+\infty} \frac{1}{k} \mathbb{E}[\log\left(\|F_0 \cdots F_k\|\right)] \leq \mathbb{E}[\log \|F_0\|] = \mu \tag{2.8}$$

and for scalar systems ($n = 1$), it holds that $\lambda = \mu$.

In the literature, λ is referred to as the Lyapunov exponent. From Theorem 2.1, it is clear that the convergence in distribution of E_t is strictly related to the sign of λ. Theorem 2.2 provides an alternative expression for λ and the useful upper-bound μ that, usually, can be explicitly computed. We can now state the main result of this section.

Proposition 2.2. *If*

$$(1-\gamma)\log(\|A\|)+\gamma\log(\|A-KC\|)<0 \tag{2.9}$$

then e_t converges in distribution to a stationary distribution.

Proof. The proof is obtained by verifying the hypotheses of Theorem 2.1 (in particular, the ones of Item 5) with $F_t = A-\gamma_t KC$ and $Z_t = w_t-\gamma_t K v_t$. It is easy to see that, under the considered model, the pairs (F_t, Z_t) are independent and identically distributed. By direct computation we have

$$\mathbb{E}\left(\log^+\|F_0\|\right) = \begin{cases} (1-\gamma)\log(\|A\|)+\gamma\log(\|A-KC\|) & \text{if } \|A-KC\|>1 \\ (1-\gamma)\log(\|A\|) & \text{otherwise.} \end{cases}$$

In both cases, $\mathbb{E}\left(\log^+\|F_0\|\right)<+\infty$, so we can use Theorem 2.2 to obtain

$$\lambda \le \mathbb{E}[\log\|F_0\|] = (1-\gamma)\log(\|A\|)+\gamma\log(\|A-KC\|)<0$$

where the last inequality follows from condition (2.9). The Lyapunov exponent is thus strictly negative. Then, what is left to prove is that there exist $r>0$ such that $\mathbb{E}\left[\|Z_0\|^r\right]<+\infty$. If we pick $r=2$ we have

$$\begin{aligned}\mathbb{E}\left[\|Z_0\|^2\right] &= \mathbb{E}\left[\operatorname{trace}\left[Z_0 Z_0'\right]\right] \\ &= \operatorname{trace}\left[\mathbb{E}\left[Z_0 Z_0'\right]\right] \\ &= \operatorname{trace}\left[\mathbb{E}[w_0 w_0' + \gamma_0^2 K v_0 v_0' K' + \gamma_0 w_0 v_0' K' + \gamma_0 K v_0 w_0']\right] \\ &= \operatorname{trace}\left[Q+\gamma K R K'\right] < +\infty\end{aligned}$$

which concludes the proof. □

Previous proposition guarantees the existence of a stationary distribution for constant estimator, thus it allows to apply Proposition 2.1 and ensures the presence of heavy-tails in the error distribution. See [95] for numerical method to find the stationary distribution.

In general, condition (2.9) is not tight since it relies on the upper-bound μ of the Lyapunov exponent. In the past fifty years, many works have addressed the derivation of lower and upper bounds for the Lyapunov exponent [96]. To date, the exact value can be explicitly computed only for special random matrices. For instance, as outlined in Theorem 2.2, μ and λ coincide for the special case of scalar systems.

The previous proposition can be used to draw some further considerations related to the stability of the estimator. In this respect, mean-square stability is the most used notion in the literature. Mathematically, the estimator is said mean-square stable if there exists a positive matrix M_0 such that the expected error covariance P_t is bounded by M_0,

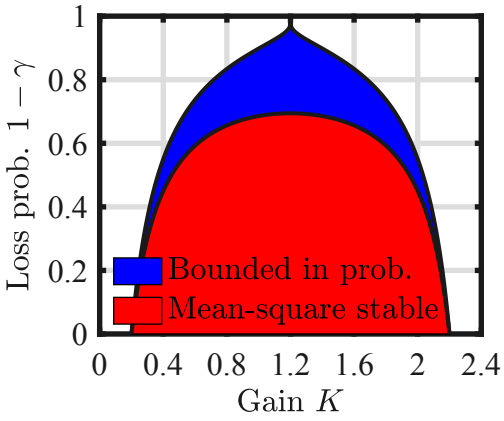

Figure 2.4: Stability regions.

that is $\mathbb{E}[P_t] < M_0$ for $t \geq 0$. For general multi-dimensional systems, with the optimal (time-varying) estimator, there exists a critical arrival rate γ_c such that the estimator is mean-square stable if and only the arrival rate γ is greater than γ_c [35]. For scalar systems, with arbitrary constant estimator, the mean-square stability condition is given by

$$(1-\gamma)A^2 + \gamma(A-KC)^2 < 1. \tag{2.10}$$

The results of this section suggest to consider the notion of bounded in probability. A sequence of random variables X_t is said bounded in probability if for any $\epsilon > 0$ there exists a N_ϵ such that $\mathbf{P}[X_t > N_\epsilon] < \epsilon$ for $t \geq 0$. Intuitively, it means that the probability of large values is uniformly bounded. It can be shown that, if e_t converges to a stationary distribution, then it is bounded in probability. It follows that the error is bounded in probability if (2.9) holds and, for scalar systems, the condition is tight since Theorem 2.2.

In general, mean-square stability is a sufficient condition for stability in probability. If the error distribution were Gaussian, then mean-square stability and stability in probability would coincide. This is the case without packet loss. However, in the problem at hand, the stationary distribution of the error is heavy-tailed and therefore not Gaussian. It follows that, when the estimator is mean-square stable, the error is bounded in probability, while there may be cases where the error is bounded in probability but the estimator is not mean-square stable. This happens, for example, for scalar systems, for which condition (2.10) is more stringent than condition (2.9). A pictorial representation for the toy system introduced above (but arbitrary K) is reported in Figure 2.4. It can be seen that mean-square stability guarantees that the sequence e_t is bounded in probability. In the case without measurement noise, with the optimal constant estimator satisfying $CK = A$, we have that the estimator is mean-square stable if and only if $\gamma > \gamma_c = 1 - 1/|\lambda_{\max}|^2 = 1 - 1/A^2$, while the error is bounded in probability if and only if $\gamma > 0$.

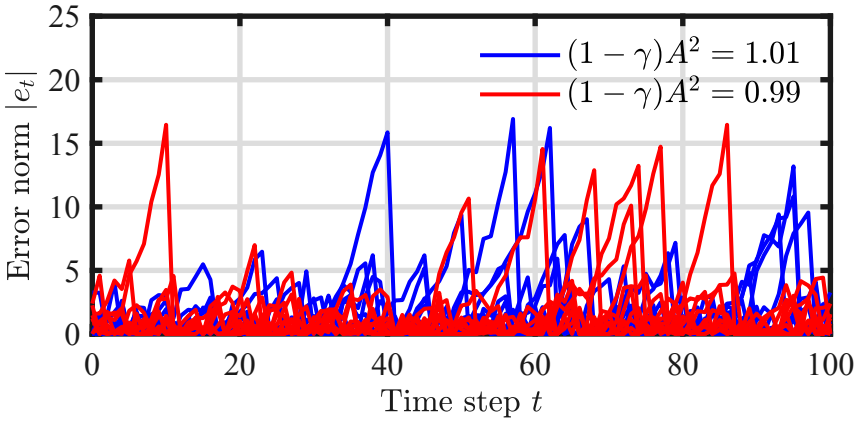

Figure 2.5: Error norm evolutions for a toy system. A violation of the threshold for mean-square stability does not result in a qualitative difference in the error norm.

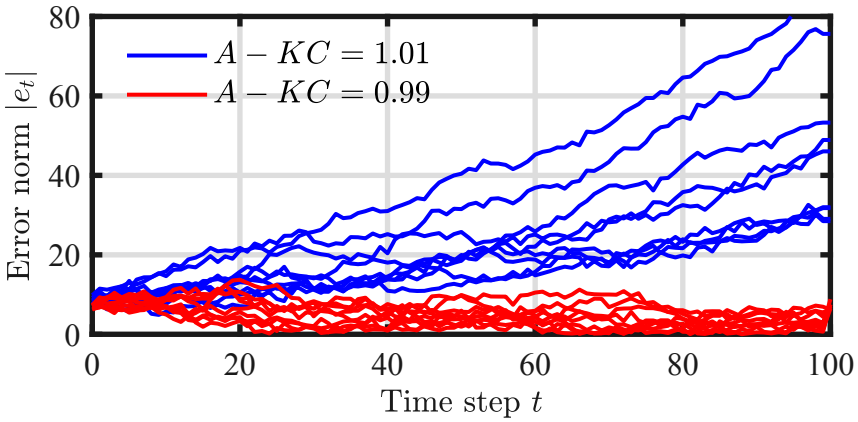

Figure 2.6: Error norm evolutions for a toy system. A violation of the threshold for mean-square stability in the case of ideal channel results in a drastically different evolution.

Differently from the case without packet loss, we see that the two notions of stability are not coincident. In past years, a large attention has been given to the study of the threshold γ_c, since it distinguishes bounded and divergent evolutions of the error covariance. However, even if the error covariance is unbounded, since the distribution is not Gaussian, the error may be bounded in probability. We explore the implications through the toy example introduced above. We set the loss probability $1-\gamma$ equal to 0.99 times and 1.01 times the critical loss probability $1/A^2$. In this way, in the first case, the estimator is mean-square stable, while, in the second, the expected error covariance diverges. In Figure 2.5 we report 10 evolutions of the error norm $|e_t|$ for both the cases. We can see that no qualitative differences are present. For sake of comparison, we report the evolution for the same toy example with ideal channel. Also in this case, we consider a mean-square stable estimator, whose gain K is chosen to satisfy $(A - KC) = 0.99$, and

an unstable one, with K such that $(A-KC) = 1.01$. In this case, the threshold behavior is evident. From these results, we expect that, increasing the packet loss probability, the estimation performances smoothly deteriorate, rather than diverging once the stability threshold is violated. We conclude that the notion of mean-square stability may be misleading in the case of control over wireless.

2.4 Analytical characterization: power-law distribution

For sake of completeness, in this section we provide additional details on the stationary distribution of the error for scalar systems with constant estimator. In particular, we show that, under mild assumptions, the stationary distribution asymptotically decays as a power law and we characterize the decay rate.

We say that a random variable is non-arithmetic if its support is not a set of form $r\mathbb{Z}$, for an arbitrary $r \in \mathbb{R}$. Roughly speaking, it means that the support is not included in the set of the multipliers of r. Now we can recall the results from the Renewal theory needed for our study.

Theorem 2.3 (Theorem 2.3 [97] and Theorem 2.2.4 [94])**.** *Let F and Z be two random variables. Assume (i) $\{F \geq 0\}$ with probability 1, (ii) $\log(F)$ conditioned on $F > 0$ is non-arithmetic, (iii) there exists $\alpha > 0$ such that $\mathbb{E}[|F|^\alpha] = 1$, $\mathbb{E}[|Z|^\alpha] < +\infty$, and $\mathbb{E}[|F|^\alpha \log^+(F)] < +\infty$, (iv) $\mathbf{P}(Fx + Z = x) < 1$ for all $x \in \mathbb{R}$. Then there exists a random variable E that satisfies $E = FE + Z$ in distribution, and E is independent of F and Z. Moreover it holds that*

$$\lim_{x \to +\infty} x^\alpha \mathbf{P}(E > \quad x) = c_+ \tag{2.11}$$

$$\lim_{x \to +\infty} x^\alpha \mathbf{P}(E < -x) = c_- \tag{2.12}$$

where c_+ and c_- are strictly positive constants.

The first result of the previous theorem is that a stationary distribution exists. Indeed, under assumptions (i)-(iii), it can be shown that $\mathbb{E}[\log^+(F)] < +\infty$ and that $\mathbb{E}[\log(F)] < 0$, so the existence of a stationary distribution is implied by Theorem 2.1. The novelty of the theorem is the characterization of the limit behavior of the distribution of E for large values in the support. Roughly speaking, the theorem states that the distribution $\mathbf{P}(E > x)$ asymptotically converges to 0 as $c_+ x^{-\alpha}$, namely the tail probability follows a suitable power law. Since c_+ and c_- are strictly positive, the cases where the limit is zero is excluded. This excludes that $\mathbf{P}(E > x)$ converges faster than $x^{-\alpha}$. Expressions to compute the positive constants c_+ and c_- can be found in [97] and [94]. Since they are quite involved, they are omitted here.

We now apply the previous theorem for the case at hand.

Proposition 2.3. *Consider a scalar unstable system with $A > 1$. Assume that $A - KC > 0$ and $A - KC < 1$. Assume that $\log(A)/\log(A - KC) \notin \mathbb{Z}$. Assume that*

$$(1 - \gamma)\log(A) + \gamma \log(A - KC) < 0 \tag{2.13}$$

Then, there exist an unique $\alpha > 0$ and $c > 0$ such that

$$\lim_{x \to +\infty} x^{\alpha} \mathbf{P}(|E| > x) = c \tag{2.14}$$

and α satisfies

$$(1 - \gamma)A^{\alpha} + \gamma(A - KC)^{\alpha} = 1 \tag{2.15}$$

Proof. The proof is obtained by verifying the hypotheses of Theorem 2.3 with $F = A - \gamma_t KC$ and $Z = w_t - \gamma_t K v_t$ for an arbitrary t. Since $F = A > 0$ with probability $1 - \gamma$ and $F = A - KC > 0$ with probability γ, Assumption (i) holds. Since all the elements of the support of F are strictly positive, the support of $\log(F)$ conditioned on $F > 0$ is equal to the support of $\log(F)$. Then, Assumption (ii) follows from the fact that $\log(A)/\log(A - KC) \notin \mathbb{Z}$. Denote $f(\alpha) = (1 - \gamma)A^{\alpha} + \gamma(A - KC)^{\alpha}$. We take the derivative and we obtain

$$f'(\alpha) = (1 - \gamma)\log(A)A^{\alpha} + \gamma \log(A - KC)(A - KC)^{\alpha}$$

With simple manipulations, we can find that $f'(\alpha) > 0$ if and only if $\alpha > \bar{\alpha}$ with

$$\bar{\alpha} = \frac{\log\left(-\frac{\gamma \log(A-KC)}{(1-\gamma)\log(A)}\right)}{\log\left(\frac{A}{A-KC}\right)}$$

We can conclude that $f(\alpha)$ is convex. It follows that, since $f(0) = 1$, there exists a (unique) $\alpha > 0$ such that $f(\alpha) = 1$, thus satisfying (2.15), if and only if $\bar{\alpha} > 0$. Since $A > A - KC$, $\bar{\alpha} > 0$ if and only if the argument of the logarithm at numerator in the equation above is strictly greater than 1. This is verified under the condition (2.13). For such an α, $\mathbb{E}[|F|^{\alpha}] = 1$, $\mathbb{E}[|Z|^{\alpha}] = \mathbb{E}[|w_t + \gamma_t K v_t|^{\alpha}] = (1-\gamma)\mathbb{E}[|w_t|^{\alpha}] + \gamma \mathbb{E}[|w_t + K v_t|^{\alpha}] < +\infty$ since Gaussian random variable have finite moments, and $\mathbb{E}[|F|^{\alpha} \log^{+}(F)] = \gamma |A|^{\alpha} \log(A) < +\infty$. This proves that Assumption (iii) holds. Assumption (iv) trivially holds because the distribution of Z is continuous, while the distribution of F is discrete with finite support. We can now apply Theorem 2.3, concluding the proof. □

For the scalar case with constant estimator, under some additional technical assumptions, the previous proposition shows that the distribution of the error is not only heavy-tailed, namely $\lim_{x \to +\infty} e^{\alpha x} \mathbf{P}(X > x) = +\infty$, but is fat-tailed, namely it satisfies $\lim_{x \to +\infty} x^{\alpha} \mathbf{P}(X > x) = c$. We can conclude that the probability of the tails is even larger than what ensured by Proposition 2.1.

The previous proposition provides also the expression of the decay rate α. In particular, the smaller the arrival rate γ is, the smaller $\bar{\alpha}$ is, and the smaller α is. Similarly, the greater A is, the smaller α is.

Interestingly, the previous proposition cannot be applied in the case without measurement noise and with the optimal (constant) estimator. In fact, in that case, $K = A/C$ and the support of F is $\{A, 0\}$, so the support of $\log(F)$ conditioned on $\{F > 0\}$ is not arithmetic. In that case, other arguments from Renewal theory can be used to show that the stationary distribution of the error asymptotically follows a power law.

2.5 Conclusion

In this section, we have presented further advances in the understanding of the estimation problem with intermittent observations. In particular, we have shown that the error distribution is heavy-tailed, we have outlined the differences between the mean-square stability and boundedness in probability, and we have analytically characterized the distribution in the case of scalar systems. The results of this chapter have an important practical consequence: since both the distribution of the estimation error with Bernoulli packet losses and the distribution of blackouts in Wi-Fi networks are heavy-tailed, large deviations of the system trajectory are likely to occur even if the system is mean-square stable. To deal with this problem, we need to move from the concept of stability to a new concept of safety, more suitable for practical applications.

3

Reference Governor over Wireless

Outside research laboratories, where technological solutions are used on the field, an unexpected behavior or a failure of the control system may lead to dangerous or even catastrophic events. When point-to-point dedicated connections or wired networks are used, high safety levels are usually guaranteed with a suitable control design. However, when wireless networks are used to close the feedback loop, safety guarantees are dramatically jeopardized due to packet loss. To investigate this problem, we first need to more properly define the concept of safety.

In general, safety is strongly related to mean-square stability. A system is said mean-square stable if the (expected) state covariance is bounded. Similarly, the estimator is said mean-square stable if the (expected) estimation error covariance is bounded. Unfortunately, even with ideal communications, the boundedness of the state covariance does not exclude large transient deviations from the expected trajectory. This behavior is drastically emphasized with packet losses if the open-loop system is unstable. For instance, it is known from the literature that the error covariance (and the probability of large error) grows when a packet loss occurs. Moreover, as we have shown in the previous chapter, the distribution of the estimation error is heavy-tailed so, even if the error covariance is not large, large errors occur more often than in the Gaussian case. For these reasons, mean-square stability is not sufficient to guarantee safety and a new definition needs to be introduced.

Consider now some illustrative examples. First, consider the imminent large-scale deployment of self-driving cars. This application will require each vehicle to communicate with the others in order to safely share the road and to manage crossroads and turns. In this case, a dangerous crush can happen if a car crosses the road center line or passes too close to another car. We can see that crashes can be avoided if certain limitations in terms of position and speed are satisfied. A similar reasoning can be done for platooning of vehicles. A second example is the use of robots in the industrial scenario. Think of a set of robotic arms that collaborate to assemble an object. In this case, a damage to the object may be caused by undesired oscillations of an arm or uncoordinated movements. Again,

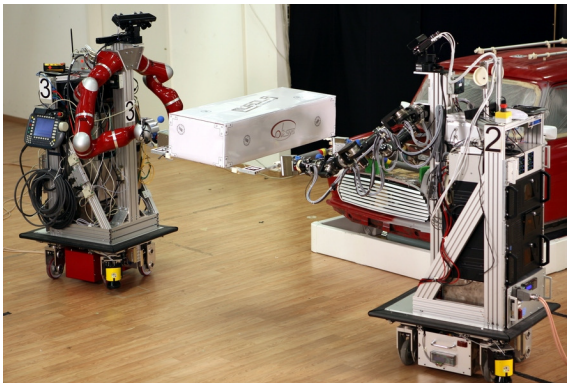

Figure 3.1: Typical task in multi-agent systems. Two dual-arm mobile robots collaborate to transport a load. Limits on their positions have to be satisfied to avoid obstacles and harms to the object. Courtesy of [98].

harms can be avoided if suitable constraints are satisfied. The same is valid for mobile robots that transport an object. In the latter case, also collisions with obstacles or humans can be expressed through limits on the system state. A typical example is depicted in Figure 3.1. Finally, consider the Segway-like robot introduced in Appendix A.2 and assume that we want to move it forward by a certain distance. Even if this is a simple single-agent system and the task is a simple constant set-point tracking, we need to avoid the tilt angle to be larger than a limit value, above which the robot will fall. This example is particularly interesting from the technical point of view because, on one hand, we want to increase the tilt angle to increase the speed of the robot and, on the other, we want to keep it below the critical value.

These examples suggest a strong connection between safety and satisfaction of suitable constraints. In the following we say that safety is ensured if constraints are satisfied. Our objective is to design a control algorithm that ensures safety in presence of packet loss.

As we have shown in section 1.1.1, in the case of fast communications relying on fast networks like Wi-Fi or 5G, blackouts are not excluded. Unfortunately, during blackouts, the feedback loop is interrupted and the system evolves in open-loop. If the open-loop system is unstable, the state diverges and constraints are violated. For this reason, in this chapter, we require that the open-loop system is stable.

For the case with ideal communications, several constrained control algorithms have been studied in the literature. In particular, Model Predictive Control (MPC) is one of the most used solutions. However, the problem of reference tracking under constraints with stable systems can be solved efficiently with Reference Governor (RG). A RG is an add-on scheme that enforces constraints on a stable system by modifying the reference input whenever necessary [79]. More specifically, the reference input is changed if the predicted trajectory under the unchanged reference will lead to a constraint violation. Similarly to MPC, at each instant, RG updates the input by solving a constrained optimization problem. However, the horizon during which the predicted trajectory must satisfy the

constraints is infinite, the input is kept constant over the horizon, and the cost function is independent of the state but depends only on the distance to the desired reference. Traditionally, RG is appealing for its low computational complexity compared to MPC. In the simplest formulation, it can be solved by finding the minimum element of a vector obtained through simple matrix multiplications and so it can be implemented also on some on-board embedded systems. RG is particularly attractive also for NCSs, because, once a reference is applied, it can be kept constant for an arbitrarily long period without violating the constraints. This means that the resulting scheme is naturally robust against infinitely long blackouts.

To date, some works have studied RG with non-ideal communications. The case of bounded delays has been considered e.g. by [99][100][101], where the reference input is designed to be robust whatever delay will occur. Conversely, the case of possibly random and possibly unbounded delays has been addressed in the works [102][103]. In these works, the main idea is to admit a fixed period between the computation instant of the reference input and its application so that it can be delivered before the instant when it is needed with a high probability. A recovery procedure is introduced to address the case where the reference input is not available. An alternative idea, proposed in [102][103], is to compute an input that is robust with respect to all the possible sequences of inputs applied at the plant. This allows to update the applied input as soon as possible and to satisfy the constraints for an arbitrarily long blackout without any recovery procedure. In this chapter, we follow a similar idea.

First, we consider two simple strategies to be implemented at the plant side: a zero-order hold, which keeps the current value until a new packet arrives, and a discrete integrator, which adds the new arrived value to the previous output. Then, we design two RG schemes to work in combination with the two strategies at the plant side: the Reference Reset, to be used in combination with the zero-order hold, and the Additive Update, to be used with the discrete integrator. Following the idea of [102][103], to overcome the uncertainty on the system state due to the lossy communications, we impose that the new quantity provided by the RG is admissible for any possible applied input trajectory. We prove that theoretical properties as recursive feasibility and convergence, usually achieved by standard RG, are guaranteed. Interestingly, through accurate simulations we show that none of the two strategies is optimal and which is better may depend on the specific system and on the constraints. Moreover, we provide an accurate validation of the scheme in a wireless-in-the-loop setup where communication data are obtained from experiments with a real Wi-Fi network and we show the benefits of the proposed strategy compared to other solutions based on RG and on MPC. Finally, the proposed algorithm has been implemented on a real system, the Segway-like robot introduced in Appendix A.2. The experimental results indicate that the proposed RG is a suitable solution for constrained control over wireless.

3.1 Problem formulation

We consider a discrete-time linear system

$$x_{t+1} = Ax_t + Bu_t + w_t \tag{3.1}$$

where $x_t \in \mathbb{R}^n$ is the state, $u_t \in \mathbb{R}^m$ is the applied input, $w_t \in W \subset \mathbb{R}^n$ is an unknown disturbance, with W compact and containing the null vector. We assume that all the eigenvalues of the matrix A are strictly inside the unitary circle, corresponding to the case where the system is stable, possibly thanks to an inner control loop. The system has to fulfill the set of constraints

$$H(Cx_t + Du_t) \leq h \quad \forall t \geq 0 \tag{3.2}$$

with $C \in \mathbb{R}^{p\times n}$, $D \in \mathbb{R}^{p\times m}$, $H \in \mathbb{R}^{q\times p}$, and $h \in \mathbb{R}^q$. For instance, matrices C, D, H, and h can be set in order to avoid the system trajectory to enter dangerous regions of the state space, like obstacle positions for a mobile robot. The constraints can be conveniently reformulated through the set Y defined as

$$Y = \{y : Hy \leq h\}. \tag{3.3}$$

Then, constraints (3.2) are equivalent to

$$Cx_t + Du_t \in Y \quad \forall t \geq 0 \tag{3.4}$$

The objective is to design the input u_t in order to track a prescribed desired reference r_t and so that the system always satisfies the constraints. According to the application, the desired reference is provided by a higher trajectory planner or by a user request. The simplest example is $r_t = r$ so that $(I-A)^{-1}Br$ is a desired target state.

To solve this problem we introduce a control unit that, at each time step, computes an input v_t based on the estimate of the state x_t and on the desired reference r_t. We assume that the plant and the control unit are connected through a wireless network introducing delays and packet losses in the loop, see Figure 3.2. It follows that the applied input u_t can not be readily manipulated and the control unit has not direct access to the state x_t of the plant. More specifically, we assume that, at time instant t, the plant transmits a packet containing the pair (x_t, u_t) and we introduce the arrival process $\gamma_t \in \{0, 1\}$ defined as

$$\gamma_t = \begin{cases} 1 & \text{if } (x_t, u_t) \text{ is available to the control unit to compute } v_{t+1} \\ 0 & \text{otherwise} \end{cases} \tag{3.5}$$

At the same way, we assume that, during the period between time instant $t-1$ and time

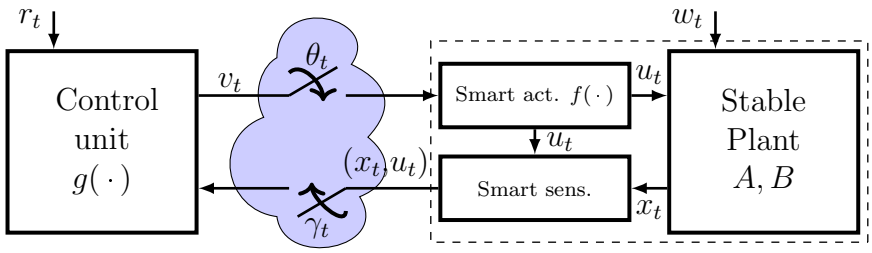

Figure 3.2: Setup. In this chapter, the remote control unit is based on Reference Governor and the plant is pre-stabilized.

instant t, just after the computation, the control unit transmits the computed input v_t and we introduce the arrival process $\theta_t \in \{0, 1\}$ defined as

$$\theta_t = \begin{cases} 1 & \text{if } v_t \text{ is available to the smart actuator at time } t \\ 0 & \text{otherwise.} \end{cases} \tag{3.6}$$

Arrival processes take into account both random delays and packet losses. In particular, delays are treated as losses if the corresponding packet is not available when required. In order to let the network be as general as possible, at this stage, no assumptions are made on the distribution of γ_t and θ_t.

We define the information available to the control unit when computing v_t as

$$\mathcal{I}_t^{\mathrm{C}} = \{v_0, \dots, v_{t-1}, \gamma_0 u_0, \dots, \gamma_{t-1} u_{t-1}, \gamma_0 x_0, \dots, \gamma_{t-1} x_{t-1}\} \tag{3.7}$$

where, with a little abuse of notation, if $\gamma_k = 0$ then $\gamma_k x_k = \emptyset$. Similarly, we define the information available to the plant when applying u_t as

$$\mathcal{I}_t^{\mathrm{P}} = \{\theta_0 v_0, \dots, \theta_t v_t, u_0, \dots, u_{t-1}\} \tag{3.8}$$

Then, we are interested in the problem of designing the laws $f(\cdot)$ and $g(\cdot)$

$$u_t = f(\mathcal{I}_t^{\mathrm{P}}) \qquad v_t = g(\mathcal{I}_t^{\mathrm{C}}) \tag{3.9}$$

such that constraints (3.2) are satisfied and the input u_t tracks the desired reference r_t.

In order to solve this problem, in this chapter, we adapt the standard RG scheme to the considered setup. Before providing the proposed solution, in order to introduce the basic concepts of RG, we outline the solution with ideal channels. Before proceeding, we need to introduce some notation. Given two sets $X, Y \subset \mathbb{R}^n$, the Minkowsky Set Sum is defined as $X \oplus Y = \{x + y : x \in X,\ y \in Y\}$, while the Minkowsky Set Difference is defined as $X \sim Y = \{x : x - y \in X,\ \forall y \in Y\}$. Further details are given in Appendix A.1.

3.2 Background: ideal channel

Note that, with ideal channel, it is always possible to choose $u_t = v_t$. So, the problem boils down to the design of $g(\,\cdot\,)$.

First, we recall the Maximal Output Admissible Set studied in [104]. Preliminarily, we define

$$\hat{x}(k|x,u) = A^k x + \sum_{\ell=0}^{k-1} A^{k-\ell-1} B u \tag{3.10}$$

$$F_k = C \bigoplus_{\ell=0}^{k} A^\ell W. \tag{3.11}$$

We can see that $\hat{x}(k|x,u)$ is the nominal prediction k steps ahead of the system state starting from initial condition x and under constant input u. The set F_k is the reachable set in k steps starting from the origin for a (disturbance) input belonging to W. Roughly speaking, F_k represents the set of the possible effects of a sequence of disturbances with length k on the system state. Then, the Maximal Output Admissible Set (MOAS) is defined as

$$O_\infty = \{(x,u) : C\hat{x}(k|x,u) + Du \in Y \sim F_k \ \forall k \geq 0\}. \tag{3.12}$$

For a fixed x, O_∞ represents the largest set of constant inputs u which guarantee that the system evolution starting from x will always satisfy the constraints for any possible sequence of disturbances.

In general, O_∞ consists of infinitely many inequalities, and thus it may be intractable for practical applications. Interestingly, this problem can be avoided using an inner approximation of O_∞ that can be made arbitrarily close to it. Introduce

$$O_\epsilon = \{(x,u) : C(I-A)^{-1}Bu + Du \in (1-\epsilon)(Y \sim F_\infty)\} \tag{3.13}$$

with an arbitrary $\epsilon \in (0,1)$ and $F_\infty = \lim_{k\to+\infty} F_k$. The limit exists and is bounded since A is stable and W is compact containing the origin. Now introduce

$$\tilde{O}_\infty = O_\infty \cap O_\epsilon. \tag{3.14}$$

The set $\tilde{O}_\infty$ is the set of pairs (x,u) for which the evolution of the system starting from x with input u is always admissible and such that the steady state satisfies the constraints with a small margin ϵ. Under very mild technical assumptions, it can be shown that $\tilde{O}_\infty$ consists of a finite number of inequalities [104]. Moreover, there exists an iterative procedure to obtain $\tilde{O}_\infty$ in a finite number of steps. An exhausting description of $\tilde{O}_\infty$ can be obtained from [105] for the case without disturbances and from [106] for the case with disturbances.

Based on $\tilde{O}_\infty$, the Reference Governor can be expressed in general as

$$v_t = \arg\min_v \mathcal{C}(r_t, u_{t-1}, v) \tag{3.15}$$

$$\text{s.t. } (Ax_{t-1} + Bu_{t-1}, v) \in \tilde{O}_\infty \tag{3.16}$$

where $\mathcal{C}(r_t, u_{t-1}, v)$ is a suitable cost function. A typical choice is $\mathcal{C}(r_t, u_{t-1}, v) = \|r_t - v\|_Q^2$ with $Q \geq 0$, and the resulting algorithm is called Command Governor [107]. To reduce the computational burden, it is common to restrict v to be $v = \alpha r_t + (1-\alpha)u_{t-1}$ with $\alpha \in [0, 1]$. In this case, the resulting algorithm is properly referred to as Reference Governor [108][104]. More elaborated choices are also possible, see e.g. [109] and [110].

Reference and Command Governors have several important theoretical properties. First, under the assumption that the optimization problem is feasible at time instant $t = 0$, the optimization problem is feasible for any $t > 0$ thanks to the particular definition of $\tilde{O}_\infty$. Second, by construction, the system evolution satisfies the constraints for any $t \geq 0$. Third, it can be shown that, if r_t is constant, u_t converges to the closest admissible input in finite time. For the proofs see e.g. [104].

3.3 Maximal Output Admissible Set with Packet Loss

In order to extend RG for the case with lossy channels, we introduce the Maximal Output Admissible Set with Packet Loss defined as

$$O_\infty(i) = \{(x, u) : C\hat{x}(k|x, u) + Du \in Y \sim F_{k+i} \ \forall k \geq 0\}. \tag{3.17}$$

Differently from the case with ideal channel, the Maximal Output Admissible Set with Packet Loss depends on $i \in \mathbb{N}$. More specifically, the predicted nominal trajectory $C\hat{x}(k|x, u) + Du$ is required to belong to the more tightened set $Y \sim F_{k+i}$ instead of $Y \sim F_k$. In this way, we can take into account the larger uncertainty (at the control unit) on the current state due to the past disturbances when the last i packets (transmitted from the plant) have been lost. We can see that $O_\infty(0) = O_\infty$ and, if $W = \{0\}$, $O_\infty(i) = O_\infty$ for any $i \geq 0$.

As done in the case of ideal channel, we consider a tightened version of $O_\infty(i)$ obtained by imposing the steady state to satisfy the constraints with a small margin $\epsilon > 0$. We obtain

$$\tilde{O}_\infty(i) = O_\infty(i) \cap O_\epsilon \tag{3.18}$$

where O_ϵ is defined in (3.13).

Preliminarily, we introduce the set

$$O_t(i) = \{(x, u) : C\hat{x}(k|x, u) + Du \in Y \sim F_{k+i} \ k \leq t\}. \tag{3.19}$$

We now provide the main properties of $\tilde{O}_\infty(i)$.

Theorem 3.1. *Assume that A is asymptotically stable and (A, C) is observable. Assume that Y and W are compact sets containing the origin. Then, the following properties hold for $i \geq 0$*

1. $\tilde{O}_\infty(i+1) \subseteq \tilde{O}_\infty(i)$.
2. $\tilde{O}_\infty(i)$ *is compact if* $C(I-A)^{-1}B + D$ *has rank* m.
3. $\tilde{O}_\infty(i)$ *is convex if* Y *is convex.*
4. $\tilde{O}_\infty(i)$ *is symmetric if* Y *and* W *are symmetric.*
5. $\tilde{O}_\infty(i)$ *is not-empty if* $Y \sim F_\infty$ *contains the origin.*
6. $\tilde{O}_\infty(i)$ *is finitely determined, namely there exists a* t_i *such that* $\tilde{O}_\infty(i) = O_t(i) \cap O_\epsilon$ *for* $t \geq t_i$. *Moreover* $t_{i+1} \leq t_i$.
7. $\tilde{O}_\infty(i)$ *is positively invariant, namely if* $(x, u) \in \tilde{O}_\infty(i)$ *then* $(Ax + Bu, u) \in \tilde{O}_\infty(i)$ *and* $(Ax + Bu, u) \in \tilde{O}_\infty(i+1)$.

Proof. Point 1 follows from $F_{k+i} \subseteq F_{k+i+1}$ that holds since W is compact containing the origin. Point 2 follows from the compactness of $\tilde{O}_\infty(0)$ [104]. For sake of completeness, we report the complete proof following Theorem 5.1 from [106]. Denote $Y_k = Y \sim F_k$. Consider the extended system

$$\bar{A} = \begin{bmatrix} A & B \\ 0 & I_m \end{bmatrix} \qquad \bar{C} = \begin{bmatrix} C & D \end{bmatrix}$$

Let $\mathcal{H} = (\bar{C}', (\bar{C}\bar{A})', (\bar{C}\bar{A}^2)', \cdots, (\bar{C}\bar{A}^{n+m-1})')'$. If $\mathcal{H}$ is full-rank, $\mathcal{H}^\dagger = (\mathcal{H}'\mathcal{H})^{-1}\mathcal{H}'$ exists and $O_{n+m-1}(i) = \mathcal{H}^\dagger(Y_i \times Y_{i+1} \times \cdots \times Y_{i+n+m-1})$. Since Y is compact, also $O_{n+m-1}(i)$ is compact. Since $\tilde{O}_\infty(i) \subseteq O_{n+m-1}(i)$, $\tilde{O}_\infty(i)$ is compact. So we have to show that $\mathcal{H}$ is full-rank. It is known that $\mathcal{H}$ is full-rank if and only if $(\bar{A}, \bar{C})$ is observable. Using a suitable change of coordinate T we can obtain the equivalent pair $(\bar{\bar{A}}, \bar{\bar{C}})$ where

$$T = \begin{bmatrix} I_n & (I_n - A)^{-1}B \\ 0 & I_m \end{bmatrix} \quad \bar{\bar{A}} = \begin{bmatrix} A & 0 \\ 0 & I_m \end{bmatrix} \quad \bar{\bar{C}} = \begin{bmatrix} C & D + C(I_n - A)^{-1}B \end{bmatrix}$$

Using the PBH criterion of observability, we can show that $(\bar{\bar{A}}, \bar{\bar{C}})$ is observable if (A, C) is observable and $D + C(I_n - A)^{-1}B$ has rank m. This proves Point 2.

If Y is convex, F_k is convex due to basic properties of the Minkowski set difference, see Appendix A.1 (note that no assumptions on W are needed). Expressing the constraints in $O_\infty(i)$ as $\bar{C}\bar{A}^k(x', u')' \in Y \sim F_{k+i}$, we can conclude that $O_\infty(i)$ is convex. Similarly,

it is possible to prove that O_ϵ is convex. We can conclude that $\tilde{O}_\infty(i)$ is convex, proving Point 3.

If W is symmetric, $A^k W$ is symmetric. It follows that, due to basic properties of the Minkowski set sum, F_k is symmetric. If also Y is symmetric, due to basic properties of the Minkowski set difference, Y_k is symmetric. With the same reasoning of the previous Point, we can conclude that $\tilde{O}_\infty(i)$ is symmetric, proving Point 4.

If $Y \sim F_\infty$ contains the origin both $(1-\epsilon)(Y \sim F_\infty)$ and $Y \sim F_k$ contain the origin. It follows that $\tilde{O}_\infty(i)$ contains at least the origin.

To prove Point 6 we start from the case with $i = 0$, for which we can follow [104]. We start considering the case where $(\bar{\bar{A}}, \bar{\bar{C}})$ is observable and Y is compact, so that $O_{n+m-1}(0)$ is compact. We have that

$$\bar{\bar{C}}\bar{\bar{A}}^t = \begin{bmatrix} CA^t & D + C(I-A)^{-1}B \end{bmatrix} \to \begin{bmatrix} 0 & D + C(I-A)^{-1}B \end{bmatrix} \text{ for } t \to +\infty.$$

Denote $\tilde{O}_t(i) = O_t(i) \cap O_\epsilon$. By construction, for $(x, u) \in \tilde{O}_t(0)$ we have

$$\begin{bmatrix} 0 & D + C(I-A)^{-1}B \end{bmatrix} \begin{bmatrix} x \\ u \end{bmatrix} \in (1-\epsilon)(Y \sim F_\infty).$$

Plugging these two conditions together we get

$$\bar{\bar{C}}\bar{\bar{A}}^{t+1}\tilde{O}_{n+m-1}(0) \to (1-\epsilon)(Y \sim F_\infty) \text{ for } t \to +\infty.$$

Note that this holds only if (x, u) is finite, so it requires $\tilde{O}_{n+m-1}(0)$ to be compact. If $0 \in \text{int}(Y \sim F_\infty)$, then $(1-\epsilon)(Y \sim F_\infty) \subset Y \sim F_\infty$. It follows that

$$\bar{\bar{C}}\bar{\bar{A}}^{t+1}\tilde{O}_{n+m-1}(0) \subseteq Y \sim F_\infty \subseteq Y \sim F_{t+1}$$

for some large t. Let t_0 be the smallest t for which the previous inequality holds. If $t_0 > n + m - 1$, we have that $\tilde{O}_{t_0}(0) \subseteq \tilde{O}_{n+m-1}(0)$ and thus

$$\bar{\bar{C}}\bar{\bar{A}}^{t_0+1}\tilde{O}_{t_0}(0) \subseteq \bar{\bar{C}}\bar{\bar{A}}^{t_0+1}\tilde{O}_{n+m-1}(0) \subseteq Y \sim F_{t_0+1}.$$

For $(x, u) \in \tilde{O}_{t_0}(0)$ it holds that $\bar{\bar{C}}\bar{\bar{A}}^k(x', u')' \in Y \sim F_k$ for any $k \leq t_0$, but from the previous inclusion we have that $\bar{\bar{C}}\bar{\bar{A}}^{t_0+1}(x', u')' \in Y \sim F_{t_0+1}$. This means that $\tilde{O}_{t_0}(0) \subseteq \tilde{O}_{t_0+1}(0)$. Since $\tilde{O}_{t_0+1}(0) \subseteq \tilde{O}_{t_0}(0)$, we can conclude that $\tilde{O}_{t_0}(0) = \tilde{O}_{t_0+1}(0)$. With the same argument we have that $\tilde{O}_t(0) = \tilde{O}_{t_0}(0)$ for any $t \geq t_0$. This proves Point 4 for $i = 0$. The following chain of inequalities holds

$$\bar{\bar{C}}\bar{\bar{A}}^{t_0+1}\tilde{O}_{n+m-1}(i) \subseteq \bar{\bar{C}}\bar{\bar{A}}^{t_0+1}\tilde{O}_{n+m-1}(0) \subseteq Y \sim F_\infty \subseteq Y \sim F_{t_0+1+i}$$

This can used to prove Point 4 for any i. The argument also holds for t_i defined as the smallest t for which $\bar{\bar{C}}\bar{\bar{A}}^{t+1}\tilde{O}_{n+m-1}(i) \subseteq Y \sim F_{t_i+1}$ holds true. At most $t_i = t_0$, while in general $t_i \leq t_0$. In the case $(\bar{\bar{A}}, \bar{\bar{C}})$ is not observable, we can change the basis in order to split observable subspace and unobservable subspace. The latter does not affect the constraints. We can repeat the procedure on the observable subspace, for which it is finitely determined if Y is compact. Since $\tilde{O}_\infty(i)$ is equivalent for equivalent systems, this proves Point 5.

To check positive invariance let $(x, u) \in \tilde{O}_\infty(i)$. Then we have by definition that

$$C\left(A^k x + \sum_{\ell=0}^{k-1} A^\ell B u\right) + Du \in Y \sim F_{k+i}$$

for $k \geq 0$. By using the change of variable $\bar{k} = k - 1$ we have

$$C\left(A^{\bar{k}+1} x + \sum_{\ell=0}^{\bar{k}} A^\ell B u\right) + Du \in Y \sim F_{\bar{k}+1+i}$$

and

$$C\left(A^{\bar{k}} \bar{x} + \sum_{\ell=0}^{\bar{k}-1} A^\ell B u\right) + Dv \in Y \sim F_{\bar{k}+1+i}$$

for $\bar{k} \geq -1$ with $\bar{x} = Ax + Bu$. If it holds for $\bar{k} \geq -1$ it holds also for $\bar{k} \geq 0$ proving that $(\bar{x}, v) \in \tilde{O}_\infty(i+1) \subseteq \tilde{O}_\infty(i)$. □

Previous properties have important consequences from the computational point of view. In particular, Point 2 (compactness) and Point 3 (convexity) guarantee that the optimal point is unique and can be found with efficient optimization algorithms. Point 4 simplifies the construction of the set. Point 5 allows to know in advance if the set is not empty, so if the optimization problem is well posed. Note that if Y and W are symmetric, $Y \sim F_\infty$ is not empty if and only if it contains the origin. In that case, Point 5 can be specialized and the if condition becomes an if and only if implication.

Since the set is finitely determined, infinite-horizon constraints required to be robust against future communication blackouts can be expressed by a finite (tractable) number of inequalities. Moreover, also algorithmic derivation of $\tilde{O}_\infty(i)$ is possible by iterating the computation of $\tilde{O}_t(i)$ until $\tilde{O}_{t+1}(i) = \tilde{O}_t(i)$, that is verified for $t \geq t_i$ (see [106]). Interestingly, since $t_{i+1} \leq t_i$ $\tilde{O}_t(i)$ can be obtained from $\tilde{O}_t(0)$ by tightening the constraints $C\hat{x}(k|x, u) + Du \in Y$ subtracting set F_{k+i} from set Y. This provides $O_{t_0}(i) \cap O_\epsilon$ that is equal to $O_{t_i}(i) \cap O_\epsilon$ with possibly some redundant inequalities. The (set) subtraction can be done easily if W is expressed thorough linear inequalities. In the notable case where $W = \{w : I_n w \leq \mathrm{w} \text{ and } -I_n w \leq -\mathrm{w}\}$, it consists of simple vector subtractions.

Since the set is positively invariant, if an admissible input v is applied, it would be

admissible at the next time step, even if the updated state does not arrive at the control unit. Unfortunately, if v is not applied and the previous input u is hold, v may be not admissible at the next time instant. Consider the following toy example without disturbances: $A = -1/2$, $B = 2$, $-1 \leq x \leq 1$, $r_t = 0.9$, and at time $t = 0$ system is at the equilibrium $(x_0, u_0) = (-0.9, -0.9)$. Consider that v_t is chosen according (3.15) and $u_t = \theta_t v_t + (1 - \theta_t)u_t$. If $\gamma_0 = 1$, then $v_1 = 0.37$, and if $\theta_1 = 1$ then $u_1 = v_1$ and the system moves to $x_2 = 1$. If $\gamma_1 = 1$, then $v_2 = 0.9$. However if $\theta_2 = 0$ the system moves to $x_3 = 0.61$. In that case the input $v = 0.9$ is no more admissible and $v_3 = 0.87$. We can see that the computed input v_t may not have a monotonic behavior even for a fixed desired r_t, differently from what happens in standard RG.

3.4 Design of the Smart Actuator

We start from the design of the Smart Actuator and we consider two different laws $f(\cdot)$. As a first choice, let the function $f(\cdot)$ be a Zero-Order Hold that keeps the current value until a new packet arrives

$$u_t = \theta_t v_t + (1 - \theta_t)u_{t-1}. \tag{3.20}$$

This solution comes out naturally from the positively invariance of the MOAS (see Point 6 of Theorem 3.1). The second alternative is a discrete integrator that adds the new arrived value to the previous output

$$u_t = u_{t-1} + \theta_t v_t \tag{3.21}$$

For instance, this choice can be interesting when the system is sensitive to large increments of the reference and when system dynamics are sufficiently fast to follow (almost) instantaneously an admissible increment.

Both the proposed $f(\cdot)$ laws are really simple, so all the complexity is relegated to the control unit. In particular, function $g(\cdot)$ needs to take into account the missing information from the plant, due to possible past states x that have been lost, and for missing information at the plant, due to the future updates of the input v that may be lost.

3.5 Design of the Remote Constrained Controller

We start considering the case where $f(\cdot)$ is a Zero-Order Hold as in (3.20). The resulting strategy is called Reference Reset (RR) since when a new packet arrives, it resets the applied input to the new value.

The first step is to retrieve the estimate of the current state and the corresponding applied input. Let i_t denote the number of consecutive packet losses on the link from

the plant to the controller at time instant t. It follows that, when computing v_t, the last known applied input is u_{t-i_t-1}. Since that, the computed inputs $v_{t-i_t}, \dots, v_{t-1}$ have been transmitted and arrived according to the realization of the random sequence $\theta_{t-i_t}, \dots, \theta_{t-1}$. Since for a binary random sequence of length i we have 2^i possible realizations, we have 2^{i_t} possible sequences of applied inputs. Let $\Theta = (\vartheta_1, \dots, \vartheta_i)$ be an arbitrary binary vector of length i and denote

$$U_{t-i:t} = \begin{bmatrix} v_{t-1} \\ \cdots \\ v_{t-i} \\ u_{t-i-1} \end{bmatrix} \tag{3.22}$$

In the case where the arrival sequence $\theta_{t-i_t}, \dots, \theta_{t-1}$ is equal to Θ, the corresponding estimate of the state at time t is

$$\hat{x}(t, \Theta) = A^{i_t+1} x_{t-i_t-1} + A^{i_t} B u_{t-i_t-1} + \mathcal{R}_{i_t} \Lambda_{\Theta}^{\mathrm{RR}} U_{t-i_t:t} \tag{3.23}$$

where $\mathcal{R}_i$ is the reachability matrix in i steps

$$\mathcal{R}_i = \begin{bmatrix} B & AB & \cdots & A^{i-2}B & A^{i-1}B \end{bmatrix} \tag{3.24}$$

and $\Lambda_{\Theta}^{\mathrm{RR}}$ is the selection matrix given by the sequence Θ under the Reference Reset strategy

$$\Lambda_{\Theta}^{\mathrm{RR}} = \begin{bmatrix} \vartheta_1 \mathrm{I}_m & (1-\vartheta_1)\vartheta_2 \mathrm{I}_m & \dots & \prod_{\ell=1}^{i_t} (1-\vartheta_\ell) \mathrm{I}_m \\ 0 & \vartheta_2 \mathrm{I}_m & \dots & \prod_{\ell=2}^{i_t} (1-\vartheta_\ell) \mathrm{I}_m \\ 0 & 0 & \dots & \dots \\ 0 & 0 & \vartheta_{i_t} \mathrm{I}_m & (1-\vartheta_{i_t}) \mathrm{I}_m \end{bmatrix}. \tag{3.25}$$

From the previous analysis, we can see that there exists a different estimate for each possible past input sequence, namely for any $\Theta \in \{0,1\}^{i_t}$.

In order to manage the uncertainty on the current state due to the unknown past applied inputs since the last received packet, we impose that the new computed input v_t satisfies the constraints for any possible past sequence of applied inputs. Formally, the function $g(\,\cdot\,)$ is implicitly defined as the following optimization problem

$$v_t = \arg\min_{v} \|r_t - v\|^2 \tag{3.26}$$

$$\text{s.t. } (\hat{x}(t, \Theta), v) \in \tilde{O}_\infty(i_t), \ \Theta \in \{0,1\}^{i_t} \tag{3.27}$$

If the problem is infeasible at time t, v_t does not exist. In that case, in order to keep the formalism introduced for the arrival process, the remote control unit transmits an

empty packet which, even if received, does not produce any effect at the smart actuator. Moreover, we also assume that if $\|r_t - v_t\| > \|r_t - u_{t-i_t-1}\|$, v_t is discarded. Again, an empty packet is transmitted.

Note that, in order to manage the uncertainty on the current state due to past disturbances since the last received packet, we use the Maximal Output Admissible Set with Packet Loss $\tilde{O}_\infty(i_t)$. The number of constraints grows exponentially with the length of the blackout i_t and the problem may become intractable. To take into account this situation, let the bound L be such that the optimization problem can be solved before the transmission instant when $i_t \leq L$. Then, if $i_t > L$, namely the remote control unit is not able to solve the optimization problem in time, an empty packet is transmitted.

Following the same reasoning, we repeat the procedure for the case where $f(\,\cdot\,)$ is a discrete integrator as in (3.21). The resulting strategy is called Additive Update (AU) since when a new packet arrives, it is added to the applied input.

For an arbitrary sequence Θ, the corresponding estimate of the state at time t is

$$\hat{x}(t,\Theta) = A^{i_t+1}x_{t-i_t-1} + A^{i_t}Bu_{t-i_t-1} + \mathcal{R}_{i_t}\Lambda_\Theta^{\mathrm{AU}}U_{t-i_t:i} \tag{3.28}$$

where $\Lambda_\Theta^{\mathrm{AU}}$ is the selection matrix given by the sequence Θ under the Additive Update strategy

$$\Lambda_\Theta^{\mathrm{AU}} = \begin{bmatrix} \vartheta_1\mathrm{I}_m & \vartheta_2\mathrm{I}_m & \cdots & \vartheta_{i_t}\mathrm{I}_m & \mathrm{I}_m \\ 0 & \vartheta_2\mathrm{I}_m & \cdots & & \\ 0 & 0 & \cdots & & \\ 0 & 0 & 0 & \vartheta_{i_t}\mathrm{I}_m & \mathrm{I}_m \\ 0 & 0 & 0 & 0 & \mathrm{I}_m \end{bmatrix} \tag{3.29}$$

In the case of the AU strategy we also need to retrieve the applied input corresponding to the estimate $\hat{x}(t,\Theta)$. In particular, given the arrival sequence Θ, the corresponding applied input at time instant $t-1$ is

$$\hat{u}(t-1,\Theta) = \begin{bmatrix} \vartheta_1\mathrm{I}_m & \vartheta_2\mathrm{I}_m & \cdots & \vartheta_{i_t}\mathrm{I}_m & \mathrm{I}_m \end{bmatrix} U_{t-i_t:t}. \tag{3.30}$$

In this case, the function $g(\,\cdot\,)$ is implicitly defined as the following optimization problem

$$v_t = \arg\min_v \left(\min_\Theta \|r_t - (\hat{u}(t-1,\Theta) + v)\|^2 \right) \tag{3.31}$$

$$\text{s.t. } (\hat{x}(t,\Theta), \hat{u}(t-1,\Theta) + v) \in \tilde{O}_\infty(i_t),\ \Theta \in \{0,1\}^{i_t} \tag{3.32}$$

It can be shown that when the applied input and the current state are known, the two optimization problems are equivalent. This holds also if the current state is not known but the applied input is known for any past instant, so that the set of state

estimates is a singleton. We can conclude that, if at least a link is completely reliable, for instance in the notable case where the RG is collocated with the smart actuator, the two strategies are equivalent. Conversely, when both links are lossy, a possible asymmetry in the information sets may arise and the optimal design of both $g(\cdot)$ and $f(\cdot)$ is not trivial, as we underline in [111]. We point out that also alternative strategies can be devised. For example, the optimal input for any possible state estimate can be computed and sent. Also hybrid strategies can be devised, where both the problems are solved and both the solutions are sent, and then the smart actuator chooses the best to apply. In all these cases, the critical point is the possible asymmetry of information between the two sides of the system.

3.6 Theoretical properties

In this section, we study the theoretical properties of the proposed strategy. We focus on the RR strategy but they can be adapted also for the AU strategy.

A well-known property of standard RG schemes is the recursive feasibility of the underlying optimization problem, guaranteed since $\tilde{O}_\infty(0)$ is positively invariant, under the assumption that the problem is feasible at $t = 0$. Under the RR strategy, feasibility of the optimization problem may be temporarily lost due to the more stringent constraints if $i_t > 0$. It is however possible to state the following theorem.

Proposition 3.1. *Assume that* $(x_0, u_0) \in \tilde{O}_\infty(0)$. *Then,* $(\hat{x}(t, \emptyset), u_{t-1}) \in \tilde{O}_\infty(0)$ *and the optimization problem* (3.26) *is feasible for any* $t \geq 0$ *s.t.* $\gamma_{t-1} = 1$.

Proof. Let j such that $\theta_{t-j} = 1$ and $\theta_k = 0$ for $t - j < k < t$. Let $\Theta = (\theta_{t-i_t}, \cdots, \theta_t)$ the actual arrival sequence occurred in the link from the controller to the plant, and let $\bar{\Theta} = (\theta_{t-i_t}, \cdots, \theta_{t-j})$. Then it holds that

$$
\begin{aligned}
x_t &= A^{i_t+1} x_{t-i_t-1} + A^{i_t} B u_{t-i_t-1} + \mathcal{R}_{i_t} \Lambda_\Theta^{\mathrm{RR}} U_{t-i_t:t} + \sum_{k=0}^{i_t} A^k w_{t-k} \\
&= A^{i_t+1} x_{t-i_t-1} + A^{i_t} B u_{t-i_t-1} + A^j \mathcal{R}_{i_t-j} \Lambda_\Theta^{\mathrm{RR}} U_{t-i_t:t-j} + \sum_{k=0}^{i_t-j} A^k B v_{t-j} + \sum_{k=0}^{i_t} A^k w_{t-k} \\
&= A^j \hat{x}(t-j, \bar{\Theta}) + \sum_{k=0}^{i_t-j} A^k B v_{t-j} + \sum_{k=0}^{i_t} A^k w_{t-k}
\end{aligned}
$$

By construction $(\hat{x}(t-j, \bar{\Theta}), v_{t-j}) \in \tilde{O}_\infty(i_t - j)$. Since $\tilde{O}_\infty(i)$ is positively invariant (see Theorem 3.1), it holds that $(A^j \hat{x}(t-j, \bar{\Theta}) + \sum_{k=0}^{i_t-j} A^k B v_{t-j}, v_{t-j}) \in \tilde{O}_\infty(i_t)$. Since $\sum_{k=0}^{i_t} A^k w_{t-k} \in F_{i_t}$, we can choose $v_t = v_{t-j}$. So $(x_t, v_t) \in \tilde{O}_\infty(0)$ and the optimization problem is feasible. □

According to the previous proposition, feasibility is guaranteed as soon as a packet has been received by the control unit. In particular, during periods characterized by an ideal communication without losses, the proposed scheme works exactly like a standard governor and the problem is recursively feasible. If the problem is infeasible during blackouts, it becomes feasible as soon as a packet is received and a new update can be sent (and eventually applied) without any resynchronization procedure as e.g. in [103].

Safety and constraint satisfaction for any packet loss sequence follows from the previous proposition. For sake of completeness, we formalize the statement here.

Proposition 3.2. *Assume that* $(x_0, u_0) \in \tilde{O}_\infty(0)$. *Then, constraints* (3.2) *are satisfied with probability 1 for any* $t \geq 0$.

Interestingly, the above safety property is the most general possible since it does not require any assumption on the network. The robustness of the ideal case, in terms of hard constraint satisfaction, is achieved through the proposed solution for any network and channel condition, even in presence of blackouts. Conversely, in order to achieve tracking of reference signals, additional assumptions on the network are required.

Assumption 3.1. Assume that $\mathbf{P}(\bigcap_{k>0}\{\theta_{t_k}\gamma_{t_k} = 0\}) = 0$ for any infinite sequence $\{t_k\}_{k=0}^{+\infty}$ with $t_{k+1} > t_k$.

We can now state the main theorem.

Proposition 3.3. *Assume that* $(x_0, u_0) \in \tilde{O}_\infty(0)$, *and* $r_t = r$ *for* $t \geq 0$. *If* $W = \{0\}$, *under Assumption 3.1, the applied input* u_t *reaches the reference* r^* *and the state converges to* $(I - A)^{-1}Br^*$, *where* $r^* = \arg\min_v \|r - v\|^2$ *such that* $((I - A)^{-1}Bv, v) \in \tilde{O}_\infty(0)$.

Proof. The proof consists of 3 steps.

First step: consider an input u and denote

$$\bar{x}_u = (I - A)^{-1}Bu \qquad \bar{y}_u = C\bar{x}_u + Du.$$

Assume that $(\bar{x}_u, u) \in \tilde{O}_\infty(0)$. In particular, it implies that $\bar{y}_u \in (1 - \epsilon)Y$. Consider now an arbitrary initial state as $\bar{x}_0$. We have

$$\begin{aligned} y_k &= CA^k\bar{x}_0 + C\sum_{\ell=0}^{k-1} A^\ell Bu + Du \\ &= CA^k\bar{x}_0 + C\sum_{\ell=0}^{k-1} A^\ell Bu + Du + CA^k\bar{x}_u - CA^k\bar{x}_u \\ &= \bar{y}_u + (CA^k\bar{x}_0 - CA^k\bar{x}_u) \end{aligned}$$

Since by construction $\bar{y}_u \in (1 - \epsilon)Y$, we have that $y_k \in Y$ if $H(CA^k\bar{x}_0 - CA^k\bar{x}_u) \in \mathcal{B}_\epsilon(0)$. Since A is stable, we know that there exists a δ such that if $\|\bar{x}_0 - \bar{x}_u\| < \delta$

then $HCA^k(\bar{x}_0 - \bar{x}_u) \in \mathcal{B}_\epsilon(0)$, and consequently $y_k \in Y$. We can conclude that for any $(\bar{x}_u, u) \in \tilde{O}_\infty(0)$ then there exists a $\delta > 0$ such that if $\bar{x}_0 \in \mathcal{B}_\delta(\bar{x}_u)$ then $(\bar{x}_0, u) \in \tilde{O}_\infty(0)$. In other words, from any point $\bar{x}_0$ it is possible to move arbitrarily close to any steady-state admissible point $\bar{x}_u$, provided that they are close enough.

Second step: let $\{s_t\}_{t=0}^{+\infty}$ be the sequence of applied inputs that have been (sent back and) received by the control unit, that is $s_t = u_{t-i_t-1}$. Since v_t is assumed to be discarded when $\|v_t - r\| > \|u_{t-i_t-1} - r\|$ we have that $\|s_t - r\| \geq \|u_t - r\|$, that implies

$$\|s_{t+1} - r\| = \gamma_t \|u_t - r\| + (1 - \gamma_t)\|s_t - r\| \leq \|s_t - r\|$$

We have that the sequence $\|s_t - r\|$ is monotonically non-increasing and bounded by 0, so it converges to $\|v - r\|$. With standard arguments, we can show that s_t converges to v. Consider the sequence of time instants $\{t_k\}_{k=0}^{+\infty}$ such that v_{t_k} is defined, while it is not defined elsewhere. If v_{t_k} converges, it must converge to v. Assume by contradiction that v_{t_k} does not converge. Equivalently, there exists a $\delta > 0$ and a sequence $\{\tau_k\}_{k=0}^{+\infty}$ included in the sequence $\{t_k\}_{k=0}^{+\infty}$ such that $\|v_{\tau_k} - r\| > \delta$. Now, pick $\epsilon = \delta/2$. Since s_t is converging to v, there exists a t_ϵ such that $\|s_t - v\| < \epsilon$ for any $t > t_\epsilon$. By Assumption 3.1, with probability 1, there exists a $\tau > t_\epsilon$ belonging to the sequence $\{\tau_k\}$ such that $\theta_\tau \gamma_\tau = 1$. By construction, $s_\tau = v_\tau$, that implies $\|s_\tau - r\| = \|v_{\tau_k} - r\| > \delta$, reaching an absurd.

Third step: assume by contradiction that $v \neq r^*$. Given a $\delta_1 > 0$, there exists t_1 such that $\|u_t - v\| < \delta_1$ for $t > t_1$. Given a $\delta_2 > \delta_1$, there exists a $t_2 > t_1$ such that $\|x_t - \bar{x}_v\| < \delta_2$ for $t > t_2$. Introduce $v_\alpha = \alpha r^* + (1-\alpha)v$. Given a $\delta_3 > 0$, there exists a $\bar{\alpha} > 0$ sufficiently small such that $\|\bar{x}_{v_\alpha} - \bar{x}_v\| < \delta_3$ for $\alpha < \bar{\alpha}$. We can conclude that for $\delta = \delta_3 + \delta_2$ then $\|x_t - \bar{x}_{v_\alpha}\| < \delta$ for $\alpha < \bar{\alpha}$ and $t > t_2$. It follows from the first step that $(x_t, v_\alpha) \in \tilde{O}_\infty(0)$. But we have that

$$\begin{aligned} \|v_\alpha - r\| &= \|(1-\alpha)v_t + \alpha r^* - r\| \\ &\leq (1-\alpha)\|v_t - r\| + \alpha\|r^* - r\| \\ &\leq \|v_t - r\| \end{aligned}$$

by convexity of the norm, reaching an absurd and proving the convergence of the applied input to r^*. The convergence of the state immediately follows. The case with general W can be treated analogously. □

Essentially, if the desired reference r is constant, the applied input u_t will reach the best admissible approximation r^* of the desired reference r. Clearly, if the desired reference r is admissible, u_t will reach it. The result can be generalized for time-varying references that converge to a steady-state constant value. In the literature similar results exist also for other governors without packet losses: the proposition guarantees that the proposed governor behaves "as expected", converging to the desired point despite the packet loss.

3.7 Simulations: assessment of the proposed strategies

In order to compare the two proposed strategies and to assess their performances, we carry out a simulation test featuring two plants and different channel conditions.

As for the channel, the arrival processes γ_t and θ_t are modeled as independent and identically distributed random variables with Bernoulli distribution and time-varying (piecewise constant) mean. In particular, we set $\mathbb{E}[\gamma_t]$ and $\mathbb{E}[\theta_t]$ equal to 1 (no packet loss) in the first period (from 0 to τ, for a given period τ), equal to 0.6 in the second period (from τ to 2τ), and equal to 0.2 (bad channel) in the third period from (from 2τ to 3τ). In the following, the link from the control unit to the actuator is referred to as uplink, while the link from the sensor to the control unit is referred to as downlink.

As a first plant, we consider a simple double-integrator system with sampling period $T = 0.01$ s characterized by

$$A_{ol} = \begin{bmatrix} 1 & T \\ 0 & 1 \end{bmatrix} \qquad B_{ol} = \begin{bmatrix} \frac{T^2}{2} \\ T \end{bmatrix}$$

with disturbance belonging to the set

$$W = \{w = (w_1, w_2)' : -0.05 \leq w_1 \leq 0.05,\ w_2 = 0\}$$

Through state feedback, we allocate the eigenvalues at $\pm 0.5i$ and we implement nominal tracking. The constraints are set as

$$C = \begin{bmatrix} 0 & 1 \end{bmatrix} \qquad D = 0 \qquad Y = \{y : -10 \leq y \leq 10\}$$

and the desired reference r is set equal to 1. Intuitively, the system models the dynamics of a simple mass in one-dimensional space driven by an external force. So, the first component of the state is the position, the second one is the velocity, and the system input is the applied force. According to this analogy, the objective is to drive the system to a desired position while keeping the velocity bounded.

The communication blackouts, defined as the period elapsed at the current time instant since the last received packet, obtained during the simulation, are reported in Figure 3.3. We can see that, in the first period, the duration of communication blackouts is always 0, while, in the third period, long blackouts up to 0.2 s are present. The realization of the arrival processes during the simulation can be easily inferred.

Top panel of Figure 3.4 reports the evolutions of the system position for the proposed strategies under the channel conditions represented in Figure 3.3. As expected, in the period from 0 s to 2 s where packet loss is not present, the system responses are identical for the two strategies. Also in the period from 2 s to 4 s, the evolution under the two

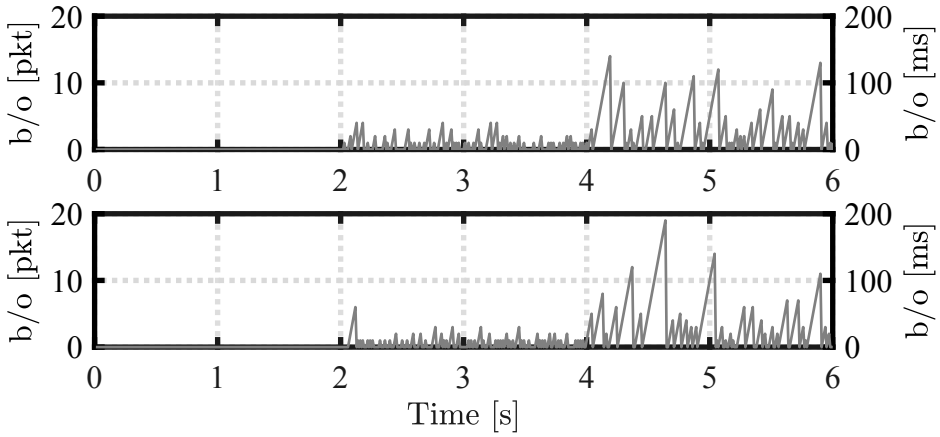

Figure 3.3: Blackouts (b/o). Top: uplink. Bottom: downlink

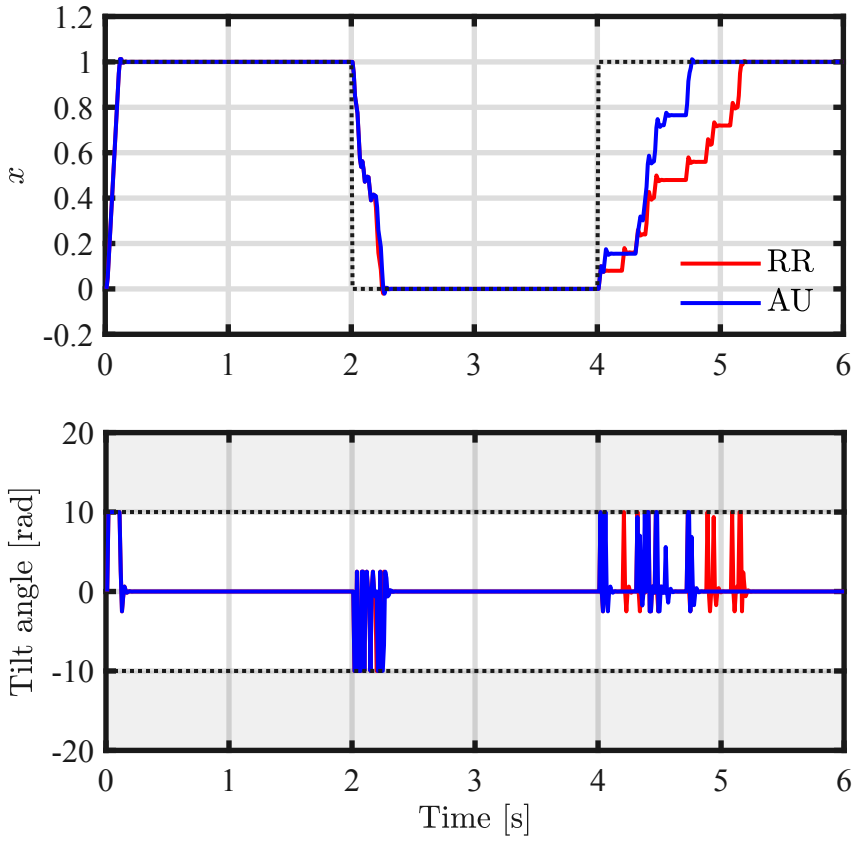

Figure 3.4: System response with simulated channels. System: double integrator. Comparison between RR strategy (3.26) and AU strategy (3.31). AU outperforms RR.

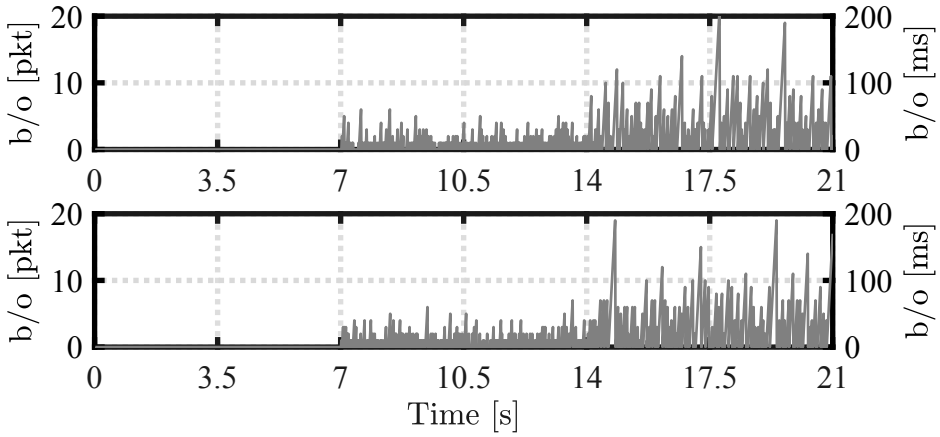

Figure 3.5: Blackouts (b/o). Top: uplink. Bottom: downlink

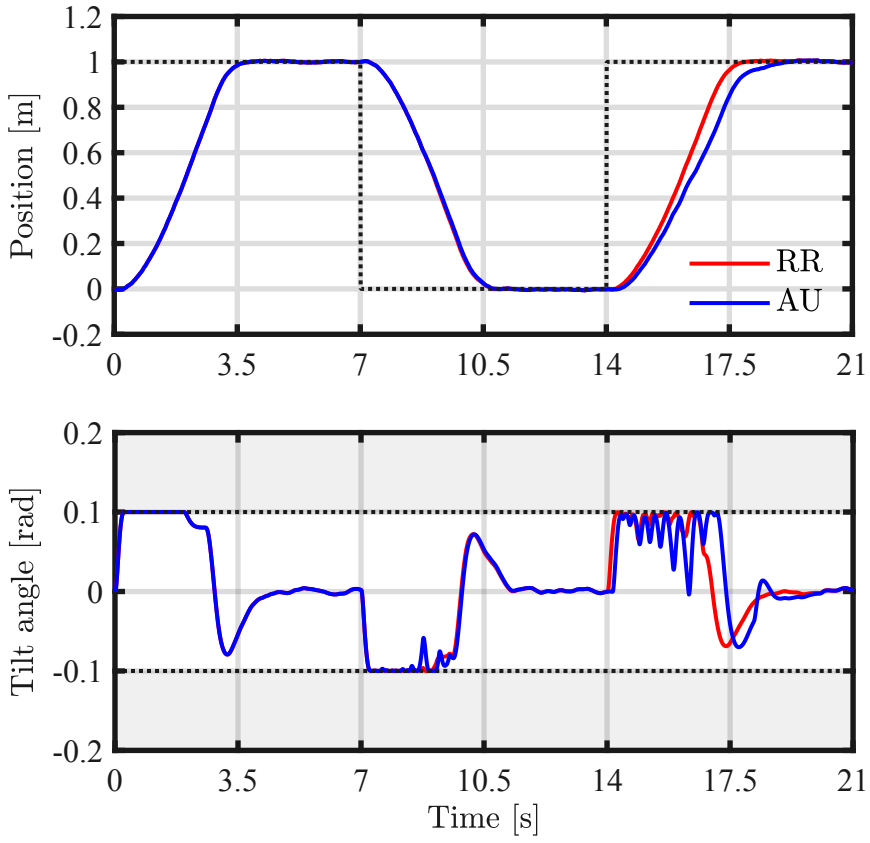

Figure 3.6: System response with simulated channels. System: Segway. Comparison between RR strategy (3.26) and AU strategy (3.31). In this case, RR outperforms AU.

strategies are almost identical and no clear differences are present in terms of settling time. Conversely, in the period from 4 s to 6 s, the two strategies obtain substantially different evolutions. We can see that AU takes approximately half the time of RR to reach the desired reference. For this particular system, AU scheme addresses the losses more efficiently. This can be due to the presence of oscillations in the response of the controlled system and the fast response to a new reference. Indeed, in different states, there exists a quantity that can be added to the current input without violating the constraints but there may not exist an input (or it is more conservative) that is admissible for all.

Bottom panel of Figure 3.4 shows the velocities achieved with the two strategies and the non-admissible region according to the constraints (indicated in gray). We see that both the strategies analyzed in this chapter succeed in satisfying the constraints even with high loss probabilities.

Interestingly, the proposed strategies naturally adapt to the channel quality. As long as the channel condition gets worse, e.g. moving from the first period to the second, or from the second to the third, longer periods are required to reach the desired reference. The proposed strategies naturally deteriorate the performances in order to guarantee the safety of the remote system.

As a second plant, we simulate the pre-stabilized linear model of the Segway-like robot described in Appendix A.2 with sampling period $T = 10$ ms. In particular, matrices C, D, H, and h are set to take into account the limits on the input fed to the motors, that is required to remain in the interval $[-11\text{ V}, 11\text{ V}]$, and the safety constraints on the tilt angle, that is required to remain in the interval $[-0.1\text{ rad}, 0.1\text{ rad}]$. The communication blackouts during the simulation are reported in Figure 3.5, while the system responses for the proposed strategies are reported in Figure 3.6.

Similarly to the double integrator, the two strategies are almost identical in the first two periods. However, conversely to the previous case, RR outperforms AU when loss probability is high. Also for the Segway-like robot, the proposed strategies adapt to the channel conditions but the performances of RR in terms of settling time are only marginally affected by (i.i.d. Bernoulli arrival processes with) high loss probability. This motivates the choice of RR for the following experimental tests involving the Segway.

These two simple examples show that none of the two strategies is optimal and which is better may depend on the specific system and on the constraints.

3.8 WiFi-in-the-loop simulations: comparisons

In this section, we set up an accurate simulation test featuring communication data from a real Wi-Fi network. As for the plant, we consider the Segway-like robot described in Appendix A.2. The sampling period is $T = 5$ ms and we pre-stabilize the system by a linear state feedback. We accurately simulate the nonlinear plant dynamics, the local

linear controller, the sensing devices (encoders and MPU), and the actuator saturation. Computational time is neglected. As for the network, we use the communication data collected with the experimental setup of Appendix A.3. For control design purposes, the model is linearized. We consider the constraints on the tilt angle and on the input fed to the motors. In the following, we compare the RR strategy, since it achieves better performances than AU when applied to the Segway, with other two strategies.

As a first strategy, we consider a simple event-based RG: the control unit is triggered when a packet is received, it solves the standard RG problem and transmits the computed input. If no packets arrive from the plant, the event-based RG does not update the previous computed input and keeps sending the same quantity. This strategy is relevant because it is representative of what it is done in practice e.g. with drones: in normal channel conditions, a new input is computed by a remote computer in a suitable way (not necessarily with RG) to avoid obstacles but, if the connection is temporarily down, the previous input is re-transmitted until a new measurement is received. The main advantage of this strategy is that it is simple to implement. However it may lead to constraint violations because the input computed in the past may be no more admissible.

As a second strategy, we adapt the Networked MPC devised in [59] for the case at hand. The key idea is to keep the first τ inputs of the previous control sequence also in the next sequence, and to initialize the MPC problem on the state prediction τ steps ahead. In this way, each input is sent τ times and the solution is unaffected if the number of consecutive packet losses on the uplink is smaller than τ. At the controller side, a buffer is used to store the computed inputs and the past received measurements. At the plant side, a buffer is used to store the last received control sequence, and a suitable logic is implemented to extract the input associated to the current time instant. Formally, let i_t denote the number of consecutive packet losses on the link from the plant to the controller at time instant t. Then, the algorithm consists of the state estimator

$$\hat{x}_{k+1} = A\hat{x}_k + Bv_k^{k-\tau} \qquad k = t - i_t, \ldots, t + \tau$$

and of the controller

$$\begin{aligned}(v_{t+\tau}^t, \ldots, v_{t+\tau+N-1}^t) = \arg\min_{\mathbf{u}} \; & \sum_{k=0}^{N-1} \|x(k) - \bar{x}\|_Q^2 + \|u(k) - \bar{u}\|_R^2 + \|x(N) - \bar{x}\|_P^2 \\ & x(k+1) = Ax(k) + Bu(k) \qquad x(0) = \hat{x}_{t+\tau} \\ & Cx(k) + Du(k) \in Y \sim F_{k+\tau+i_t} \qquad k = 0, \ldots, N-1 \\ & x(N) \in X_f(\bar{x})\end{aligned}$$

with $\mathbf{u} = (u(0), u(1), \ldots, u(N-1))$, $\bar{x}$ is the desired set-point, and $\bar{u}$ such that $\bar{x} = A\bar{x} + B\bar{u}$. The transmitted packet U_t is obtained by merging the new computed sequence

with the first elements of the previous transmitted packet, obtaining

$$U_t = (v_t^{t-\tau}, v_{t+1}^{t+1-\tau}, \dots, v_{t+\tau}^{t}, \dots v_{t+\tau+N-1}^{t}).$$

If the bound τ is never violated, the applied input is always $u_t = v_t^{t-\tau}$. In order to overcome violations of the bound τ, we propose to use the next inputs of the received sequence, eventually holding the last input when the sequence is finished. Recursive feasibility, constraint satisfaction, and convergence to the desired set-point $\bar{x}$ require the number of consecutive packet losses both on the downlink and on the uplink to be bounded, together with some technical assumptions on the system and on the design of P and $X_f(\bar{x})$.

The resulting solution is not robust against blackouts longer than τ packets. In fact, when more than τ consecutive packets are lost, the estimate computed at the control unit is no more aligned with the actual system state and the computed input sequence may be no more valid. In line of principle, if the open-loop system is stable, τ can be taken arbitrarily large, expanding the set of channel conditions for which safety is theoretically ensured. However, this comes at the price of a loss of performances especially in good channel conditions, since applied inputs are derived from long open-loop prediction. Moreover, note that, if the open-loop system is unstable, there may exist a k such that $Y \sim F_k$ is empty, so τ cannot be chosen arbitrarily large.

The following results have been obtained under the optimistic design assumption of blackouts of at most $\tau = 20$ transmissions. Moreover we choose $N = 50$, $Q = P = G'G$, $R = 1$, with $G = (1\ 0\ 0\ 0)$. Since we consider time-varying set-points, also the terminal set $X_f(\bar{x})$ should be time-varying. However, this would require to design a suitable algorithm to change $X_f(\bar{x})$, for which there do not exist simple solutions in the literature. For this reason, we remove the terminal constraints. Unfortunately, this choice, together with the occurrence of blackouts longer than τ, may lead the optimization problem to be unfeasible for some time instant. In those cases, the problem is relaxed converting the hard constraints into soft ones.

We consider the system response with a desired reference r_t equal to a step signal, with size 1 m and step time 3 s. The channel evolution used in the test is reported in Figure 3.7 and the responses are reported in Figure 3.8. In the top panel, reporting the position of the robot, we see that the proposed strategy converges faster to the desired reference r with respect to the event-based RG. The advantage of the proposed solution is cumulating over time and the desired reference is reached in approximately 1.2 s less (30% less). Also the performances of the Networked MPC are worse than the proposed strategy. In the bottom panel we have the evolution of the tilt angle, where the constraints are indicated in gray. We see that, as expected, the proposed RG always satisfies the constraints. We stress that, when the segway-like robot is proceeding forward, the best

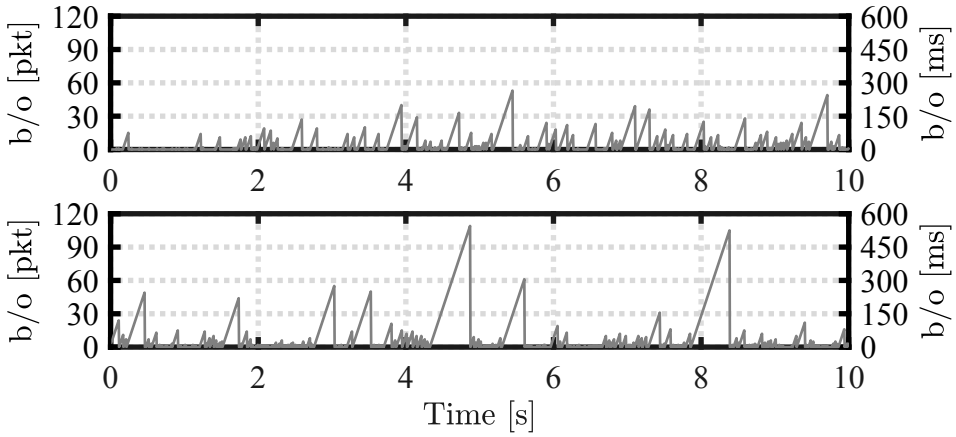

Figure 3.7: Blackouts (b/o). Top: uplink. Bottom: downlink

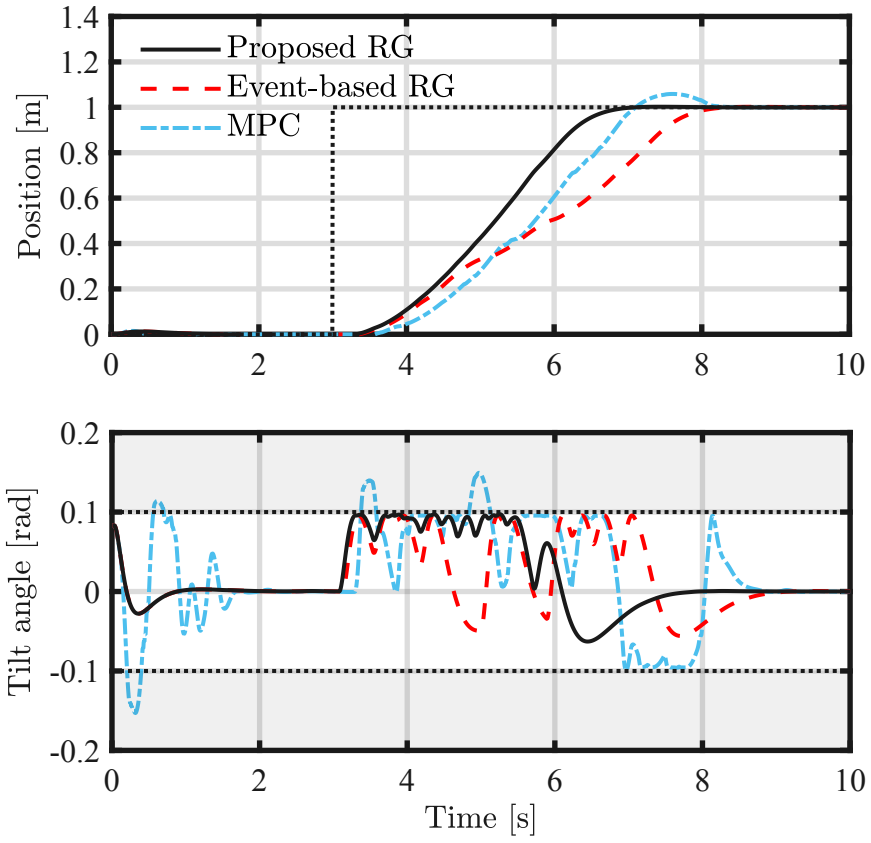

Figure 3.8: System response with WiFi-in-the-loop setup. Comparison between proposed solution, an Event-based RG, and standard Networked MPC [59].

tilt angle satisfying the constraints is equal to 0.1 rad, while the tilt angle decreases when the segway is stopping. When the tilt angle is decreasing in the period between 3 s and 7 s, we can infer that u_t has not been updated due to packet losses (see also top panel of Figure 3.7). Roughly speaking, this can be seen as the way that RG implements in order to operate safely. As for the MPC, we can see that constraints are not satisfied in many cases due to blackouts longer than τ, leading to the worse tracking performances and possibly also to instability. This occurs, for instance, when longer blackouts are present in the link from the control unit to the plant. Other WiFi-in-the-loop tests with different channel conditions can be found in [112].

3.9 Experiments

In this section, we test the proposed RG on a full experimental setup. The experiment involves a remote PC, which plays the role of the control unit, the Segway robot, which plays the role of the plant, and the Wi-Fi network. The mathematical model of the Segway robot is given in Appendix A.2, while the mechanical and electronic characteristics of the prototype are given in Appendix A.4. In particular, the Segway is equipped with a Raspberry board, to manage wireless communications, and an Arduino microcrontroller, for low level computations. Accordingly, the proposed RG is implemented on the PC, the smart actuator is implemented on the Raspberry board, while the stabilizing inner loop is implemented on the Arduino microcrontroller. The sampling period is $T = 5$ ms, control design is carried out as in Appendix A.2, while network parameters are set as in Appendix A.3.

Differently from the WiFi-in-the-loop experiments, where the dynamics of the system were accurately simulated but the model parameters were assumed to be known, in this experiment, model errors are unavoidable and largely affect the control performances. Indeed, high accuracy is not possible in practice due to the complicated shape and mass distribution of the Segway. Due to nature of prototype, the mechanical design of the robot is not ideal and several small inaccuracies are present. First, the presence of a mechanical backlash in the motor gearbox produces oscillations, within a band of a few degrees, at steady-state. Moreover, the mass distribution is not perfect. This implies that the equilibrium position is not perfectly vertical, and most importantly, degrades the quality of the predictions. Furthermore, an offset in the measurements from the IMU is present. We correct it with a rudimentary cancellation, but a small error is still present. Finally, the battery cannot always supply the nominal voltage, equal to 11.1 V. To avoid the cases where the supplied power is less than expected, which may give wrong predictions and uncontrolled movements, we reduce the limit of voltage input to 9 V.

During the experiments, the channel condition was good, with a packet loss probability of 0.05 and blackouts always shorter than 6 packets. The system response is reported in

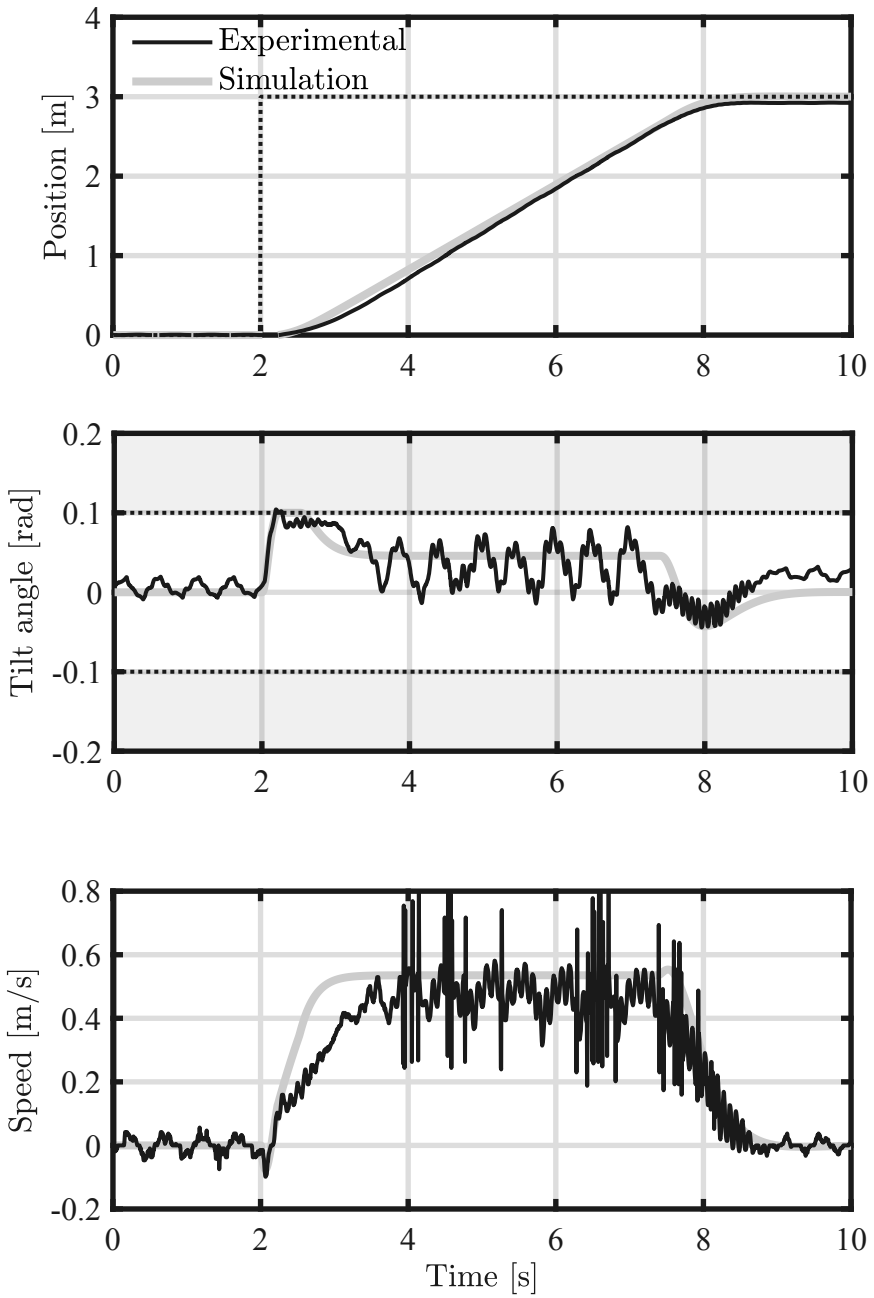

Figure 3.9: System response. Simulation with ideal communication and full experiment on Segway. Despite the non-ideal mechanical design and model errors, constraints are satisfied and the desired set-point is reached.

Figure 3.9. For sake of readability, we also report the expected (and desired) behavior obtained from simulations with ideal model and ideal channel. As we can see in the center panel, the experimental tilt angle evolution is really noisy. Even at the equilibrium (in the period from 0 s to 2 s), oscillations of 0.02 rad are present. They are due to the non-ideal mass distribution and backlash in the motor gearbox, as confirmed by extensive experimental campaigns also with different setups. Larger oscillations of the tilt angle are present when the Segway is moving (in the period from 4 s to 7 s). They are probably due to the incorrect system model used in the prediction: alternately, the RG slows down the segway, because it predicts a possible future constraint violation, and accelerates, because the state is later than expected from the model. This behavior is emphasized by the rudimentary state estimator, which computes the speed by simple differentiation of the position measurement. In the bottom panel, we can see both the oscillations of the speed with respect to the simulated model and the high-frequency error due to the basic estimator.

Despite the inaccurate state estimate and the wrong model, the system always satisfies the constraints. The evolution is qualitatively comparable with the simulated plant, and the system response is satisfactory. The settling time to cover 3 m is less than 4 s and it is identical to the one obtained with the simulated matched model with ideal channel.

It can be noticed that a small steady-state error is present. This is due to the model error and it can be removed by adding an integrator in the inner control loop. This setup can be easily managed by RG with an additional state.

We would like to point out that, with the considered prototype, small violations may be present because of the inaccurate model and the noisy state feedback. However, this is a problem of the specific control application, and we believe that it would not be present in systems with a more sophisticated mechanical design. Nonetheless, also in the considered setup, this can be regarded by enlarging the set W of possible disturbances at the price of additional conservativeness. Note that this is not required by the presence of the network, differently e.g. from [59], where additional conservativeness (the fictitious delay τ) is added to the networked solution with respect to the case with ideal communication.

The presented results show the feasibility of constrained control applications over wireless. From the outcomes of the experiments, we think that the performances of the proposed algorithm under average channel conditions do not differ much from the performances of standard solutions with dedicated cables. On the other hand, wireless networks enable much larger flexibility and open the door to an incredible number of applications, like multi-agent mobile manipulation and transportation, where dedicated wired cables can be unlikely employed. In bad, but still rare channel conditions, we expect that the proposed solution would be outperformed by standard solutions with dedicated cables. However, the WiFi-in-the-loop experiments seem to indicate that safety can be guaranteed in any condition.

3.10 Conclusion

Based on the observation that safety of the control system can be described through suitable constraints, in this chapter we have addressed the problem of constrained control over wireless networks. Due to the presence of communication blackouts, we have required the plant to be stabilized by an inner control loop. We have proposed a detailed solution based on RG that is particularly appealing from the computational point of view. Theoretical guarantees and experimental results obtained using real Wi-Fi data and a real robot make the proposed scheme a valid candidate to address constrained control over wireless. However, we guess that the performances may be limited by the inner control loop and by the short-horizon state-independent cost function of the RG, especially if the desired reference is more elaborated than a simple set-point. In the following chapter, we look for a more advanced strategy based on MPC.

4

MPC for Tracking over Wireless

The safety of control systems over wireless networks can be expressed through suitable constraints. In the previous chapter, we have shown that constraints can be enforced even in presence of communication blackouts if the plant is stable. For this reason, we have first introduced a local inner control loop closed over reliable links that stabilizes the system. Then, we have designed an outer control loop based on RG that, even with packet loss, provides suitable inputs to enforce constraints and to track general reference signals. The experimental results obtained including a real Wi-Fi network are promising. However, the inner control loop and the simple cost function may reduce the performances, especially for more elaborated reference signals. A possible way to improve the performances is to consider a more advanced strategy based on MPC.

Several MPC schemes are available in the literature to deal with packet loss and random delays. The main idea is to use the sequence of future inputs, that is computed by MPC as by-product to obtain the current control input, to cope with future communication flaws. The work [50] studies the case where the link between sensor and MPC is ideal for nonlinear systems without disturbances. The solution has been extended in [51] for the case with bounded disturbances. A key aspect of these works is that MPC and sensor are co-located, so the current state is always known. Conversely, if the link between sensor and MPC is affected by packet loss, in order to estimate the state to compute an admissible input sequence, the controller needs exact knowledge of the past inputs applied by the actuator. A similar problem arises when delayed control sequences are not discarded: if the last applied inputs do not coincide with the first elements of the new received sequence, it is not guaranteed that the subsequent elements of the new sequence are admissible. In the literature, this problem is referred to as *input consistency*, that is the consistency between the input trajectory as known by the controller and the actual applied input trajectory at the actuator. Similarly, *state consistency* is achieved when the input trajectory used to estimate the state coincides with the actual applied input trajectory at the actuator. Note that, state consistency does not imply that the estimate and the actual state are coincident but that they differ at most by the effects

of the disturbance. When both links are lossy, input and state consistency are therefore a crucial point to guarantee the validity of the new control sequence. The work [113] guarantees input consistency by computing and transmitting, at each time instant, a different control sequence for any possible delay and for any possible combination of applied inputs. A smart actuator is employed to select the right sequence from the received packet. The work [52] uses a reliable acknowledgment mechanism to guarantee input consistency. According to this strategy, the optimization problem is not solved at each time instant but only if either a new measurement has been arrived, or the last measurement has been arrived i steps ago and all the last i control sequences have been lost. The most general case with both unreliable links and without acknowledgment has been studied in the work [59] whose main idea is to preserve the validity of any computed sequence introducing a fictitious delay. A detailed description of the algorithm is given in section 3.8. The solution is adapted for the simpler case with acknowledgment in [53]. A similar approach for continuous-time systems without disturbances is studied in [114]. In this case, the controller is triggered by a received packet and the sensor may transmit also not periodically. The same idea has been adapted in [115] for the case with acknowledgment. Unfortunately, aforementioned works guarantee constraint satisfaction and stability only if the interval between two consecutive received packets is bounded. This point is particularly limiting because, as shown in section 1.1.1, communication blackouts are unavoidable in fast networks as Wi-Fi.

Interestingly, unbounded sequences of packet losses can be allowed if state constraints are excluded. For instance, the work [116] considers Markovian packet losses without state and input constraints. Along the same line, the work [117] considers also random delays, the work [118] considers finite quantization levels, and the work [119] considers limited bit-rate. More recently, input constraints have been included. The work [120] considers the case with linear systems with possibly unbounded disturbances and independent identically distributed losses on the link from the controller to the actuator. The solution has been extended in [121] and [122], for stabilization and tracking problems, respectively, in the case where both links are affected by independent identically distributed losses. However, we do require constraints on the state since they are fundamental to guarantee safety.

From the above analysis, we can conclude that existing works allow unbounded sequences of packet losses at the price of excluding state constraints, and the other way around. Moreover, aforementioned works (except for [122]) focus only on stabilization, and general tracking problems are not considered. Indeed, while it is possible to generalize existing solutions to consider fixed references, modifications to deal with time-varying set-points are not trivial due to the changes required on the terminal condition.

In this chapter, we aim to overcome these limits. On one side, we adopt the MPC for Tracking, originally devised in [123], and then extended in [124][125]. On the other

side, we adopt a smart actuator to manage the input sequences from the remote MPC. We assume that the smart actuator is able to implement a simple local state feedback controller. The main idea is to use, when the control sequence from the MPC is expired, a local auxiliary tracking law to drive the system to an intermediate safe reference specifically provided by the MPC to be reached in an admissible way. This structure is less general than other existing schemes, e.g. [59], because it requires the sensor and the actuator to be co-located. However, differently from chapter 3, we do not require the system to be stable but we provide the smart actuator with a stabilizing control law to be used only in presence of long blackouts. In this way we get rid of the inner control loop during good channel conditions and an optimal input trajectory can be used. We show that constraints are enforced without any assumption on the network model. Under mild assumptions on the arrival processes and without requiring the number of consecutive packet losses to be bounded, we prove the convergence to any admissible set-points.

4.1 Problem formulation

We consider a discrete-time linear system

$$x_{t+1} = Ax_t + Bu_t \tag{4.1}$$
$$y_t = C_{\text{out}}x_t \tag{4.2}$$

where $x_t \in \mathbb{R}^n$ is the state, $u_t \in \mathbb{R}^m$ is the applied input, and $y_t \in \mathbb{R}^p$ is the system output. The system has to fulfill the set of constraints

$$H(Cx_t + Du_t) \leq h \quad \forall t \geq 0 \tag{4.3}$$

with $C \in \mathbb{R}^{p\times n}$, $D \in \mathbb{R}^{p\times m}$, $H \in \mathbb{R}^{q\times p}$, and $h \in \mathbb{R}^q$.

The objective is to design the input u_t such that the system output y_t tracks a prescribed reference signal r_t and so that the system always satisfies the constraints. To this end, we introduce a remote controller, provided with computational power to tackle the problem of reference tracking under constraints, and a smart actuator, provided with limited computational capabilities and access to the system state. We assume that the smart actuator does not have sufficient computational power to implement the sophisticated control algorithms required to enforce constraints but it is able, if needed, to implement a simple stabilizing law. We assume that the plant and the controller are connected through a network introducing delays and packet loss in the loop. The setup is depicted in Figure 4.1.

Let U_t denote the packet transmitted by the controller during the period $(t-1, t)$, and X_t the packet transmitted by the plant during the period $(t, t+1)$. The packet U_t contains a sequence of $N+1$ future inputs together with the time stamp q_t of the last

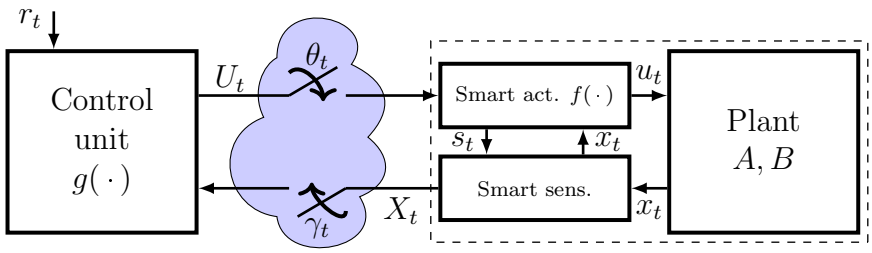

Figure 4.1: Setup. In this chapter the remote control unit is based on MPC.

packet received by the controller

$$U_t = \left\{u_t^t,\, u_{t+1}^t,\, \dots,\, u_{t+N}^t, q_t\right\}. \tag{4.4}$$

In particular, $q_t = k$ if X_k is the most recent packet received by the controller when computing U_t, with $k < t$. Similarly, the packet X_t contains the current state together with the time stamp s_t of the last packet used by the plant

$$X_t = \{x_t,\, s_t\}. \tag{4.5}$$

Specifically, $s_t = k$ if u_t is extracted from the packet U_k, with $k \leq t$. To represent the stochastic behavior of the network, we introduce the arrival process $\theta_t \in \{0, 1\}$ associated to the link from the control unit to the plant, defined as

$$\theta_t = \begin{cases} 1 & \text{if } U_t \text{ is available to the smart actuator at time } t \\ 0 & \text{otherwise,} \end{cases} \tag{4.6}$$

and the arrival process $\gamma_t \in \{0, 1\}$ associated to the link from the plant to the control unit, defined as

$$\gamma_t = \begin{cases} 1 & \text{if } X_t \text{ is available to the control unit to compute } U_{t+1} \\ 0 & \text{otherwise.} \end{cases} \tag{4.7}$$

Arrival processes take into account both random delays and packet losses. In particular, delays are treated as losses if the corresponding packet is not available when required. In order to let the network be as general as possible, at this stage, no assumptions are made on the distribution of γ_t and θ_t.

We define the information available to the plant when applying u_t as

$$\mathcal{I}_t^{\mathrm{P}} = \{\theta_0 U_0,\, \dots,\, \theta_t U_t, x_0,\, \dots,\, x_t, u_0,\, \dots,\, u_{t-1}\}$$

where, with a little abuse of notation, if $\theta_k = 0$ then $\theta_k U_k = \emptyset$. Similarly, we define the

information available to the control unit when computing U_t as

$$\mathcal{I}_t^{\mathrm{C}} = \{U_0, \dots, U_{t-1}, \gamma_0 X_0, \dots, \gamma_{t-1} X_{t-1}\}.$$

Referring to Figure 4.1, we want to design the laws $f(\cdot)$ and $g(\cdot)$

$$u_t = f(\mathcal{I}_t^{\mathrm{P}}) \qquad (u_t^t, u_{t+1}^t, \dots, u_{t+N}^t) = g(\mathcal{I}_t^{\mathrm{C}})$$

such that the constraints are satisfied and the system output y_t tracks the desired reference signal r_t.

In order to solve this problem, in this chapter, we adapt the MPC for Tracking devised in [123] to the considered setup. Before providing the proposed solution, in order to introduce the original algorithm and the notation used, we outline the solution with ideal channels.

4.2 Background: ideal channel

Let $\bar{x}$ denote a steady state, and let $\bar{u}$ and $\bar{y}$ be the corresponding steady-state input and output, respectively. It is possible to characterize the relation between $\bar{x}$, $\bar{u}$, and $\bar{y}$ through the following condition

$$\begin{bmatrix} A-I & B & 0 \\ C & 0 & -I \end{bmatrix} \begin{bmatrix} \bar{x} \\ \bar{u} \\ \bar{y} \end{bmatrix} = \begin{bmatrix} 0 \\ 0 \end{bmatrix}. \tag{4.8}$$

A non-trivial solution exists if and only if (A, B) is stabilizable.

For a given steady-state pair $(\bar{x}, \bar{u})$ and a stabilizing gain K, we introduce the auxiliary (tracking) control law

$$u = \bar{u} + K(x - \bar{x}). \tag{4.9}$$

The evolution of the system (4.1) under (4.9) can be expressed using the extended state $z = (x, \bar{x}, \bar{u})$ and the corresponding auxiliary controlled system

$$z_{t+1} = A_e z_t, \qquad A_e = \left[\begin{array}{c|cc} A + BK & -BK & B \\ 0 & I & \end{array}\right]. \tag{4.10}$$

Similarly, also the constraints (4.3) under the auxiliary law (4.9) can be formulated using the extended state as

$$z_t \in Z \qquad Z = \big\{z = (x, \bar{x}, \bar{u}) : HCx + HD(\bar{u} + K(x - \bar{x})) \leq h\big\}. \tag{4.11}$$

Then, a set S is an *admissible invariant set for tracking* if $S \subseteq Z$ and, if $z \in S$, then

$A_e^k z \in S$ for any $k \geq 0$. The maximal admissible invariant set for tracking is

$$O_\infty = \{z : A_e^k z \in Z,\ k \geq 0\}, \tag{4.12}$$

which corresponds to the Maximal Output Admissible Set for the auxiliary controlled system. As explained in section 3.3, O_∞ is not finitely determined but it is possible to approximate it as closely as desired by a set $\tilde{O}_\infty$ that is finitely determined

$$\tilde{O}_\infty = O_\infty \cap O_\epsilon \qquad O_\epsilon = \{z = (x, \bar{x}, \bar{u}) : (\bar{x}, \bar{x}, \bar{u}) \in (1-\epsilon)Z\} \tag{4.13}$$

with an arbitrary $\epsilon \in (0, 1)$. The set $\tilde{O}_\infty$ is the set of $z = (x, \bar{x}, \bar{u})$ such that the evolution of the original system starting from x with input $u = \bar{u} + K(x - \bar{x})$ is always admissible and such that the steady state satisfies the constraints with a small margin ϵ.

Consider the cost function

$$V(\mathbf{x}, \mathbf{u}, \bar{x}, \bar{u}, \bar{y}, r) = \sum_{k=0}^{N-1} \|x(k) - \bar{x}\|_Q^2 + \|u(k) - \bar{u}\|_R^2 + \|x(N) - \bar{x}\|_P^2 + \|\bar{y} - r\|_T^2 \tag{4.14}$$

with $\mathbf{u} = (u(0), u(1), \ldots, u(N-1))$, $\mathbf{x} = (x(0), x(1), \ldots, x(N))$. The resulting MPC problem $\mathcal{P}(x, r)$ is

$$\begin{aligned} &\min_{\mathbf{u}, \bar{u}, \bar{x}} V(\mathbf{x}, \mathbf{u}, \bar{x}, \bar{u}, \bar{y}, r) \\ &\quad x(k+1) = Ax(k) + Bu(k), \quad x(0) = x, \\ &\quad HCx(k) + HDu(k) \leq h, \quad k = 0, 1, \ldots, N-1, \\ &\quad (x(N), \bar{x}, \bar{u}) \in S, \quad \bar{x},\ \bar{u},\ \bar{y} \text{ satisfy (4.8)}, \end{aligned} \tag{4.15}$$

where S is an admissible invariant set for tracking. Typical choices of S are $\tilde{O}_\infty$, that is the largest possible set, or the singleton $\{(\bar{x}, \bar{x}, \bar{u})\}$, that is the smallest one. In standard MPC for Tracking [123], at each time step t, the optimization problem is solved with initial condition $x = x_t$ and the applied control input u_t is the first element $\mathbf{u}^t(0)$ of the minimizer of the optimization problem. Due to the lossy network, this is not always possible so we modify the procedure to consider the cases when x_t is not available to the controller and when $\mathbf{u}^t(0)$ is not available to the actuator

4.3 Design of the Remote Constrained Controller

Due to the non-zero delay introduced by the communications and the computations, even in ideal channel conditions, the state x_{t+1} is not available at the remote control unit when computing U_{t+1}, but it has to be estimated. When the packet X_t arrives, the estimate $\hat{x}_{t+1|t}$ of x_{t+1} can be derived from x_t and u_t, provided that the latter can be retrieved

from s_t using $f(\cdot)$. However, if the packet X_t has been lost, the controller does not have the knowledge of the applied input and there exists a different estimate for each possible past input sequence. It is then crucial to guarantee that the estimate and the state are consistent, namely obtained with the same past input values, otherwise the future inputs may lead to a constraint violation. To guarantee state consistency we propose to solve the MPC problem using the state estimate obtained as if the last packets transmitted by the controller were applied to the system. Then, the smart actuator is designed to discard the received input sequence in the case that the estimate used to generate it is not consistent with the current state.

We now provide the details of the remote constrained controller. First, the control unit estimates the state as if the last packets transmitted by the controller were arrived. This can be formalized as

$$\hat{u}_{t|t} = \gamma_t u_t + (1-\gamma_t) u_t^t \tag{4.16}$$

$$\hat{x}_{t|t} = \gamma_t x_t + (1-\gamma_t) \hat{x}_{t|t-1} \tag{4.17}$$

$$\hat{x}_{t+1|t} = A\hat{x}_{t|t} + B\hat{u}_{t|t} \tag{4.18}$$

starting from $\hat{u}_{0|0} = u_0$ and $\hat{x}_{0|0} = x_0$. Based on the state estimate, the controller solves the MPC for Tracking problem $\mathcal{P}(\hat{x}_{t|t-1}, r_t)$. Let $\mathbf{u}^t = (\mathbf{u}^t(0), \dots, \mathbf{u}^t(N-1))$, $\bar{u}^t$, $\bar{x}^t$ denote the corresponding minimizers, and denote $\bar{y}^t = C\bar{x}^t$. The law $g(\cdot)$ is defined as

$$u_{t+k}^t = \begin{cases} \mathbf{u}^t(k) & \text{for } 0 \le k < N \\ \bar{u}^t - K\bar{x}^t & \text{for } k = N. \end{cases} \tag{4.19}$$

Note that the first N inputs are directly obtained from the optimal sequence $\mathbf{u}^t$, while the last one wraps the information on the pair $\bar{x}^t, \bar{u}^t$. The sequence u_{t+k}^t is then encapsulated together with the time stamp q_t, iteratively obtained as $q_{t+1} = \gamma_t t + (1-\gamma_t) q_t$.

4.4 Design of the Smart Actuator

As explained in the previous section, in order to guarantee state consistency, the actuator has to decide whether to keep or discard the most recently received sequence by checking if it was obtained with an estimate consistent with the real state. To this end, we introduce a mismatch detection variable Θ_t defined as

$$\Theta_t = \begin{cases} \prod_{k=q_t+1}^{t} \theta_k & \text{if } \theta_t = 1 \\ 0 & \text{otherwise.} \end{cases} \tag{4.20}$$

Note that if $\theta_t = 1$ then q_t is available to the smart actuator and the product can be computed. If the previous packet from the plant has been received by the controller, i.e., $q_t = t - 1$, then $\Theta_t = \theta_t$. On the other hand, if the last ℓ packets from the plant have not been received by the controller, i.e., $q_t = t - \ell$, then $\Theta_t = 1$ if and only if all the previous ℓ packets from the controller have been received. If at least one of them has been lost, the input trajectory used by the estimator and the actual applied input trajectory at the actuator are different: in that case even if $\theta_t = 1$, U_t has to be discarded. Then the sequence U_k to be used is the last one for which $\Theta_k = 1$. The extraction of the suitable input from the suitable sequence can be done using the variable s_t, that is the time stamp corresponding to the input sequence currently applied at the plant. It can be seen as an internal state of the smart actuator and it can be computed as

$$s_t = \Theta_t t + (1 - \Theta_t) s_{t-1}. \tag{4.21}$$

Based on the available input sequences, the input to be applied is derived according to the law $f(\,\cdot\,)$ implicitly defined as

$$u_t = \begin{cases} u_t^{s_t} & \text{if } t - s_t < N \\ u_{s_t+N}^{s_t} + Kx_t = \bar{u}^{s_t} + K(x_t - \bar{x}^{s_t}) & \text{otherwise.} \end{cases} \tag{4.22}$$

When a new sequence is arrived, if not discarded, it is stored and the first input is used. When a packet is lost or discarded, the previous sequence is shifted and the first input is applied. The procedure is iteratively repeated until the sequence is expired, when the last input is held. However, while the first N inputs, if used, are directly applied to the system, the last one is superposed on the state feedback, obtaining the auxiliary tracking law. In that case, the smart actuator becomes de facto a local controller. For this reason it must have access to the measured state. An important exception is when the plant is already stable (possibly thanks to an inner control loop), so that $K = 0$.

4.5 Theoretical properties

We start this section showing that, under the proposed strategy, the estimate is consistent with the actual state.

Lemma 4.1. *If $\Theta_t = 1$, then $x_t = \hat{x}_{t|t-1}$.*

Proof. Let $\tau \leq t$ be such that $\gamma_\tau = 1$ and $\gamma_{\tau+\ell} = 0$ for $0 \leq \ell < L = t - \tau$, namely the last packet has been received by the controller L steps ago. It follows that $q_t = \tau$ and $\hat{x}_{t|t-1} = A^L x_\tau + \sum_{\ell=0}^{L-1} A^{L-1-\ell} B u_{\tau+\ell}^{\tau+\ell}$. Moreover if $\Theta_t = 1$ by definition we have that $\theta_{\tau+\ell} = 1$ for $0 \leq \ell < L$, namely the last L packets has been received by the plant. It follows that $x_t = A^L x_\tau + \sum_{\ell=1}^{L-1} A^{L-1-\ell} B u_{\tau+\ell}^{\tau+\ell}$, so $x_t = \hat{x}_{t|t-1}$. □

Even if, in general, x_t may be different from $\hat{x}_{t|t-1}$, in particular when $\Theta_t = 0$, the previous proposition guarantees that consistency between actual state and estimated one is always guaranteed when it is needed, namely in the time instants when the sequence used by the actuator changes.

Based on the previous lemma, we can show that the proposed strategy is able to guarantee recursive feasibility and constraint satisfaction for any arbitrary network condition. This is in contrast with existing MPC schemes for lossy channels, which require strong assumptions on the network, like perfect acknowledgement [52][121] or a limited number of consecutive packet losses [51],[59],[114]. We first prove the recursive feasibility of the optimization problem.

Proposition 4.1. *Assume there exists a t_0 s.t. $\gamma_{t_0-1} = 1$ and $\theta_{t_0} = 1$. Assume that the optimization problem $\mathcal{P}(x_{t_0}, r_{t_0})$ is feasible. Then, the optimization problem $\mathcal{P}(\hat{x}_{t|t-1}, r_t)$ is feasible for any $t \geq t_0$.*

Proof. The proposition is proved by induction. The basic case holds for t_0 by assumption. Now assume that the problem is feasible for any $\tau < t$. We have three distinct cases: $\gamma_t = 0$, $\gamma_t = 1$ with $\Theta_{t-1} = 1$, and $\gamma_t = 1$ with $\Theta_{t-1} = 0$. When $\gamma_t = 0$, i.e., when the last packet sent by the plant has been lost, the recursive feasibility at time t is shown from the feasibility at time $t-1$ using standard arguments. When $\gamma_t = 1$ and $\Theta_{t-1} = 1$, the proposed logic ensures that $x_t = \hat{x}_{t|t-1}$ according to Lemma 4.1, so the problem is equivalent to the former case with $\gamma_t = 0$. When $\gamma_t = 1$ and $\Theta_{t-1} = 0$, then there exists a $\tau < t$ such that $\Theta_{\tau+\ell} = 0$ for $0 < \ell \leq L = t - \tau$ and $\Theta_\tau = 1$. According to Lemma 4.1, we have $x_\tau = \hat{x}_{\tau|\tau-1}$. By assumption of the inductive argument, the problem is feasible at time τ and it provides the sequence $u^\tau_{\tau+k}$ such that $HCx(k) + HDu^\tau_{\tau+k} \leq h$ with $x(k+1) = Ax(k) + Bu^\tau_{\tau+k}$, $x(0) = \hat{x}_{\tau|\tau-1} = x_\tau$. If $L < N$ then $x_t = x(L)$ and an admissible sequence is given by the remaining $N - L$ inputs from the sequence at time τ and L inputs obtained from the auxiliary law. If $L \geq N$ then $(x_t, \bar{x}^\tau, \bar{u}^\tau) \in S$ and an admissible sequence is given by the auxiliary law. □

From the above proposition, it immediately follows the constraint satisfaction without any assumption on the network.

Proposition 4.2. *Assume there exists a t_0 s.t. $\gamma_{t_0-1} = 1$ and $\theta_{t_0} = 1$. Assume that the optimization problem $\mathcal{P}(x_{t_0}, r_{t_0})$ is feasible. Then, constraints (4.3) are satisfied with probability 1 for any $t \geq t_0$.*

This property is particularly important because it ensures that, no matter how bad is the network quality, the system evolves within the constraints. In practice, the mild assumption is intended to require that the control unit is able to communicate with the plant before it is "too late". In other words, in the period before receiving the first admissible sequence, the plant has to evolve in a safe way without the MPC. As a special

case, feasibility and constraint satisfaction are guaranteed if $x_0 = \bar{x}$, $u_t = \bar{u}$, $t < t_0$, with $(\bar{x}, \bar{x}, \bar{u}) \in \tilde{O}_\infty$, namely if the system is initially in an admissible steady state condition.

Note that, so far, no assumption is required on the reference. In particular, the recursive feasibility under an arbitrary r_t is achieved in the considered framework. This extends the applicability of the proposed solution with respect to most existing algorithms, which require the reference to be fixed (typically, the origin). A simplistic method to employ existing algorithms under time-varying references is to remove the terminal constraint. However, when dealing with lossy networks, this may be critical because, if we do not require the terminal state to belong to an admissible invariant set, after a sufficient long blackout on the uplink, the system can violate the constraints (even if it is provided with the auxiliary stabilizing law) or the optimization problem may become unfeasible, leading to possible future constraint violations.

Provided that recursive feasibility and constraint satisfaction are guaranteed for any reference r_t, it is important to assess the tracking properties of the proposed solution. To this end, we now focus on a constant reference $r_t = r$. We denote the corresponding steady state and input as $(\bar{x}_r, \bar{u}_r)$, $\bar{x}_r = A\bar{x}_r + B\bar{u}_r$, $r = C\bar{x}_r$. The following additional assumptions both on the controller and on the network are made.

Assumption 4.1. The following conditions hold:

1. Q, R, T are positive definite.
2. K is a constant gain s.t. $(A + BK)$ is Hurtwitz.
3. P satisfies $P = (A + BK)'P(A + BK) + Q + K'RK$.
4. $S = \tilde{O}_\infty$.
5. $\Pr(\cap_{t \geq k} \{\gamma_{t-1}\theta_t = 0\}) = 0 \ \forall k \geq 0$.

We have the following result.

Proposition 4.3. *Suppose that Assumption 4.1 holds and that feasibility is guaranteed. Assume that $r_t = r$ and r is such that $(\bar{x}_r, \bar{x}_r, \bar{u}_r) \in (1 - \epsilon)Z$. Then, the system output y_t converges to r with probability 1.*

Proof. In order to prove the proposition, we start with some notation. Since the cost function is evaluated along the trajectory $\mathbf{x}$ and it is completely determined by the input sequence $\mathbf{u}$ and by $x(0)$, we use the notation $V(\mathbf{x}, \mathbf{u}, \bar{x}, \bar{u}, \bar{y}, r) = V(x(0), \mathbf{u}, \bar{x}, \bar{u}, \bar{y})$, where we also drop the dependence on r. Denote the optimal value of the cost function of $\mathcal{P}(x, r)$ as $V^*(x)$. Denote the system evolution driven by the auxiliary tracking law determined by $\bar{x}, \bar{u}$ starting from x as

$$
\begin{aligned}
u(k|x, \bar{x}, \bar{u}) &= \bar{u} + K(x(k|x, \bar{x}, \bar{u}) - \bar{x}) \\
x(k+1|x, \bar{x}, \bar{u}) &= Ax(k|x, \bar{x}, \bar{u}) + Bu(k|x, \bar{x}, \bar{u}).
\end{aligned}
$$

Now introduce the *virtual sequence of future inputs at plant side*, consisting of the remaining inputs from the last received sequence and of the auxiliary tracking law based on the last received intermediate reference. It can be defined as

$$\tilde{\mathbf{u}}_{t+1} = \begin{cases} \mathbf{u}^{t+1} & \text{if } \Theta_{t+1} = 1 \\ (\tilde{\mathbf{u}}_t(1), \dots, \tilde{\mathbf{u}}_t(N-1), \bar{u}^{s_t} + K(x_{t+N} - \bar{x}^{s_t})) & \text{otherwise.} \end{cases}$$

It can be seen as the buffer at the plant side storing the current version of the next N inputs. We call it virtual because in general it is different both from the optimal sequence computed by the MPC and from the sequence that will be applied. Based on the virtual input sequence, we define the virtual value function at the plant side

$$\mathcal{V}(x_t) = V(x_t, \tilde{\mathbf{u}}_t, \bar{x}^{s_t}, \bar{u}^{s_t}, \bar{y}^{s_t}).$$

Now we provide some preliminarily results that will be used in the proof. In particular it is immediate to see that

$$x(k+1|x, \bar{x}, \bar{u}) - \bar{x} = (A + BK)(x(k|x, \bar{x}, \bar{u}) - \bar{x}).$$

Then, due to Item 3 in Assumption 4.1, it can be shown that

$$\begin{aligned} &\|x(k|x, \bar{x}, \bar{u}) - \bar{x}\|_Q^2 + \|u(k|x, \bar{x}, \bar{u}) - \bar{u}\|_R^2 \\ &\qquad = \|x(k|x, \bar{x}, \bar{u}) - \bar{x}\|_P^2 - \|x(k+1|x, \bar{x}, \bar{u}) - \bar{x}\|_P^2 \end{aligned} \tag{4.23}$$

The proof then consists of 3 steps.

Step 1. At each time step we have

$$\begin{aligned} \mathcal{V}(x_{t+1}) &= V(x_{t+1}, \tilde{\mathbf{u}}_{t+1}, \bar{x}^{s_{t+1}}, \bar{u}^{s_{t+1}}, \bar{y}^{s_{t+1}}) \\ &\leq V(x_t, \tilde{\mathbf{u}}_t, \bar{x}^{s_t}, \bar{u}^{s_t}, \bar{y}^{s_{t+1}}) - \|x_t - \bar{x}^{s_t}\|_Q^2 - \|\tilde{\mathbf{u}}_t(0) - \bar{u}^{s_t}\|_R^2 \\ &\leq \mathcal{V}(x_t) - \|x_t - \bar{x}^{s_t}\|_Q^2 \end{aligned}$$

where the first inequality, following from (4.23), is indeed an equality if $\Theta_{t+1} = 0$, while it is an inequality if $\Theta_{t+1} = 1$ since $\mathcal{V}(x_{t+1}) = V^*(x_{t+1})$ and the virtual sequence with $\Theta_{t+1} = 0$ is admissible, thus possibly suboptimal. Since $\mathcal{V}(x_t) \geq 0$, $\mathcal{V}(x_t)$ converges and $\lim_{t \to +\infty} \|x_t - \bar{x}^{s_t}\|_Q^2 \overset{a.s.}{=} 0$.

Step 2. Define the sequence $\{t_k\}$ such that $\Theta_{t_k} = 1$ and $\Theta_t = 0$ for any $t_{k-1} < t < t_k$. It corresponds to the sequence of time instants where the state and the estimate coincide, so $\hat{x}_{t_k|t_k-1} = x_{t_k}$. Moreover, by definition of s_t, we have that $s_{t_k} = t_k$. It follows that $\|\hat{x}_{t_k|t_k-1} - \bar{x}^{t_k}\|_Q^2 = \|x_{t_k} - \bar{x}^{s_{t_k}}\|_Q^2$. Since Item 5 in Assumption 4.1, we have that t_k is defined for any $k \geq 0$, so we can take the limit. From Step 1 we have $\lim_{k \to +\infty} \|\hat{x}_{t_k|t_k-1} - \bar{x}^{t_k}\|_Q^2 \overset{a.s.}{=} 0$.

Applying Lemma 3 in [123] it must be $\lim_{k\to+\infty} \|C\hat{x}_{t_k|t_k-1} - r\|_T^2 \overset{a.s.}{=} 0$ and finally we have $\lim_{k\to+\infty} \|Cx_{t_k} - r\|_T^2 \overset{a.s.}{=} 0$.

Step 3. We have the following chain of inequalities

$$\|C\bar{x}^{s_t} - r\|_T^2 \leq \mathcal{V}(x_t) \leq \|x_t - \bar{x}^{s_t}\|_P^2 + \|C\bar{x}^{s_t} - r\|_T^2$$

where the last inequality, provided by Lemma 2 in [123], holds if $x_t \in \tilde{O}_\infty \cap \{(x, \bar{x}, \bar{u}) : \bar{x} = \bar{x}^{s_t}, \bar{u} = \bar{u}^{s_t}\}$, i.e. when x_t is sufficiently close to $\bar{x}^{s_t}$ s.t. the auxiliary law is admissible. It follows that $\mathcal{V}(x_t)$ asymptotically tends to $\|C\bar{x}^{s_t} - r\|_T^2$ but $\mathcal{V}(x_t)$ converges according to Step 1, so $\|C\bar{x}^{s_t} - r\|_T^2$ converges and also $\|Cx_t - r\|_T^2$ converges. Since it converges to 0 on the subsequence $\{t_k\}$ due to Step 2, we have that it converges to 0 on t, concluding the proof. □

Interestingly, convergence with the proposed algorithm does not require many more assumptions than needed by standard MPC for Tracking. What is additionally required is only Item 5 in Assumption 4.1. However it is very mild since it only requires that there always exists an infinite sequence of instants where two consecutive successful receptions, one per side, occur. Indeed, in the interval between two successful transmissions from the plant, the input sequence used by the actuator changes if and only if the first sequence transmitted by the controller in that interval is received. If it does not happen, all the subsequent packets are not compatible with the actual state, so they are discarded and the system does not converge to r. Similarly, if one of the two links is down from t onward and $C\bar{x}^t \neq r$, then there is no chance the system converges to r. In these cases it is immediate to see that y_t converges to $C\bar{x}^k$ where k is the largest time instant for which $\Theta_k = 1$. Clearly, these situations are very rare in practice, and the assumption is less restrictive than to require the number of consecutive packet losses to be bounded.

4.6 Simulations: assessment of the proposed strategy

In this section, we assess the performances of the proposed strategy for different control design parameters through simulations. Since the terminal condition is strictly related to the safety against blackouts, it is interesting to test different terminal sets S.

As for the channel, the arrival processes γ_t and θ_t are modeled as independent and identically distributed random variables with Bernoulli distribution and constant mean $\mathbb{E}[\gamma_t] = \mathbb{E}[\theta_t] = 0.25$.

As for the plant, we simulate the unstable linearized model of the Segway described in Appendix A.2 with sampling period $T = 10$ ms. In particular, matrices C, D, H, and h are set to take into account the limits on the input fed to the motors, that is required to remain in the interval $[-11\text{ V}, 11\text{ V}]$, and the safety constraints on the tilt angle, that is required to remain in the interval $[-0.1\text{ rad}, 0.1\text{ rad}]$.

We set the control parameters as $R = 1$, $Q = \text{diag}\{10, 1000, 1, 1\}$, $T = 10P$, and P as in Item 3 of Assumption 4.1. We consider two possible terminal sets. On one hand, we choose $S = \tilde{O}_\infty$, that is the largest terminal set possible and guarantees the convergence to the any admissible set-point. In this case, we set $N = 50$. On the other hand, we restrict the terminal state $x(N)$ to be equal to the steady-state $\bar{x}$. Clearly, we need also to require $HC\bar{x} + HD\bar{u} \leq h$, equivalent to $(\bar{x}, \bar{x}, \bar{u}) \in Z$, so that the steady-state is admissible. Note that, if we further reduce the terminal set by the small quantity ϵ, namely we impose the terminal conditions $(x(N), \bar{x}, \bar{u}) \in (1 - \epsilon)Z$, the terminal set S is equivalently described by the conditions $(x(N), \bar{x}, \bar{u}) \in \tilde{O}_\infty$ and $x(N) = \bar{x}$. This more clearly shows the reduction on the possible terminal states introduced in the latter case. Since the system state needs to be driven at the equilibrium at the end of the horizon, the control sequence is usually less aggressive and system response is slower. For this reason, in this case, we set $N = 100$. In the case with ideal communications, for the system at hand, the two solutions have very similar performances.

The system responses under the channel evolution of Figure 4.2 are reported in Figure 4.3. As we can see in the top panel, the controller designed with $S = \tilde{O}_\infty$ converges faster to the desired reference. In fact, during blackouts, subsequents elements of the control sequence are used and, for the case with $x(N) = \bar{x}$, they drive the system to the equilibrium in N steps. Therefore, the system slows down. This can be seen also in the bottom panel, since an higher tilt angle corresponds to an higher speed. It is worth mentioning that both the designs are able to satisfy the constraints even in presence of packet loss. This confirms that the proposed strategy is able to guarantee safety of the system.

4.7 WiFi-in-the-loop simulations: comparisons

In this section, we test the proposed MPC for Tracking in a WiFi-in-the-loop setup. We consider the Segway-like robot described in Appendix A.2 with sampling period $T = 5$ ms. Differently from section 3.8, we do not include the inner stabilizing loop, so the open-loop system is unstable. The simulation comprises the complete nonlinear model of the plant, including the non-ideliaties of sensors (quantization) and actuators (saturation), and real Wi-Fi communication data collected with the experimental setup of Appendix A.3. We use the same realization used in section 3.8.

We compare the proposed solution with the standard Networked MPC adapted from [59], detailed in section 3.8. The main idea of [59] is to postpone the initial point of the optimization problem τ steps ahead in order to be robust against up to τ consecutive packet losses.

The constrained control algorithms are designed on the linearized model of the robot. We consider the constraints on the tilt angle and on the input fed to the motors. For both

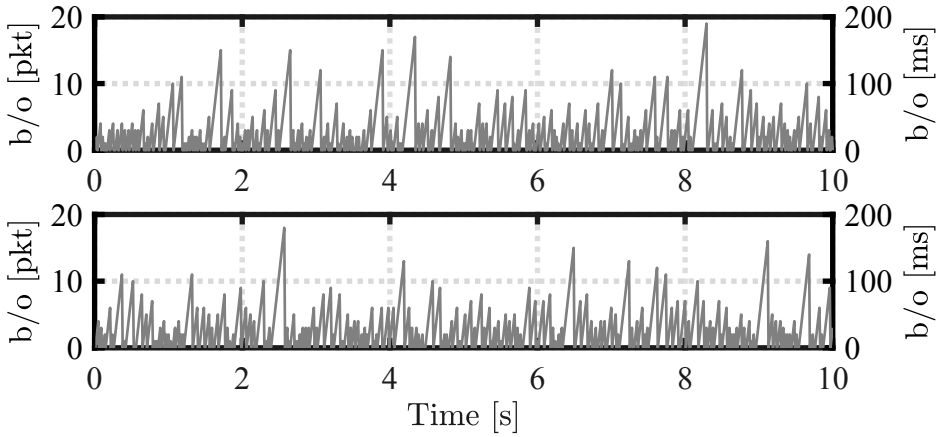

Figure 4.2: Blackouts (b/o). Top: uplink. Bottom: downlink

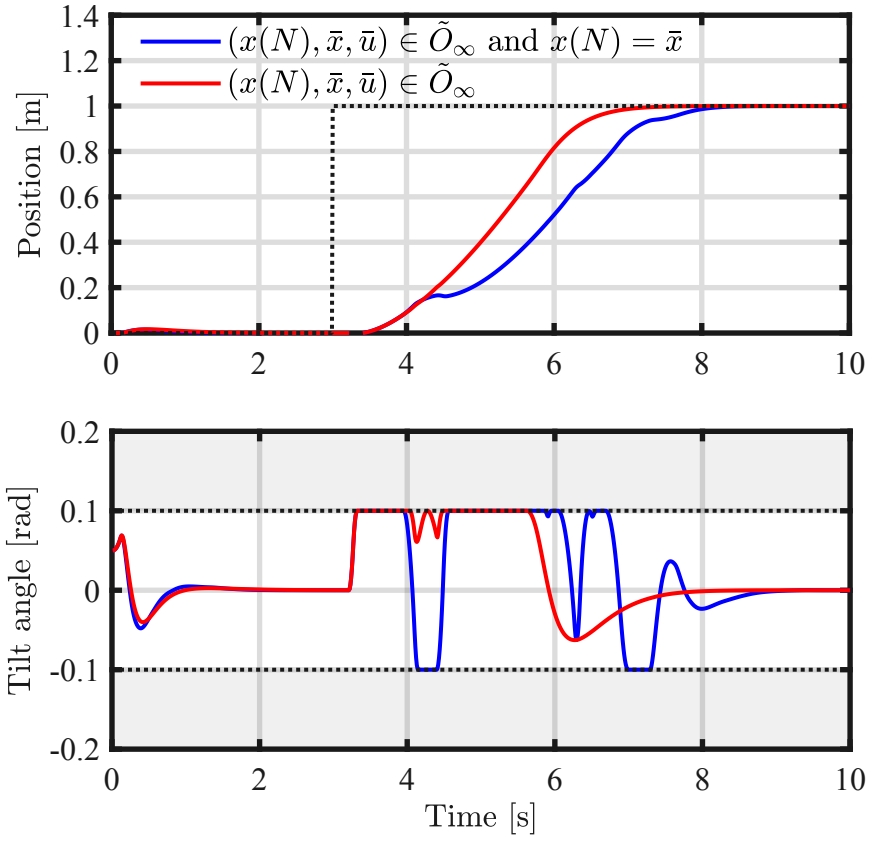

Figure 4.3: System response with simulated channels. Comparison between different terminal set S. Choosing a larger terminal set improves the performances when packet loss is present.

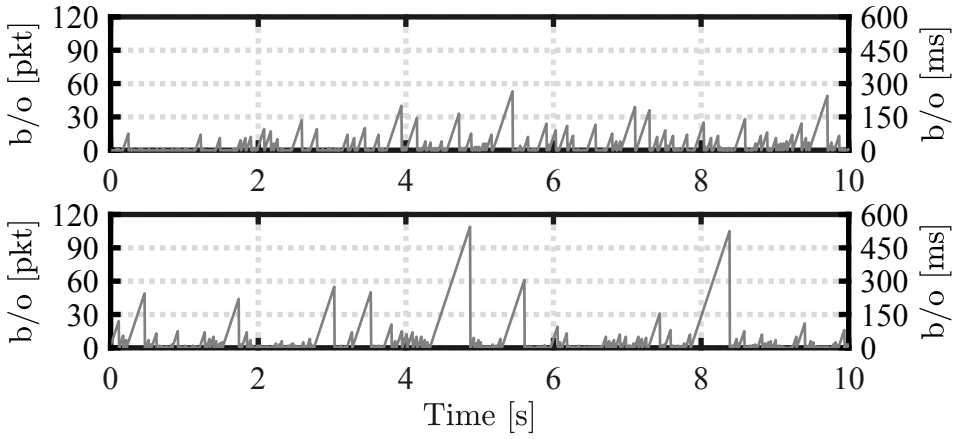

Figure 4.4: Blackouts (b/o). Top: uplink. Bottom: downlink

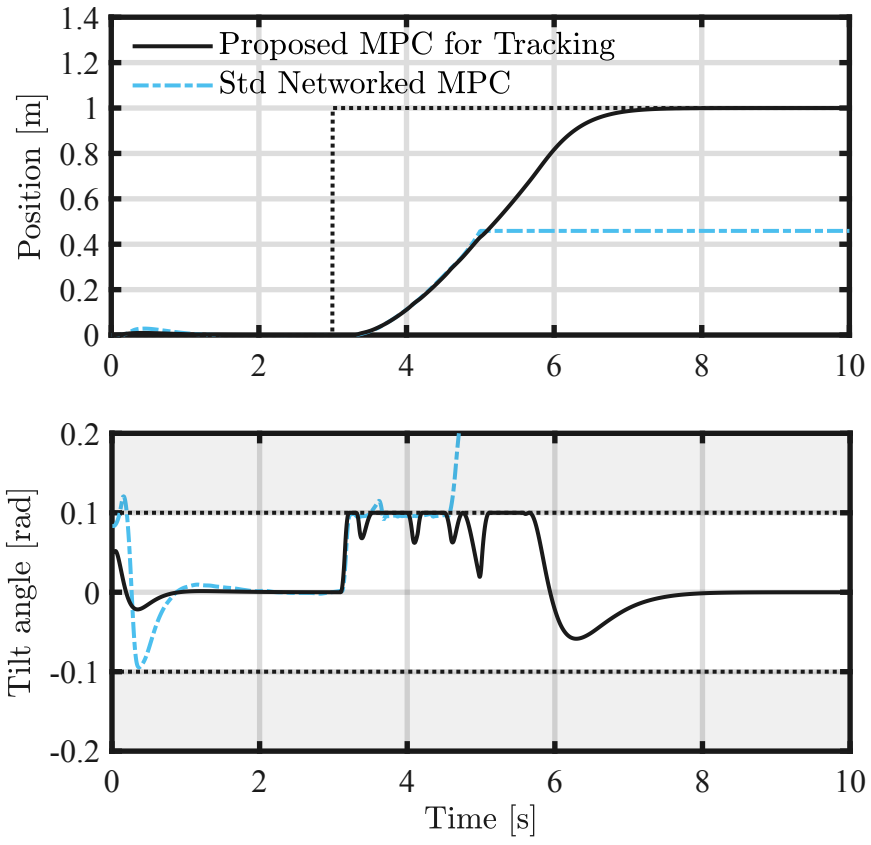

Figure 4.5: System response with WiFi-in-the-loop setup. Comparison between proposed solution and standard Networked MPC [59]. Due to long blackouts, the Segawy falls when controlled by standard Networked MPC.

the algorithms we set $N = 50$, $R = 1$, $Q = \text{diag}\{10, 1000, 1, 1\}$, and P as in Item 3 of Assumption 4.1. For the proposed algorithm, we set $K = -(B'PB+R)^{-1}BPA$, $T = 10P$, an terminal condition $S = \tilde{O}_\infty$. For the standard Networked MPC, we set $\tau = 30$ and we do not include terminal constraints to easily manage time-varying reference. When infeasible, the problem is relaxed converting the hard constraints into soft ones. In this chapter, computational time is neglected. This is a crucial point since the MPC problem may be not always solved in the prescribed period. Nevertheless, note that a violation of the required execution time can be treated as a packet loss.

In Figure 4.4, reporting the blackout lengths, we can see that the bound τ is violated. Consequently, the standard Networked MPC does no more guarantee constraint satisfaction and, in fact, as shown in Figure 4.5, the bound on the tilt angle is immediately violated. Later in the simulation, due to other long blackouts, the segway falls down: the robot lays horizontally (the tilt angle is equal to $\pi/2$) and cannot proceed anymore. Conversely, the proposed strategy always satisfies the constraints despite the packet losses. Roughly speaking this is achieved by "slowing down": during blackouts, instead of proceeding forward with the maximum tilt angle allowed, namely at the maximum speed, the tilt angle decreases, indicating that the Segway robot starts to stop. This behavior implies that the settling time is approximately 0.5 s slower than in the ideal scenario, but safety is guaranteed. Other WiFi-in-the-loop tests with a different sampling period and different channel conditions can be found in [126].

4.8 Conclusion

In this chapter, we have proposed an algorithm based on MPC for tracking reference signals under constraints and over wireless. We have shown that constraints are satisfied for arbitrary channel condition, and we have shown that the desired signal is tracked under mild requirements. WiFi-in-the-loop experiments have confirmed that constraints are always satisfied even under severe noise conditions and have shown the validity of the proposed strategy for industrial and safety-critical applications. With respect to the RG devised in chapter 3 we do not explicitly require the open-loop system to be stable, but we require the smart actuator to have access to the system state in order to apply an auxiliary law during blackouts. For simple constant reference tracking problems, the performances of the proposed RG and of the proposed MPC for Tracking are comparable, as indicated by the WiFi-in-the-loop tests. However, MPC for Tracking has more degrees of freedom than RG, so we expect better performances in more challenging tasks. Nonetheless, differently from RG presented chapter 3, the presented MPC is not conceived for systems with disturbances. To generalize the presented solution to the case with bounded disturbances we can employ the Tube-based MPC for Tracking [124]. Similarly to chapter 3, this requires to add an inner control loop always activated.

5

Reference Governor for Multi-Agent Systems

Many interesting and trending control applications comprise multiple spatially distributed sensors and actuators. For instance, in cooperative robotics, the actuators are physically located on the different agents, and the sensors as well. In those applications, wired connections to put into communication the agents are usually an annoying obstacle, especially with drones and mobile robots. To date, to avoid wired links, there exist mainly three alternatives. First, a solution with (almost) *no communication* can be used. In this case, each agent is provided with an off-line suitable reference trajectory to be followed independently of the other agents. This solution is however not robust, since no feedback from the other agents is used, and it is probably conservative. A second solution makes use of *implicit communications*. In this case, each agent is equipped with an advanced sensing apparatus that allows to (partially) measure the state of the other agents. Depending on the application, typical examples are cameras to retrieve positions and relative angles, time-of-flight sensors to retrieve the distance, and force sensors to retrieve the force applied by the other agents. Typical algorithms are [127][128]. With this solution, a desired reference trajectory is provided to some special agents, called leaders, that have to track it, while the remaining agents, called followers, are in charge to follow the leaders according to a prescribed local control law. This solution is definitely more robust than the solution with no communications but still some drawbacks are present. In fact, the overall performances are limited by the computational capabilities on-board and by the accuracy of the sensors. More importantly, only information on the current state can be obtained through sensors and no knowledge on the future intentions can be exploited. This limit can be overcome only using explicit communications. In fact, the third alternative employs *wireless communications*. With this solution, both the state and the future inputs can be transmitted and performances can be improved using predictive strategies. Both centralized [129][130] and distributed algorithms [131][132] are available in the literature. To date, most of the control algorithms that consider communications in multi-agent systems makes the assumption that the links are ideal. Indeed, when slow communication rates are used (less than 10 transmissions per second),

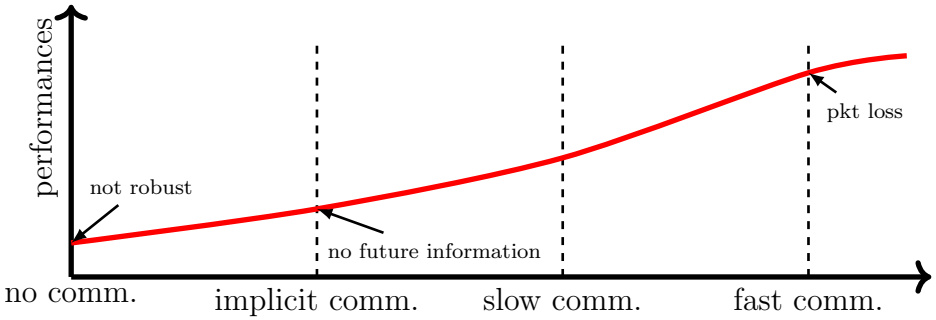

Figure 5.1: Qualitative expected performances for the different solutions.

transmissions are usually quite reliable and packet losses can be neglected. This solution is satisfactory in several applications characterized by slow dynamics, like HVAC systems in buildings. On the other hand, this can be limiting in systems that require small sampling periods, like cooperative robotics. To push the performances to the limit, we need to use fast communications, which may introduce both packet losses and blackouts. The control algorithm has to be modified to take into account them. The benefits of fast wireless networks in multi-agent mobile manipulation have been shown e.g. in [75], but packet losses have not been considered so far. A pictorial representation of the expected performances for the different solutions is reported in Figure 5.1.

In this chapter, we propose a first solution to the problem of control of multi-agent systems with packet loss and constraints starting from the RG presented in chapter 3. In the literature, only a handful of works considers a similar problem. The work [103] proposes two centralized solutions that explicitly take into account (possibly unbounded) delays due to the communication network, but they require resynchronization procedures and they are computationally demanding. The work [133] devises a sequential distributed RG scheme where only an agent for time instant is allowed to update its input. The work [134] extends the solution of [133] using the graph colorability theory. According to [134], agents with decoupled dynamics and constraints, colored in the same way, are allowed to update the input simultaneously. The turn-based approach of [133] can be suitable to avoid the cases where an admissible input leads to a constraint violation because applied only by some actuators. However, solutions [133][134] do not take into account packet losses.

The proposed solution is a suitable extension of RG presented in chapter 3 with features of [133] to solve the multi-agent constrained control problem with wireless communication. Suitable strategies have been introduced to deal with the fact that actuators are spatially distributed, so the new input may be only partially applied due to packet losses. Recursive feasibility and constraint satisfaction have been proved without any assumption on the network. Convergence to a desired constant set-point is guaranteed under very mild hypothesis on the network and with small conservativeness introduced on the set of

admissible inputs. Simulations show that the proposed strategy is better than the solution with implicit communication (even with ideal hardware) and than the solution with slow (ideal) communications.

5.1 Problem formulation

We consider a set of N_A spatially distributed actuators and a set of N_S spatially distributed sensors. This generalizes the case of $N = N_A = N_S$ agents, each one equipped with a local sensor and a local actuator, to include the cases where additional sensors are present e.g. on the load or in the environment. We denote

$$x(t) = \begin{pmatrix} x_1(t) \\ x_2(t) \\ \cdots \\ x_{N_S}(t) \end{pmatrix} \quad u(t) = \begin{pmatrix} u_1(t) \\ u_2(t) \\ \cdots \\ u_{N_A}(t) \end{pmatrix} \tag{5.1}$$

where $x(t) \in \mathbb{R}^n$ is the system state, with $x_i(t) \in \mathbb{R}^{n_i}$, and $u(t) \in \mathbb{R}^m$ is the system input, with $u_i(t) \in \mathbb{R}^{m_i}$. Accordingly, sensor i has direct access to $x_i(t)$, while actuator i directly manipulates $u_i(t)$. The system is modeled as

$$x(t+1) = Ax(t) + Bu(t). \tag{5.2}$$

We assume that all the eigenvalues of the matrix A are strictly inside the unitary circle. The system has to fulfill the constraints

$$y(t) \in Y \tag{5.3}$$

where $y(t) \in \mathbb{R}^c$ is the constrained output defined as

$$y(t) = Cx(t) + Du(t) \tag{5.4}$$

and $Y \subset \mathbb{R}^c$. We assume that the pair (A, C) is observable and that Y is closed containing the origin.

The objective is to design the input $u(t)$ such that the system output $y_{\text{out}}(t) = C_{\text{out}}x(t)$ tracks a prescribed desired reference signal $r(t)$ while enforcing the constraints $y(t) \in Y$. For sake of simplicity, we assume that $C_{\text{out}}(I - A)^{-1}B = I$ and we consider the simplified problem where the input $u(t)$ has to follow the desired reference $r(t)$.

We propose to solve the problem through a central control unit and to use a shared wireless network to connect the control unit with the actuators and the sensors. Specifically, the wireless network is used for transmissions 1) from the sensors to the control unit, 2) from the control unit to the actuators, and 3) from the actuators back to the

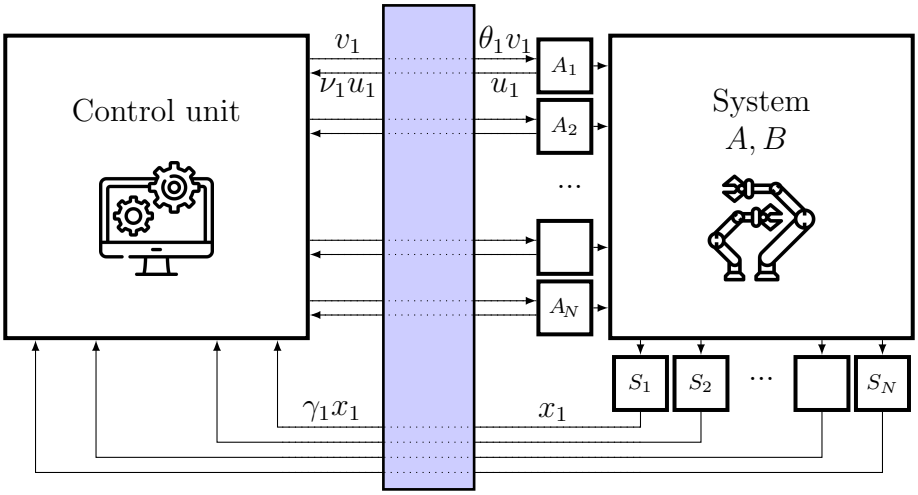

Figure 5.2: Setup. The blue box represents a shared wireless network.

control unit. The latter is equivalent to the acknowledgment of the transmissions from the control unit to the actuators. In line of principle, we would like that all the communications take place during each sampling period with success. However, this may overload the network and deteriorate the performances. To avoid this problem a suitable transmission scheduling algorithm may be studied. We do not consider this problem in this chapter.

At each time step, the central control unit computes the input $v(t) = (v_1'(t), \cdots, v_{N_A}'(t))'$, with $v_i(t) \in \mathbb{R}^{m_i}$, based on the estimate of the state $x(t)$ and on the desired reference $r(t) = (r_1'(t), \cdots, r_{N_A}'(t))'$, $r_i(t) \in \mathbb{R}^{m_i}$. However, since the wireless network introduces delays and packet losses in the loop, the input $u(t)$ can not be readily manipulated according to $v(t)$ and the control unit has not direct access to the state $x(t)$ of the system. More specifically, we assume that, at time instant t, the sensor i transmits the measure $x_i(t)$ and we introduce the arrival process $\gamma_i(t) \in \{0, 1\}$ defined as

$$\gamma_i(t) = \begin{cases} 1 & \text{if } x_i(t) \text{ is available to the control unit to compute } v(t+1) \\ 0 & \text{otherwise.} \end{cases} \tag{5.5}$$

This definition captures also the case where the transmission of $x_i(t)$ is not scheduled, opportunely setting $\gamma_i(t) = 0$. Also actuators communicate to the control unit the current applied input. To model this, we introduce the arrival process $\nu_i(t) \in \{0, 1\}$ defined as

$$\nu_i(t) = \begin{cases} 1 & \text{if } u_i(t) \text{ is available to the control unit to compute } v(t+1) \\ 0 & \text{otherwise.} \end{cases} \tag{5.6}$$

Finally, we assume that, during the period between time instant $t-1$ and time instant t, just after the computation, the control unit transmits $v_i(t)$ and we introduce the arrival

process $\theta_i(t) \in \{0, 1\}$ defined as

$$\theta_i(t) = \begin{cases} 1 & \text{if } v_i(t) \text{ is available to the actuator } i \text{ at time } t \\ 0 & \text{otherwise.} \end{cases} \tag{5.7}$$

Based on the arrival processes, we define the information available to the central control unit when computing $v(t)$ as

$$\begin{aligned} \mathcal{I}^{\mathrm{C}}(t) = \big\{v(0), \cdots, v(t-1)\big\} \cup \big\{\gamma_i(0)x_i(0), \cdots, \gamma_i(t-1)x_i(t-1) \,:\, i \in \{1, \dots, N_S\}\big\} \\ \cup \big\{\nu_i(0)u_i(0), \cdots, \nu_i(t-1)u_i(t-1) \,:\, i \in \{1, \dots, N_A\}\big\} \end{aligned}$$

while we define the information available to actuator i at time instant t as

$$\mathcal{I}_i(t) = \big\{u_i(0), u_i(1), \cdots, u_i(t-1)\big\} \cup \big\{\theta_i(0)v_i(0), \cdots, \theta_i(t-1)v_i(t-1)\big\}$$

for any $i \in \{1, \dots, N_A\}$. Then, we are interested in the problem of designing the laws $f_i(\,\cdot\,)$ and $g(\,\cdot\,)$

$$u_i(t) = f_i(\mathcal{I}_i(t)) \qquad v(t) = g(\mathcal{I}^{\mathrm{C}}(t)) \tag{5.8}$$

for $i \in \{1, \dots, N_A\}$ such that constraints (5.3) are satisfied.

5.2 Design of the Smart Actuators

The first step is to design the laws $f_i(\,\cdot\,)$ implemented at the smart actuators. As done in the single-agent case of chapter 3, the function $f_i(\,\cdot\,)$ is a simple Zero-Order Hold that keeps the current value until a new packet arrives

$$u_i(t) = \theta_i(t)v_i(t) + (1 - \theta_i(t))u_i(t-1). \tag{5.9}$$

5.3 Design of the Actuator Scheduler

With respect to the single-agent case, the problem is more difficult due to the presence of multiple channels. The peculiar issues of the considered problem can be summarized in two points: 1) if a new input is computed to be admissible if applied by all the actuators, constraints may be violated in situations where the packet has been received and used only by some actuators, 2) when a new input is sent but no information is received back at the control unit, the number of possible states doubles, thus it grows exponentially with the number of consecutive packet losses in the link from each actuator to the control unit. To solve these problems, we propose to consider a smart Actuator Scheduler.

To solve problem 1), similarly to the single-agent case, we propose to design $v_i(t)$ to

be robust for any possible $u_j(t)$, $j \neq i$. However, this would require that the system evolutions for all the 2^{N_A} possible combinations of $u_i(t)$ satisfy the constraints, and the corresponding problem may be cumbersome. For this reason, taking inspiration from [133], we propose to use an asynchronous approach where, at each time instant t, only the input $v_i(t)$ for the actuator i is computed, while other inputs are not changed. To formalize this solution, we introduce the binary selection variable $\alpha_i(t) \in \{0, 1\}$ defined as

$$\alpha_i(t) = \begin{cases} 1 & \text{if actuator } i \text{ is selected at time } t \\ 0 & \text{otherwise.} \end{cases} \tag{5.10}$$

Then, the asynchronous approach is characterized by the constraint

$$\sum_{i=1}^{N_A} \alpha_i(t) \leq 1. \tag{5.11}$$

Then, the input $v_i(t)$ is computed and transmitted if $\alpha_i(t) = 1$, while it is not if $\alpha_i(t) = 0$. In this sense, $\alpha_i(t)$ regulates both the computation and the transmissions. Accordingly, we always have $\theta_i(t) = 0$ if $\alpha_i(t) = 0$. Technically, for actuators such that $\alpha_i(t) = 0$, $v_i(t)$ can be set equal to any value because, since it is not transmitted, it does not have any effect.

According to the asynchronous approach, any agent can be chosen at any time instant. However, the number of possible states depends on the number of past transmitted inputs that have not been followed by a packet received at the control unit so far. That is, if L inputs have been transmitted to actuator i during a period in which no packet from i has been received, the number of possible states is at least 2^L. Then, to solve problem 2), we propose to compute a new input $v_i(t)$ only for actuators whose applied input $u_i(t-1)$ is known. This limits the number of possible states to be equal to 2^{N_A} in the worst case, but in general much smaller, and even equal to 1 in good channel conditions.

To formalize this solution we introduce an eligibility variable $\beta_i(t) \in \{0, 1\}$ defined as

$$\beta_i(t) = \begin{cases} 1 & \text{if } \nu_i(t) = 1 \\ 0 & \text{if } \nu_i(t) = 0 \text{ and } \alpha_i(t-1) = 1 \\ \beta_i(t-1) & \text{if } \nu_i(t) = 0 \text{ and } \alpha_i(t-1) = 0 \end{cases} \tag{5.12}$$

It is easy to see that, if $\beta_i(t) = 1$, then the applied input $u_i(t-1)$ is known at the control unit. So, the actuator i can be selected at time t only if $\beta_i(t) = 1$. Equivalently, we can introduce the counter $\Delta_i(t)$, defined as the period elapsed since the last known applied input at the actuator i. It can be recursively obtained as

$$\Delta_i(t) = (1 - \beta_i(t))(\Delta_i(t) + 1) \tag{5.13}$$

Then, the actuator i can be selected at time t only if $\Delta_i(t) = 0$.

Finally, the actuator scheduling is obtained through the following optimization problem

$$\alpha(t) = \arg\min_{\alpha} \mathcal{C}(\alpha) \tag{5.14}$$

$$\text{s.t.} \sum_{i=1}^{N_A} \alpha_i \leq 1 \tag{5.15}$$

$$\sum_{i=1}^{N_A} (1 - \beta_i(t))\alpha_i = 0 \tag{5.16}$$

where $\mathcal{C}(\,\cdot\,)$ is a suitable cost function. The first constraint imposes that at most an actuator is selected. The second constraint imposes that only eligible actuators are chosen. In the following, we choose as cost $\mathcal{C}(\alpha)$ the linear function $\sum_{i=1}^{N_A} c_i\alpha_i$, where we set c_i equal to the number of steps since the last time α_i was equal to 1. In this way, we implement a modified round-robin allocation protocol. More sophisticated functions, possibly state dependent, can be designed following e.g. [135][136].

5.4 Design of the State Estimator

For sake of clarity, we preliminarily introduce a set of buffers $U_i^{0:t}$, containing the past known inputs of actuator i. Specifically, the buffer $U_i^{0:t}$ is recursively obtained by adding an entry at the end of $U_i^{0:t-1}$, starting from $U_i^{0:0} = u_i(0)$. If $\nu_i(t) = 1$, then the last $\Delta_i(t-1)+1$ entries of the buffer are set equal to $u_i(t)$. If $\nu_i(t) = 0$, the last entry of $U_i^{0:t}$ is set equal to the last entry of $U_i^{0:t-1}$, eventually keeping it empty if no value was present. It is easy to see that only the last $\Delta_i(t)$ entries may be empty and they are filled as soon as $\nu_i(t) = 1$, while the first $t - \Delta_i(t) + 1$ entries contain the sequence $u_i(k)$ for k from 0 to $t - \Delta_i(t)$.

In order to obtain any possible current state, we need to store also the sequences of non-acknowledged inputs of any actuator. To this end we introduce

$$\hat{u}_i^+(t) = \nu_i(t)u_i(t)+\alpha_i(t)(1-\nu_i(t))v_i(t)+(1-\alpha_i(t))(1-\nu_i(t))\hat{u}_i^+(t-1) \tag{5.17}$$

$$\hat{u}_i^-(t) = \nu_i(t)u_i(t) + (1 - \nu_i(t))\hat{u}_i^-(t-1) \tag{5.18}$$

stating from $\hat{u}_i^+(t) = \hat{u}_i^-(t) = u_i(0)$. They represent the two possible inputs applied at actuator i. We now split the problem of obtaining the state estimate in two parts: we first compute the (unique) estimate of the state at the last time instant for which the applied inputs are known, and then we compute all the estimates of the possible current states obtained from any possible past input trajectory.

5.4.1 Estimate up to the last known applied input

When computing $v(t)$, we obtain $\hat{u}(k) = (\hat{u}_1'(k), \dots, \hat{u}_{N_S}'(k))'$ from the buffers $U_i^{0:t-1}$ as

$$\hat{u}_i(k) = U_i^{0:t-1}(k) \tag{5.19}$$

for k from $t-1-\Delta(t-1)$ to $t-1-\Delta(t)$. The state is estimated according to the following standard recursive procedure

$$\hat{x}(k|k) = \begin{bmatrix} \gamma_1(k) & 0 & 0 \\ 0 & \cdots & 0 \\ 0 & 0 & \gamma_N(k) \end{bmatrix} x(k) + \begin{bmatrix} 1-\gamma_1(k) & 0 & 0 \\ 0 & \cdots & 0 \\ 0 & 0 & 1-\gamma_N(k) \end{bmatrix} \hat{x}(k|k-1) \tag{5.20}$$

$$\hat{x}(k+1|k) = A\hat{x}(k|k) + B\hat{u}(k) \tag{5.21}$$

for k from $t-1-\Delta(t-1)$ to $t-1-\Delta(t)$. Note that, at each time instant, this procedure is iterated from $\hat{x}(t-1-\Delta(t-1)|t-2-\Delta(t-1))$, obtained at the previous time instant, to $\hat{x}(t-\Delta(t)|t-1-\Delta(t))$. At the first time instant, the procedure is initialized at $\hat{u}(0) = u(0)$, $\hat{x}(0|0) = x(0)$. When $\Delta(t) = \Delta(t-1)+1$ no steps are performed while, in general, $\Delta(t-1)+1-\Delta(t)$ steps are performed. If $\Delta(t) = 0$, this procedure returns $\hat{x}(t|t-1)$.

5.4.2 Estimates compatible with the possible inputs

When computing $v(t)$, $\hat{x}(t-\Delta(t)|t-1-\Delta(t))$ is given by the previous procedure. To efficiently obtain any possible current state we keep updated the following three quantities

$$\hat{z}_i^0(t) = \sum_{\ell=\Delta_i(t)}^{\Delta(t)-1} A^{\Delta_i(t)} A^{\ell} B_i \hat{u}_i(t-1-\ell) \tag{5.22}$$

$$\hat{z}_i^+(t) = \sum_{\ell=0}^{\Delta_i(t)-1} A^{\ell} B_i \hat{u}_i^+(t-1-\ell) \tag{5.23}$$

$$\hat{z}_i^-(t) = \sum_{\ell=0}^{\Delta_i(t)-1} A^{\ell} B_i \hat{u}_i^-(t-1-\ell) \tag{5.24}$$

with $B_i = B\mathbf{1}_i$ where $\mathbf{1}_i \in \mathbb{R}^{n \times m_i}$ is equal to $\mathbf{1}_i = (0, 0, I_{m_i}, 0, 0)'$. The first term represents the forced response of the system at time t due to the input sequence $\hat{u}_i(t-1-\ell)$ at actuator i, ℓ from $\Delta_i(t)$ to $\Delta(t)-1$, while keeping the input of all the other actuators to 0. Recalling that $\hat{u}_i^+(t-1-\ell) = v(t-\Delta_i(t))$ and $\hat{u}_i^-(t-1-\ell) = u(t-1-\Delta_i(t))$ for ℓ from 0 to $\Delta_i(t)-1$, the terms $\hat{z}_i^+(t)$ and $\hat{z}_i^-(t)$ represent the forced responses of the system at time t under the two possible input sequences applied at actuator i starting from $t-\Delta_i(t)$.

Note that $\hat{z}_i^+(t)$ and $\hat{z}_i^-(t)$ are 0 if $\Delta_i(t) = 0$, while $\hat{z}_i^0(t) = 0$ if $\Delta_i(t) = \Delta(t)$. We can use them to retrieve

$$\hat{x}_i^+(t) = \hat{z}_i^0(t) + \hat{z}_i^+(t) \tag{5.25}$$

$$\hat{x}_i^-(t) = \hat{z}_i^0(t) + \hat{z}_i^-(t) \tag{5.26}$$

that represent the two possible forced responses of the system at time t under the two possible input sequences applied at actuator i starting from $t - \Delta(t)$. These quantities will be used to retrieve in a efficient way any possible state compatible with the available information to the control unit.

Let $\Lambda = (\lambda_1, \ldots, \lambda_{N_A})$ be a binary sequence of length N_A. We define

$$\hat{x}(t, \Lambda) = A^{\Delta(t)}\hat{x}(t - \Delta(t)|t - 1 - \Delta(t)) + \sum_{i=1}^{N_A} \lambda_i \hat{x}_i^+(t) + (1 - \lambda_i)\hat{x}_i^-(t) \tag{5.27}$$

$$\hat{u}(t, \Lambda) = \sum_{i=1}^{N_A} \mathbf{1}_i(\lambda_i \hat{u}_i^+(t) + (1 - \lambda_i)\hat{u}_i^-(t)) \tag{5.28}$$

Varying Λ we get any possible pair of state and input that is compatible with available information at the control unit.

5.5 Design of the Remote Constrained Controller

To be robust against arbitrarily long blackouts, we propose to design $v(t)$ such that, if kept constant, the predicted evolution of the system over the infinite horizon will satisfy the constraints. This will be achieved using the Maximal Output Admissible Set (MOAS) and adapting the standard RG for the considered case. We now recall the MOAS already introduced in section 3.2. Denote

$$\hat{x}(k|x, u) = A^k x + \sum_{\ell=0}^{k-1} A^{k-\ell-1} B u. \tag{5.29}$$

Then, the MOAS is defined as

$$O_\infty = \{(x, u) : C\hat{x}(k|x, u) + Du \in Y \ \forall k \geq 0\}. \tag{5.30}$$

Since, in general, it is not finitely determined, we consider the inner approximation $\tilde{O}_\infty$ obtained as

$$\tilde{O}_\infty = O_\infty \cap O_\epsilon \qquad O_\epsilon = \{(x, u) : C(I - A)^{-1}Bu + Du \in (1 - \epsilon)Y\}. \tag{5.31}$$

The set $\tilde{O}_\infty$ is the set of pairs (x, u) for which the evolution of the system starting from x with input u is always admissible and such that the steady state satisfies the constraints with a small margin ϵ. Under mild technical assumptions, $\tilde{O}_\infty$ is compact, finitely determined, and positively invariant, see section 3.3.

Let i be such that $\alpha_i(t) = 1$. The input $v_i(t)$ is obtained by solving the optimization problem expressed as

$$v_i(t) = \arg\min_v \|r_i(t) - v\|^2_{Q_i} \tag{5.32}$$

$$\text{s.t. } (\hat{x}(t, \Lambda), \hat{u}(t-1, \Lambda) + \mathbf{1}_i(v - \hat{u}_i(t-1, \Lambda)) \in \tilde{O}_\infty \quad \forall \Lambda \in \{0, 1\}^N \tag{5.33}$$

The law $f(\,\cdot\,)$ can be implicitly expressed as the concatenation of the optimization problems (5.14) and (5.32).

5.6 Theoretical properties

In this section we prove the main theoretical properties of the proposed solution. In particular, we show that the optimization problem is recursively feasible, constraints are satisfied with probability 1, and the system converges to the desired set-point.

For easy of notation let $N_A = N$ and denote $a_i^U(t)$ the period elapsed at the current time instant t since the last time the input at actuator i has been computed. We start with the following preliminary lemma.

Lemma 5.1. *Let $\Lambda = (\lambda_1, \dots, \lambda_i \dots, \lambda_N) \in \{0, 1\}^N$ and $\bar{\Lambda} = (\bar{\lambda}_1, \dots, \bar{\lambda}_i \dots, \bar{\lambda}_N) \in \{0, 1\}^N$. If $\bar{\lambda}_i = (1 - \nu_i(t))\lambda_i + \nu_i(t)\theta_i(t - a_i^U(t))$ for any $i \in \{1, \dots, N\}$, then it holds that*

$$\hat{x}(t+1, \Lambda) = A\hat{x}(t, \bar{\Lambda}) + B\hat{u}(t, \bar{\Lambda})$$

$$\hat{u}(t, \Lambda) = \hat{u}(t-1, \bar{\Lambda}) + \sum_{i=1}^{N} \alpha_i(t)\mathbf{1}_i \left(\bar{\lambda}_i v_i(t) + (1 - \bar{\lambda}_i)\hat{u}_i(t-1, \bar{\Lambda}) - \hat{u}_i(t-1, \bar{\Lambda})\right)$$

Proof. The proof follows from standard computations. Since it is quite long, it is omitted for sake of readability. □

Previous lemma shows how the set of possible estimates changes at each time instant. In particular, when $\nu_i(t) = 1$, there is no uncertainty on the input applied at the actuator i, and both $\hat{x}(t+1, \Lambda)$ and $\hat{u}(t, \Lambda)$ are indeed independent of λ_i. The independence at a generic time τ propagates at the next time instant $\tau + 1$ as long as $\alpha_i(\tau + 1) = 0$. It follows that, even if $\nu_i(t) = 0$ but the input applied at the actuator i is known, the estimate $\hat{x}(t+1, \Lambda)$ and $\hat{u}(t, \Lambda)$ are the same both for $\lambda_i = 1$ and $\lambda_i = 0$. This result is what we expected from the proposed design. Roughly speaking, first the possible

states double due to the new possible input at the selected actuator, and then the set of possible states is shrunk thanks to the information feedback from the actuators. We use the previous lemma to relate the estimate at the next time instant to the estimate at the previous time instant through the relation between $\bar{\Lambda}$ and Λ. We need this relation to show the recursive feasibility and constraint satisfaction of the proposed solution.

Proposition 5.1. *Assume that* $(x(0), u(0)) \in \tilde{O}_\infty$. *Then, we have that* $(\hat{x}(t,\Lambda), \hat{u}(t-1,\Lambda)) \in \tilde{O}_\infty$, $\Lambda \in \{0,1\}^N$, *for any* $t \geq 0$, *and the optimization problem* (5.32) *is feasible for any* $t \geq 0$ *such that* $\beta_i(t) = 1$.

Proof. We prove the theorem by inductive argument. For the considered initial conditions, $\hat{x}(t,\Lambda) = Ax(0) + Bu(0)$ for any Λ. Pick an arbitrary $i \in \{1, \dots, N\}$. By choosing $v = u_i(0)$, $\hat{u}(0,\Lambda) + \mathbf{1}_i v = u(0)$ and it is a feasible solution of the optimization problem at time $t = 1$ since $(Ax(0) + Bu(0), u(0)) \in \tilde{O}_\infty$ because $\tilde{O}_\infty$ is positively invariant. So the statements holds at time $t = 1$.

Assume that the statement holds for t, namely $(\hat{x}(t,\Lambda), \hat{u}(t,\Lambda)) \in \tilde{O}_\infty$ for any $\Lambda \in \{0,1\}^N$. If there exists a $i \in \{1, \dots, N\}$ $\beta_i(t) = 1$ then $\Delta_i(t) = 0$ and $\hat{u}_i(t,\Lambda) = u_i(t)$ for any $\Lambda \in \{0,1\}^N$. If we choose $\alpha_i(t+1) = 1$ and $v_i(t+1) = u_i(t)$, then $\hat{u}(t,\Lambda) = \hat{u}(t,\Lambda) + \mathbf{1}_i(v - \hat{u}_i(t,\Lambda))$ for any $\Lambda \in \{0,1\}^N$ and $(A\hat{x}(t,\Lambda) + B\hat{u}(t,\Lambda), \hat{u}(t,\Lambda) + \mathbf{1}_i(v - \hat{u}_i(t,\Lambda)) \in \tilde{O}_\infty$ since $\tilde{O}_\infty$ is positively invariant. This proves the feasibility at time $t+1$. Recall now that $\hat{x}(t+1,\Lambda) = A\hat{x}(t,\bar{\Lambda}) + B\hat{x}(t,\bar{\Lambda})$ for a given $\bar{\lambda}$, according to the previous Lemma.

If $\bar{\lambda}_i = 0$, $\hat{u}(t+1,\Lambda) = u(t,\bar{\Lambda})$. By inductive hypothesis, $(\hat{x}(t,\bar{\Lambda}), \hat{x}(t,\bar{\Lambda})) \in \tilde{O}_\infty$. Since $\tilde{O}_\infty$ is positively invariant, $(A\hat{x}(t,\bar{\Lambda}) + Bu(t,\bar{\Lambda}), u(t,\bar{\Lambda})) \in \tilde{O}_\infty$, and thus $(\hat{x}(t+1,\Lambda), \hat{u}(t+1,\Lambda)) \in \tilde{O}_\infty$.

If $\bar{\lambda}_i = 1$, $\hat{u}(t+1,\Lambda) = \hat{u}(t,\bar{\Lambda}) + \alpha_i(t)\mathbf{1}_i\left(v_i(t+1) - \hat{u}_i(t,\bar{\Lambda})\right)$. By construction, we have that $(A\hat{x}(t,\bar{\Lambda}) + Bu(t,\bar{\Lambda}), u(t,\bar{\Lambda}) + \sum_{i=1}^N \alpha_i(t)\mathbf{1}_i\left(v_i(t+1) - \hat{u}_i(t,\bar{\Lambda})\right)) \in \tilde{O}_\infty$ and $(\hat{x}(t+1,\Lambda), \hat{u}(t+1,\Lambda)) \in \tilde{O}_\infty$, concluding the proof. □

Since the optimization problem (5.32) is feasible if $\beta_i(t) = 1$, and it is solved if and only if $\alpha_i(t) = 1$, when $\alpha(t)$ is chosen according to (5.14), we can conclude that the overall strategy (5.14)-(5.32) always provides a new admissible input $v_i(t)$. The only case when a new input is not computed is when $\beta_i(t) = 0$ for any i. This happens when the input of every actuator is not known at the remote control unit. In this case, the optimization problem (5.32) is not solved for any i and the control unit waits until a packet from at least an actuator is received. In general, the optimization problem may be feasible also if $\beta_i(t) = 0$, but this may increase exponentially the number of possible states.

Under the proposed strategy, safety is guaranteed for any sequence of packet losses. We formalize the result in the following statement, the proof immediately follows from the previous proposition.

Proposition 5.2. *Assume that* $(x(0), u(0)) \in \tilde{O}_\infty$. *Then, constraints* (5.3) *are satisfied with probability 1 for any* $t \geq 0$.

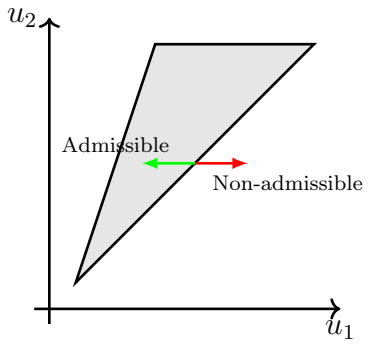

Figure 5.3: Admissible (green) and non-admissible (red) directions.

As for the single-agent case, this is the most general result possible since it does not require any assumption on the network. Even if an agent is disconnected for long periods due to issues on the communication hardware or due to noisy channel conditions, safety is guaranteed. Clearly, in that case, it is not possible in general to guarantee the convergence to any desired set-point. Indeed, it is easy to see that, when a long blackout occurs, the system converges to an intermediate set-point, suboptimal but still safe. Under some mild hypotheses, however, we can guarantee that the system asymptotically converges to the optimal set-point with probability 1. It is intuitive that, similarly to the single-agent case, we need some minimal assumptions on the network to avoid communication blackouts of infinite length. In addition, differently from the single-agent case, we require some mild assumptions on the constraints. Indeed, due to the asynchronous updates, the control problem becomes a game between the agents and so we may reach a suboptimal equilibrium. Based on the results of [133] for distributed RG, we can avoid this problem with a minimal reduction of the set of admissible inputs, as we outline in the remaining part of the section.

We start with some definitions. First recall that $u = (u_1', \cdots, u_N')'$ with dimensions $u_i \in \mathbb{R}^{m_i}$ and $m = \sum_{i=1}^{N} m_i$. We recall the notation $\bar{x}_u = (I - A)^{-1}Bu$ and $\bar{y}_u = C\bar{x}_u + Du$. Moreover we define the set

$$U = \{u \in \mathbb{R}^m : \bar{y}_u \in (1 - \epsilon)Y\} \tag{5.34}$$

We introduce the following definitions from [133].

Definition 5.1. A vector $\mathrm{v} \in \mathbb{R}^m$ is an admissible direction at u in U if $\exists \bar{\alpha} > 0$ such that $u + \alpha \mathrm{v} \in U$ for any $\alpha \in [0, \bar{\alpha}]$

Roughly speaking, a direction is admissible at u if small shifts along it are still in the set U. A pictorial representation of an admissible direction and a non-admissible direction is reported in Figure 5.3.

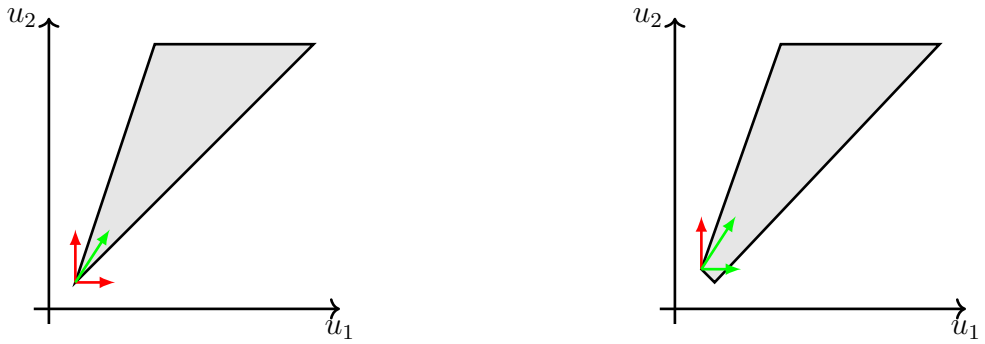

Figure 5.4: A non-viable point (left panel) and a viable point (right panel). Admissible directions are indicated in green, while non-admissible directions are in red. Note that sets U (in gray) are slightly different in the two panels.

Definition 5.2. A point $u \in U$ is viable if, for any vector $\mathrm{v} = (\mathrm{v}_1', \ldots, \mathrm{v}_i', \ldots, \mathrm{v}_N')' \in \mathbb{R}^m$ that is an admissible direction at u in U, there exists an i such that the vector $\mathbf{1}_i \mathrm{v}_i \in \mathbb{R}^m$ is an admissible direction at u in U.

Roughly speaking, to be viable, a point requires that, for any direction v obtained by simultaneously acting on all the actuators that is admissible, there exists at least a sub-direction, namely a direction obtained by acting only on an actuator, that is admissible. In other words, at any point u, we must avoid the case where there exist admissible directions that require to act on more than an actuator simultaneously. A pictorial representation of a viable and a non-viable point for two slightly different sets U is reported in Figure 5.3. Viability property of points in the set U will be fundamental to prove the convergence.

For sake of completeness, we also recall the definition of Pareto-optimal point in the considered setup.

Definition 5.3. A vector $u \in U \subset \mathbb{R}^n$ is Pareto-optimal if there does not exist a vector $\mathrm{v} = (\mathrm{v}_1', \ldots, \mathrm{v}_N')' \in \mathbb{R}^m$, $\mathrm{v}_i \in \mathbb{R}^{m_i}$ such that $u + \mathrm{v} \in U$ and

$$\begin{aligned} &\|u_j + \mathbf{1}_j \mathrm{v}_j - r_j\|_{Q_j} \leq \|u_j - r_j\|_{Q_j} \quad \text{for any } j \in \{1, \ldots, N\} \\ &\|u_i + \mathbf{1}_i \mathrm{v}_i - r_i\|_{Q_i} < \|u_i - r_i\|_{Q_i} \quad \text{for at least a } i \in \{1, \ldots, N\} \end{aligned}$$

In order to prove the main theorem, we need three preliminary lemmas, given and explained in the following.

Lemma 5.2. *If $(\bar{x}_u, u) \in \tilde{O}_\infty$ then $\exists \bar{\bar{\alpha}} > 0$ such that $(\bar{x}_u, u + \alpha \mathrm{v}) \in O_\infty$ for any $\alpha \in [0, \bar{\bar{\alpha}}]$ and for any $\mathrm{v} \in \mathbb{R}^m$ with $\|v\| = 1$.*

Proof. Since A is stable, there exists a $\delta > 0$ such that $\|C \sum_{\ell=0}^{k-1} A^\ell B + D\| < \delta$ for $k \geq 0$. It follows that $(C \sum_{\ell=0}^{k-1} A^\ell B + D)\mathrm{v} \in \mathcal{B}_\delta$ for $k \geq 0$, where $\mathcal{B}_r$ is a ball of suitable

dimensions with radius r. Since $(\bar{x}_u, u) \in \tilde{O}_\infty$, if the the origin is strictly included in Y, there exists a $\bar{\delta} > 0$ such that $C\bar{x}_u + Du \in Y \sim \mathcal{B}_{\bar{\delta}}$. It follows that

$$\begin{aligned}\hat{y}(k|\bar{x}_u, u + \alpha \mathrm{v}) &= CA^k\bar{x}_u + C\sum_{\ell=0}^{k-1} A^\ell Bu + \alpha C\sum_{\ell=0}^{k-1} A^\ell B\mathrm{v} + Du + \alpha D\mathrm{v} \\ &= \underbrace{C\bar{x}_u + Du}_{Y\sim\mathcal{B}_\delta} + \alpha \underbrace{\left(C\sum_{\ell=0}^{k-1} A^\ell B + D\right)}_{\mathcal{B}_{\bar{\delta}}} \mathrm{v}\end{aligned}$$

If we pick $\bar{\bar{\alpha}} > 0$ such that $\bar{\bar{\alpha}}\bar{\bar{\delta}} < \delta$ then $\hat{y}(k|\bar{x}_u, u + \alpha \mathrm{v}) \in Y$, concluding the proof. □

Please note that $(\bar{x}_u, u) \in \tilde{O}_\infty$ while $(\bar{x}_u, u+\alpha \mathrm{v}) \in O_\infty$. It follows that the input $u+\alpha \mathrm{v}$ may not satisfy the steady-state condition, namely $(\bar{x}_{u+\alpha \mathrm{v}}, u+\alpha \mathrm{v})$ may not belong to O_ϵ. However, the previous lemma shows that, for any steady-state admissible pair $(\bar{x}_u, u)$, a small change of u along any direction satisfies the constraints (5.3). This allows us to prove the following lemma.

Lemma 5.3. *If the input u is viable in U then, for any $\mathrm{v} = (\mathrm{v}_1', \ldots, \mathrm{v}_i', \ldots, \mathrm{v}_N')'$ that is an admissible direction at u in U, there exists an i and an $\tilde{\alpha} > 0$ such that $(\bar{x}_u, u + \alpha \mathbf{1}_i \mathrm{v}_i) \in \tilde{O}_\infty$ for any $\alpha \in [0, \tilde{\alpha}]$.*

Proof. By definition of viability, if we pick an arbitrary admissible direction $\bar{\mathrm{v}}$ at u in U, there exist an i and an $\bar{\alpha} > 0$ such that $u + \alpha \mathbf{1}_i \bar{\mathrm{v}}_i \in U$ for $\alpha \in [0, \bar{\alpha}]$. Since $u \in U$, then $(\bar{x}_u, u) \in \tilde{O}_\infty$. From the previous lemma, it follows that there exists a $\bar{\bar{\alpha}} > 0$ such that $(\bar{x}_u, u + \alpha \mathbf{1}_i \bar{\mathrm{v}}_i/\|\bar{\mathrm{v}}_i\|) \in O_\infty$ for $\alpha \in [0, \bar{\bar{\alpha}}]$. If we pick $\tilde{\alpha} = \min(\bar{\alpha}, \bar{\bar{\alpha}}/\|\bar{\mathrm{v}}_i\|)$, we have that $(\bar{x}_u, u + \alpha \mathbf{1}_i \bar{\mathrm{v}}_i) \in O_\infty$ and $u + \alpha \mathbf{1}_i \bar{\mathrm{v}}_i \in U$ for $\alpha < \tilde{\alpha}$. Merging these two conditions it follows that $(\bar{x}_u, u + \alpha \mathbf{1}_i \bar{\mathrm{v}}_i) \in \tilde{O}_\infty$ for $\alpha < \tilde{\alpha}$. Since $\bar{\mathrm{v}}$ is arbitrary, this concludes the proof. □

According to the previous lemma, viability in U implies a similar property in the MOAS. For the convergence result, the following Lemma proved in [133] will be useful.

Lemma 5.4. *Each point belonging to U is viable in U if and only if each point belonging to ∂U is viable in U, where ∂U is the frontier of U.*

It follows that, to check if the points of set U are viable, it is enough to check if the points of the frontier of U are viable (in U).

We now make the following assumption.

Assumption 5.1. The following conditions hold:

1. Actuators are selected according to a modified round-robin protocol, namely $\mathcal{C}(\alpha) = \sum_{i=1}^N a_i^U(t)\alpha_i$

2. Each point belonging to ∂U is viable in U

3. $\mathbf{P}[\cap_{k>t}\{\nu_i(k)=0\}]=0$ for any $t>0$ and $\mathbf{P}[\cap_{k>0}\{\theta_i(t_k)=0\}]=0$ for any infinite sequence $\{t_k\}_{k=0}^{+\infty}$ with $t_{k+1}>t_k$

We are now ready to provide the convergence theorem.

Proposition 5.3. *Assume that $(x(0),u(0))\in\tilde{O}_\infty$, and $r(t)=r$ for $t\geq 0$. Then, under Assumption 5.1, $u(t)$ reaches a Pareto-optimal point u^* and $x(t)$ converges to $(I-A)^{-1}Bu^*$.*

Proof. For easy of notation, we omit the weight of the norm. If $\alpha_i(t)=0$, then $\|r_i-u_i(t)\|^2=\|r_i-u_i(t-1)\|^2$. Consider now $\alpha_i(t)=1$. It requires that $\hat{u}_i(t-1,\Lambda)=u_i(t-1)$ for any Λ. As shown in Proposition 5.1, $u_i(t-1)$ is an admissible solution of the optimization problem, it follows that

$$\|r_i-v_i(t)\|^2\leq\|r_i-u_i(t-1)\|^2.$$

Moreover

$$\begin{aligned}\|r_i-u_i(t)\|^2&=\theta_i(t)\|r_i-v_i(t)\|^2+(1-\theta_i(t))\|r_i-u_i(t-1)\|^2\\&\leq\theta_i(t)\|r_i-u_i(t-1)\|^2+(1-\theta_i(t))\|r_i-u_i(t-1)\|^2\\&=\|r_i-u_i(t-1)\|^2.\end{aligned}$$

We have that the sequence $\|r_i-u_i(t)\|^2$ is monotonically not-increasing and lower-bounded by 0, so it converges. With standard argument we can show that $u_i(t)$ converges to a point u_i. Let $u=(u_1',\ldots,u_N')'$ and $u(t)$ converges to u. It follows that $x(t)$ converges to $\bar{x}_u$.

Consider the sequence t_k defined as follows: $t_0=0$ and t_k such that $\alpha_i(t)=0$ for $t_{k-1}<t<t_k$ and $\alpha_i(t_k)=1$. It correspond to the sequence where a new input for actuator i is computed. Under the modified round-robin algorithm (Assumption 5.1.1) and the hypothesis on the links from the actuators to the control unit (Assumption 5.1.3), we have that t_k is defined for any $k>0$, so we can take the limit. By contradiction, assume that $v_i(t_k)$ is not converging to u_i. Equivalently, there exists a $\delta>0$ and a sequence $\{\tau_k\}_{k=0}^{+\infty}$ such that $\|v_i(\tau_k)-u_i\|>\delta$. Now, pick $\epsilon=\delta/2$. Since $u_i(t)$ is converging to u_i, there exists a t_ϵ such that $\|u_i(t)-u_i\|<\epsilon$ for any $t>t_\epsilon$. By the hypothesis on the links from the control unit to the actuator (Assumption 5.1.3), with probability 1, there exists a $\tau>t_\epsilon$ belonging to the sequence $\{\tau_k\}$ such that $\theta_i(\tau)=1$. By construction, $v_i(\tau)=u_i(\tau)$, that implies $\|u_i(\tau)-u_i\|>\epsilon$, reaching an absurd.

By definition, $\hat{u}_i^+(t)$ is either equal to $v_i(t-a_i^U(t))$ or $u_i(t)$, while $\hat{u}_i^-(t)$ is either equal to $u_i(t-a_i^U(t)-1)$ or $u_i(t)$. From the convergence of $u_i(t)$ and $v_i(t)$, we have that $\hat{u}_i^+(t)$ and

$\hat{u}_i^-(t)$ converge to u_i, and the same also for $\hat{u}_i(t,\Lambda)$ for any Λ. By construction, $\hat{x}(t,\Lambda)$ converge to $\bar{x}_u$ for any Λ.

Similarly to Step 1 in the proof of Proposition 3.3, it can be proved that for any $(\bar{x}_u, u) \in \tilde{O}_\infty$ then there exists a $\delta > 0$ such that if $x \in \mathcal{B}_\delta(\bar{x}_u)$ then $(x,u) \in \tilde{O}_\infty$. It means that $v_i(t) = u_i$ for some t, and it follows that $\hat{u}(t,\Lambda) = u$ from a certain t onward.

Suppose by contradiction that $u \in S$ is not Pareto-optimal, namely there exists a vector $\mathrm{v} = (\mathrm{v}_1', \ldots, \mathrm{v}_N')' \in \mathbb{R}^m$, $\mathrm{v}_i \in \mathbb{R}^{m_i}$ such that $u + \mathrm{v} \in S$ and

$$\begin{aligned} &\|u_j + \mathbf{1}_j \mathrm{v}_j - r_j\|_{Q_j} \leq \|u_j - r_j\|_{Q_j} \quad \text{for any } j \in \{1,\ldots,N\} \\ &\|u_i + \mathbf{1}_i \mathrm{v}_i - r_i\|_{Q_i} < \|u_i - r_i\|_{Q_i} \quad \text{for at least a } j \in \{1,\ldots,N\} \end{aligned}$$

Consider now the convex combination $\alpha(u_j + \mathbf{1}_j \mathrm{v}_j) + (1-\alpha)u_j$. By convexity of the norm we have

$$\|\alpha(u_j + \mathbf{1}_j \mathrm{v}_j) + (1-\alpha)u_j - r\|_{Q_j} < \alpha\|u_j + \mathbf{1}_j \mathrm{v}_j - r\|_{Q_j} + (1-\alpha)\|u_j - r\|_{Q_j}$$

for any $\alpha \in (0,1)$ and any j. By subtracting at both sides $\|u_j - r\|_{Q_j}$ we get

$$\|\alpha(u_j + \mathbf{1}_j \mathrm{v}_j) + (1-\alpha)u_j - r\|_{Q_j} - \|u_j - r\|_{Q_j} < \alpha(\|u_j + \mathbf{1}_j \mathrm{v}_j - r\|_{Q_j} - \|u_j - r\|_{Q_j})$$

The right hand side is ≤ 0 by the choice of v, so

$$\|\alpha(u_j + \mathbf{1}_j \mathrm{v}_j) + (1-\alpha)u_j - r\|_{Q_j} - \|u_j - r\|_{Q_j} < 0$$

for any $\alpha \in (0,1)$ and any j. From Assumption 5.1.2 and Lemma 5.4, u is viable. By Lemma 5.3, there exist an i and an $\tilde{\alpha} > 0$ such that $(\bar{x}_u, u + \alpha \mathbf{1}_i \mathrm{v}_i) \in \tilde{O}_\infty$ for $\alpha \in [0, \tilde{\alpha}]$. According to the previous inequality, this violates the optimality of the current applied input, reaching an absurd. □

The previous Proposition guarantees that the system converges to the desired set-point under very mild hypotheses.

Assumption 5.1.1 is needed to exclude the pathological cases where actuators with no admissible direction are always selected instead of the actuator that makes the current point viable. Indeed, more sophisticated costs in the scheduling problem, possibly state-dependent, can be considered to improve the performances. For instance, we may take $\mathcal{C}(\alpha) = \sum_{i=1}^N \alpha_i \|r_i - u_i(t)\|$. In that case, Assumption 5.1.1 can be relaxed but it is still necessary to avoid that the actuators with an admissible improvement are always excluded. A possible solution is to temporarily exclude an actuator from the set of eligible actuators if its previous optimal input was equal to the applied input, namely $v(t - a_i^U(t)) = u(t - a_i^U(t) - 1)$. Also, stochastic schedulers can be considered.

Assumption 5.1.2 is required to avoid the system to be stuck in a non (Pareto) optimal

point. Since we consider a centralized approach, it is always possible to check if the overall constraints satisfy the conditions. Note that it is enough to guarantee the viability of the points of the frontier of U, since it implies the viability of any point of U. The work [133] provides a useful procedure to check if all the points of ∂U are viable. Even more, they show that there exists an inner approximation U' arbitrarily close to U whose points are viable. Intuitively, the procedure consists in cutting the vertices of U that are not viable. This idea is graphically shown in Figure 5.4

Assumption 5.1.3 outlines the mild requirements on the communication network. In particular, it ensures that blackouts of infinite length are excluded for any link. Note that the assumption on the arrival processes $\theta_i(t)$ is slightly more restrictive than the condition on $\nu_i(t)$. On one hand, the condition on $\nu_i(t)$ excludes the existence of infinite sequences of consecutive packet losses from any t onward. On the other, the condition on $\theta_i(t)$ excludes the existence of infinite sequences of packet losses, also not consecutive. This is required because we do not transmit a new input $v_i(t)$ at any t but only when $\alpha_i(t) = 1$ and, since the sequence of transmission instants is not known in advance but depends on the sequence $\nu_i(t)$ and on the cost $C(\alpha)$, we require the condition to hold for any possible sequence of transmissions. Note that no assumption on the arrival processes $\gamma_i(t)$ are made because the feedback needed by the control algorithm is given by the information transmitted by the actuators. However, the communications from the sensors are essential to improve the performances of the system in the case with disturbances. In that case, it also plays an important role in the convergence theorem, since long blackouts on the link from the sensors to the control unit reduce the set of admissible inputs as shown in the single-agent problem (see section 3.3).

5.7 Simulations: assessment of the proposed strategy

In this section, we assess the performances of the proposed centralized strategy on a multi-agent systems. For illustrative purposes, we provide also the typical results that can be achieved using implicit communications and slow wireless communications.

We consider a cooperative load transportation task implemented using two Segway-like robots. A pictorial representation of the setup is reported in Figure 5.5. The two robots are facing each other and they hold the two ends of a rope. Attached to the rope, at its mid point, there is a plate used to carry a small load. The objective is to transport the load to a desired position while preventing the plate from touching the floor and the rope from being completely tight. These constraints can be easily formalized through a minimum and a maximum distance between the two robots. Even if the load transportation using two segways is not particularly efficient, it is an interesting case of study because it includes both coupled constraints (on the distance between the two agents) and decoupled constraints (on the tilt angle and on the voltage input).

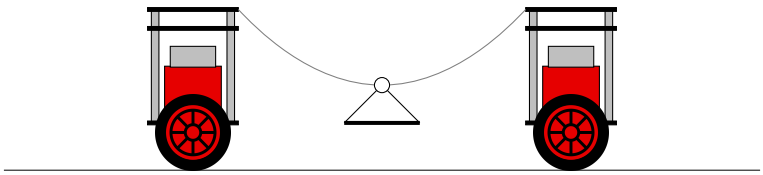

Figure 5.5: Representation of the considered setup (side view).

At this stage, we consider that the load is light so that the force of the rope on the two agents can be neglected. The dynamics are therefore decoupled and the overall model can be directly derived from the model of the segway

$$A_{\text{ma}} = \begin{bmatrix} A & 0 \\ 0 & A \end{bmatrix} \qquad B_{\text{ma}} = \begin{bmatrix} B & 0 \\ 0 & B \end{bmatrix}$$

where A and B are the closed-loop system matrices introduced in Appendix A.2 with sampling period $T = 0.01$ s. We require that the tilt angles are within the interval $[-0.1 \text{ rad}, 0.1 \text{ rad}]$, the control inputs are in $[-11 \text{ V}, 11 \text{ V}]$ and the distance between the agents (simple derived from the states of the two agents) is in $[0.40 \text{ m}, 0.60 \text{ m}]$. Matrices C and D are derived accordingly.

The arrival processes $\theta_i(t), \gamma_i(t), \nu_i(t)$ are modeled as independent and identically distributed Bernoulli random variables with mean equal to 0.5. The objective is to transport the load 1 m ahead, that corresponds to a move of both the segways 1 m ahead.

The results are depicted in Figure 5.6. In the top panel, we can see that both the agents reach the desired reference, from which we can deduce that the load reaches the desired position. The settling time is approximately of 3.5 s. If we look at the center panel and at the bottom panel, we can see that constraints are always satisfied despite the packet loss. Interestingly, we see that Agent 1 is slowing down in the period $[1 \text{ s}, 2 \text{ s}]$, probably due to a blackout on the links with the control unit. Indeed, Agent 2 gets closer, but the constraint on the minimum distance is always satisfied.

We now compare the proposed algorithm to a solution with slow communications. In particular, we consider a centralized standard RG with sampling period $T = 0.1$ s and we assume that it is not affected by packet loss, since wireless networks are usually enough reliable at this communication rate. In the case without disturbances, the response is approximately identical to the proposed algorithm. However, in the case with disturbances (set as in Appendix A.2), the solution with slow communications is more conservative because the disturbance set is larger due to the longer sampling period. Figure 5.7 reports the position of Agent 1 under the proposed algorithm with good channel conditions (loss probability equal to 0.1), with bad channel conditions (loss probability equal to 0.5), and under the alternative solution with ideal channel (loss probability equal to 0). The conservativeness introduced due to the disturbance produces an evident degradation of

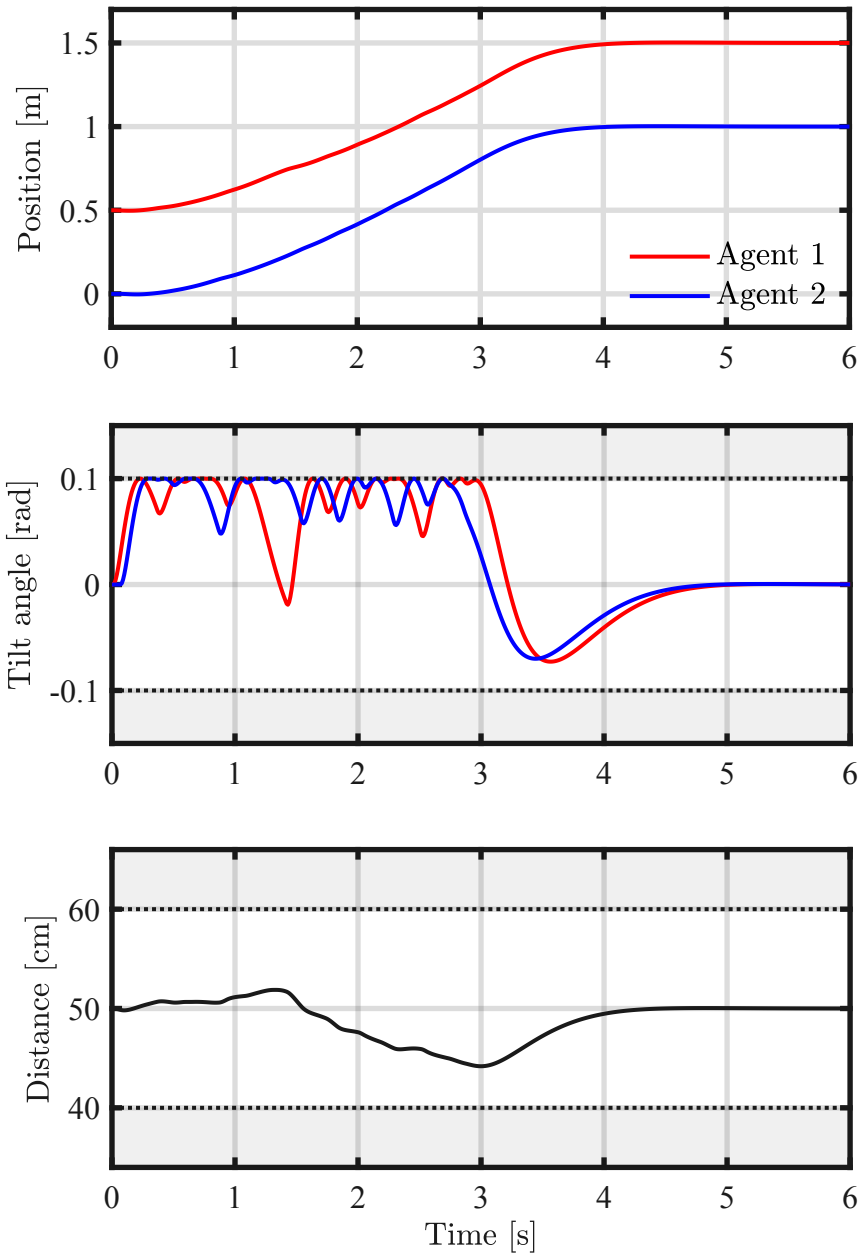

Figure 5.6: System response with simulated channels. Constraints on the tilt angles and on the distance between the two Segways are satisfied.

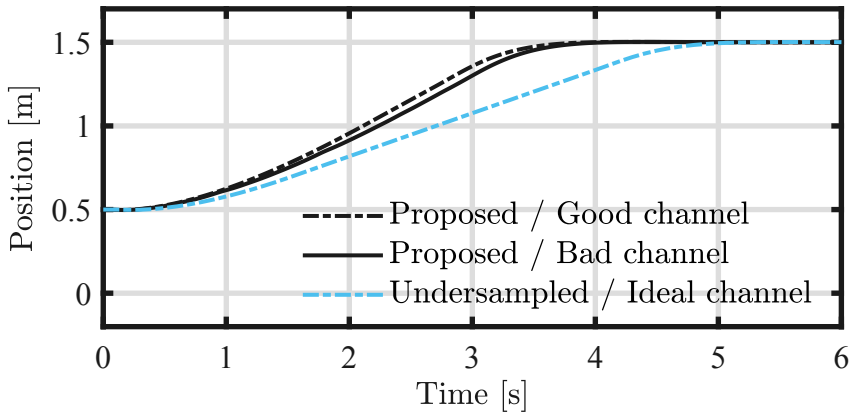

Figure 5.7: System response with fast communications (black lines) and slow communication (blue line). To increase the transmission rate is beneficial if the resulting packet losses are addressed.

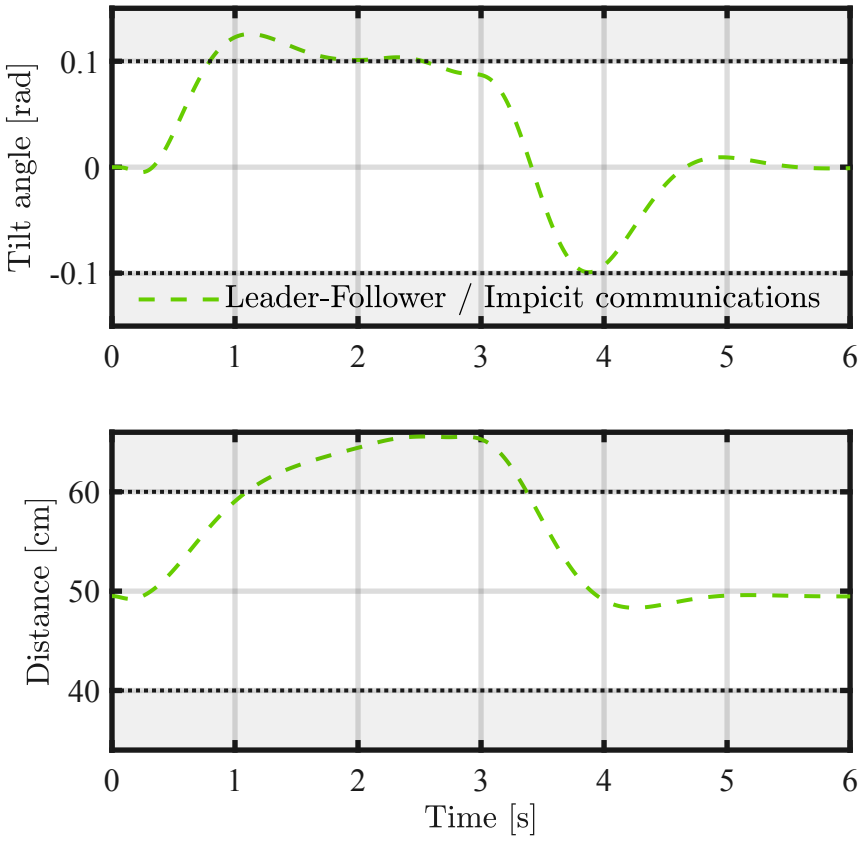

Figure 5.8: System response with implicit communications. It is not possible to enforce the constraints with simple leader-follower strategies.

the settling time. Note that the solution devised in this chapter is not conceived for the case with disturbances. However, if dynamics are decoupled, the proposed algorithm can be easily generalized using a suitable MOAS with packet loss similar to section 3.3.

To underline the benefits of the proposed algorithm, we simulate the system evolution with a solution based on implicit communication. In particular, we assume that Agent 1, playing the role of the leader, is provided with an ideal trajectory that has to follow independently of Agent 2. Conversely, Agent 2, playing the role of the follower, is equipped with an ideal sensing apparatus that is able to retrieve the position of Agent 1. Then, it derives the desired position reference through the simple local law $u_2(t) = K(d(t) - d^*)$ where $d(t)$ is the distance from the Agent 1, $d^* = 0.5$ m is the desired distance, and K is a suitable gain. More sophisticated constrained control algorithms like MPC cannot be used since they cannot be implemented on-board. This control law is commonly used in the literature of formation control. We set the gain K with a trial-and-error procedure in order to enforce constraints. Surprisingly, we discover that there does not exist a gain K such that the constraints are satisfied. In fact, if an higher K is chosen, the response is fast enough to guarantee that the maximum distance is never violated, but the tilt angle increases above the limit. Conversely, if a smaller K is chosen, the response is slow enough to keep the tilt angle inside the boundary but the maximum distance is not satisfied. The best evolution possible is achieved with $K = 0.25$ and it is reported in Figure 5.8. In particular, we can see that distance between the two agents reaches a maximum of 0.65 m. In that circumstances, the rope is completely tight, the force of the rope on the two agents is no more negligible, and each agent affects the other. The overall system evolution will not meet the desired specifics in terms of smoothness and catastrophic events may happen, e.g. the breaking of the rope and of the load. Including disturbances in the dynamics, noise and delays in the measurement, or stricter constraints, the performances are expected to get worse.

Due to the asynchronous approach, the scalability of the proposed solution is one of the major concerns. In fact, with respect to the parallel approach where the input of each actuator is updated at each sampling instant, in the proposed asynchronous approach, the input of an actuator is updated, on average, once every N_A sampling instant. In general, we expect the performance to deteriorate increasing the number of agents. To understand how much, we set up a simulation test based on the system introduced above but considering a line of N segway robots. More specifically, each Segway holds the two ends of two different ropes, each hanging a load. The other ends of the two ropes are held by the proceeding and the following robot in the line. This does not happen for the first and the last robot of the line, which hold only a rope.

The dynamics of the system are a simple generalization of the model introduced above for the case of two Segways, as well as the constraints on the tilt angles, the relative distances, and the control inputs. The arrival processes are modeled as independent and

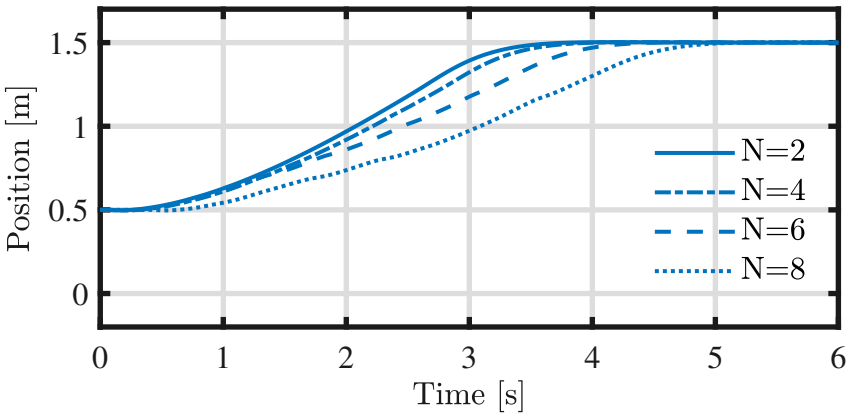

Figure 5.9: System response with different number of agents in good channel conditions. The performances deteriorate by increasing the number of agents. For the problem at hand, the proposed solution is effective up to 5 agents, while for more agents it needs to be improved, possibly applying the graph colorability theory.

identically distributed Bernoulli random variables with mean equal to 0.9. The objective is to transport every load 1 m ahead, that corresponds to a move of all the Segways 1 m ahead.

The position of a representative agent for the different cases is reported in Figure 5.9. We can see that in the case of $N = 4$ agents the response is only slightly slower than the case with $N = 2$ agents, with a settling time 0.2 s longer (5.5% worse). Performances deteriorate more clearly for $N = 6$ and $N = 8$ agents, with a settling time 0.6 s longer (16.5% worse) and 1.1 s longer (33% worse), respectively. On one hand, these results confirm that the proposed solution is effective for systems with some agents, roughly up to 5 for the considered system. On the other hand, the proposed solution achieves worse performances by increasing the number of agents and it is not suitable for the cases with many actuators and sensors.

There are several ways to improve the performances obtained for large N. First, the sampling period in the asynchronous approach does not need to be equal to the sampling period chosen in the parallel approach, but it can be taken N times smaller if this is allowed by the computational and communication resources. In this way, the performances are not limited by the delay of N sampling periods before updating the applied input. Moreover, the inner control loop, usually implemented by each agent, can run at an arbitrary higher rate, improving the response of the system. Finally, the proposed solution can be improved by exploiting the idea of [134] and the graph colorability theory. Consider, for instance, the case with $N = 3$ Segways. The first and the last robot do not directly affect each other, since dynamics are decoupled and no constraint involves the state of both. It follows that the input of the first robot can be evaluated regardless of the input of the last, and the other way around, and thus both the

inputs can be reliably updated at the same sampling instant. For the considered system, this allows to group the Segways in two sets and to alternately update the inputs of a set of agents and of the other. This solution drastically reduces the period between two following updates for the same agent and can lead to better performances.

Even if these improvements are possible, computational and communication resources are an important bottleneck. More sensors and more actuators require more communications, and more computations as well. Smart transmission scheduling schemes are needed in order to provide the required information without redundancy to the control unit. At the same way, it is important to reduce the computational complexity of the optimization problem.

It is important to stress that the proposed solution focus on the problem of cooperative robotics and so, in many relevant cases, the number of agents is small. The proposed centralized asynchronous solution with wireless communications is tailored to achieve coordination and safety in this kind of application.

5.8 Conclusion

In this chapter, we have devised a centralized solution to the problem of control of multi-agent systems with packet loss and constraints. We have obtained it by merging the RG over wireless proposed for the single-agent case in chapter 3 and the distributed RG devised in [133], with suitable improvements. In the future, following the same reasoning, we can extend the MPC for Tracking over wireless proposed in chapter 4 to the multi-agent case by resorting known results on distributed MPC [137][138]. Moreover, a distributed version of the proposed solution can be devised with simple modifications. It requires to adopt a fixed actuator scheduling policy, like the standard round-robin protocol, and to allow an agent to update its input only if other applied inputs are known. This solution may introduce additional conservativeness but it can be limited using the colored approach by [134]. Finally, to enhance the applicability of the proposed algorithm for mobile manipulation, we can study how to add on the top of the proposed RG a centralized motion planner available in the literature. The motion planner can provide to the proposed RG a possible trajectory, and the RG is in charge of enforcing the constraints by opportunely acting on each agent and by taking into account the possible communication losses.

6

Sensor Selection and Power Allocation for Remote Estimation over Wireless

In the previous chapter we let the problem of transmission scheduling open. However, how the sensors and the actuators access to the shared network can have a dramatic impact on the performances of the system. For instance, if two agents periodically try to communicate and they are almost synchronized, one of the two will always find the network busy. Also, the hidden terminal problem can arise with harmful effects on the control performances. Transmission scheduling at the control layer is the most settled method in the literature to mitigate these problems. In particular, a significant number of works have focused on the well-known sensor scheduling problem: for each time slot, a set of sensors is selected to transmit in order to optimize the remote estimation performances while avoiding collisions or undesirable delays and minimizing transmission power consumption.

Since the joint scheduling of the acknowledgments from the actuators and of the measurements from the sensors is particularly challenging, we start from the simpler problem of sensor selection. Indeed, the interest in this problem goes beyond multi-agent systems. It is reflected in various applications, especially those related to the Internet of Things, like smart homes, smart cities, wearable devices, advanced healthcare, and it is worth studying by itself. For this reason, we consider a more general setup than in chapter 5 with unstable systems, partial observations, and Gaussian disturbances.

Usually, the access to the wireless medium is implicitly regulated at the application layer, so the MAC protocol can be kept as is (e.g. CSMA/CA with Wi-Fi). Conversely, in this chapter, we consider a *cross-layer design* where not only transmission instants but also the transmission powers used at the Physical layer are set according to the control performances. Transmission power control on a packet basis is in fact allowed by the most recent wireless standards (e.g. see the case of IEEE 802.11ax [139] and 5G [140]) and supported by many off-the-shelf devices (a practical implementation on Wi-Fi has been devised by [141]). Moreover, differently from most existing solutions, we

admit multiple simultaneous transmissions to exploit the time-frequency resources to the maximum. This setup is particularly appealing for the problem considered in chapter 5, where we would like to retrieve as much information as possible from the system in order to reduce the conservativeness of the constrained control algorithm. The capability of demodulating multiple signals in the presence of mutual interference, also known as multi-user detection, is well-known in the field of broadband wireless communications, see [142]. Multi-packet reception is a particular type of multi-user detection technique where the receiver is equipped to decode multiple simultaneous transmissions. This can be achieved in many ways, such as at the signal modulation level (CDMA), by multiple antennas at transmitter and receiver (MIMO), or by using collision resolution methods based on signal processing as discussed in [143]. These techniques have proven to be very appealing for the next-generation wireless networks. Applications to Wi-Fi have been studied e.g. in [144], while 5G includes Non-Orthogonal Multiple Access (NOMA), which enables multi-packet reception using Successive Interference Cancellation (SIC). See [145][146] for a comprehensive overview. In the automation field, ZigBee has been adapted to include this feature [147].

In this chapter, we consider the optimal power allocation for remote estimation with multi-packet reception capabilities. The problem is more general than solutions already available in the literature. In fact, most of the existing works have considered the problem of sensor selection: for example, optimal periodic policies have been studied in [148][149], general optimal (infinite-horizon) policies in [150][151], decentralized event-based trigger solution in [152][153], and the case with packet losses is considered in [154]. Transmission power allocation for control applications has been explicitly considered in a few works. The case with a single sensor, thus without mutual interference, has been studied in [153][155] with only two (non-null) power levels and in [156] with a continuous bounded range of powers. More recently, also the problem of transmission power allocation with multiple possibly interfering nodes has been analyzed. The work [157] has studied the properties of the one-step-ahead optimal policy for remote estimation when the transmission power may take continuous unbounded values. Power allocation with multiple receivers has been recently studied in [158], where multiple systems communicate at each time instant to a dedicated remote estimator. Powers are then allocated in order to match minimum arrival probabilities for each system so that a minimum estimation quality is enforced.

The aim of this chapter is to introduce a tool to accommodate future sensor networks and control systems that will rely on next-generation wireless networks supporting power selection at the transmitter and multi-packet reception at the receiver. We introduce a very general system model including multiple sensors, multiple transmission power levels, a realistic fading channel model with mutual interference and arrival probabilities based on received SINR, and two different receiver design schemes, namely with and

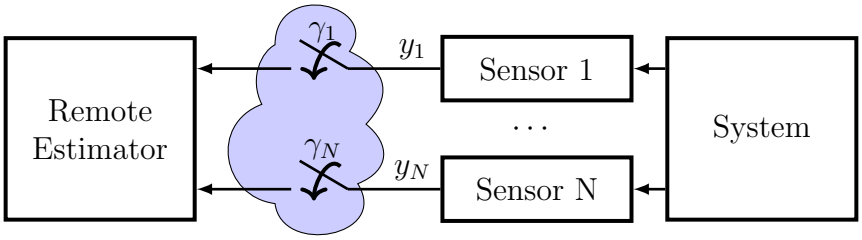

Figure 6.1: Setup. Sensors can choose among a finite set of possible tranmission powers. Arrival processes $\gamma_1, \ldots, \gamma_N$ are not independent but depend on the transmission powers of every sensor. We assume that the transmission power is computed at the remote estimator and transmitted to the sensors without errors.

without SIC. Under the considered framework we derive the optimal power allocation strategy by solving an (infinite or finite-horizon) optimization problem that accounts for the average estimation quality and penalizes the total average transmission power. We theoretically characterize the existence conditions of the infinite-horizon optimal policy and the structural properties of the one-step-ahead policy, with particular attention to multi-agent systems. By simulations on realistic systems, we show the improvements in terms of estimation quality given by SIC, that halves the error covariance with respect to simpler coding-decoding algorithms in the case of two segway-like robots.

6.1 Problem formulation

We consider a system equipped with a set of N spatially distributed sensors and we use a wireless network to connect the sensors to a remote estimator, see Figure 6.1. We assume that the sensors are provided with an advanced transmitter whose transmission power can be selected on a packet basis. Moreover, we assume that the remote unit is provided with an advanced receiver that is able to decode multiple incoming signals. We are interested into the problem of designing the law that maps the current error covariance to the next transmission powers. In this preliminary work, we assume that the transmission power $P^{\text{tx}}(t)$ is computed at the remote estimator and transmitted to the sensors without errors. The underlying assumption is that the remote estimator can use high transmission powers without energy concerns (as in the case where it is connected to the main power supply) and that the optimal transmission power can be encoded using few bits (as in the case where the number of sensors and powers is relatively small) so that high redundancy can be used in the transmission without wasting bandwidth. In the following we provide a complete description of the model considered.

6.1.1 System model

We consider a discrete-time linear system

$$x(t+1) = Ax(t) + w(t) \tag{6.1}$$

where $x(t) \in \mathbb{R}^n$ is the system state and $w(t) \in \mathbb{R}^n$ is the process noise. We consider a set of N sensors. The measurement process is modeled as

$$y_i(t) = C_i x(t) + v_i(t) \tag{6.2}$$

where $y_i(t) \in \mathbb{R}^{p_i}$ is the measurement of the i-th sensor and $v_i(t) \in \mathbb{R}^{p_i}$ is the measurement noise. We assume that process and measurement noise are independent and identically distributed random vectors with Gaussian distribution, namely $w(t) \sim \mathcal{N}(0, Q)$ for $t \geq 0$, $v_i(t) \sim \mathcal{N}(0, R_i)$ for $t \geq 0$, $w(t)$ is independent of $w(k)$ for $t \neq k$, $v_i(t)$ is independent of $v_i(k)$ for $t \neq k$, $v_i(t)$ is independent of $v_j(k)$ for $i \neq j$ and for $t, k \geq 0$, and $w(t)$ is independent of $v_i(k)$ for any i and for $t, k \geq 0$. We also assume that the initial state $x(0)$ is a Gaussian random vector independent of the process and measurement noise, namely $x(0) \sim \mathcal{N}(\bar{x}(0), P(0))$ and $x(0)$ is independent of $w(t)$ and $v_i(t)$ for any i and for $t \geq 0$.

At time instant t, the i-th sensor transmits a packet containing $y_i(t)$ to a remote estimator over a wireless network. We introduce the arrival process $\gamma_i(t) \in \{0, 1\}$ defined as

$$\gamma_i(t) = \begin{cases} 1 & \text{if } y_i(t) \text{ is available to the estimator} \\ 0 & \text{otherwise} \end{cases} \tag{6.3}$$

Complete characterization of the arrival process $\gamma_i(t)$ will be provided in the following subsections.

In this chapter, we consider the optimal estimator. To this end, we define the information available to the control unit as

$$\mathcal{I}(t) = \bigcup_{i=1}^{N} \mathcal{I}_i(t), \qquad \mathcal{I}_i(t) = \big\{\gamma_i(0)y_i(0), \ldots, \gamma_i(k-1)y_i(k-1)\big\} \tag{6.4}$$

where, with a little abuse of notation, if $\gamma_i(k) = 0$ then $\gamma_i(k)y_i(k) = \emptyset$. Now we define

$$\widehat{x}(t|t-1) = \mathbb{E}[x(t) \,|\, \mathcal{I}(t)] \tag{6.5}$$

$$P(t|t-1) = \mathbb{E}[(x(t) - \widehat{x}(t|t-1))(x(t) - \widehat{x}(t|t-1))' \,|\, \mathcal{I}(t)]. \tag{6.6}$$

According to [159], $\widehat{x}(t|t-1)$ is the optimal estimator given $\mathcal{I}(t)$, and the matrix $P(t|t-1)$ denotes the corresponding estimation error covariance matrix. In the considered setting with intermittent partial observations, under the assumption that $\gamma_i(t)$ is independent of

$x(k)$, the optimal estimator has been obtained in [47]. In order to more easily manage the update of the error covariance matrix, we arrange the results of [47] with the information form of the optimal estimator given by [160], obtaining

$$P(t|t) = \left(P^{-1}(t|t-1) + \sum_{i=1}^{N} \gamma_i(t) C_i' R_i^{-1} C_i \right)^{-1} \tag{6.7}$$

$$P(t+1|t) = A(t|t)A' + Q \tag{6.8}$$

initialized at $P(0|0) = P(0)$. Above equations can be obtained using the same reasoning of [38] and applying the Matrix Inversion Lemma.

6.1.2 Channel model

The wireless medium is modeled as a fading channel with Additive White Gaussian Noise (AWGN) whose average power at the remote estimator is σ^2. The transmission power $P_i^{\text{tx}}(t)$ used by the i-th sensor to transmit $y_i(t)$ is selected from a finite set $\mathcal{P}_i$

$$\mathcal{P}_i = \left\{0,\, P_{i,1}^{\text{tx}},\, P_{i,2}^{\text{tx}},\, \ldots\, ,\, P_{i,\max}^{\text{tx}}\right\}. \tag{6.9}$$

Let s_i denote the slow fading component of the channel power gain (usually dependent on path loss etc.) from the i-th sensor to the remote estimator, while $r_i(t)$ is the fast fading component of the same channel during the t-th sampling period. We assume that slow fading components are constant, while we assume that fast fading components are independent and identically distributed random variables with Exponential distribution and unit mean, namely $r_i(t) \sim Exp(1)$, $r_i(t)$ is independent of $r_i(k)$ for $t \neq k$, and $r_i(t)$ is independent of $r_j(k)$ for $i \neq j$ and for $t, k \geq 0$. It follows that the received power (at the remote estimator) $P_i^{\text{rc}}(t)$ from the i-th sensor is

$$P_i^{\text{rc}}(t) = s_i r_i(t) P_i^{\text{tx}}(t). \tag{6.10}$$

It follows that the received power $P_i^{\text{rc}}(t)$ is an exponential random variable with mean $s_i P_i^{\text{tx}}(t)$, i.e. $P_i^{\text{rc}}(t) \sim Exp(\lambda_i(t))$ with $\lambda_i(t) = (s_i P_i^{\text{tx}}(t))^{-1}$. Due to the independence of fast fading gains $r_i(t)$, received powers are temporally and spatially independent, namely $P_i^{\text{rc}}(t)$ is independent of $P_i^{\text{rc}}(k)$ for $t \neq k$ and $P_i^{\text{rc}}(t)$ is independent of $P_j^{\text{rc}}(k)$ for $i \neq j$ and for $t, k \geq 0$. This model, commonly referred to as Rayleigh fading, is related to the case when the number of reflected paths is large, such as in a factory or in an urban environment with many scatterers. In that case, the received electric field can be decomposed into two orthogonal components: each one is given by the sum of a large number of (zero-mean) terms and so it can be approximated by a Gaussian random variable. Therefore, the channel power gain is the sum of the squares of two Gaussian

random variables, resulting in an exponential distribution (see e.g. [161, Ch. 3.2] and [162, Ch. 14.1]). In the following we denote $P^{\text{rc}}(t) = (P_1^{\text{rc}}(t), P_2^{\text{rc}}(t), \dots, P_N^{\text{rc}}(t))$ and $P^{\text{tx}}(t) = (P_1^{\text{tx}}(t), P_2^{\text{tx}}(t), \dots, P_N^{\text{tx}}(t))$.

6.1.3 Receiver model

In contrast with most of the literature on transmission scheduling for remote estimation, we assume that the receiver has multi-packet reception capabilities, namely, it is able to decode multiple incoming signals. Successful reception of a packet requires that the signal carrying the information is strong enough with respect to the amount of interference and noise that disturb the transmission. In this view, following e.g. [163], the arrival process $\gamma_i(t)$ is modelled as

$$\gamma_i(t) = f_i(P^{\text{rc}}(t)) = \begin{cases} 1 & \text{if } \text{SINR}_i(P^{\text{rc}}(t)) > \alpha \\ 0 & \text{otherwise} \end{cases} \tag{6.11}$$

where $\text{SINR}_i(P^{\text{rc}}(t))$ is the Signal-to-Interference-and-Noise Ratio (at the decoding instant) corresponding to the packet containing $y_i(t)$, while $\alpha > 0$ is the reception threshold. The reception threshold depends on communication parameters like the modulation, the coding scheme, and the symbol rate. Since the received powers are independent across time slots, $\gamma_i(t)$ are independent across time slots, too. However $\gamma_i(t), \gamma_j(t)$ for $j \neq i$ may be dependent on each other due to interference within a given time slot. In this chapter, we consider two different receiver design schemes, implementing two different reception techniques, that result in two different expressions for the SINR.

The first receiver, referred to as *simple receiver*, decodes each signal independently so that the SINR is

$$\text{SINR}_i(P^{\text{rc}}(t)) = \frac{P_i^{\text{rc}}(t)}{\sum_{j \neq i} P_j^{\text{rc}}(t) + \sigma^2}. \tag{6.12}$$

According to this definition, the transmission from sensor i is affected by the interference of the transmissions from each other sensor $j \neq i$ [161, Ch. 6.1.1]. In typical information theoretic fashion, the received interference power is simply added to the noise power. The underlying assumption is that interference is statistically independent of combined channel and receiver noise. This is motivated by the use of random Gaussian codebooks at the transmitters to achieve the channel capacity for various types of fading channels, such as multiple-access, broadcast, and interference channels [164]. In this case we need to have $\alpha \in (0, 1)$ to enable multi-packet reception.

The second examined receiver differs from the first for the implementation of *Successive*

Interference Cancellation (SIC) algorithm. In this case, the sensor with the highest received power is decoded first and the reconstructed signal is subtracted out from the total received signal so that the second strongest signal can be decoded next when the strongest interference is no more present. In this way, after the first successful reception, other packets are decoded under an improved SINR and the probability of simultaneous received packets is definitely increased. According to a formal information theoretic treatment [165], sensors are usually relabeled by sorting the received powers in descending order so that the interference power is due only to subsequent sensors in the new order. We equivalently define the set $\mathcal{J}_i(t)$ containing the indices of the sensors whose received powers are higher than the received power from i-th sensor

$$\mathcal{J}_i(t) = \left\{ j \,:\, P_j^{\mathrm{rc}}(t) > P_i^{\mathrm{rc}}(t) \right\}. \tag{6.13}$$

Then, the SINR for the i-th sensor in this case is given by

$$\mathrm{SINR}_i(P^{\mathrm{rc}}(t)) = \begin{cases} \dfrac{P_i^{\mathrm{rc}}(t)}{\sum\limits_{\substack{j \notin \mathcal{J}_i(t) \\ j \neq i}} P_j^{\mathrm{rc}}(t) + \sigma^2} & \text{if } \mathrm{SINR}_j(P^{\mathrm{rc}}(t)) > \alpha \text{ for any } j \in \mathcal{J}_i(t) \\ \dfrac{P_i^{\mathrm{rc}}(t)}{\sum\limits_{j \neq i} P_j^{\mathrm{rc}}(t) + \sigma^2} & \text{otherwise.} \end{cases} \tag{6.14}$$

According to this definition, the transmission from sensor i is affected by the interference of the transmissions from each other sensor not decoded yet, possibly all the sensors $j \neq i$ if packets with higher received power have not been decoded [165]. Note that, even if $\alpha \geq 1$ multi-packet reception is possible with SIC.

6.2 Channel characterization

In this section we provide the probabilities of the arrival process as a function of the transmission powers. To this end, if $P_i^{\mathrm{tx}} > 0$ then $\lambda_i = (P_i^{\mathrm{tx}} s_i)^{-1}$ is well-defined and the joint distribution of received powers given the transmitted ones is

$$p(P_1^{\mathrm{rc}}, \ldots, P_N^{\mathrm{rc}} \,|\, P_1^{\mathrm{tx}}, \ldots, P_N^{\mathrm{tx}}) = \prod_{i=1}^{N} \lambda_i e^{-\lambda_i P_i^{\mathrm{rc}}} \tag{6.15}$$

since channel gains are independent. Adapted to the σ-algebra of the random variable P^{rc}, we can define the subset $R(\gamma)$ for $\gamma = (\gamma_1, \ldots, \gamma_N)$ as

$$R(\gamma) = \{P^{\mathrm{rc}} \,:\, f_i(P^{\mathrm{rc}}) = \gamma_i \;\; i = 1, \ldots, N\} \tag{6.16}$$

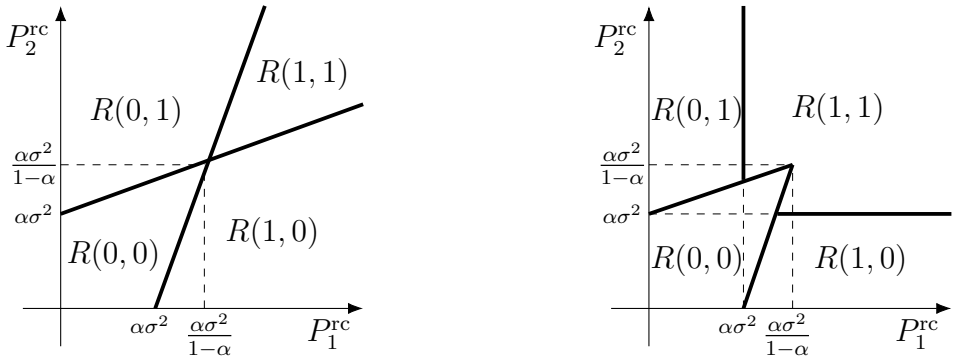

Figure 6.2: Possible received powers and corresponding outcome of the arrival process. Left panel: without SIC. Right panel: with SIC.

that is the subset of the possible received powers indicating whether packets have arrived or not as defined by γ. Explicit expressions for sets $R(\gamma)$ can be retrieved by combining (6.11) with (6.12) or (6.14). Note that they are different in general for the case with and without SIC, see for example the case with two sensors reported in Figure 6.2. A remarkable exception is $R(0,\dots,0)$, namely where no packets are correctly received, since, if the packet with the highest received power is not decoded, no advantages are given by SIC. Finally we can obtain the probability $P(\gamma|P^{\text{tx}}=u)$ of γ given the transmitted power $P^{\text{tx}}=u$ as the N-dimensional integral

$$P(\gamma \,|\, P^{\text{tx}}=u) = \int\int\cdots\int_{R(\gamma)} p(P^{\text{rc}} \,|\, P^{\text{tx}}=u)dP^{\text{rc}}. \tag{6.17}$$

The arrival probabilities can be computed either analytically or numerically. In the case where $P_i^{\text{tx}}=0$, λ_i is not defined and the joint distribution needs to be modified accordingly in order to consider that $P_i^{\text{rc}}=0$ with probability 1. The expression is omitted for sake of readability.

In the following we highlight the dependence of the arrival random variable γ_i on the transmitted power $P^{\text{tx}}=u$ as

$$\gamma_i(u) = f_i(s_i r_i u) \tag{6.18}$$

according to (6.10) and (6.11), and its expected value

$$p_i(u) = P(\gamma_i=1 \,|\, P^{\text{tx}}=u) = \mathbb{E}[\gamma_i(u)]. \tag{6.19}$$

It is easy to show that the probability $p_i(u)$ of receiving a packet from sensor i is monotonically increasing with respect to the power P_i^{tx} allocated to sensor i and monotonically decreasing with respect to P_j^{tx} for $j\neq i$.

We conclude this section providing the exact expressions for the case with 2 sensors, as an example. We denote by $p_{ij}(u)$ the probability that $\gamma_1=i$ and $\gamma_2=j$, with $i,j\in\{0,1\}$,

under the allocated power $u = ([u]_1, [u]_2)$. More specifically,

$$\begin{aligned}
p_{11}(u) &= \mathbf{P}(\gamma_1 = 1,\, \gamma_2 = 1 \,|\, P_1^{\text{tx}} = [u]_1,\, P_2^{\text{tx}} = [u]_2) \\
p_{10}(u) &= \mathbf{P}(\gamma_1 = 1,\, \gamma_2 = 0 \,|\, P_1^{\text{tx}} = [u]_1,\, P_2^{\text{tx}} = [u]_2) \\
p_{01}(u) &= \mathbf{P}(\gamma_1 = 0,\, \gamma_2 = 1 \,|\, P_1^{\text{tx}} = [u]_1,\, P_2^{\text{tx}} = [u]_2) \\
p_{00}(u) &= \mathbf{P}(\gamma_1 = 0,\, \gamma_2 = 0 \,|\, P_1^{\text{tx}} = [u]_1,\, P_2^{\text{tx}} = [u]_2)
\end{aligned}$$

If $P_1^{\text{tx}} > 0$ and $P_2^{\text{tx}} > 0$, under the assumption that $\alpha \in (0,1)$, we have

$$p_{11} = \left(\frac{\lambda_1}{\lambda_1 + \alpha\lambda_2} + \frac{\lambda_2}{\lambda_2 + \alpha\lambda_1} - 1 \right) e^{-(\lambda_1+\lambda_2)\frac{\alpha}{1-\alpha}\sigma^2} \tag{6.20}$$

$$p_{10} = \frac{\lambda_2}{\lambda_2 + \alpha\lambda_1}\, e^{-\alpha\lambda_1\sigma^2} - p_{11} \tag{6.21}$$

$$p_{01} = \frac{\lambda_1}{\lambda_1 + \alpha\lambda_2}\, e^{-\alpha\lambda_2\sigma^2} - p_{11} \tag{6.22}$$

$$\begin{aligned}
p_{00} &= 1 - (p_{11} + p_{10}) - (p_{11} + p_{01}) + p_{11} \\
&= 1 - \frac{\lambda_2}{\lambda_2 + \alpha\lambda_1}\, e^{-\alpha\lambda_1\sigma^2} - \frac{\lambda_1}{\lambda_1 + \alpha\lambda_2}\, e^{-\alpha\lambda_2\sigma^2} \\
&\qquad + \left(\frac{\lambda_1}{\lambda_1 + \alpha\lambda_2} + \frac{\lambda_2}{\lambda_2 + \alpha\lambda_1} - 1 \right) e^{-(\lambda_1+\lambda_2)\frac{\alpha}{1-\alpha}\sigma^2}
\end{aligned} \tag{6.23}$$

If $P_1^{\text{tx}} > 0$ and $P_2^{\text{tx}} = 0$ we have

$$p_{11} = 0 \quad p_{10} = e^{-\alpha\lambda_1\sigma^2} \quad p_{01} = 0 \quad p_{00} = 1 - e^{-\alpha\lambda_1\sigma^2} \tag{6.24}$$

while if $P_1^{\text{tx}} = 0$ and $P_2^{\text{tx}} > 0$ we have

$$p_{11} = 0 \quad p_{10} = 0 \quad p_{01} = e^{-\alpha\lambda_2\sigma^2} \quad p_{00} = 1 - e^{-\alpha\lambda_2\sigma^2}. \tag{6.25}$$

Clearly, if $P_1^{\text{tx}} = P_2^{\text{tx}} = 0$ then $p_{11} = p_{10} = p_{01} = 0$, $p_{00} = 1$.

When SIC is employed, the corresponding probabilities (denoted by the superscript SIC) are given by

$$\begin{aligned}
p_{11}^{SIC} &= \left(\frac{\lambda_2}{\lambda_2 + \alpha\lambda_1} e^{-\lambda_1\alpha\sigma^2} + \frac{\lambda_1}{\lambda_1 + \alpha\lambda_2} e^{-\lambda_2\alpha\sigma^2} \right) e^{-(\lambda_1+\lambda_2)\alpha\sigma^2} \\
&\qquad + \left(1 - \frac{\lambda_2}{\lambda_2 + \alpha\lambda_1} - \frac{\lambda_1}{\lambda_1 + \alpha\lambda_2} \right) e^{-(\lambda_1+\lambda_2)\frac{\alpha}{1-\alpha}\sigma^2}
\end{aligned} \tag{6.26}$$

$$p_{10}^{SIC} = \frac{\lambda_2}{\lambda_2 + \alpha\lambda_1} e^{-\alpha\sigma^2\lambda_1} \left(1 - e^{-\alpha\sigma^2(\lambda_2+\alpha\lambda_1)} \right) \tag{6.27}$$

$$p_{01}^{SIC} = \frac{\lambda_1}{\lambda_1 + \alpha\lambda_2} e^{-\alpha\sigma^2\lambda_2} \left(1 - e^{-\alpha\sigma^2(\lambda_1+\alpha\lambda_2)} \right) \tag{6.28}$$

$$p_{00}^{SIC} = p_{00}. \tag{6.29}$$

The cases where at least one transmitted power is null are equivalent to the case without SIC. As we can see, the expressions are quite involved and it is difficult to obtain general equations for an arbitrary number of sensors N.

6.3 Optimal power allocation: infinite horizon

We cast the power allocation task as a stochastic control problem. In particular, we define the state space $\mathcal{X}$ as the set of positive definite matrices of dimension $n \times n$, and the action space $\mathcal{U} \subset \mathbb{R}^N$ as the set of possible combination of transmission powers, namely

$$\mathcal{U} = \left\{ P^{\text{tx}} = (P_1^{\text{tx}}, \dots, P_N^{\text{tx}}) : P_i^{\text{tx}} \in \mathcal{P}_i \right\}. \tag{6.30}$$

An infinite-horizon policy is expressed as

$$U = \{u_1, u_2, u_3 \dots\} \tag{6.31}$$

where $u_t : \mathcal{X} \to \mathcal{U}$ is the function mapping the states $P(t|t-1)$ into the control action $P^{\text{tx}}(t) = u_t(P(t|t-1))$. We are interested in the policy that minimizes the infinite-horizon discounted cost

$$J(U, P(0)) = \lim_{K \to \infty} \mathbb{E}\left[\sum_{t=0}^{K-1} \beta^k \mathcal{C}(P(t+1|t), u_{t+1}(P(t+1|t))) \middle| P(0) \right] \tag{6.32}$$

where $\beta \in (0,1)$ is the discount factor and $\mathcal{C}(P,u)$ is the one-step-ahead cost from state P with action u. The use of a discount factor is common in infinite-horizon stochastic control problems to put more emphasis on current cost terms and less importance on costs incurred in the distant future. The discounted problem is more amenable from the theoretical point of view since the assumptions for the existence of the stationary optimal policy are milder than those for the average cost problem. However, the latter can still be considered for our problem at the price of added technical assumptions.

We choose

$$\mathcal{C}(P,u) = \mathbb{E}[\text{Tr}(g(P,u))|P,u] + \bar{\mu}u \tag{6.33}$$

where $\bar{\mu} = (\mu, \mu, \dots, \mu)$ is a regularization parameter and the function $g(P,u)$ is the Riccati-like operator

$$g(P,u) = A\left(P^{-1} + \sum_{i=1}^{N} \gamma_i(u) C_i' R_i^{-1} C_i \right)^{-1} A' + Q. \tag{6.34}$$

that provides the next error covariance starting from P with arrival process $\gamma_i(u)$. The cost balances the estimation quality, given by the trace of the error covariance, and

the transmission power consumption of the sensors through the regularization parameter μ. Minimizing the cost for different values of μ corresponds to minimizing the error covariance under different energy constraints: a larger μ implies a more stringent energy budget. Formally the problem is then

$$U^* = \arg\min_U J\left(U, P(0)\right) \tag{6.35}$$

resembling a discounted infinite-horizon Markov Decision Process (MDP).

In general the problem may not admit a solution. Moreover, even if the solution exists, the optimal action for a given error covariance may be time-dependent and thus not tractable for practical implementations. Several results are available in the literature of optimal control for MDP, providing sufficient conditions for the existence of an optimal solution that is stationary, namely that does not depend on time. A very strong condition is to have the one-step-ahead cost $\mathcal{C}(P, u)$ bounded, that is not true in our case. A weaker sufficient condition requires the existence of a positive scalar $m > 0$ and of a measurable function $w : \mathcal{X} \to \mathbb{R}^+$ such that

$$\mathcal{C}(P, u) < mw(P) \quad \text{and} \quad \sum_{z \in \mathcal{X}} w(z)\mathbf{P}(z|P, u) < w(P)$$

for any pair (P, u), $P \in \mathcal{X}$, $u \in \mathcal{U}$. Roughly speaking, this requires the cost to be (bounded by a function that is) a contraction in mean for any possible action. The most general condition to prove is the existence of a policy $\bar{U} = (\bar{u}_1, \bar{u}_2, \dots)$ such that $J(\bar{U}, P(0)) < \infty$ for any $P(0) \in \mathcal{X}$. See [166] for a full treatment. In the remainder of this section, based on the last condition, we show that a stationary optimal policy exists if it is possible to keep the evolution of the expected error covariance bounded.

Let $\mathcal{J}$ be a set of indices of sensors. Then consider the output matrix $C_{\mathcal{J}}$ as the stacked version of the output matrices C_i for $i \in \mathcal{J}$. It can be noticed that 2^N possible combinations of sensors can be selected, so essentially we have 2^N possible different $C_{\mathcal{J}}$. Among all the possible sets, choose a set $\mathcal{J}$ such that $(A, C_{\mathcal{J}})$ is detectable. Denote by $R_{\mathcal{J}}$ the corresponding block-diagonal matrix obtained from the matrices R_i for $i \in \mathcal{J}$. Then, for the given set, we can introduce two power allocation policies, characterized, respectively, by the perfect multi-packet reception probability, defined as

$$p_{\text{mp}} = \mathbf{P}(\gamma_i = 1,\, i \in \mathcal{J} \,|\, P_i^{\text{tx}} = P_{i,\max}^{\text{tx}},\, i \in \mathcal{J} \text{ and } P_j^{\text{tx}} = 0,\, j \notin \mathcal{J}) \tag{6.36}$$

and the worst-channel arrival probability, defined as

$$p_{\text{wc}} = \min_{i \in \mathcal{J}} \mathbf{P}(\gamma_i = 1 \,|\, P_i^{\text{tx}} = P_{i,\max}^{\text{tx}} \text{ and } P_j^{\text{tx}} = 0,\, j \neq i) \tag{6.37}$$

Let $\Lambda(A) = 1 - 1/\prod_\ell |\lambda_\ell^u(A)|^2$ where $\lambda_\ell^u(A)$ is the ℓ-th unstable eigenvalue of A. Then, we have the following sufficient stability condition.

Lemma 6.1. *Let the set $\mathcal{J}$ be such that the pair $(A, C_\mathcal{J})$ is detectable and let the pair $(A, \sqrt{Q})$ be reachable. Assume that at least one of the following conditions holds*

1. $p_{\text{mp}} > \Lambda(A)$,
2. $p_{\text{wc}} > \Lambda(A^{|\mathcal{J}|})$.

Then, there exists a policy $\bar{U}$ such that $\exists M_{P(0)} > 0$ for which $\mathbb{E}[P(t|t-1)] \leq M_{P(0)}$ for any $t \geq 0$.

Proof. We first assume that condition 1 holds. Consider the policy $\bar{U} = \{\bar{u}_1, \bar{u}_2, \dots\}$ where at each time instant all the sensors belonging to the set $\mathcal{J}$ transmit at the maximum power

$$[\bar{u}_t]_i = \begin{cases} P_{i,\max}^{\text{tx}} & \text{if } i \in \mathcal{J} \\ 0 & \text{otherwise} \end{cases}$$

where $[u]_i$ is the i-th entry of the vector u. Denote by $\mathbf{1}_\mathcal{J}$ the binary vector whose i-th entry is equal to 1 if $i \in \mathcal{J}$, and 0 otherwise. We can define the operator

$$\bar{g}(X) = AXA' + Q - p_{\text{mp}} AXC_\mathcal{J}'(C_\mathcal{J} X C_\mathcal{J}' + R)^{-1} C_\mathcal{J} X A'$$

and the sequence

$$\bar{P}_{t+1} = \bar{g}(\bar{P}_t) \text{ from } \bar{P}_1 = P(1|0)$$

By induction we can show that $\mathbb{E}[P(t|t-1)] \leq \bar{P}_t$ under the proposed policy. To this end, assume that $\mathbb{E}[P(t|t-1)] \leq \bar{P}_t$ for an arbitrary $t > 0$. Then we have

$$\begin{aligned}
\mathbb{E}[P(t+1|t)] &= \mathbb{E}\left[A\left(P(t|t-1)^{-1} + \sum_{i\in\mathcal{J}} \gamma_i C_i' R_i^{-1} C_i\right)^{-1} A' + Q\right] \\
&= \mathbb{E}\left[A\left(P(t|t-1)^{-1} + \sum_{i\in\mathcal{J}} C_i' R_i^{-1} C_i\right)^{-1} A' \middle| \gamma = \mathbf{1}_\mathcal{J}\right] p_{\text{mp}} + Q \\
&\quad + \mathbb{E}\left[A\left(P(t|t-1)^{-1} + \sum_{i\in\mathcal{J}} \gamma_i C_i' R_i^{-1} C_i\right)^{-1} A' \middle| \gamma \neq \mathbf{1}_\mathcal{J}\right] (1 - p_{\text{mp}}) \\
&\leq \mathbb{E}\left[A\left(P(t|t-1)^{-1} + \sum_{i\in\mathcal{J}} C_i' R_i^{-1} C_i\right)^{-1} A'\right] p_{\text{mp}} + Q + \mathbb{E}[AP(t|t-1)A'](1 - p_{\text{mp}}) \\
&\leq A\bar{P}_t A' + Q - p_{\text{mp}} A\bar{P}_t C_\mathcal{J}'(C_\mathcal{J} \bar{P}_t C_\mathcal{J}' + R_\mathcal{J})^{-1} C_\mathcal{J} \bar{P}_t A' = \bar{P}_{t+1}
\end{aligned}$$

where we use the Matrix Inversion Lemma and the Jensen's inequality. We can conclude that $\mathbb{E}[P(t|t-1)] \leq \bar{P}_t$ for any $t \geq 0$. In addition from [35][38] we know that if $p_{\text{mp}} > \Lambda(A)$

there exists a $M_{P(0)}$ such that $\bar{P}_t \leq M_{P(0)}$. It follows that $\mathbb{E}[P(t|t-1)] \leq M_{P(0)}$ concluding the proof.

We now assume that condition 2 holds. Consider the periodic policy $\bar{U} = \{\bar{u}_1, \bar{u}_2, \dots\}$ where at each time instant a sensor $i \in \mathcal{J}$ transmits at the maximum power, while other sensors do not communicate. If we relabel the sensors so that $\mathcal{J} = \{1, 2, \dots, L\}$, a possible policy is

$$[\bar{u}_t]_i = \begin{cases} P^{\text{tx}}_{i,\max} & \text{if } i \in \mathcal{J} \text{ and } \exists k \in \mathbb{N} : t = Lk + i \\ 0 & \text{otherwise} \end{cases}$$

where $[u]_i$ is the i-th entry of the vector u. For sake of clarity, we prove the lemma for $\mathcal{J} = \{1, 2, 3, 4\}$ but the general case can be proved analogously. Introduce the following operators

$$\begin{aligned} h(X) &= AXA' + Q \\ g_i(X) &= X - p_i X C_i'(X + C_i R_i C_i')^{-1} C_i X = (X^{-1} + p_i C_i R_i^{-1} C_i)^{-1} \\ \tilde{g}_i(X) &= X - p_{\text{wc}} X C_i'(X + C_i R_i C_i')^{-1} C_i X = (X^{-1} + p_{\text{wc}} C_i R_i^{-1} C_i)^{-1}. \end{aligned}$$

Under the proposed periodic policy we have

$$\begin{aligned} \mathbb{E}[P(4t+4|4t-3)] &\leq h \circ g_4 \circ h \circ g_3 \circ h \circ g_2 \circ h \circ g_1 \left(\mathbb{E}[P(4t|4t-1)]\right) \\ &\leq h \circ \tilde{g}_4 \circ h \circ \tilde{g}_3 \circ h \circ \tilde{g}_2 \circ h \circ \tilde{g}_1 \left(\mathbb{E}[P(4t|4t-1)]\right) \\ &\leq h \circ h \circ h \circ h \circ \tilde{g}_4 \circ \tilde{g}_3 \circ \tilde{g}_2 \circ \tilde{g}_1 \left(\mathbb{E}[P(4t|4t-1)]\right) \end{aligned}$$

where the first inequality holds because $h \circ g_i(X)$ is concave [35], the second holds because $h \circ g_i(X)$ is monotonically decreasing w.r.t. p_i, and the third holds if $Q > \sum_{i \in \mathcal{J}} (C_i' R_i^{-1} C_i)$ [167], otherwise a similar relation can be obtained with some manipulations.

Consider now the system $\bar{A} = A^4$, $\bar{Q} = \sum_{k=0}^{3} A^k Q$, $\bar{C} = C_{\mathcal{J}}$, $\bar{R} = R_{\mathcal{J}}$. We can define the operator

$$\bar{g}(X) = AXA' + Q - p_{\text{wc}} A X C_{\mathcal{J}}'(C_{\mathcal{J}} X C_{\mathcal{J}}') + R)^{-1} C_{\mathcal{J}} X A'$$

and the sequence

$$\bar{P}_{t+1} = \bar{g}(\bar{P}_t) \text{ from } \bar{P}_1 = P(1|0)$$

We have that $\bar{g}(X) = h \circ h \circ h \circ h \circ \tilde{g}_4 \circ \tilde{g}_3 \circ \tilde{g}_2 \circ \tilde{g}_1(X)$ by [11]. Similarly to what done above, we can prove by induction that $\mathbb{E}[P(4t|4t-1)] \leq \bar{P}_t$ for any $t \geq 0$. It is known from [35][38] that if $p_{\text{wc}} > \Lambda(\bar{A})$, then $\exists M_{P(0)} > 0$ such that $\bar{P}_t \leq M_{P(0)}$. It follows that $\mathbb{E}[P(t|t-1)] \leq M_{P(0)}$ concluding the proof. □

The previous theorem provides two sufficient but not necessary conditions for the boundedness of the error covariance, equivalent to the mean-square stability of the estimator. The first one is related to the arrival rate when all the measurements required for the system to be detectable are simultaneously transmitted. The second one relates the stability of the remote estimate to the characteristic of the worst channel and to the under-sampled system, as if the outputs are transmitted in a unique packet every $|\mathcal{J}|$ sampling periods. Note that the set of indices $\mathcal{J}$ can be chosen according to an optimization problem where p_{mp} or p_{wc} can be maximized. Moreover, in line of principle, the stability condition may be made less stringent by using intermediate solutions, e.g. coupling 4 sensors in two pairs and so on. It is worth mentioning that condition (2) is the same for any kind of receiver, while condition (1) is never valid for receivers without multi-packet reception capabilities. In this sense, there are cases where stability is guaranteed if multi-packet reception is enabled, while it may not be for a standard receiver. This improvement is clearly visible with SIC since it enhances the probability of receiving multiple packet simultaneously, and so also p_{mp}: e.g., for a system with a single unstable eigenvalue $\lambda^u(A)$, $\mathcal{J} = \{1, 2\}$, $P^{\text{tx}}_{i,\max} = 1$, $s_i = 1$, $\sigma^2 = 0.1$, it can be numerically derived that condition (2) requires $\lambda^u(A) < 1.6$, whereas condition (1) without SIC is $\lambda^u(A) < 1.05$, while condition (1) with SIC is $\lambda^u(A) < 2.6$.

We are now ready to state the existence of a (stationary) optimal policy for problem (6.35). Define the Value function

$$V_\beta(P) = \min_U J(U, P) \tag{6.38}$$

and let $\mathcal{X}^+(P)$ denote the finite set of possible error covariances that can be reached in one step from P

$$\mathcal{X}^+(P) = \left\{ z \in \mathcal{X} : z = A \left(P^{-1} + \sum_{i=1}^{N} \gamma_i C_i' R_i^{-1} C_i \right)^{-1} A' + Q,\ \gamma_i \in \{0, 1\} \right\} \tag{6.39}$$

Then we have the following result.

Proposition 6.1. *Under the hypothesis of Lemma 6.1, there exists an optimal infinite-horizon policy that is stationary. The optimal action $u^*(P)$ can be found by solving the optimality equation*

$$V_\beta(P) = \mathcal{C}(P, u^*(P)) + \beta \sum_{z \in \mathcal{X}^+(P)} V_\beta(z) \mathbf{P}(z | P, u^*(P)) \tag{6.40}$$

Proof. To prove the theorem we rely on the results given by [168] for the existence of an optimal stationary policy in general state space and finite action set. Essentially, the

existence of the stationary optimal policy requires the Value function to be finite. This can be proved as follows. By Lemma 6.1 there exists a policy $\bar{U} = (\bar{u}_1, \bar{u}_2 \dots)$ and a $M_{P(0)}$ such that $\mathbb{E}[P(t|t-1)] < M_{P(0)}$. It follows that

$$\begin{aligned}
&\mathbb{E}[\mathcal{C}(P(t+1|t), \bar{u}_{t+1}(P(t+1|t)))|P(0) = P] \\
&\qquad \leq \mathbb{E}\left[\mathrm{Tr}(AP(t+1|t)A' + Q)|P(0) = P\right] + \bar{\mu}\mathbb{E}\left[\bar{u}_{t+1}(P(t+1|t))|P(0) = P\right] \\
&\qquad \leq \mathrm{Tr}(AM_P A' + Q) + \bar{\mu}N = \overline{M}_P
\end{aligned}$$

Then

$$\begin{aligned}
J(\bar{U}, P) &= \mathbb{E}\left[\sum_{t=0}^{\infty} \beta^t \mathcal{C}(P(t+1|t), \bar{u}_{t+1}(P(t+1|t)))\Big| P(0) = P\right] \\
&= \sum_{t=0}^{\infty} \beta^t \mathbb{E}\left[\mathcal{C}(P(t+1|t), \bar{u}_{t+1}(P(t+1|t)))\Big| P(0) = P\right] \\
&\leq \sum_{t=0}^{\infty} \beta^t \overline{M}_P = \frac{\overline{M}_P}{1-\beta}
\end{aligned}$$

Finally,

$$V_\beta(P) = \inf_U J(U, P) \leq J(\bar{U}, P) \leq \overline{M}_P/(1-\beta)$$

namely the Value function is finite. Then, the existence of an optimal stationary policy follows from Theorem 1 in [168]. The optimality equation can be obtained by noting that only a finite number of values of the error covariance $P(t+1|t)$ can be reached from $P(t|t-1)$ in one step. □

The previous proposition ensures that the problem admits a feasible solution and allows us to limit our search in the set of stationary policies. To this end, there are many well-known algorithms based on dynamic programming tools such as the *Value Iteration algorithm* and the *Relative Value Iteration algorithm* [169].

6.4 Optimal power allocation: finite horizon

Similarly to what done for the infinite-horizon case, we can formulate also the finite-horizon power allocation problem. Indeed, depending on the application, the finite-horizon optimal policy may bring practical advantages, for example, when the system can be observed only for a fixed amount of time known in advance. For an arbitrary horizon of length K, the problem is to find a policy U

$$U = \{u_1, u_2, u_3, \dots, u_K\} \tag{6.41}$$

that minimizes the finite-horizon cost

$$J\left(U, P(0)\right) = \sum_{t=0}^{K-1} \beta^t \mathcal{C}(P(t|t-1), u_t(P(t|t-1))) \tag{6.42}$$

with $\beta \in (0, 1]$. In that case, the existence of the optimal policy is straightforward since stability is not required.

We conclude the section with a surprising result for the optimal policy with one-step-ahead horizon.

Proposition 6.2. *Consider $K = 1$ and $\mathcal{P}_i = \{0,\ P^{\text{tx}}_{i,\max}\}$. Assume that the sensors sample distinct outputs, namely such that $C_i C_j' = 0$ for any $i \neq j$. Then, there always exists an error covariance matrix $\bar{P}$ where the optimal action $u^*(\bar{P})$ is such that $P_i^{\text{tx}} = P^{\text{tx}}_{i,\max}$ for any i.*

Proof. For sake of simplicity we prove the theorem for the easiest case with two sensors. Preliminarily let us denote $q_1 = p_{10}(1, 0)$ and $q_2 = p_{01}(0, 1)$, while for simplicity we denote $p_{11} = p_{11}(1, 1)$, $p_{10} = p_{10}(1, 1)$, $p_{01} = p_{01}(1, 1)$, and $p_{00} = p_{00}(1, 1)$. With the new notation, according to formulas of section 6.2, we have

$$p_{11} + p_{10} = q_1 \frac{\lambda_2}{\lambda_2 + \alpha\lambda_1} \qquad p_{11} + p_{01} = q_2 \frac{\lambda_1}{\lambda_1 + \alpha\lambda_2}$$

Then for $\alpha \in (0, 1)$ we have

$$q_1 q_2 - q_1(p_{11} + p_{01}) - q_2(p_{11} + p_{01}) = q_1 q_2 \left(1 - \frac{\lambda_1}{\lambda_1 + \alpha\lambda_2} - \frac{\lambda_2}{\lambda_2 + \alpha\lambda_1}\right) < 0$$

where the inequality holds because the term in parentheses in monotonically increasing with respect to α and equal to 0 at $\alpha = 1$. We will use this result in the following.

By hypothesis $C_1 C_2' = 0$ and without loss of generality we assume $C_1 C_1' = C_2 C_2' = 1$. Then we can choose a set of $n - 2$ vectors $v_3, v_4, \ldots, v_n$ (row for convenience) such that $C_i v_j' = 0$, $i = 1, 2$, $j = 3, 4, \ldots, n$, $v_\ell v_j' = 0$, $\ell, j = 3, 4, \ldots, n$, and $v_j v_j' = 1$, $j = 3, 4, \ldots, n$, obtaining an orthonormal basis of the space $\mathbb{R}^n$. Using such a basis we define the set $\mathcal{X}_\sigma$ of symmetric positive definite matrices of the form

$$P_\sigma = \sigma_1 C_1' C_1 + \sigma_2 C_2' C_2 + \sum_{j=3}^{n} \sigma_j v_j v_j'$$

for any arbitrary combination of the eigenvalues $\sigma_1, \sigma_2, \sigma_j > 0$. We now evaluate the

Riccati-like operator on an arbitrary $P_\sigma \in \mathcal{X}_\sigma$ and for an arbitrary action u

$$\begin{aligned} g(P_\sigma, u) =& A\left(P_\sigma^{-1} + \gamma_1 C_1' R_1^{-1} C_1 + \gamma_2 C_2' R_2^{-1} C_2\right)^{-1} A' + Q \\ =& A\Big(\sigma_1^{-1} C_1' C_1 + \sigma_2^{-1} C_2' C_2 + \sum\nolimits_j \sigma_j^{-1} v_j' v_j + \gamma_1 C_1' R_1^{-1} C_1 + \gamma_2 C_2' R_2^{-1} C_2\Big)^{-1} A' + Q \\ =& A\Big((\sigma_1^{-1} + \gamma_1 R_1^{-1}) C_1' C_1 + (\sigma_2^{-1} + \gamma_2 R_2^{-1}) C_2' C_2 + \sum\nolimits_j \sigma_j^{-1} v_j' v_j\Big)^{-1} A' + Q \\ =& A\left(\frac{R_1\sigma_1}{R_1 + \gamma_1\sigma_1} C_1' C_1 + \frac{R_2\sigma_2}{R_1 + \gamma_2\sigma_2} C_2' C_2 + \sum\nolimits_j \sigma_j v_j' v_j\right) A' + Q \end{aligned}$$

where the dependence of γ on u is omitted for clarity. Based on this, we get

$$\mathcal{C}(P_\sigma, (1,0)) - \mathcal{C}(P_\sigma, (0,1)) = q_1 \frac{\sigma_2^2}{\sigma_2 + R_2} \mathrm{Tr}(A C_2' C_2 A') - q_2 \frac{\sigma_1^2}{\sigma_1 + R_1} \mathrm{Tr}(A C_1' C_1 A')$$

Within the set $\mathcal{X}_\sigma$ we now restrict to the subset of matrices $P_{\bar\sigma}$ characterized by $\bar\sigma_1, \bar\sigma_2, \bar\sigma_j$ for which $\mathcal{C}(P_{\bar\sigma}, (1,0)) = \mathcal{C}(P_{\bar\sigma}, (0,1))$, namely satisfying

$$\frac{\bar\sigma_2^2}{\bar\sigma_2 + R_2} \mathrm{Tr}(A C_2' C_2 A') = \frac{q_1}{q_2} \frac{\bar\sigma_1^2}{\bar\sigma_1 + R_1} \mathrm{Tr}(A C_1' C_1 A')$$

Now consider

$$\begin{aligned} &\mathcal{C}(P_{\bar\sigma}, (1,1)) - \mathcal{C}(P_{\bar\sigma}, (1,0)) \\ &\quad = \mathcal{C}(P_{\bar\sigma}, (1,1)) - \frac{1}{2}(\mathcal{C}(P_{\bar\sigma}, (1,0)) + \mathcal{C}(P_{\bar\sigma}, (1,0))) \\ &\quad = \left(\frac{q_1}{2} - (p_{11} + p_{10})\right) \frac{\bar\sigma_1^2}{\bar\sigma_1 + R_1} \mathrm{Tr}(A C_1' C_1 A') + \left(\frac{q_2}{2} - (p_{11} + p_{01})\right) \frac{\bar\sigma_2^2}{\bar\sigma_2 + R_2} \mathrm{Tr}(A C_2' C_2 A') + \mu \\ &\quad = \left(q_1 - (p_{11} + p_{10}) - (p_{11} + p_{01}) \frac{q_1}{q_2}\right) \frac{\bar\sigma_1^2}{\bar\sigma_1 + R_1} \mathrm{Tr}(A C_1' C_1 A') + \mu \end{aligned}$$

Since the term in parentheses is negative, we can see that the right hand side is monotonically decreasing with respect to $\bar\sigma_1$ and unbounded. It follows that $\exists \bar{\bar\sigma}_1 > 0$ such that $\mathcal{C}(P_{\bar\sigma}, (1,1)) < \mathcal{C}(P_{\bar\sigma}, (1,0))$ for $\bar\sigma_1 > \bar{\bar\sigma}_1$. We can conclude that the action $u = (1,1)$ is optimal at least for the matrices $P_{\bar\sigma}$ with $\bar\sigma_1 > \bar{\bar\sigma}_1$, $\bar\sigma_2$ such that $\mathcal{C}(P_{\bar\sigma}, (1,0)) = \mathcal{C}(P_{\bar\sigma}, (0,1))$, and arbitrary $\bar\sigma_j > 0$. □

Interestingly enough, this proposition holds in general but not for scalar systems, where all the sensors observe noisy versions of the same quantity and so the assumption $C_i C_j' = 0$ does not hold. In fact, it can be numerically shown that there are configurations of the parameters for which there does not exist an error variance such that multiple simultaneous transmissions are optimal. Conversely, previous proposition applies, among the others, for the notable case where each sensor observes a different component of the state. Even if the previous proposition shows that there always exists a covariance

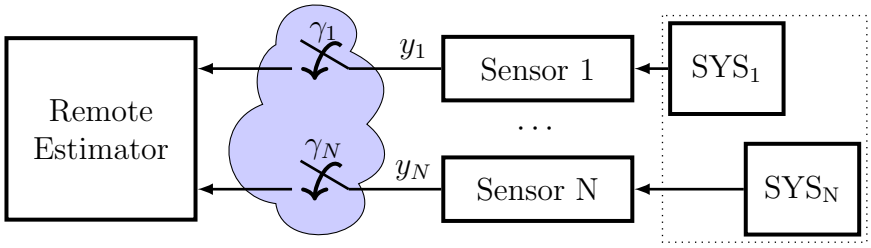

Figure 6.3: Setup. Dynamics of SYS$_1$ and SYS$_N$ are decoupled.

matrix such that employing multiple simultaneous transmissions is convenient, that error covariance may be not reachable along every sample path.

6.5 Special case: decoupled systems

In this section we present the analytical characterization of the optimal policy with horizon of length $K = 1$ for the case of decoupled systems. Indeed, considering decoupled systems is interesting because it resembles the case where multiple independent systems are observed by a central unit. This scenario has been specifically considered e.g. by [170][171][158]. Even more, in industrial WSNs, the dynamics of the monitored systems is often decoupled. The system considered in section 5.7 is a possible example of practical interest.

We assume that each subsystem is equipped with a (possibly multi-dimensional) sensor and we denote

$$A = \begin{bmatrix} A_1 & & 0 \\ & \cdots & \\ 0 & & A_N \end{bmatrix} \quad C = \begin{bmatrix} C_{10} & & 0 \\ & \cdots & \\ 0 & & C_{N0} \end{bmatrix} \quad Q = \begin{bmatrix} Q_1 & & 0 \\ & \cdots & \\ 0 & & Q_N \end{bmatrix} \quad P = \begin{bmatrix} P_1 & & 0 \\ & \cdots & \\ 0 & & P_N \end{bmatrix}$$

where 0 should be interpreted as a block of suitable dimension with all null entries, and $u = ([u]_1, \dots, [u]_N)'$. The considered setup is represented in Figure 6.3.

Introduce the following function

$$\psi_i(P_i) = \mathrm{Tr}\left[A_i P_i C_{i0}' (C_{i0} P_i C_{i0}' + R_i)^{-1} C_{i0} P_i A_i'\right] \tag{6.43}$$

and $\psi(P) = (\psi_1(P_1), \dots, \psi_N(P_N))$. Roughly speaking, it is the term by which the trace of the estimation error covariance is reduced if a measurement is received. In this sense it can be seen as the gain given by a new measurement with respect to the case where it has been lost. The function $\psi_i(\,\cdot\,)$ has the following property.

Lemma 6.2. *The function $\psi_i(X)$ is monotonically increasing with respect to X.*

Proof. Define $\overline{\psi}_i(X) = \mathrm{Tr}(X - (X^{-1} + C_i' R_i^{-1} C_i)^{-1})$. Note that if $\overline{\psi}_i(X)$ is monoton-

ically increasing, the same holds for $\psi_i(X)$. Given $f(\cdot)$ a differentiable function of an (invertible) matrix X^{-1}, from [172] (see also Sec. 2.2 of [173]) we have that

$$\frac{df(X)}{dX^{-1}} = -X' \frac{df(X)}{dX} X'$$

and thus

$$\frac{df(X)}{dX} = -X^{-T} \frac{df(X)}{dX^{-1}} X^{-T}$$

Let $f(X) = \mathrm{Tr}((X^{-1} + C'_{i0} R_i^{-1} C_{i0})^{-1}$. For X symmetric, it follows that

$$\begin{aligned}
\frac{df(X)}{dX} &= \frac{d\mathrm{Tr}((X^{-1} + C'_{i0} R_i^{-1} C_{i0})^{-1})}{dX} \\
&= -X^{-1} \frac{d(X^{-1} + C'_{i0} R_i^{-1} C_{i0})^{-1}}{dX^{-1}} X^{-1} \\
&= X^{-1} (X^{-1} + C'_{i0} R_i^{-1} C_{i0})^{-2} X^{-1}
\end{aligned}$$

where we use Equation (64) from [173]. Then we have

$$\frac{d\overline{\psi}_i(X)}{dX} = I - X^{-1} (X^{-1} + C'_{i0} R_i^{-1} C_{i0})^{-2} X^{-1}$$

Pre and post-multiplying by X we obtain

$$X \frac{d\overline{\psi}_i(X)}{dX} X = X^2 - (X^{-1} + C'_{i0} R_i^{-1} C_{i0})^{-2} \geq 0$$

concluding the proof. □

The monotonicity of $\psi_i(\cdot)$ entails the structural properties of the optimal policy, as shown in the following. We start from the derivation of an optimality condition.

Proposition 6.3. *Consider a decoupled system and horizon $K = 1$. Then $J(u, P) < J(v, P)$ if and only if*

$$\sum_{i=1}^{N} \psi_i(P_i) p_i(u) + \bar{\mu} u > \sum_{i=1}^{N} \psi_i(P_i) p_i(v) + \bar{\mu} v \tag{6.44}$$

Proof. For easy of notation, we consider the case of two systems. The theorem is proved by using the trick of splitting the cost in two parts, based on the following decomposition

$$\begin{aligned}
&\left(P^{-1} + \gamma_1(u) C_1' R_1^{-1} C_1 + \gamma_2(u) C_2' R_2^{-1} C_2\right)^{-1} \\
&\qquad = \begin{bmatrix} P_1^{-1} + \gamma_1(u) C_{10}' R_1^{-1} C_{10} & 0 \\ 0 & P_1^{-1} + \gamma_2(u) C_{20}' R_2^{-1} C_{20} \end{bmatrix}^{-1}
\end{aligned}$$

We can express the expected value as

$$\begin{aligned}
&\mathbb{E}[\mathrm{Tr}(A(P^{-1}+\gamma_1(u)C_1'R_1^{-1}C_1+\gamma_2(u)C_2'R_2^{-1}C_2)^{-1}A')|P,u] \\
&\quad=\mathbb{E}[\mathrm{Tr}(A_1(P_1^{-1}+\gamma_1(u)C_{10}'R_1^{-1}C_{10})^{-1}A_1'|P,u]+ \\
&\qquad\mathbb{E}[\mathrm{Tr}(A_2(P_2^{-1}+\gamma_2(u)C_{20}'R_2^{-1}C_{20})^{-1}A_2')|P,u] \\
&\quad=(1-p_1(u))\mathrm{Tr}(A_1P_1A_1)+(1-p_2(u))\mathrm{Tr}(A_2P_2A_2') \\
&\qquad+p_1(u)\mathrm{Tr}(A_1(P_1^{-1}+C_{10}'R_1^{-1}C_{10})^{-1}A_1') \\
&\qquad\quad+p_2(u)\mathrm{Tr}(A_2(P_2^{-1}+C_{20}'R_2^{-1}C_{20})^{-1}A_2')
\end{aligned}$$

so that we can rewrite the one-step-ahead cost as

$$\begin{aligned}
J(P,u)&=\mathcal{C}(P,u) \\
&=(1-p_1(u))\mathrm{Tr}(A_1P_1A_1')+(1-p_2(u))\mathrm{Tr}(A_2P_2A_2') \\
&\qquad+p_1(u)\mathrm{Tr}(A_1(P_1^{-1}+C_{10}'R_1^{-1}C_{10})^{-1}A_1') \\
&\qquad+p_2(u)\mathrm{Tr}(A_2(P_2^{-1}+C_{20}'R_2^{-1}C_{20})^{-1}A_2') \\
&\qquad\qquad+Q_1+Q_2+\mu u
\end{aligned}$$

If we define

$$\begin{aligned}
\psi_i(P_i)&=\mathrm{Tr}(A_iP_iA_i')-\mathrm{Tr}(A_i(P_i^{-1}+C_{i0}'R_i^{-1}C_{i0})^{-1}A_i') \\
&=\mathrm{Tr}(A_iP_iC_{i0}'(C_{i0}P_iC_{i0}'+R_i)^{-1}C_{i0}P_iA_i')\geq 0
\end{aligned}$$

where we used the Matrix Inversion Lemma, the minimization of $J(P,u)$ is equivalent to the maximization of $\psi_1(P_1)p_1(u)+\psi_2(P_2)p_2(u)+\mu u$, concluding the proof. □

Intuitively, since $\psi_i(P)>0$ and p_i is monotonically increasing with respect to the power allocated to the i-th sensor, the optimal policy allocates more power to the sensor with the largest $\psi_i(P)$. On the other hand, since p_i is monotonically decreasing with respect to the power allocated to j-th sensor, the optimal policy looks for a balance of the allocated powers weighted by $\psi_i(P)$.

As an immediate consequence, the previous theorem shows that the optimal policy has a threshold-like behaviour with respect to the scalar transformation $\psi(P)$ of P. Indeed for any possible control action u we can set a system of $|\mathcal{U}|$ linear inequalities in the variables $\psi_i(P_i)$ obtaining the region where the control action u is optimal. It follows that the optimal action can be easily expressed using an indicator function and can be implemented using finite memory to store the thresholds. Using the monotonicity of $\psi_i(P_i)$, this result can be enhanced obtaining the following characterization with respect to the error covariance P_i.

Proposition 6.4. *Consider a decoupled system and horizon $K=1$. If $\tilde{P}_i\geq P_i$ and $\tilde{P}_j=P_j$ for $j\neq i$, then for the optimal action u^* it holds that $[u^*(\tilde{P})]_i\geq[u^*(P)]_i$.*

Proof. For easy of notation, we consider the case of two systems. Consider P_2 and $[u]_2$ fixed. We highlight this by denoting $\mathcal{C}(P_1,[u]_1)=\mathcal{C}(P,([u]_1,[u]_2))$. Moreover let

$$\tilde{P}=\begin{bmatrix}\tilde{P}_1 & 0\\ 0 & P_2\end{bmatrix}$$

with $\tilde{P}_1\geq P_1$ and $\tilde{u}=([\tilde{u}]_1,[u]_2)$ with $[\tilde{u}]_1\geq[u]_1$. Then we have

$$\begin{aligned}\mathcal{C}(\tilde{P}_1,[u]_1)-\mathcal{C}(P_1,[u]_1)&=(1-p_1(u))\mathrm{Tr}(A_1\tilde{P}_1A_1')+(1-p_1(u))\mathrm{Tr}(A_1P_1A_1')\\&\quad+p_1(u)\mathrm{Tr}(A_1(\tilde{P}_1^{-1}+C_{10}'R_1^{-1}C_{10})^{-1}A_1')\\&\quad+p_1(u)\mathrm{Tr}(A_1(P_1^{-1}+C_{10}'R_1^{-1}C_{10})^{-1}A_1')\\&=\mathrm{Tr}(A_1(\tilde{P}_1-P_1)A_1')-p_1(u)(\psi_1(\tilde{P}_1)-\psi_1(P_1))\\&\geq\mathrm{Tr}(A_1(\tilde{P}_1-P_1)A_1')-p_1(\tilde{u})(\psi_1(\tilde{P}_1)-\psi_1(P_1))\\&=\mathcal{C}(\tilde{P}_1,[\tilde{u}]_1)-\mathcal{C}(P_1,[\tilde{u}]_1)\end{aligned}$$

where the inequality holds because $\psi_i(P_i)$ is monotonically increasing w.r.t. P_i and $p_i(u)$ is monotonically increasing w.r.t. $[u]_i$ for fixed $[u]_j$, $j\neq i$. We can conclude that

$$\mathcal{C}(\tilde{P}_1,[\tilde{u}]_1)-\mathcal{C}(P_1,[\tilde{u}]_1)\leq\mathcal{C}(\tilde{P}_1,[u]_1)-\mathcal{C}(P_1,[u]_1)$$

From Theorem 2.6.1 by [174] $\mathcal{C}(P_1,[u]_1)$ is submodular in $(P_1,[u]_1)$. From Theorem 2.8.1 by [174] submodularity is a sufficient condition for optimality of monotone increasing policies. See also the proof of Theorem 6.1 in [175]. In particular since $\mathcal{C}(P_1,[u]_1)$ is submodular in $(P_1,[u]_1)$, then $[u^*(P_1)]_1=\arg\min\mathcal{C}(P_1,[u]_1)$ is non-decreasing in P_1. □

As shown in section 6.2, p_i is a complicated function of allocated powers and it is not possible in general to have further insight on the structure of the optimal policy. The following proposition clarifies the easiest case, where only two power levels are available.

Proposition 6.5. *Consider a decoupled system, $N=2$ subsystems, horizon $K=1$, and $\mathcal{P}_i=\{0,\,P_{i,\max}^{\mathrm{tx}}\}$. Define*

$$\begin{aligned}S_{00}&=\left\{P:\psi_1(P_1)<\frac{\mu}{p_{10}(1,0)},\,\psi_2(P_2)<\frac{\mu}{p_{01}(0,1)}\right\}\\S_{11}&=\{P:(p_{10}(1,0)-p_1(1,1))\psi_1(P_1)+\mu<p_2(1,1)\psi_2(P_2)\\&\qquad\textit{and }(p_{01}(0,1)-p_2(1,1))\psi_2(P_2)+\mu<p_1(1,1)\psi_1(P_1)\}\\S_{10}&=\{P:p_{10}(1,0)\psi_1(P_1)>p_{01}(0,1)\psi_2(P_2)\}\setminus\{S_{00}\cup S_{11}\}\\S_{10}&=\{P:p_{10}(1,0)\psi_1(P_1)<p_{01}(0,1)\psi_2(P_2)\}\setminus\{S_{00}\cup S_{11}\}\end{aligned}$$

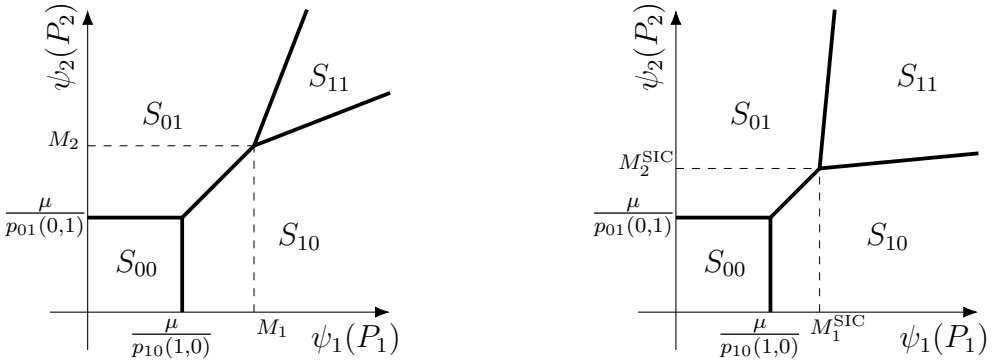

Figure 6.4: Optimal policy without SIC (left panel) and with SIC (right panel) with $M_1 = \mu p_{01}(0,1)/p_e$ and $M_2 = \mu p_{10}(1,0)/p_e$, where $p_e = p_1(1,1)p_{10}(1,0) + p_2(1,1)p_{01}(0,1) - p_{10}(1,0)p_{01}(0,1)$ and similarly with SIC. It is easy to show that $M_1 > M_1^{\text{SIC}}$, $M_2 > M_2^{\text{SIC}}$, and S_{11} is larger with SIC.

Then we have that

$$U^*(P) = \begin{cases} (0,\, 0) & \text{if } P \in S_{00} \\ (0,\, P_{2,\max}^{\text{tx}}) & \text{if } P \in S_{01} \\ (P_{1,\max}^{\text{tx}},\, 0) & \text{if } P \in S_{10} \\ (P_{1,\max}^{\text{tx}},\, P_{2,\max}^{\text{tx}}) & \text{if } P \in S_{11} \end{cases} \tag{6.45}$$

Proof. It easily follows from Proposition 6.3 using standard calculus tools. □

The previous proposition identifies 4 simple regions given by the optimality conditions provided by Proposition 6.3. Figure 6.4 reports the typical shape of the regions for the case with and without SIC. The reader can find an analogy between Figure 6.2, that depicts the received powers and the corresponding value of the arrival variable, and Figure 6.4, that depicts the values of the functions $\psi_i(\,\cdot\,)$ of the error covariance and the corresponding optimal action. Remarkably, R_{00} and S_{00} are the same with and without SIC, while R_{11} and S_{11} without SIC are strictly included in R_{11} and S_{11} with SIC. Unfortunately, in general, it is not possible to analytically associate the error covariance matrix P to the optimal action $u^*(P)$ without passing through $\psi_i(\,\cdot\,)$. However this is possible if A_i is scalar, where it is easy to invert the functions $\psi_i(\,\cdot\,)$, see [176].

6.6 Simulations: assessment of the proposed strategies

We start this section by providing some implementation details on the derivation of the proposed optimal infinite-horizon policy. For numerical purposes, it is convenient to discretize the action and state spaces. In our case, while the action space $\mathcal{U}$ is already discrete and finite, the state space $\mathcal{X}$ is the infinite-dimensional set of positive semidefinite matrices, for which a universal quantization mechanism does not exist. In this section,

we propose to obtain a discrete set as follows: first we collect multiple sample paths generated with random arrival processes and random initial conditions, then we cluster them into D different clusters based on the Frobenius norm mimicking what is done by the k-means algorithm for vector quantization, finally we obtain the set $\mathcal{X}_d$ by including the clusters' centroids. In this way, D can be tuned to obtain a trade-off between the accuracy of the quantization and the computational burden, while the focus is on the matrices given by the actual updates of the covariance matrix instead of exploring the whole space $\mathcal{X}$. Based on the discretized state space $\mathcal{X}_d$, we find the optimal policy off-line. To this end, we proceed as follows: first, the finite set $\mathcal{X}_d^+(P)$ of the discretized error covariance matrices that can be reached in one step from P is computed for any $P \in \mathcal{X}_d$, then, an iterative procedure is carried out to find the fixed point of the optimality equation (6.40) based on the Value Iteration algorithm. The optimal policy consists of a map from any matrix in $\mathcal{X}_d$ to the corresponding optimal action and it can be stored in a lookup table. Then, at time instant t, we find the matrix belonging to $\mathcal{X}_d$ that minimizes the distance to $P(t+1|t)$ and we use the corresponding optimal action. Further implementation details are given in [177].

Since multi-packet reception is naturally applicable in control of multi-agent systems, we consider a system featuring 2 identical drones that communicate their own positions to a remote control unit. The use of multiple drones is interesting for many different applications like environmental monitoring and object transportation. The system parameters are chosen as

$$A_1 = A_2 = \begin{bmatrix} 1 & T \\ 0 & 1 \end{bmatrix} \quad C_{10} = C_{20} = \begin{bmatrix} 1 & 0 \end{bmatrix} \quad Q = 0.1I$$

where $T = 0.1\,\mathrm{s}$ is the sampling period. This model is used also for other systems like ground robots or simple vehicles. It is reasonable to assume that both on-board transmitting systems are identical, and, if the drones are close to each other with respect to the central unit without obstacles on the line-of-sight, also the channels can be considered identical. For this reason we set

$$P_{1,\max}^{\mathrm{tx}} = P_{2,\max}^{\mathrm{tx}} = 1 \quad s_1 = s_2 = 1 \quad \sigma^2 = 0.1$$

where we have normalized the powers and the channel power gains. We set $M = 4$, $\alpha = 0.75$ and $\beta = 0.9$.

We start by reporting a pictorial representation of the optimal policy with SIC. To this end, we may use the function $\psi(P)$. Indeed, using the function $\psi(P)$, each covariance matrix P can be mapped to a point of the plane $\psi_1(P_1) \times \psi_2(P_2)$, where P_i is the error covariance matrix relative to subsystem i. Then, using the relation in Proposition 6.3,

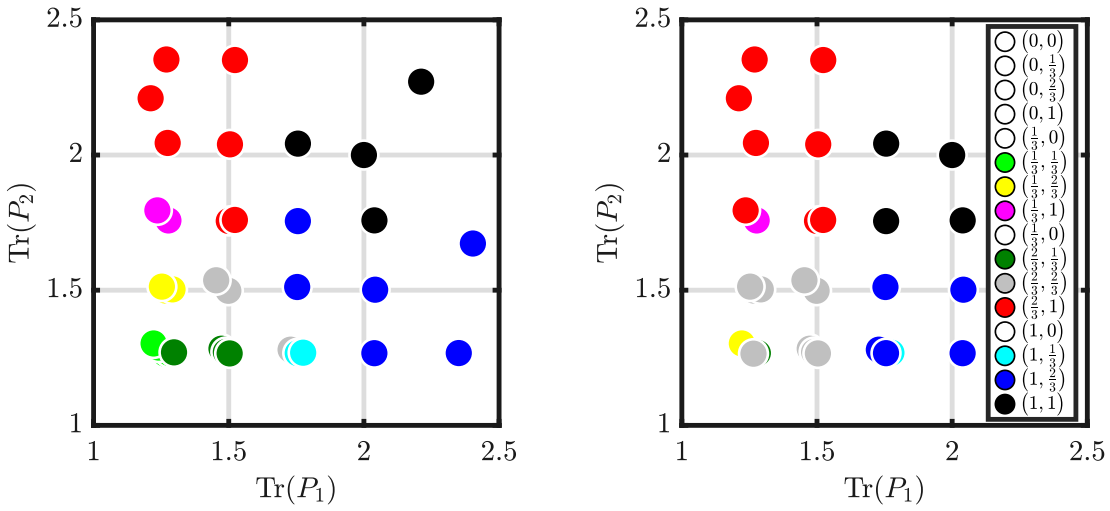

Figure 6.5: Optimal policy with SIC ($\mu = 0.1$). Left panel: $K = 1$. Right panel: $K = \infty$. System: two drones. In the legend, no colors are assigned to actions not used on $\mathcal{X}_d$. Note that the optimal policy always allocates strictly non-null powers to both the sensors.

the plane $\psi_1(P_1) \times \psi_2(P_2)$ can be divided into a finite number of subregions, each of them associated to a specific optimal action, producing a plot similar to Figure 6.4. Here, however, we prefer to represent the plane $\mathrm{Tr}(P_1) \times \mathrm{Tr}(P_2)$, where $\mathrm{Tr}(P_i)$ is the trace of P_i, instead of the plane $\psi_1(P_1) \times \psi_2(P_2)$. In fact, $\mathrm{Tr}(P_i)$ gives an immediate understanding of the quality of the current estimate of the state of subsystem i: the higher $\mathrm{Tr}(P_i)$, the worse the knowledge on subsystem i is. The optimal one-step-ahead policy and the optimal infinite-horizon policy with SIC are reported in the left and right panels of Figure 6.5, respectively. In the two plots, the points are not uniformly distributed because they are taken from the discretized state space $\mathcal{X}_d$, which is not distributed over the whole space. In the left panel, we can see that, for a fixed $\mathrm{Tr}(P_2)$, the optimal one-step-ahead power allocated to sensor 1 is not decreasing with respect to $\mathrm{Tr}(P_1)$. The same holds for sensor 2. Similarly, the total power increases by moving along a straight line starting from the origin. Since larger P_i entails larger $\mathrm{Tr}(P_i)$, this is expected from Proposition 6.4, which states that the optimal one-step-ahead transmission power of sensor i increases for larger P_i for a fixed P_j. It is interesting to stress that for $\mathrm{Tr}(P_1) = \mathrm{Tr}(P_2) \simeq 1.8$ it holds that $\min_U J(U, P) = J\left(\left(1, \frac{2}{3}\right), P\right) = J\left(\left(\frac{2}{3}, 1\right), P\right)$. In that case we decide to fix $U^* = \left(1, \frac{2}{3}\right)$. It causes an asymmetry in the optimal policy even if the system consists of two independent identical subsystems. As it can be seen in the right panel, the optimal infinite-horizon policy has similar features. Differences are present especially in the bottom left corner of the plane: the optimal action for error covariances P such that $\mathrm{Tr}(P_1) \simeq 1.25$, $\mathrm{Tr}(P_2) \simeq 1.5$ shifts from $\left(\frac{1}{3}, \frac{2}{3}\right)$ to $U^* = \left(\frac{2}{3}, \frac{2}{3}\right)$, and the same happens for $\mathrm{Tr}(P_1) \simeq 1.5$, $\mathrm{Tr}(P_2) \simeq 1.25$, while the set of error covariances with

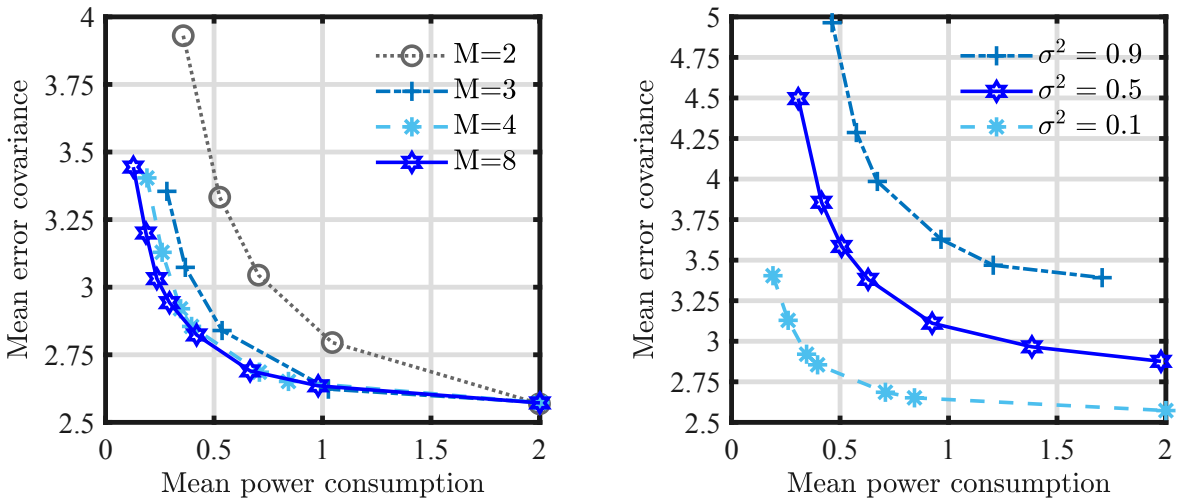

Figure 6.6: Assessment of the optimal infinite-horizon policy with SIC for different numbers of available power levels M (left panel) and noise σ^2 (right panel). System: two drones.

$\mathrm{Tr}(P_1) \simeq \mathrm{Tr}(P_2) \simeq 1.25$ is split into three different regions, and the most conservative action $\left(\frac{1}{3}, \frac{1}{3}\right)$ is no more optimal for any considered covariance. Interestingly, the optimal policy allocates non-null power to both sensors for any $P \in \mathcal{X}_d$, namely multi-packet reception is always used.

We now focus on the performances of the proposed policies. The following plots report the mean trace of the error covariance matrix for different mean power consumptions (normalized over the consumption for a single transmission at the maximum power). Such a plot allows comparing different policies (or the same policy with different parameters) in a fair way by providing the different estimation performances achieved with the same power consumption. To obtain the following plots, we set different values of μ and we simulate the system evolution over a long time horizon under the corresponding policy. To assess how the optimal infinite-horizon policy with SIC behaves for different hardware and network conditions, we vary the number of available transmission power levels (Figure 6.6, left panel) and the background noise (Figure 6.6, right panel). In the left panel of Figure 6.6 we can see that increasing the number of levels M improves the estimation quality for the same mean power consumption. On one hand, the improvement is particularly clear for low power consumptions, where we can see that, with more transmission levels, the energy is more efficiently employed. On the other hand, the improvement tends to saturate when increasing the number of levels, especially when the energy bound is not stringent (right part of the plot): the mean error covariance with a mean power consumption of 2 is identical for any considered value of M, and with a mean power consumption higher than 0.4 for $M = 4$ and $M = 8$. In the right panel of

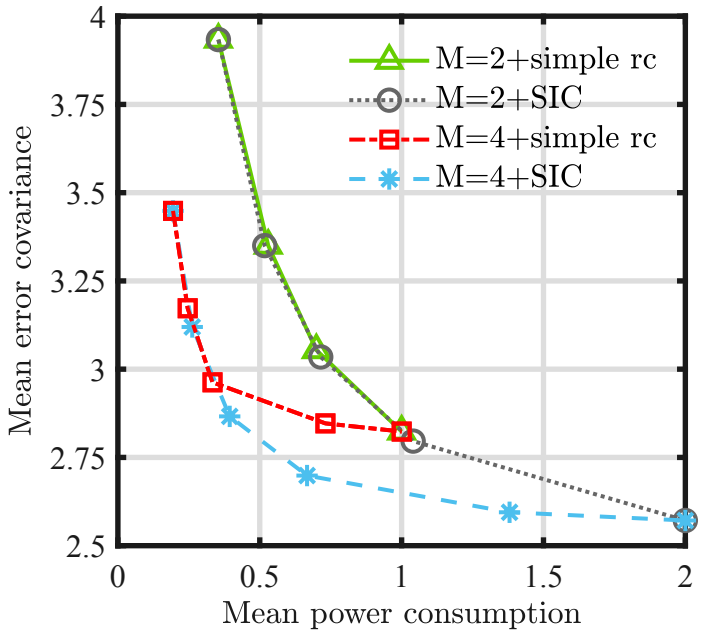

Figure 6.7: Assessment of the optimal infinite-horizon policies for different receivers (with and without SIC) and different numbers of available power levels M. System: two drones.

Figure 6.6, we can see that with better network conditions, i.e. lower background noise σ^2, the estimation quality is improved for the same mean power consumption. In general, a lower error covariance can be achieved with lower σ^2 but some error covariances can be achieved also with higher σ^2 at the price of higher mean power consumptions. For instance, a mean error covariance of 3.4 can be achieved with a mean power consumption of 0.2 with $\sigma^2 = 0.1$, of 0.6 with $\sigma^2 = 0.5$, and of 1.7 with $\sigma^2 = 0.9$.

We now compare the performances of the infinite-horizon optimal policy for both the receivers, namely with and without SIC, and for transmitters with different numbers of available power levels, specifically $M = 2$ and $M = 4$. Results are reported in Figure 6.7. We can see that, allowing more than 2 power levels, the mean error covariance is smaller. The difference is particularly evident when we impose a stringent constraint on the power consumption (left part of the plot). The performance without SIC is similar to the counterpart with SIC when the mean power consumption is small. This is due to the fact that communications are highly penalized so that simultaneous transmissions are selected for error covariances that the system reaches less often. The difference becomes more evident when the energy constraint is less stringent: with $M = 4$, we achieve a reduction of the mean trace of error covariance up to 10%. Note that in the case of SIC, both with $M = 2$ and $M = 4$, the optimal policy tends to be more aggressive in terms of power allocation: indeed, for small μ, with SIC, simultaneous transmissions at the maximum

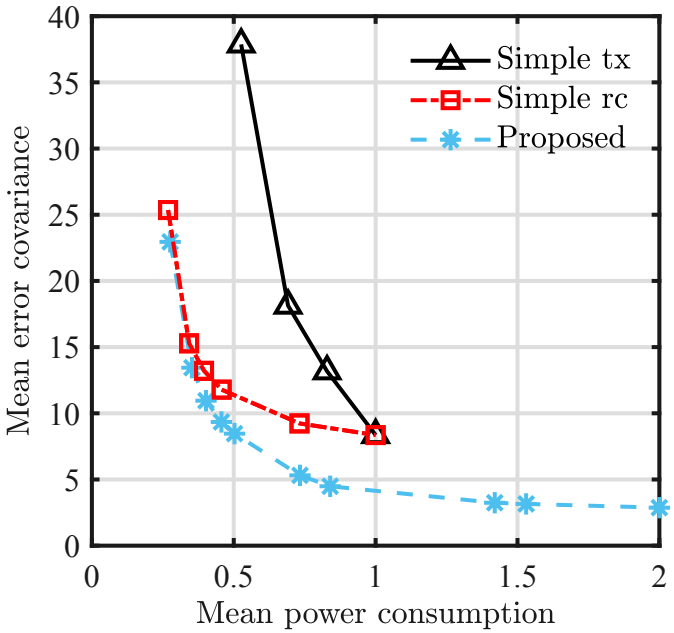

Figure 6.8: Comparison between existing algorithms ($K = 1$). Simple tx [154]. Simple rc [157]. Proposed: $M = 4$ with SIC. System: two segways.

power are often scheduled, while in the case without SIC, even with $\mu = 0$ the mean power consumption is equal to 1. This is due to the fact that alternating transmissions from sensor 1 to sensor 2 are preferred because the loss probability with simultaneous transmissions is high. Presented results indicate the importance of SIC in order to always optimally allocate the available power when it is limited (left part of the plot), and to further decrease the mean error covariance when requirements on the power consumption are not stringent (right part).

To validate the proposed algorithm we compare it with other existing algorithms that rely on a simpler hardware. In particular, we consider the simplest solution studied in [154] where transmitters have only two power levels and the receiver has no multi-packet reception capabilities (only one sensor is scheduled at a given time). We will refer to it as "Simple tx". Then we consider a more advanced solution adapted from [157] where the transmitters have 4 power levels and the receiver is able to decode multiple simultaneous packets but does not implement SIC. We will refer to it as "Simple rc". Finally, we consider the proposed policy as derived in section 6.4 with SIC and $M = 4$. We carry out the test on a more extreme case where the system consists of two segways. For sake of simplicity, in this chapter, we consider the simplified model obtained by the discretization

with $T = 0.01$ s of the linearized continuous-time system

$$A_1 = A_2 = \begin{bmatrix} 0 & 1 \\ g/\ell & 0 \end{bmatrix} \quad C_{10} = C_{20} = \begin{bmatrix} 1 & 0 \end{bmatrix} \quad Q = 0.1I$$

where g is the gravitational acceleration and $\ell = 0.25$, equivalent to the case of a rigid body with height 20 cm. This model can capture the simplified dynamics of wheeled robots transporting an object. Differently from the system with two drones, the dynamics are unstable, so the estimation and the power allocation problem are more challenging. Communication parameters are set as for the previous example. Results are reported in Figure 6.8. We can see that the proposed strategy outperforms the existing algorithms. In particular, the difference with respect to Simple tx is evident when the energy requirements are strict, i.e., when the mean power consumption is small. On the other hand, the difference with respect to Simple rc is the largest for a mean power consumption equal to 1, for which the mean error covariance achieved by the proposed strategy using SIC is half of the existing algorithm. Note that Simple rc achieves the same error covariance of Simple tx and it is not able to go beyond a mean power consumption of 1, namely a single transmission at the maximum power at each time step. Conversely, with SIC, it is convenient to have simultaneous transmissions to get information from both the systems more often. This shows that simultaneous transmissions are really advantageous with the concurrent implementation of SIC.

6.7 Conclusion

In this chapter, we have explored the power allocation problem for remote estimation in the case where multiple incoming packets from simultaneous transmissions can be decoded by the receiver. We have shown the existence of a stationary optimal policy for the infinite-horizon problem and we have shown that the optimal one-step-ahead policy has a threshold behavior with respect to a scalar transformation of the error covariance if the system is decoupled. Through extensive numerical simulations, we have shown the improvements of the proposed strategy, especially when SIC is implemented. The proposed solution is suitable for multi-agent systems, as well for the Internet of Things.

7 Conclusions

In this thesis, we have started from the observation that stability does not imply safety when the feedback loop is closed over wireless. This has been theoretically explained in chapter 2, where we have focused on the problem of remote estimation for the single-agent case. We have considered the widespread setup with Gaussian noise and without control input. First, using simple arguments, we have shown that the stationary distribution of the estimation error, if it exists, is heavy-tailed. Then, using results of the Renewal theory, we have derived a sufficient condition for the existence of the stationary distribution. From these results, it follows that large deviations of the system trajectory are likely to occur even if the system is mean-square stable. To deal with this problem, we have proposed to move from the concept of stability to a new concept of safety, more suitable for practical applications.

Based on practical examples, we have proposed to represent safety requirements through suitable constraints on the system evolution. The objective of the thesis was to devise control algorithms able to guarantee constraint satisfaction without making assumptions on the wireless network.

In chapter 3 and chapter 4, we have focused on the problem of constrained control over wireless for the single-agent case. In both cases, as often done in the literature of constrained control, we have assumed that the sensor has access to the complete state of the system. In chapter 3 we have proposed a solution based on RG. We have first extended the theory of Maximal Output Admissible Set for the case of packet losses. We have shown that, under the proposed strategy, safety is always satisfied without any assumption on the network. Then, we have proved that the system converges to any admissible desired set-point if infinite sequences of packet losses have probability 0.

In chapter 4 we have extended the MPC for Tracking to the case with packet losses. By using a local smart actuator able to stabilize the system in presence of blackouts, we have proved that safety is always guaranteed without any requirement on the network. The scheme achieves convergence to any admissible desired set-point if there exists an infinite sequence of time instants where two consecutive receptions, one per link, occur.

In chapter 5 we have addressed the problem of multi-agent constrained control over wireless. The proposed centralized solution features a suitable actuator scheduler, that selects only the agents whose applied input is known, and a remote estimator, that computes any possible state of the system. We have shown that safety is guaranteed without any assumption on the network. Using results on distributed RG, we have shown that the convergence to any admissible desired set-point is achieved under suitable mild assumptions on the actuator scheduler, on the constraint set, and on the network.

In chapter 6 we have considered the problem of sensor transmission power allocation for remote estimation in the case where the receiver is able to simultaneously decode multiple incoming packets. We have considered two different receivers, one implementing standard multi-packet reception techniques, and one implementing SIC. Based on fundamental results on wireless communications, we have derived a detailed analytical model of the network. For the infinite-horizon power allocation problem, using results from the theory of Kalman filtering with intermittent observations, we have derived two sufficient conditions for the existence of a stationary optimal policy. For the one-step-horizon problem, if the system is decoupled, we have shown that the optimal policy has a threshold behavior with respect to a scalar transformation of the error covariance.

Accurate simulations have shown the validity of the proposed algorithms. In particular, WiFi-in-the-loop simulations have proved the effectiveness of the proposed RG and MPC schemes for constrained control over the latest wireless networks. The solutions guarantee both safety in bad channel conditions and high performances in good channel conditions. Results achieved by the proposed RG in experimental tests involving the Segway-like robot are promising: despite non-ideal mechanical design and model errors, the constraints are satisfied and the desired reference is reached very quickly.

This thesis has verified both theoretically and experimentally that constrained control with fast wireless communications is feasible. This result raises new research questions.

Regarding the single-agent problem, it is reasonable to ask when it is convenient to shift from the legacy wired controller to a remote controller. In general, the local controller cannot be very sophisticated but, depending on the application, its performances may be altogether comparable to the performances of advanced schemes like MPC. Is it possible to determine which is the optimal choice between the wired and the wireless alternatives? Are there system characteristics that can be used to decide which architecture gives the best performances?

This question is less relevant for multi-agent systems, since wireless communications are unavoidable. However, it is still not clear which is the optimal amount of computational resources that can be made available to the plant side. We have assumed that the smart actuator can only implement a logic to select the control input from a finite set of values, and eventually implement a state-feedback controller. It is important to understand if performances can be improved allowing the actuator to implement more

elaborated control laws. Possible hybrid solutions with a centralized control unit and a local algorithm based on formation control theory can be effective, especially in the case of time-varying constraints. What is the optimal distribution of roles between the centralized controller and the local controller? Which is the trade-off between communication rate and communication reliability that optimizes the performances of the systems? In the next years, we will pursuit the answer to these questions.

A
Appendix

A.1 Minkowsky Set Sum and Difference

In this thesis we widely use set operations. In the following we recall some basic definitions and properties. Let $X \subseteq \mathbb{R}^n$ and $Y \subseteq \mathbb{R}^n$ be two sets, and let $\alpha \in \mathbb{R}$. The scalar multiplication of a set is defined as

$$\alpha X = \{\alpha x : x \in X\}. \tag{A.1}$$

The matrix multiplication AX with $A \subseteq \mathbb{R}^{m \times n}$ is defined analogously. The Minkowsky Set Sum is defined as

$$X \oplus Y = \{x + y : x \in X,\ y \in Y\}. \tag{A.2}$$

The Minkowsky Set Difference, also referred to as the Pontryagin set difference, is defined as

$$X \sim Y = \{x : x - y \in X,\ \forall y \in Y\}. \tag{A.3}$$

A pictorial representation of the Minkowsky Set Sum and of the Minkowsky Set Difference is reported in Figure A.1. Efficient algorithms based on linear programming have been devised to compute the Minkowsky Set Sum and Difference in the case of polyendron. The case of more general sets is more cumbersome but it is still possible to find suitable approximations. In the following theorem we summarize some useful properties of set operations.

Theorem A.1. *The following statements hold: (i)* $\alpha X \subset X$ *if and only if* $\alpha \in [0, 1)$ *and* $0 \in \text{int}(X)$ *(ii)* $(\alpha_1 + \alpha_2)X = \alpha_1 X \oplus \alpha_2 X$ *if* $\alpha_1 \geq 0$, $\alpha_2 \geq 0$, *and* X *is convex (iii)* $X \oplus Y$ *is bounded if* X *and* Y *are bounded (iv)* $X \oplus Y$ *is closed if* X *and* Y *are closed (v)* $X \oplus Y$ *is convex if* X *and* Y *are convex (vi)* $X \oplus Y$ *is symmetric if* X *and* Y *are symmetric (vii)* $X \sim Y \subseteq X$ *if* $0 \in Y$ *(viii)* $(X \sim Y) \oplus Y \subseteq X$ *(ix)* $X \sim Y$ *is bounded if* X *is bounded (x)* $X \sim Y$ *is closed if* X *is closed (xi)* $X \sim Y$ *is convex if* X *is convex (xii)* $X \sim Y$ *is symmetric if* X *and* Y *are symmetric*

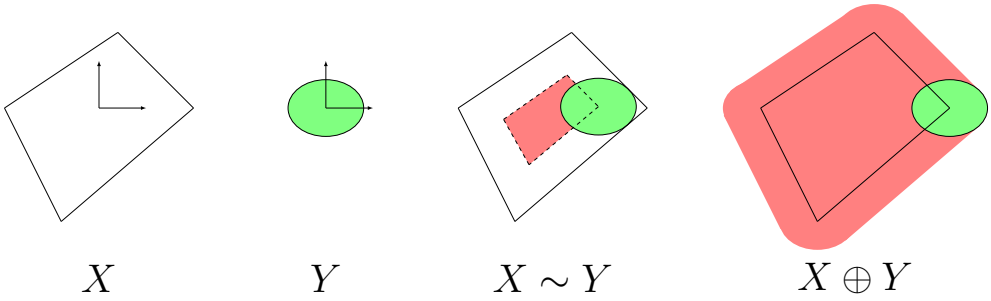

Figure A.1: Set operations.

For more details, see [106]. In particular, it is interesting to stress that $(X \sim Y) \oplus Y$ does not return the whole X, but a subset of X. This can be seen also in Figure A.1, third panel.

A.2 Testbed: the Segway-like Robot

For most of the numerical examples carried out in this thesis, we consider an accurate model of the two-wheeled balancing robot depicted in Figure A.2, often referred to as Segway-like robot or simply Segway. It consists of a rigid chassis with two wheels, that results in an inverted-pendulum-like structure and can be regarded as a small-scale version of a Segway electric vehicle. In the figure, we can discern the battery, the electronic boards, and, in the bottom part of the rigid chassis, the dc motors connected to the wheels. Approximately, the rigid chassis has dimensions 20 cm $\times$ 20 cm $\times$ 10 cm and the radius of the wheels is 3.4 cm.

Under the assumption that steering is not allowed (so wheels are always coupled), the system state consists of the wheel angle (which provides the position of the center-of-mass of the wheel along a straight line), the tilt angle (namely the angle between the vertical axes of the robot chassis and the line orthogonal to the plane), and their derivatives. The control input is the voltage supplied to the dc motors moving the wheels, and the

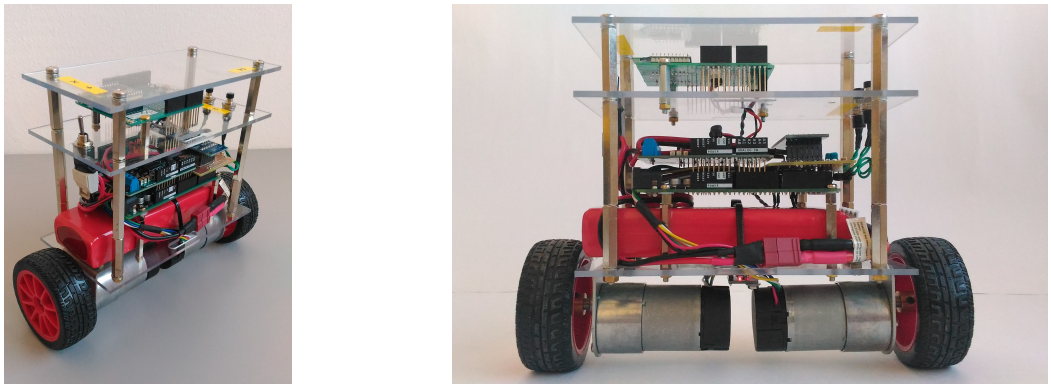

Figure A.2: The Segway-like robot

system outputs are the measurements from a on-board MPU and encoders on the motors. The continuous-time nonlinear mathematical model is derived following the Lagrangian approach [178]. For the purposes of this thesis, the system is linearized around the equilibrium, characterized by null tilt angle (and null derivatives). Finally, the system is discretized using exact discretization. With sampling period $T = 0.01$ s, the system matrices are

$$A_{ol} = \begin{bmatrix} 1 & 0.0022 & 0.0098 & 0.0001 \\ 0 & 1.0027 & 0.0001 & 0.0099 \\ 0 & 0.4345 & 0.9624 & 0.0359 \\ 0 & 0.5488 & 0.0198 & 0.9801 \end{bmatrix} \qquad B_{ol} = \begin{bmatrix} 0.0002 \\ -0.001 \\ 0.0472 \\ -0.0317 \end{bmatrix}$$

Note that the system is unstable with unstable eigenvalue equal to 1.0741. When needed, we implement a LQR controller with weights

$$Q = \begin{bmatrix} 100 & 0 & 0 & 0 \\ 0 & 1000 & 0 & 0 \\ 0 & 0 & 1 & 0 \\ 0 & 0 & 0 & 1 \end{bmatrix} \qquad R = 10$$

and we consider nominal tracking design. The resulting state feedback gain and the feedforward gain are

$$K = \begin{bmatrix} -2.8747 & -83.6534 & -2.1875 & -8.8631 \end{bmatrix} \qquad N_r = -2.8747$$

so the closed-loop system matrices are

$$A = A_{ol} - KB_{ol} \qquad B = N_r B_{ol}$$

In this thesis, the system output matrix is chosen equal to $C_{\text{out}} = (1\ 0\ 0\ 0)$ or to the identity matrix, depending on the case, while the measurement noise is either a independent and identically distributed Gaussian random variable with zero mean and variance R or null.

In order to avoid significant deviations of the linear model from the nonlinear dynamics, we consider to limit the tilt angle in the interval $[-0.1 \text{ rad}, 0.1 \text{ rad}]$, while the input is constrained in the interval $[-11 \text{ V}, 11 \text{ V}]$ due to limits in the actuation system. This can be formalized introducing the constrained output $y_t^{\text{cstr}} = Cx_t + Du_t$ with

$$C = \begin{bmatrix} 0 & 1 & 0 & 0 \\ & & -K & \end{bmatrix} \qquad D = \begin{bmatrix} 0 \\ N_r \end{bmatrix}$$

and imposing $y_t^{\text{cstr}} \in Y = \{y : Hy \leq h\}$ with

$$H = \begin{bmatrix} 1 & 0 \\ -1 & 0 \\ 0 & 1 \\ 0 & -1 \end{bmatrix} \qquad h = \begin{bmatrix} 0.1 \\ 0.1 \\ 11 \\ 11 \end{bmatrix}.$$

To capture model inaccuracies and approximations due to the linearization, disturbances are also considered. Different models are used in the thesis according to the applications. For estimation purposes, the disturbance process w_t is assumed to be an independent and identically distributed Gaussian random vector with zero mean and covariance Q. For constrained control applications, the disturbance w_t is assumed bounded, belonging to the set $W = AB_w\overline{W}$ with

$$B_w = \begin{bmatrix} 0.01 \\ 0.001 \\ 0 \\ 0 \end{bmatrix} \qquad \overline{W} = \{w : -1 \leq w \leq 1\}$$

A.3 Experimental setup for communication data collection

The experimental setup, originally presented in [23], comprises an host PC (Intel Core i5-6400, 2.70 GHz, 16GB RAM, Ubuntu 17.04 with wireless Qualcomm Atheros AR9227 chip and PC-link interface) and a target board (Raspberry Pi 3 mod. B with Broadcom BCM2837 Wi-Fi module). The host PC, set as access point, creates the Wi-Fi network (IEEE 802.11n standard) that is joined by the target board only. Communication parameters have been set as indicated in [24]. In particular, at the Physical layer, MCS index is taken as HT7, corresponding to 64-QAM modulation, 5/6 coding rate, with a resulting bitrate of 65 Mbit/s. At the Data Link layer, the MAC transmission retries is set equal to 1. At the Transport layer, UDP protocol is implemented. Since both the devices run GNU/Linux operating system, networks parameters are set by resorting to the nl80211 library, that provides a set of functions to manage IEEE 802.11 standard features from the user space. External disturbance is produced through another Wi-Fi network connecting a smartphone and another PC.

The experiment consists of the transmission of time-stamped packets from the host PC to the target board and the other way around, with a fixed time-span between two following transmissions from each machine. This is achieved by running two suitably coded programs. Using the time-stamps of the packets, it is possible to retrieve the arrival processes, and from the arrival processes it is possible to derive the blackouts. For instance, let γ_t be the arrival process of the packet transmitted from the board to the

host PC, where $\gamma_t = 1$ if the t-th packet from the board is arrived at the PC before that the $(t+1)$-th packet is transmitted from the PC. Then, the blackout bo_t at time instant t on the link from the board to the PC can be computed recursively as

$$bo_{t+1} = \begin{cases} 0 & \text{if } \gamma_t = 1 \\ bo_t + 1 & \text{if } \gamma_t = 0. \end{cases}$$

The setup mimics the communication at sampling instants between a plant and a remote control unit.

A.4 Experimental setup for constrained control of Segway

The experimental setup comprises a host PC and the Segway connected through a Wi-Fi network.

The Segway used in the experiments is a custom prototype devised and built in our laboratory at the Department of Information Engineering of the University of Padova by dr. Riccardo Antonello. The prototype is equipped with a Raspberry Pi 3B+ and with an Arduino Mega 2560 microcontroller, interfaced with the Raspberry Pi 3B+ via UART serial connection. The Raspberry board provides the connection to Wi-Fi networks and it is used to connect the robot and the remote computer. The Arduino board provides the voltage commands to the two brushed DC gearmotors (Pololu 30:1 Metal Gearmotor 37Dx68L mm) through a dual H-bridge voltage driver (Arduino motor shield based on ST L298). Moreover, the Arduino board performs the inertial measurement readings, interfacing with an IMU sensor (GY521 module based on Invensense MPU6050) via I2C serial connection, and wheel angle readings, interfacing with encoder counter board (Superdroid Dual Quadrature Encoder Buffer based on LSI/CSI LS7366R) connected via SPI. Power to the vehicle is provided by a LiPo battery pack (11.1V, 4300mAh). The host PC and the Wi-Fi network are set as in the previous section.

Differently from the model used in the simulations, in the experimental setup we have considered a cascade of three control loops. The first inner loop consists of two independent speed PID controllers for the two wheel angles. It has been added to enhance robustness against model uncertainties. The second loop is a LQR balance and longitudinal position controller with input feed-forward. The output of the LQR controller, that is the acceleration reference, is then integrated, subtracted to the wheel speed, and fed as input to the two PIDs, while the input of the LQR controller is the wheel angle reference. The system state is obtained through a very simple estimator: the wheel angle is computed as the average of the measurements of the two wheel encoders, the tilt angle is derived from the IMU measurements using a complementary filter, and their derivatives are obtained with a discrete-time filter. The PID controllers, the LQR feedback, and

the estimator are implemented on the Arduino microcontroller. The third loop consists of the RG over wireless (3.26) implemented on the PC and it is closed over the Wi-Fi network. More specifically, the state estimate and the applied reference are forwarded by the Arduino microcontroller to the Raspberry board and then transmitted over the Wi-Fi network to the host PC. Based on the available information, the host PC computes the new input and transmits it to Raspberry board over Wi-Fi. If arrived, the Raspberry forwards the new input to the Arduino microcontroller, otherwise it forwards the last received input.

Note that the plant consists of the physical robot and the two inner control loops (PID and LQR), so the overall system is stable, as required by RG. The Raspberry implements both the transmission logic at the sensor and the smart actuator (ZOH). Clearly, the PC represents the remote control unit.

References

[1] Y. Lu, "Industry 4.0: A Survey on Technologies, Applications and Open Research Issues," *Journal of Industrial Information Integration*, vol. 6, pp. 1–10, 2017. (Cited on page 1.)

[2] E. Sisinni, A. Saifullah, S. Han, U. Jennehag, and M. Gidlund, "Industrial Internet of Things: Challenges, Opportunities, and Directions," *IEEE Transactions on Industrial Informatics*, vol. 14, no. 11, pp. 4724–4734, 2018. (Cited on page 1.)

[3] T. K. Hui, R. S. Sherratt, and D. D. Sánchez, "Major Requirements for Building Smart Homes in Smart Cities based on Internet of Things Technologies," *Future Generation Computer Systems*, vol. 76, pp. 358–369, 2017. (Cited on page 1.)

[4] R. Du, P. Santi, M. Xiao, A. V. Vasilakos, and C. Fischione, "The Sensable City: A Survey on the Deployment and Management for Smart City Monitoring," *IEEE Communications Surveys & Tutorials*, vol. 21, no. 2, pp. 1533–1560, 2018. (Cited on page 1.)

[5] J. Gao, Y. Xiao, J. Liu, W. Liang, and C. P. Chen, "A Survey of Communication/Networking in Smart Grids," *Future Generation Computer Systems*, vol. 28, no. 2, pp. 391–404, 2012. (Cited on page 1.)

[6] G. Lu, B. Krishnamachari, and C. S. Raghavendra, "Performance Evaluation of the IEEE 802.15. 4 MAC for Low-Rate Low-Power Wireless Networks," in *IEEE International Conference on Performance, Computing, and Communications*. IEEE, 2004, pp. 701–706. (Cited on page 2.)

[7] S. Petersen and S. Carlsen, "WirelessHART versus ISA100. 11a: The Format War Hits the Factory Floor," *IEEE Industrial Electronics Magazine*, vol. 5, no. 4, pp. 23–34, 2011. (Cited on page 2.)

[8] F. Tramarin, S. Vitturi, M. Luvisotto, and A. Zanella, "On the Use of IEEE 802.11n for Industrial Communications," *IEEE Transactions on Industrial Informatics*, vol. 12, no. 5, pp. 1877–1886, 2015. (Cited on pages 2 and 3.)

[9] W. Ikram, S. Petersen, P. Orten, and N. F. Thornhill, "Adaptive Multi-channel Transmission Power Control for Industrial Wireless Instrumentation," *IEEE Transactions on Industrial Informatics*, vol. 10, no. 2, pp. 978–990, 2014. (Cited on page 2.)

[10] S. Vitturi, L. Seno, F. Tramarin, and M. Bertocco, "On the Rate Adaptation Techniques of IEEE 802.11 Networks for Industrial Applications," *IEEE Transactions on Industrial Informatics*, vol. 9, no. 1, pp. 198–208, 2012. (Cited on page 2.)

[11] M. Pezzutto, F. Tramarin, S. Dey, and L. Schenato, "Adaptive Transmission Rate for LQG Control over Wi-Fi: A Cross-layer Approach," *Automatica*, vol. 119, p. 109092, 2020. (Cited on pages 2 and 113.)

[12] M. Luvisotto, F. Tramarin, and S. Vitturi, "A Learning Algorithm for Rate Selection in Real-Time Wireless LANs," *Computer Networks*, vol. 126, pp. 114–124, 2017. (Cited on page 2.)

[13] G. Cena, L. Seno, A. Valenzano, and C. Zunino, "On the Performance of IEEE 802.11e Wireless Infrastructures for Soft-real-time Industrial Applications," *IEEE Transactions on Industrial Informatics*, vol. 6, no. 3, pp. 425–437, 2010. (Cited on page 3.)

[14] P. Park, P. Di Marco, C. Fischione, and K. H. Johansson, "Modeling and Optimization of the IEEE 802.15.4 Protocol for Reliable and Timely Communications," *IEEE Transactions on Parallel and Distributed Systems*, vol. 24, no. 3, pp. 550–564, 2012. (Cited on page 3.)

[15] Y.-H. Wei, Q. Leng, S. Han, A. K. Mok, W. Zhang, and M. Tomizuka, "RT-WiFi: Real-time High-speed Communication Protocol for Wireless Cyber-physical Control Applications," in *2013 IEEE 34th Real-Time Systems Symposium*. IEEE, 2013, pp. 140–149. (Cited on page 3.)

[16] W. Liang, M. Zheng, J. Zhang, H. Shi, H. Yu, Y. Yang, S. Liu, W. Yang, and X. Zhao, "WIA-FA and its Applications to Digital Factory: A Wireless Network Solution for Factory Automation," *Proceedings of the IEEE*, vol. 107, no. 6, pp. 1053–1073, 2019. (Cited on page 3.)

[17] E. N. Gilbert, "Capacity of a Burst-noise Channel," *The Bell System Technical Journal*, vol. 39, no. 5, pp. 1253–1265, 1960. (Cited on page 3.)

[18] E. O. Elliott, "Estimates of Error Rates for Codes on Burst-noise Channels," *The Bell System Technical Journal*, vol. 42, no. 5, pp. 1977–1997, 1963. (Cited on page 3.)

[19] R. K. Guha and S. Sarkar, "Characterizing Temporal SNR Variation in 802.11 Networks," *IEEE Transactions on Vehicular Technology*, vol. 57, no. 4, pp. 2002–2013, 2008. (Cited on page 3.)

[20] M. Yajnik, S. Moon, J. Kurose, and D. Towsley, "Measurement and Modelling of the Temporal Dependence in Packet Loss," in *18th IEEE Conference on Computer Communications. Proceedings (INFOCOM99)*, vol. 1. IEEE, 1999, pp. 345–352. (Cited on page 3.)

[21] J. A. Hartwell and A. O. Fapojuwo, "Modeling and Characterization of Frame Loss Process in IEEE 802.11 Wireless Local Area Networks," in *IEEE 60th Vehicular Technology Conference*, vol. 6. IEEE, 2004, pp. 4481–4485. (Cited on page 3.)

[22] C. A. G. Da Silva and C. M. Pedroso, "MAC Layer Packet Loss Models for Wi-Fi Networks: A survey," *IEEE Access*, vol. 7, pp. 180 512–180 531, 2019. (Cited on page 3.)

[23] F. Branz, R. Antonello, L. Schenato, F. Tramarin, and S. Vitturi, "Time-Critical Wireless Networked Embedded Systems: Feasibility and Experimental Assessment," *IEEE Transactions on Industrial Informatics*, vol. 16, no. 12, pp. 7732–7742, 2020. (Cited on pages 3, 4, and 136.)

[24] F. Branz, R. Antonello, M. Pezzutto, S. Vitturi, F. Tramarin, and L. Schenato, "Drive-by-WiFi: Model-Based Control over Wireless at 1 kHz," *IEEE Transactions on Control Systems Technology*, 2021. (Cited on pages 4, 11, 20, and 136.)

[25] J. Nilsson, B. Bernhardsson, and B. Wittenmark, "Stochastic Analysis and Control of Real-Time Systems with Random Time Delays," *Automatica*, vol. 34, no. 1, pp. 57–64, 1998. (Cited on page 5.)

[26] G. C. Walsh, O. Beldiman, and L. G. Bushnell, "Asymptotic Behavior of Nonlinear Networked Control Systems," *IEEE Transactions on Automatic Control*, vol. 46, no. 7, pp. 1093–1097, 2001. (Cited on page 5.)

[27] G. C. Walsh, H. Ye, and L. G. Bushnell, "Stability Analysis of Networked Control Systems," *IEEE Transactions on Control Systems Technology*, vol. 10, no. 3, pp. 438–446, 2002. (Cited on page 5.)

[28] L. A. Montestruque and P. Antsaklis, "Stability of Model-based Networked Control Systems with Time-Varying Transmission Times," *IEEE Transactions on Automatic Control*, vol. 49, no. 9, pp. 1562–1572, 2004. (Cited on page 5.)

[29] D. Nešić and A. R. Teel, "Input-Output Stability Properties of Networked Control Systems," *IEEE Transactions on Automatic Control*, vol. 49, no. 10, pp. 1650–1667, 2004. (Cited on page 5.)

[30] W. P. Heemels, K. H. Johansson, and P. Tabuada, "An Introduction to Event-triggered and Self-triggered Control," in *51st IEEE Conference on Decision and Control (cdc)*. IEEE, 2012, pp. 3270–3285. (Cited on page 5.)

[31] D. Carnevale, A. R. Teel, and D. Nešić, "A Lyapunov Proof of an Improved Maximum Allowable Transfer Interval for Networked Control Systems," *IEEE Transactions on Automatic Control*, vol. 52, no. 5, pp. 892–897, 2007. (Cited on page 6.)

[32] M. Tabbara, D. Nešić, and A. R. Teel, "Stability of Wireless and Wireline Networked Control Systems," *IEEE Transactions on Automatic Control*, vol. 52, no. 9, pp. 1615–1630, 2007. (Cited on page 6.)

[33] W. M. H. Heemels, A. R. Teel, N. Van de Wouw, and D. Nešić, "Networked Control Systems with Communication Constraints: Tradeoffs between Transmission Intervals, Delays and Performance," *IEEE Transactions on Automatic Control*, vol. 55, no. 8, pp. 1781–1796, 2010. (Cited on page 6.)

[34] R. Postoyan, N. Van de Wouw, D. Nešić, and W. M. H. Heemels, "Tracking Control for Nonlinear Networked Control Systems," *IEEE Transactions on Automatic Control*, vol. 59, no. 6, pp. 1539–1554, 2014. (Cited on page 6.)

[35] B. Sinopoli, L. Schenato, M. Franceschetti, K. Poolla, M. I. Jordan, and S. S. Sastry, "Kalman Filtering with Intermittent Observations," *IEEE Transactions on Automatic Control*, vol. 49, no. 9, pp. 1453–1464, 2004. (Cited on pages 6, 7, 21, 24, 27, 112, and 113.)

[36] N. Elia, "Remote Stabilization over Fading Channels," *Systems & Control Letters*, vol. 54, no. 3, pp. 237–249, 2005. (Cited on pages 6 and 7.)

[37] O. C. Imer, S. Yüksel, and T. Başar, "Optimal Control of LTI Systems over Unreliable Communication Links," *Automatica*, vol. 42, no. 9, pp. 1429–1439, 2006. (Cited on pages 6 and 9.)

[38] L. Schenato, B. Sinopoli, M. Franceschetti, K. Poolla, and S. S. Sastry, "Foundations of Control and Estimation over Lossy Networks," *Proceedings of the IEEE*, vol. 95, no. 1, pp. 163–187, 2007. (Cited on pages 6, 7, 8, 105, 112, and 113.)

[39] M. Huang and S. Dey, "Stability of Kalman Filtering with Markovian Packet Losses," *Automatica*, vol. 43, no. 4, pp. 598–607, 2007. (Cited on page 6.)

[40] Y. Mo and B. Sinopoli, "A Characterization of the Critical Value for Kalman Filtering with Intermittent Observations," in *2008 47th IEEE Conference on Decision and Control*. IEEE, 2008, pp. 2692–2697. (Cited on pages 7 and 21.)

[41] K. Plarre and F. Bullo, "On Kalman Filtering for Detectable Systems with Intermittent Observations," *IEEE Transactions on Automatic Control*, vol. 54, no. 2, pp. 386–390, 2009. (Cited on pages 7 and 21.)

[42] Y. Mo and B. Sinopoli, "Kalman Filtering with Intermittent Observations: Tail Distribution and Critical Value," *IEEE Transactions on Automatic Control*, vol. 57, no. 3, pp. 677–689, 2011. (Cited on pages 7 and 21.)

[43] E. R. Rohr, D. Marelli, and M. Fu, "Kalman Filtering with Intermittent Observations: On the Boundedness of the Expected Error Covariance," *IEEE Transactions on Automatic Control*, vol. 59, no. 10, pp. 2724–2738, 2014. (Cited on pages 7 and 21.)

[44] X. Liu and A. Goldsmith, "Kalman Filtering with Partial Observation Losses," in *2004 43rd IEEE Conference on Decision and Control*, vol. 4. IEEE, 2004, pp. 4180–4186. (Cited on page 7.)

[45] L. Schenato, "Optimal Estimation in Networked Control Systems subject to Random Delay and Packet Drop," *IEEE Transactions on Automatic Control*, vol. 53, no. 5, pp. 1311–1317, 2008. (Cited on page 7.)

[46] V. Gupta, B. Hassibi, and R. M. Murray, "Optimal LQG Control across Packet-dropping Links," *Systems & Control Letters*, vol. 56, no. 6, pp. 439–446, 2007. (Cited on page 7.)

[47] E. Garone, B. Sinopoli, A. Goldsmith, and A. Casavola, "LQG Control for MIMO Systems over Multiple Erasure Channels with Perfect Acknowledgment," *IEEE Transactions on Automatic Control*, vol. 57, no. 2, pp. 450–456, 2011. (Cited on pages 8 and 105.)

[48] V. Gupta and N. C. Martins, "On Stability in the Presence of Analog Erasure Channel between the Controller and the Actuator," *IEEE Transactions on Automatic Control*, vol. 55, no. 1, pp. 175–179, 2009. (Cited on page 8.)

[49] L. Schenato, "To Zero or To Hold Control Inputs with Lossy Links?" *IEEE Transactions on Automatic Control*, vol. 54, no. 5, pp. 1093–1099, 2009. (Cited on page 8.)

[50] D. E. Quevedo, E. I. Silva, and G. C. Goodwin, "Packetized Predictive Control over Erasure Channels," in *2007 American Control Conference*. IEEE, 2007, pp. 1003–1008. (Cited on pages 8 and 61.)

[51] D. E. Quevedo and D. Nešić, "Input-to-State Stability of Packetized Predictive Control over Unreliable Networks Affected by Packet Dropouts," *IEEE Transactions on Automatic Control*, vol. 56, no. 2, pp. 370–375, 2010. (Cited on pages 8, 61, and 69.)

[52] H. Li and Y. Shi, "Network-based Predictive Control for Constrained Nonlinear Systems with Two-channel Packet Dropouts," *IEEE Transactions on Industrial Electronics*, vol. 61, no. 3, pp. 1574–1582, 2013. (Cited on pages 8, 62, and 69.)

[53] G. Pin and T. Parisini, "Stabilization of Networked Control Systems by Nonlinear Model Predictive Control: a Set Invariance Approach," in *Nonlinear Model Predictive Control*. Springer, 2009, pp. 195–204. (Cited on pages 8 and 62.)

[54] E. Garone, B. Sinopoli, and A. Casavola, "LQG Control over Lossy TCP-like Networks with Probabilistic Packet Acknowledgements," *International Journal of Systems, Control and Communications*, vol. 2, no. 1-3, pp. 55–81, 2010. (Cited on page 8.)

[55] H. Lin, H. Su, Z. Shu, Z.-G. Wu, and Y. Xu, "Optimal Estimation in UDP-like Networked Control Systems with Intermittent Inputs: Stability Analysis and Suboptimal Filter Design," *IEEE Transactions on Automatic Control*, vol. 61, no. 7, pp. 1794–1809, 2015. (Cited on page 8.)

[56] H. Lin, H. Su, P. Shi, R. Lu, and Z.-G. Wu, "Estimation and LQG Control over Unreliable Network with Acknowledgment Randomly Lost," *IEEE Transactions on Cybernetics*, vol. 47, no. 12, pp. 4074–4085, 2016. (Cited on page 8.)

[57] M. Epstein, L. Shi, and R. M. Murray, "Estimation Schemes for Networked Control Systems using UDP-like Communication," in *2007 46th IEEE Conference on Decision and Control*. IEEE, 2007, pp. 3945–3951. (Cited on page 9.)

[58] B. Sinopoli, L. Schenato, M. Franceschetti, K. Poolla, and S. Sastry, "Optimal Linear LQG Control over Lossy Networks without Packet Acknowledgment," *Asian Journal of Control*, vol. 10, no. 1, pp. 3–13, 2008. (Cited on page 9.)

[59] G. Pin and T. Parisini, "Networked Predictive Control of Uncertain Constrained Nonlinear Systems: Recursive feasibility and Input-to-State Stability Analysis," *IEEE Transactions on Automatic Control*, vol. 56, no. 1, pp. 72–87, 2010. (Cited on pages 9, 16, 53, 55, 58, 62, 63, 69, 73, and 75.)

[60] Emerson™, "Wireless now," https://www.emerson.com/documents/automation/article-wireless-now-featured-in-november-2008-issue-of-control-magazine-en-40872.pdf, *Control, November 2008 Special Advertising Supplement*. Accessed: 2021-09-24. (Cited on page 9.)

[61] S. Kim, S. Pakzad, D. Culler, J. Demmel, G. Fenves, S. Glaser, and M. Turon, "Health Monitoring of Civil Infrastructures using Wireless Sensor Networks," in *6th International Conference on Information Processing in Sensor Networks*, 2007, pp. 254–263. (Cited on page 9.)

[62] J. Ko, C. Lu, M. B. Srivastava, J. A. Stankovic, A. Terzis, and M. Welsh, "Wireless Sensor Networks for Healthcare," *Proceedings of the IEEE*, vol. 98, no. 11, pp. 1947–1960, 2010. (Cited on page 9.)

[63] J. Ko, J. H. Lim, Y. Chen, R. Musvaloiu-E, A. Terzis, G. M. Masson, T. Gao, W. Destler, L. Selavo, and R. P. Dutton, "MEDiSN: Medical Emergency Detection

in Sensor Networks," *ACM Transactions on Embedded Computing Systems*, vol. 10, no. 1, pp. 1–29, 2010. (Cited on page 9.)

[64] V. Shnayder, B.-r. Chen, K. Lorincz, T. R. Fulford-Jones, and M. Welsh, "Sensor Networks for Medical Care," Harvard Computer Science Group, Technical Report (TR-08-05), Tech. Rep., 2005. (Cited on page 9.)

[65] M. Magno, T. Polonelli, L. Benini, and E. Popovici, "A Low-cost Highly-scalable Wireless Sensor Network Solution to Achieve Smart LED Light Control for Green Buildings," *IEEE Sensors Journal*, vol. 15, no. 5, pp. 2963–2973, 2014. (Cited on page 10.)

[66] P. Zhou, G. Huang, and Z. Li, "Demand-based Temperature Control of Large-scale Rooms Aided by Wireless Sensor Network: Energy Saving Potential Analysis," *Energy and Buildings*, vol. 68, pp. 532–540, 2014. (Cited on page 10.)

[67] J. Gutiérrez, J. F. Villa-Medina, A. Nieto-Garibay, and M. Á. Porta-Gándara, "Automated Irrigation System using a Wireless Sensor Network and GPRS Module," *IEEE Transactions on Instrumentation and Measurement*, vol. 63, no. 1, pp. 166–176, 2013. (Cited on page 10.)

[68] A. Gasparri, G. Ulivi, N. Bono Rossello, and E. Garone, "The H2020 Project Pantheon: Precision Farming of Hazelnut Orchards," *Convegno Automatica. Florence, Italy*, 2018. (Cited on page 10.)

[69] C. Kamienski, J.-P. Soininen, M. Taumberger, R. Dantas, A. Toscano, T. Salmon Cinotti, R. Filev Maia, and A. Torre Neto, "Smart Water Management Platform: IoT-based Precision Irrigation for Agriculture," *Sensors*, vol. 19, no. 2, p. 276, 2019. (Cited on page 10.)

[70] A. Ahlén, J. Akerberg, M. Eriksson, A. J. Isaksson, T. Iwaki, K. H. Johansson, S. Knorn, T. Lindh, and H. Sandberg, "Toward Wireless Control in Industrial Process Automation: A Case Study at a Paper Mill," *IEEE Control Systems Magazine*, vol. 39, no. 5, pp. 36–57, 2019. (Cited on page 10.)

[71] S. Han, A. K. Mok, J. Meng, Y.-H. Wei, P.-C. Huang, Q. Leng, X. Zhu, L. Sentis, K. S. Kim, and R. Miikkulainen, "Architecture of a Cyberphysical Avatar," in *ACM/IEEE 4th International Conference on Cyber-Physical Systems*, 2013, pp. 189–198. (Cited on page 11.)

[72] J. Eker, A. Cervin, and A. Hörjel, "Distributed Wireless Control using Bluetooth," *IFAC Proceedings Volumes*, vol. 34, no. 22, pp. 360–365, 2001. (Cited on page 11.)

[73] N. W. Bauer, S. B. Van Loon, N. Van De Wouw, and W. M. Heemels, "Exploring the Boundaries of Robust Stability under Uncertain Communication: An NCS Toolbox Applied to a Wireless Control Setup," *IEEE Control Systems Magazine*, vol. 34, no. 4, pp. 65–86, 2014. (Cited on page 11.)

[74] D. Baumann, F. Mager, R. Jacob, L. Thiele, M. Zimmerling, and S. Trimpe, "Fast Feedback Control over Multi-hop Wireless Networks with Mode Changes and Stability Guarantees," *ACM Transactions on Cyber-Physical Systems*, vol. 4, no. 2, pp. 1–32, 2019. (Cited on page 11.)

[75] Y. Ren, S. Sosnowski, and S. Hirche, "Fully Distributed Cooperation for Networked Uncertain Mobile Manipulators," *IEEE Transactions on Robotics*, vol. 36, no. 4, pp. 984–1003, 2020. (Cited on pages 11 and 78.)

[76] J. Bae, W. Zhang, and M. Tomizuka, "Network-based Rehabilitation System for Improved Mobility and Tele-Rehabilitation," *IEEE Transactions on Control Systems Technology*, vol. 21, no. 5, pp. 1980–1987, 2012. (Cited on page 11.)

[77] W. Zhang and M. Tomizuka, "Compensation of Time Delay in a Network-based Gait Rehabilitation System with a Discrete-time Communication Disturbance Observer," *IFAC Proceedings Volumes*, vol. 46, no. 5, pp. 555–562, 2013. (Cited on page 11.)

[78] W. Zhang, X. Zhu, S. Han, N. Byl, A. K. Mok, and M. Tomizuka, "Design of a Network-based Mobile Gait Rehabilitation System," in *2012 IEEE International Conference on Robotics and Biomimetics (ROBIO)*. IEEE, 2012, pp. 1773–1778. (Cited on page 11.)

[79] E. Garone, S. Di Cairano, and I. Kolmanovsky, "Reference and Command Governors for Systems with Constraints: A Survey on Theory and Applications," *Automatica*, vol. 75, pp. 306–328, 2017. (Cited on pages 14 and 34.)

[80] D. Q. Mayne, "Model Predictive Control: Recent Developments and Future Promise," *Automatica*, vol. 50, no. 12, pp. 2967–2986, 2014. (Cited on page 14.)

[81] S. Foss, D. Korshunov, and S. Zachary, *An Introduction to Heavy-tailed and Subexponential Distributions*. Springer, 2011, vol. 6. (Cited on page 19.)

[82] B. O. Bradley and M. S. Taqqu, "Financial Risk and Heavy Tails," in *Handbook of Heavy Tailed Distributions in Finance*. Elsevier, 2003, pp. 35–103. (Cited on page 19.)

[83] M. E. Crovella, M. S. Taqqu, and A. Bestavros, "Heavy-Tailed Probability Distributions in the World Wide Web," *A Practical Guide to Heavy Tails*, vol. 1, pp. 3–26, 1998. (Cited on page 19.)

[84] A. Vázquez, J. G. Oliveira, Z. Dezsö, K.-I. Goh, I. Kondor, and A.-L. Barabási, "Modeling Bursts and Heavy Tails in Human Dynamics," *Physical Review E*, vol. 73, no. 3, p. 036127, 2006. (Cited on page 19.)

[85] A.-L. Barabási, "The Origin of Bursts and Heavy Tails in Human Dynamics," *Nature*, vol. 435, no. 7039, pp. 207–211, 2005. (Cited on page 19.)

[86] R. S. Smith and B. Bamieh, "Stochasticity in Feedback Loops: Great Expectations and Guaranteed Ruin," *IEEE Control Systems Magazine*, vol. 41, no. 2, pp. 28–44, 2021. (Cited on page 19.)

[87] J. Nair, A. Wierman, and B. Zwart, "The Fundamentals of Heavy-Tails: Properties, Emergence, and Identification," in *Proceedings of the ACM SIGMETRICS – International Conference on Measurement and Modeling of Computer systems*, 2013, pp. 387–388. (Cited on page 20.)

[88] L. Shi, M. Epstein, and R. M. Murray, "Kalman Filtering over a Packet-dropping Network: A probabilistic Perspective," *IEEE Transactions on Automatic Control*, vol. 55, no. 3, pp. 594–604, 2010. (Cited on page 21.)

[89] A. Censi, "Kalman Filtering with Intermittent Observations: Convergence for semi-Markov Chains and an Intrinsic Performance Measure," *IEEE Transactions on Automatic Control*, vol. 56, no. 2, pp. 376–381, 2010. (Cited on page 21.)

[90] S. Kar, B. Sinopoli, and J. M. Moura, "Kalman Filtering with Intermittent Observations: Weak Convergence to a Stationary Distribution," *IEEE Transactions on Automatic Control*, vol. 57, no. 2, pp. 405–420, 2011. (Cited on page 21.)

[91] M. Loeve, *Probability theory I*. Springer, 1977, vol. 4. (Cited on page 22.)

[92] H. Kesten, "Random Difference Equations and Renewal Theory for Products of Random Matrices," *Acta Mathematica*, vol. 131, pp. 207–248, 1973. (Cited on page 25.)

[93] H. Furstenberg and H. Kesten, "Products of Random Matrices," *The Annals of Mathematical Statistics*, vol. 31, no. 2, pp. 457–469, 1960. (Cited on page 25.)

[94] D. Buraczewski, E. Damek, and T. Mikosch, *Stochastic Models with Power-law Tails: The equation X=AX+B*. Springer, 2016, vol. 1. (Cited on pages 25 and 29.)

[95] M. Pezzutto, L. Schenato, and S. Dey, "Heavy-tails in Kalman Filtering with Packet Losses," *European Journal of Control*, vol. 50, pp. 62–71, 2019. (Cited on page 26.)

[96] V. Y. Protasov and R. M. Jungers, "Lower and Upper Bounds for the Largest Lyapunov Exponent of Matrices," *Linear Algebra and its Applications*, vol. 438, no. 11, pp. 4448–4468, 2013. (Cited on page 26.)

[97] C. M. Goldie, "Implicit Renewal Theory and Tails of Solutions of Random Equations," *The Annals of Applied Probability*, pp. 126–166, 1991. (Cited on page 29.)

[98] S. Erhart, D. Sieber, and S. Hirche, "An Impedance-based Control Architecture for Multi-robot Cooperative Dual-Arm Mobile Manipulation," in *2013 IEEE/RSJ International Conference on Intelligent Robots and Systems (RSJ)*. IEEE, 2013, pp. 315–322. (Cited on page 34.)

[99] S. Di Cairano and I. V. Kolmanovsky, "Rate Limited Reference Governor for Network Controlled Systems," in *Proceedings of the 2010 American Control Conference*. IEEE, 2010, pp. 3704–3709. (Cited on page 35.)

[100] ——, "Further Developments and Applications of Network Reference Governor for Constrained Systems," in *2012 American Control Conference (ACC)*. IEEE, 2012, pp. 3907–3912. (Cited on page 35.)

[101] S. Di Cairano, U. V. Kalabić, and I. V. Kolmanovsky, "Reference Governor for Network Control Systems subject to Variable Time-Delay," *Automatica*, vol. 62, pp. 77–86, 2015. (Cited on page 35.)

[102] A. Casavola, E. Mosca, and M. Papini, "Predictive Teleoperation of Constrained Dynamic Systems via Internet-like Channels," *IEEE Transactions on Control Systems Technology*, vol. 14, no. 4, pp. 681–694, 2006. (Cited on page 35.)

[103] A. Casavola, M. Papini, and G. Franzè, "Supervision of Networked Dynamical Systems under Coordination Constraints," *IEEE Transactions on Automatic Control*, vol. 51, no. 3, pp. 421–437, 2006. (Cited on pages 35, 47, and 78.)

[104] E. G. Gilbert and I. Kolmanovsky, "Fast reference governors for systems with state and control constraints and disturbance inputs," *International Journal of Robust and Nonlinear Control*, vol. 9, no. 15, pp. 1117–1141, 1999. (Cited on pages 38, 39, 40, and 41.)

[105] E. G. Gilbert and K. T. Tan, "Linear Systems with State and Control Constraints: The Theory and Application of Maximal Output Admissible Sets," *IEEE Transactions on Automatic Control*, vol. 36, no. 9, pp. 1008–1020, 1991. (Cited on page 38.)

[106] I. Kolmanovsky and E. G. Gilbert, "Theory and Computation of Disturbance Invariant Sets for Discrete-time Linear Systems," *Mathematical Problems in Engineering*, vol. 4, pp. 317–367, 1998. (Cited on pages 38, 40, 42, and 134.)

[107] A. Casavola, E. Mosca, and D. Angeli, "Robust Command Governors for Constrained Linear Systems," *IEEE Transactions on Automatic Control*, vol. 45, no. 11, pp. 2071–2077, 2000. (Cited on page 39.)

[108] E. G. Gilbert, I. Kolmanovsky, and K. T. Tan, "Discrete-time Reference Governors and the Nonlinear Control of Systems with State and Control Constraints," *International Journal of Robust and Nonlinear Control*, vol. 5, no. 5, pp. 487–504, 1995. (Cited on page 39.)

[109] A. Bemporad, A. Casavola, and E. Mosca, "Nonlinear Control of Constrained Linear Systems via Predictive Reference Management," *IEEE Transactions on Automatic Control*, vol. 42, no. 3, pp. 340–349, 1997. (Cited on page 39.)

[110] E. G. Gilbert and C.-J. Ong, "Constrained Linear Systems with Hard Constraints and Disturbances: An extended Command Governor with Large Domain of Attraction," *Automatica*, vol. 47, no. 2, pp. 334–340, 2011. (Cited on page 39.)

[111] M. Pezzutto, E. Garone, and L. Schenato, "Reference Governor for Constrained Control over Lossy Channels," *IEEE Control Systems Letters*, vol. 4, no. 2, pp. 271–276, 2019. (Cited on page 46.)

[112] ——, "Constrained Control with Communication Blackouts: Theory and Experimental Validation over Wi-Fi," in *2021 29th Mediterranean Conference on Control and Automation*. IEEE, 2021, pp. 238–243. (Cited on page 56.)

[113] D. E. Quevedo, E. I. Silva, and G. C. Goodwin, "Control over Unreliable Networks Affected by Packet Erasures and Variable Transmission Delays," *IEEE Journal on Selected Areas in Communications*, vol. 26, no. 4, pp. 672–685, 2008. (Cited on page 62.)

[114] R. Findeisen and P. Varutti, "Stabilizing Nonlinear Predictive Control over Nondeterministic Communication Networks," in *Nonlinear Model Predictive Control*. Springer, 2009, pp. 167–179. (Cited on pages 62 and 69.)

[115] P. Varutti, B. Kern, T. Faulwasser, and R. Findeisen, "Event-based Model Predictive Control for Networked Control Systems," in *48h IEEE Conference on Decision and Control and 28th Chinese Control Conference*. IEEE, 2009, pp. 567–572. (Cited on page 62.)

[116] D. E. Quevedo and D. Nešić, "Robust Stability of Packetized Predictive Control of Nonlinear Systems with Disturbances and Markovian Packet Losses," *Automatica*, vol. 48, no. 8, pp. 1803–1811, 2012. (Cited on page 62.)

[117] D. E. Quevedo and I. Jurado, "Stability of Sequence-based Control with Random Delays and Dropouts," *IEEE Transactions on Automatic Control*, vol. 59, no. 5, pp. 1296–1302, 2013. (Cited on page 62.)

[118] D. E. Quevedo, J. Ostergaard, and D. Nešić, "Packetized Predictive Control of Stochastic Systems over Bit-Rate Limited Channels with Packet Loss," *IEEE Transactions on Automatic Control*, vol. 56, no. 12, pp. 2854–2868, 2011. (Cited on page 62.)

[119] M. Nagahara, D. E. Quevedo, and J. Østergaard, "Sparse Packetized Predictive Control for Networked Control over Erasure Channels," *IEEE Transactions on Automatic Control*, vol. 59, no. 7, pp. 1899–1905, 2013. (Cited on page 62.)

[120] P. K. Mishra, D. Chatterjee, and D. E. Quevedo, "Stabilizing Stochastic Predictive Control under Bernoulli Dropouts," *IEEE Transactions on Automatic Control*, vol. 63, no. 6, pp. 1579–1590, 2017. (Cited on page 62.)

[121] ——, "Stochastic Predictive Control under Intermittent Observations and Unreliable Actions," *Automatica*, vol. 118, p. 109012, 2020. (Cited on pages 62 and 69.)

[122] P. K. Mishra, S. S. Diwale, C. N. Jones, and D. Chatterjee, "Reference Tracking Stochastic Model Predictive Control over Unreliable Channels and Bounded Control Actions," *Automatica*, vol. 127, p. 109512, 2021. (Cited on page 62.)

[123] D. Limón, I. Alvarado, T. Alamo, and E. F. Camacho, "MPC for Tracking Piecewise Constant References for Constrained Linear Systems," *Automatica*, vol. 44, no. 9, pp. 2382–2387, 2008. (Cited on pages 62, 65, 66, and 72.)

[124] ——, "Robust Tube-based MPC for Tracking of Constrained Linear Systems with Additive Disturbances," *Journal of Process Control*, vol. 20, no. 3, pp. 248–260, 2010. (Cited on pages 62 and 76.)

[125] D. Limon, M. Pereira, D. M. de la Pena, T. Alamo, C. N. Jones, and M. N. Zeilinger, "MPC for Tracking Periodic References," *IEEE Transactions on Automatic Control*, vol. 61, no. 4, pp. 1123–1128, 2015. (Cited on page 62.)

[126] M. Pezzutto, M. Farina, R. Carli, and L. Schenato, "Remote MPC for Tracking over Lossy Networks," *IEEE Control Systems Letters*, 2021. (Cited on page 76.)

[127] S. Zhao and D. Zelazo, "Bearing Rigidity Theory and its Applications for Control and Estimation of Network Systems: Life Beyond Distance Rigidity," *IEEE Control Systems Magazine*, vol. 39, no. 2, pp. 66–83, 2019. (Cited on page 77.)

[128] Z. Wang and M. Schwager, "Multi-robot Manipulation without Communication," in *Distributed Autonomous Robotic Systems*. Springer, 2016, pp. 135–149. (Cited on page 77.)

[129] H. Lee, H. Kim, and H. J. Kim, "Planning and Control for Collision-free Cooperative Aerial Transportation," *IEEE Transactions on Automation Science and Engineering*, vol. 15, no. 1, pp. 189–201, 2016. (Cited on page 77.)

[130] J. Alonso-Mora, S. Baker, and D. Rus, "Multi-robot Formation Control and Object Transport in Dynamic Environments via Constrained Optimization," *The International Journal of Robotics Research*, vol. 36, no. 9, pp. 1000–1021, 2017. (Cited on page 77.)

[131] F. Xiao, L. Wang, J. Chen, and Y. Gao, "Finite-time Formation Control for Multi-agent Systems," *Automatica*, vol. 45, no. 11, pp. 2605–2611, 2009. (Cited on page 77.)

[132] P. B. Dohmann and S. Hirche, "Distributed Control for Cooperative Manipulation with Event-Triggered Communication," *IEEE Transactions on Robotics*, vol. 36, no. 4, pp. 1038–1052, 2020. (Cited on page 77.)

[133] A. Casavola, E. Garone, and F. Tedesco, "A Distributed Multi-Agent Command Governor Strategy for the Coordination of Networked Interconnected Systems," *IEEE Transactions on Automatic Control*, vol. 59, no. 8, pp. 2099–2112, 2014. (Cited on pages 78, 82, 88, 90, 93, and 99.)

[134] ——, "A Distributed Command Governor based on Graph Colorability Theory," *International journal of robust and nonlinear control*, vol. 28, no. 8, pp. 3056–3072, 2018. (Cited on pages 78, 98, and 99.)

[135] E. Henriksson, D. E. Quevedo, E. G. Peters, H. Sandberg, and K. H. Johansson, "Multiple-loop Self-triggered Model Predictive Control for Network Scheduling and Control," *IEEE Transactions on Control Systems Technology*, vol. 23, no. 6, pp. 2167–2181, 2015. (Cited on page 83.)

[136] M. Bahraini, M. Zanon, A. Colombo, and P. Falcone, "Optimal Scheduling and Control for Constrained Multi-agent Networked Control Systems," *Optimal Control Applications and Methods*, 2021. (Cited on page 83.)

[137] A. Ferramosca, D. Limón, I. Alvarado, and E. F. Camacho, "Cooperative Distributed MPC for Tracking," *Automatica*, vol. 49, no. 4, pp. 906–914, 2013. (Cited on page 99.)

[138] C. Conte, C. N. Jones, M. Morari, and M. N. Zeilinger, "Distributed Synthesis and Stability of Cooperative Distributed Model Predictive Control for Linear Systems," *Automatica*, vol. 69, pp. 117–125, 2016. (Cited on page 99.)

[139] M. S. Afaqui, E. Garcia-Villegas, and E. Lopez-Aguilera, "IEEE 802.11 ax: Challenges and Requirements for Future High Efficiency WiFi," *IEEE Wireless Communications*, vol. 24, no. 3, pp. 130–137, 2016. (Cited on page 101.)

[140] T. O. Olwal, K. Djouani, and A. M. Kurien, "A Survey of Resource Management toward 5G Radio Access Networks," *IEEE Communications Surveys & Tutorials*, vol. 18, no. 3, pp. 1656–1686, 2016. (Cited on page 101.)

[141] T. Huehn and C. Sengul, "Practical Power and Rate Control for WiFi," in *21st International Conference on Computer Communications and Networks (ICCCN)*. IEEE, 2012, pp. 1–7. (Cited on page 101.)

[142] S. Verdu, *Multiuser Detection*. Cambridge university press, 1998. (Cited on page 102.)

[143] L. Tong, Q. Zhao, and G. Mergen, "Multipacket Reception in Random Access Wireless Networks: From Signal Processing to Optimal Medium Access Control," *IEEE Communications Magazine*, vol. 39, no. 11, pp. 108–112, 2001. (Cited on page 102.)

[144] M. Z. Ali, J. Mišić, and V. B. Mišić, "Uplink Access Protocol in IEEE 802.11 ac," *IEEE Transactions on Wireless Communications*, vol. 17, no. 8, pp. 5535–5551, 2018. (Cited on page 102.)

[145] S. R. Islam, N. Avazov, O. A. Dobre, and K.-S. Kwak, "Power-Domain Non-Orthogonal Multiple Access (NOMA) in 5G Systems: Potentials and Challenges," *IEEE Communications Surveys & Tutorials*, vol. 19, no. 2, pp. 721–742, 2016. (Cited on page 102.)

[146] Z. Ding, X. Lei, G. K. Karagiannidis, R. Schober, J. Yuan, and V. K. Bhargava, "A Survey on Non-Orthogonal Multiple Access for 5G Networks: Research Challenges and Future Trends," *IEEE Journal on Selected Areas in Communications*, vol. 35, no. 10, pp. 2181–2195, 2017. (Cited on page 102.)

[147] L. Kong and X. Liu, "mZig: Enabling Multi-Packet Reception in ZigBee," in *21st Annual International Conference on Mobile Computing and Networking*, 2015, pp. 552–565. (Cited on page 102.)

[148] L. Shi, P. Cheng, and J. Chen, "Optimal Periodic Sensor Scheduling with Limited Resources," *IEEE Transactions on Automatic Control*, vol. 56, no. 9, pp. 2190–2195, 2011. (Cited on page 102.)

[149] Z. Ren, P. Cheng, J. Chen, L. Shi, and Y. Sun, "Optimal Periodic Sensor Schedule for Steady-State Estimation under Average Transmission Energy Constraint," *IEEE Transactions on Automatic Control*, vol. 58, no. 12, pp. 3265–3271, 2013. (Cited on page 102.)

[150] Y. Mo, E. Garone, and B. Sinopoli, "On Infinite-horizon Sensor Scheduling," *Systems & Control Letters*, vol. 67, pp. 65–70, 2014. (Cited on page 102.)

[151] L. Zhao, W. Zhang, J. Hu, A. Abate, and C. J. Tomlin, "On the Optimal Solutions of the Infinite-horizon Linear Sensor Scheduling Problem," *IEEE Transactions on Automatic Control*, vol. 59, no. 10, pp. 2825–2830, 2014. (Cited on page 102.)

[152] J. Wu, Q.-S. Jia, K. H. Johansson, and L. Shi, "Event-based Sensor Data Scheduling: Trade-off between Communication Rate and Estimation Quality," *IEEE Transactions on Automatic Control*, vol. 58, no. 4, pp. 1041–1046, 2012. (Cited on page 102.)

[153] D. Han, Y. Mo, J. Wu, S. Weerakkody, B. Sinopoli, and L. Shi, "Stochastic Event-triggered Sensor Schedule for Remote State Estimation," *IEEE Transactions on Automatic Control*, vol. 60, no. 10, pp. 2661–2675, 2015. (Cited on page 102.)

[154] A. S. Leong, S. Dey, and D. E. Quevedo, "Sensor Scheduling in Variance-based Event-triggered Estimation with Packet Drops," *IEEE Transactions on Automatic Control*, vol. 62, no. 4, pp. 1880–1895, 2016. (Cited on pages 102 and 127.)

[155] Z. Ren, P. Cheng, J. Chen, L. Shi, and H. Zhang, "Dynamic Sensor Transmission Power Scheduling for Remote State Estimation," *Automatica*, vol. 50, no. 4, pp. 1235–1242, 2014. (Cited on page 102.)

[156] X. Ren, J. Wu, K. H. Johansson, G. Shi, and L. Shi, "Infinite-horizon Optimal Transmission Power Control for Remote State Estimation over Fading Channels," *IEEE Transactions on Automatic Control*, vol. 63, no. 1, pp. 85–100, 2017. (Cited on page 102.)

[157] Y. Li, C. S. Chen, and W. S. Wong, "Power Control for Multi-Sensor Remote State Estimation over Interference Channel," *Systems & Control Letters*, vol. 126, pp. 1–7, 2019. (Cited on pages 102 and 127.)

[158] S. Zoppi, T. Soleymani, M. Klügel, M. Vilgelm, S. Hirche, and W. Kellerer, "Transmission Power Control for Remote State Estimation in Industrial Wireless Sensor Networks," *arXiv preprint arXiv:1907.07018*, 2019. (Cited on pages 102 and 118.)

[159] B. D. Anderson and J. B. Moore, *Optimal Filtering*. Courier Corporation, 2012. (Cited on page 104.)

[160] H. R. Hashemipour, S. Roy, and A. J. Laub, "Decentralized Structures for Parallel Kalman Filtering," *IEEE Transactions on Automatic Control*, vol. 33, no. 1, pp. 88–94, 1988. (Cited on page 105.)

[161] A. Goldsmith, *Wireless Communications*. Cambridge university press, 2005. (Cited on page 106.)

[162] J. G. Proakis, *Digital Communications*. Mc-Graw-Hill, 2001. (Cited on page 106.)

[163] A. Ephremides, "Energy Concerns in Wireless Networks," *IEEE Wireless Communications*, vol. 9, no. 4, pp. 48–59, 2002. (Cited on page 106.)

[164] N. Jindal, S. Vishwanath, and A. Goldsmith, "On the Duality of Gaussian Multiple-Access and Broadcast Channels," *IEEE Transactions on information Theory*, vol. 50, no. 5, pp. 768–783, 2004. (Cited on page 106.)

[165] D. Tse and P. Viswanath, *Fundamentals of Wireless Communication*. Cambridge university press, 2005. (Cited on page 107.)

[166] O. Hernández-Lerma and M. Muñoz de Ozak, "Discrete-time Markov Control Processes with Discounted Unbounded Costs: Optimality Criteria," *Kybernetika*, vol. 28, no. 3, pp. 191–212, 1992. (Cited on page 111.)

[167] C. Yang and L. Shi, "Deterministic Sensor Data Scheduling under Limited Communication Resource," *IEEE Transactions on Signal Processing*, vol. 59, no. 10, pp. 5050–5056, 2011. (Cited on page 113.)

[168] R. K. Ritt and L. I. Sennott, "Optimal Stationary Policies in General State Space Markov Decision Chains with Finite Action Sets," *Mathematics of Operations Research*, vol. 17, no. 4, pp. 901–909, 1992. (Cited on pages 114 and 115.)

[169] D. P. Bertsekas, *Dynamic Programming and Optimal Control: Vol. 1*. Athena Scientific Belmont, 2000. (Cited on page 115.)

[170] L. Shi and H. Zhang, "Scheduling two Gauss–Markov Systems: An Optimal Solution for Remote State Estimation under Bandwidth Constraint," *IEEE Transactions on Signal Processing*, vol. 60, no. 4, pp. 2038–2042, 2012. (Cited on page 118.)

[171] D. Han, J. Wu, H. Zhang, and L. Shi, "Optimal Sensor Scheduling for Multiple Linear Dynamical Systems," *Automatica*, vol. 75, pp. 260–270, 2017. (Cited on page 118.)

[172] Z. He, S. Xie, S. Ding, and A. Cichocki, "Convolutive Blind Source Separation in the Frequency Domain based on Sparse Representation," *IEEE Transactions on*

Audio, Speech, and Language Processing, vol. 15, no. 5, pp. 1551–1563, 2007. (Cited on page 119.)

[173] K. B. Petersen and M. S. Pedersen, "The Matrix Cookbook," November 2012, version 2012.11.15. [Online]. Available: http://www2.compute.dtu.dk/pubdb/pubs/3274-full.html (Cited on page 119.)

[174] D. M. Topkis, *Supermodularity and Complementarity*. Princeton University Press, 1998. (Cited on page 121.)

[175] M. Nourian, A. S. Leong, and S. Dey, "Optimal Energy Allocation for Kalman Filtering over Packet Dropping Links with Imperfect Acknowledgments and Energy Harvesting Constraints," *IEEE Transactions on Automatic Control*, vol. 59, no. 8, pp. 2128–2143, 2014. (Cited on page 121.)

[176] M. Pezzutto, L. Schenato, and S. Dey, "Transmission Scheduling for Remote Estimation with Multi-packet Reception under Multi-sensor Interference," *IFAC-PapersOnLine*, vol. 53, no. 2, pp. 2628–2633, 2020. (Cited on page 122.)

[177] ——, "Transmission Power Allocation for Remote Estimation with Multi-packet Reception Capabilities," *arXiv preprint arXiv:2101.12493*, 2021. (Cited on page 123.)

[178] R. Antonello and L. Schenato, "Laboratory Activity 4: Longitudinal State-space Control of a Balancing Robot," University of Padova, Department of Information Engineering, Tech. Rep., 2017. [Online]. Available: http://automatica.dei.unipd.it/tl_files/utenti/lucaschenato/SEGWAY_GUIDE.pdf (Cited on page 135.)